Cover Page



Universiteit Leiden



The handle http://hdl.handle.net/1887/19856 holds various files of this Leiden University dissertation.

Author: Cogliati, Tiziana Paola
Title: Study and retina allotransplantation of porcine ciliary epithelium (CE)-derived cells
Date: 2012-09-27

Study and retina allotransplantation of porcine ciliary epithelium (CE)-derived cells

Study and retina allotransplantation
of porcine ciliary epithelium (CE)-derived cells

PROEFSCHRIFT

ter verkrijging van
de graad van Doctor aan de Universiteit Leiden,
op gezag van Rector Magnificus prof. mr. P.F. van der Heijden
volgens besluit van het College voor Promoties
te verdedigen op donderdag 27 september 2012
klokke 10:00 uur
door

Tiziana Paola Cogliati

geboren te Calolziocorte (Italy) in 1963

PROMOTIECOMMISSIE

Promotor

Prof. dr. A.K. Raap

Overige leden

Prof. dr. C.L. Mummery

Prof. dr. G.P.M. Luyten

Dr. M. Ader, Center for Regenerative Therapy, Dresden

Dr. V. Marigo, University of Modena and Reggio Emilia, Modena

Printed by: Proefschriftmaken.nl || Uitgeverij BOXPress

Published by: Uitgeverij BOXPress, Oisterwijk

ISBN: 9789088914713

The studies described in this thesis were performed at the Center for Vision Science, Queen's University School of Biomedical Sciences, Belfast, UK.

The author is most grateful to Prof. Raap and Dr. Jost for making this possible.

Apart from the joys of human relationships, *"with the exception of those miraculous and isolated moments fate bestows on a man, loving one's work (unfortunately, the privilege of a few) represents the best, most concrete approximation to happiness on earth."*

Adapted from: Primo Levi, The Monkey's Wrench (1987)

In memory of my late father Luigi Cogliati

TABLE OF CONTENTS

	Outline of the Thesis	**9**
Chapter 1	**General Introduction**	**11**
Chapter 2	**Immunohistochemical study of pig retinal development** Guduric-Fuchs J, Ringland LJ, Gu P, Dellett M, Archer DB, Cogliati T. *Mol Vis. 2009 Sep 21;15:1915-1928.*	**37**
Chapter 3	**Isolation of retinal progenitor and stem cells from the porcine eye** Gu P, Harwood LJ, Zhang X, Wylie M, Curry WJ, Cogliati T. *Mol Vis. 2007 Jun 29;13:1045-1057.*	**53**
Chapter 4	**Prediction of microRNAs affecting mRNA expression during retinal development** Arora A, Guduric-Fuchs J, Harwood L, Dellett M, Cogliati T, Simpson DA. *BMC Dev Biol. 2010 Jan 6;10:1.*	**69**
Chapter 5	**RPE and neuronal differentiation of allotransplantated porcine ciliary epithelium-derived cells** Guduric-Fuchs J, Chen W, Price H, Archer DB, Cogliati T. *Mol Vis. 2011;17:2580-2595.*	**87**
Chapter 6	**General Discussion**	**105**
	References	**115**
Appendices:	**Summary**	**139**
	Nederlandse Samenvatting	**141**
	Riassunto in Italiano	**145**
	Abbreviations	**147**
	List of publications	**151**
	Curriculum vitae	**155**

Outline of the Thesis

The Introduction (Chapter 1) to this thesis gives the background on retinal degenerative diseases, current therapeutic approaches and the opportunities for cell replacement. It further illustrates the regenerative mechanisms active in lower vertebrates and current research on cell types of ocular origin amenable for transplantation and retinal repair, focusing on Müller glia and ciliary epithelium (CE)-derived cells, also known as retinal stem cells (RSCs). Finally, it provides the rationale for studying CE-derived cells of porcine origin and testing their potential to generate retinal phenotypes upon transplantation.

Chapter 2 investigates the similarities between pig and human eye development, characterizes the CE at the developmental age collected to isolate and propagate RSCs, and validates tools for immunohistochemical analysis of the porcine retina. Chapters 3 and 4 describe the isolation and characterization of RSCs from neonatal porcine CE. In particular, Chapter 3 compares the proliferating properties and differentiation potential of RSCs and retinal progenitor cells (RPCs) from developing pig retina; Chapter 4 uses expression data to predict microRNAs that could be involved in retinal development, homeostasis, and in CE-derived RSCs, providing further insights into the molecular properties of the latter. In Chapter 5, CE-derived RSCs are transplanted into the young porcine retina, where they integrate and undergo differentiation into retinal pigment epithelium (RPE) and retinal cell phenotypes.

The General Discussion (Chapter 6) summarizes the findings described in the previous chapters, their contribution to our understanding of CE-derived cell biology and of their potential applications in retinal degenerative diseases. The limitations of the work presented are discussed together with the implications of the current debate on the nature of CE-derived cells. Concluding remarks discuss the standing of CE-derived cells in the current research efforts on retinal cell replacement therapies and propose their use as a model to study cell plasticity.

CHAPTER 1

GENERAL INTRODUCTION

Vision and the retina

Visual perception of the surrounding world is a complex and important physiological function that, in most instances, mediates our primary interaction with the environment. By sending approximately 30% of sensory inputs to the brain, visual stimuli greatly affect higher cognitive functions, including learning, memory and behavior (Rodieck, 1998). Inputs originate from neurons in the retina, the neurosensory structure in the eye and the most accessible portion of the nervous system. Light enters the eye after penetrating the cornea, passes through the pupillary aperture in the center of the iris and is more finely shifted by the lens to be focused on the retina at the back of the eye, where it stimulates retinal photoreceptors (Figure 1).

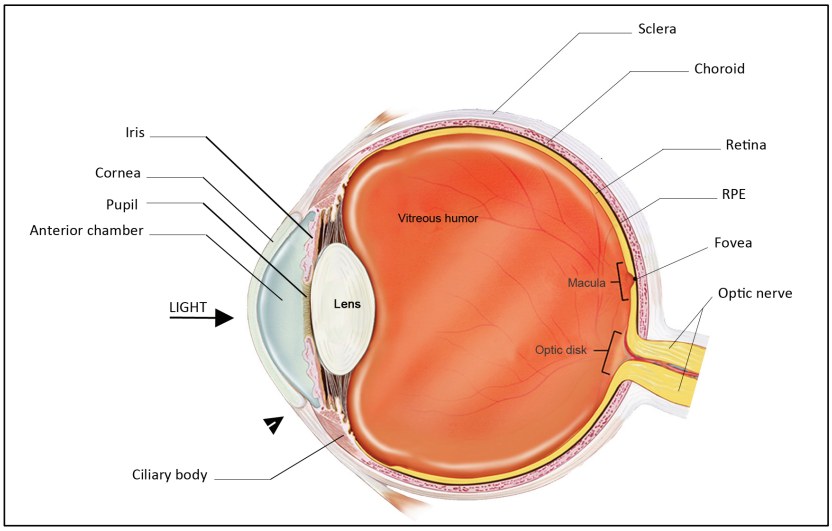


Figure 1. Anatomy of the eye. The eye is comprised of three tunics or layers. The outermost layer is the fibrous tunic, which gives shape to the eye. It consists of the sclera that extends into the cornea to the front, at the corneoscleral junction (arrowhead). The middle layer is the vascular tunic, which gives rise to the iris in the anterior eye, the ciliary body, and the choroid. The ciliary body is responsible for the production of aqueous humor, and the vasculature in the choroid supplies nourishment to the neural retina. The innermost layer is the photoreceptive tunic that comprises the retina. The space between the cornea and the iris, called the anterior chamber, is filled with aqueous humor, while the space between the lens and the retina contains vitreous humor. Light comes into the eye through the cornea, passes through the pupil aperture in the center of the iris, and is more finely shifted by the lens to focus on the retina at the back of the eye. Designed by: Lydia Kibiuk, NIH Division of Medical Arts.

The retina is a layered structure that includes six types of neurons, rod and cone photoreceptors, bipolar, horizontal, amacrine and retinal ganglion cells (RGCs) and one type of (Müller) glia (Figure 2). These cells are organized in three nuclear layers: the

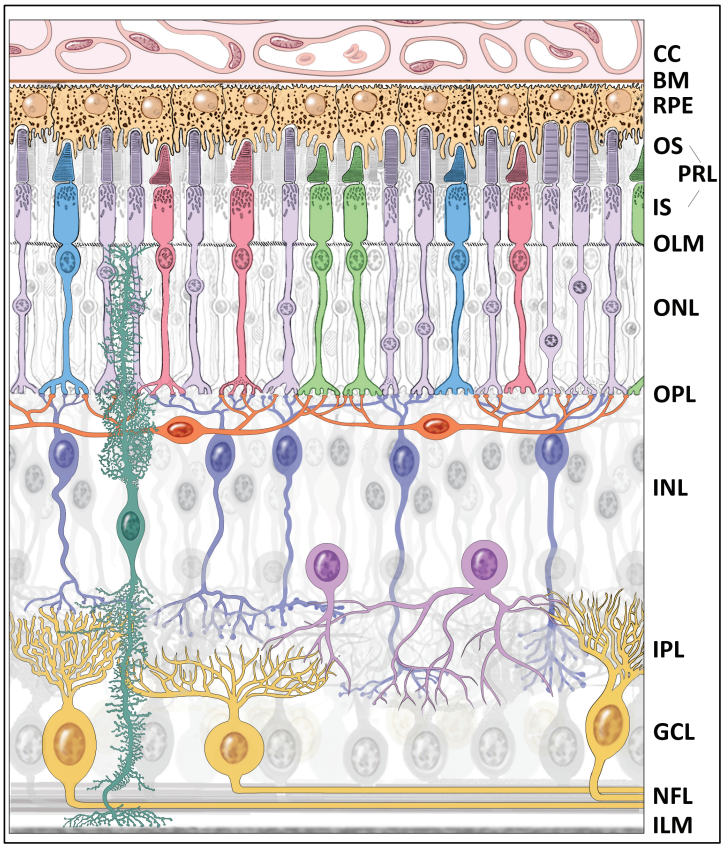


Figure 2. Retinal architecture and histology. The retina is composed of six types of neurons and one type of glia organized in three nuclear layers with synapses in two plexiform layers. The outer nuclear layer (ONL) contains rod (gray) and cone (blue, red and green) photoreceptor cell nuclei; the inner nuclear layer (INL) contains the cell bodies of bipolar (dark blue), horizontal (orange), amacrine (purple), and Müller glia (dark green) cells; and the ganglion cell layer (GCL) contains retinal ganglion cell (RGC) bodies (yellow) and displaced amacrine cells (not shown). Synapses of photoreceptors, bipolar and horizontal cells are localized in the outer plexiform layer (OPL), and synaptic connections of bipolar, RGCs, and amacrine cells in the inner plexiform layer (IPL). RGC axons extend along the inner surface of the retina to form the nerve fiber layer (NFL) and converge toward the optic disc to form the optic nerve. Rod and cone photoreceptors exist alongside each other, project their inner (IS) and outer segments (OS) toward the outer retina, and form the photoreceptor layer (PRL) in close relationship with the retinal pigment epithelium (RPE). The choriocapillaris (CC), separated from the RPE by Bruch's membrane (BM) provide nutrients to the outer retina. Outer (OLM) and inner limiting membranes (INL) are localized at the base of the IS and in the innermost retina, respectively. Designed by: Lydia Kibiuk, NIH Division of Medical Arts.

outer nuclear layer (ONL) containing rod and cone cell nuclei; the inner nuclear layer (INL) containing the cell bodies of bipolar, amacrine, horizontal and Müller glia cells; and the ganglion cell layer (GCL) containing RGCs and displaced amacrine cell bodies. Synapses between photoreceptor, bipolar, and horizontal cells are localized in the outer plexiform layer (OPL) and synapses between bipolar, RGCs and amacrine cells populate the inner plexiform layer (IPL). Müller glia cell bodies span the thickness of the retina, contributing with their end-feet to form the inner limiting membrane (ILM) and the outer limiting membrane (OLM). RGC axons extend along the inner surface of the retina to form the nerve fiber layer (NFL) and converge at the optic disc to form the optic nerve (Figure 1). Rod and cone photoreceptors (Figure 2) exist alongside each other and project their outer segments (OS) to form the photoreceptor layer (PRL).

The highly polarized retinal pigment epithelium (RPE) has intimate relationship with photoreceptor OS and is essential for their functional maintenance. In particular, the RPE phagocytizes the membranous material shed from rod and cone OS, regenerates of 11-cis retinal (a vitamin A derivative) for re-entry into the visual cycle, and absorbs excess light. Disruption of the interaction between RPE and retina is detrimental to photoreceptor function and survival.

Photoreceptor types and distribution vary among species. Rod and cone photoreceptors are differentially distributed within the human retina. At the center of the retina (on the same axis as the pupil and lens and eccentric to the optic disc), a specialized region called the macula contains a higher density of cones compared with the rest of the retina (Figure 1). This area is responsible for central color vision and visual acuity. In the middle of the macula, the retina thins to form the fovea, which contains only cones and is avascular in its center (foveola). In humans and mice, rods represent over 95% of photoreceptors. The remaining 5% (human) and 3% (mouse) are cone photoreceptor subtypes. In the mouse retina, rods are relatively homogeneously distributed and there is no structure resembling the human fovea.

Rods and cones are highly specialized sensory neurons, characterized by distinct morphology, synaptic connections, and gene expression, that reflect their unique

functions in light detection and visual process: rod photoreceptors function in dim light, whereas cones are responsible for chromatic vision and visual acuity in bright light. These differences in light sensitivity are made possible by distinct visual pigments (opsins) that belong to a family of membrane-bound guanine nucleotide binding protein-coupled receptors, and are covalently linked to a vitamin A-derived retinaldehyde chromophore. Light travels through all layers of the neural retina to reach the photoreceptor OS where it is captured by the photosensitive pigments rhodopsin (Rho) in rods and cone opsins in cones. Humans and old world primates have three subtypes of cone photoreceptors: cones sensitive to blue light express short wavelength-sensitive (S)-opsin; cones sensitive to green light express medium wavelength-sensitive (M)-opsin; whereas those sensitive to red light express long wavelength-sensitive (L)-opsin. Only S-opsin and M-opsin are expressed in mouse cone photoreceptors. Absorption of a quantum of light by the opsin results in isomerization of the retinaldehyde and activation of the phototransduction cascade, leading to hyperpolarization of the photoreceptor membrane and decrease in glutamate neurotransmitter release at the photoreceptor-bipolar cell synapse. From bipolar cells, the visual stimulus is conveyed to RGCs, whose axons converge into the optic nerve and extend outside of the orbit to relay information to several processing areas in the brain where neuronal electrical stimuli are interpreted as visual sensation. Horizontal and amacrine cells integrate and modulate visual stimuli as they are transmitted from photoreceptors to RGCs.

Photoreceptor development in human and mouse

During development, the retinal neuroepithelium is populated by proliferating, undifferentiated, multipotent retinal progenitor cells (RPCs), from which all neural retinal cell types originate in a sequence initiating from the central retina and proceeding toward the periphery (Dyer & Cepko, 2001; Livesey & Cepko, 2001). Extrinsic and intrinsic factors regulate cell cycle progression, exit and differentiation. RPCs are maintained in a proliferative and undifferentiated state by several pathways, including

those activated by epidermal growth factor (EGF), fibroblast growth factor (FGF), sonic hedgehog (SHH), Wnt, and Delta/Notch. Master genes such as *Pax6* and *Six3* regulate the intrinsic transcriptional activity.

The SHH pathway comprises SHH, its receptor PTC and the effector protein smoothened (SMO). SHH de-represses SMO from PTC control, allowing the intracellular signaling cascade that leads to activation of cell proliferation genes (Jensen & Wallace, 1997; Oliver et al, 2003). Similarly, classic Wnt signaling through Frizzled and β-catenin activate c-*myc* and *cyclins*, sustaining cell proliferation (Ahmad et al, 2004; Sanchez-Sanchez et al, 2010). Interaction of Notch with its receptor Delta initiates a cascade leading to the expression of two basic helix-loop-helix (bHLH) transcriptional repressors (HES1 and HES5) that prevent transcription of proneural genes, required for differentiation (Hatakeyama et al, 2004; Henrique et al, 1997). This phenomenon is known as "lateral inhibition". Cells that escape lateral inhibition initiate differentiation. The competence model of retinal development explains the sequence of differentiation events whereby, over time, RPCs pass through stages of competence to produce a particular subset of retinal cells (Cepko et al, 1996). RGCs are generated first, followed in overlapping waves by cone photoreceptor, amacrine, horizontal, rod photoreceptor, bipolar and finally, Müller glia cells (Marquardt, 2003).

In the stereotypical progression of cell differentiation, cone genesis is initiated from common proliferating RPCs, in a sequential manner after RGCs and before horizontal and amacrine neurons. Rod birth is initiated later compared to cone genesis, but it precedes bipolar and Müller glia cells. However, the time intervals during which full complements of cone and rod photoreceptors are generated largely overlap (Marquardt, 2003). The last cells to exit the cell cycle are those at the retinal margin. Two key elements control the commitment and differentiation of photoreceptors: gene-regulatory networks that confer competence to the RPC and dictate differentiation events, and extrinsic factors that modulate transcriptional cascades in differentiating RPCs and later modulate cell–cell communication (Figure 3 and Belliveau & Cepko, 1999; Bradford et al, 2005; Livesey & Cepko, 2001). At the time of their last mitosis and

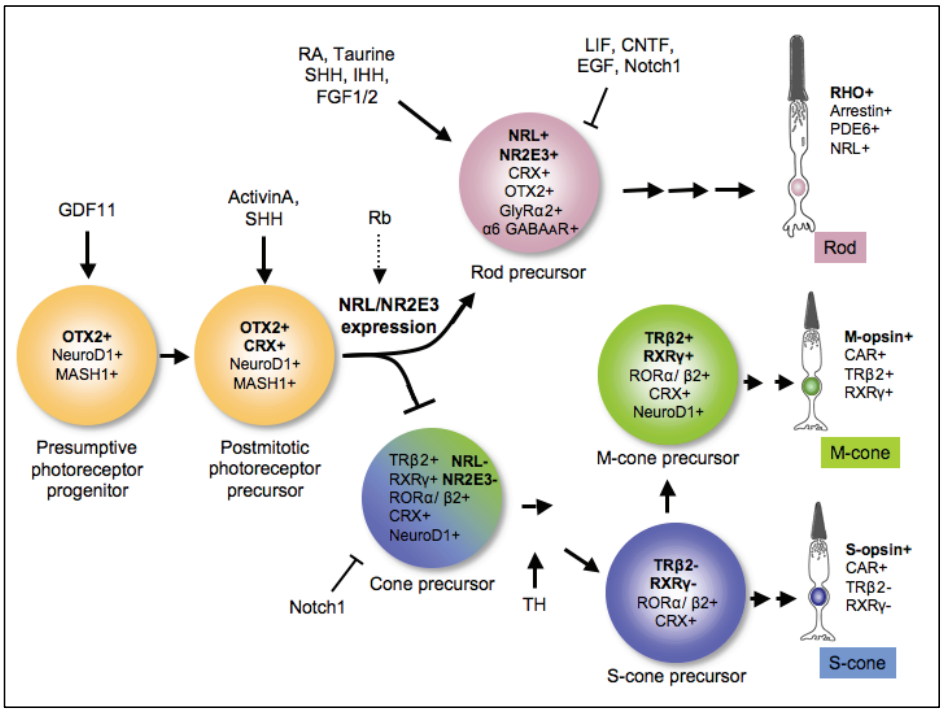


Figure 3. Model of photoreceptor development in the murine retina. Rods, S and M cones are generated from a common pool of retinal progenitor cells (RPCs), which exit the cell cycle at specific times during retinogenesis. A synergistic interaction between intrinsic and extrinsic factors progressively restricts cell fate, biasing individual cells towards differentiation into a unique mature cell type. Some of the known molecules involved are illustrated here. Proteins that appear to be major contributors to specification/determination of cell fate are shown in bold. Expression of Otx2 and Crx defines the postmitotic pool of cells fated to become photoreceptors (photoreceptor precursors). Expression of Nrl and its target Nr2e3 determines rod photoreceptor cell fate. Photoreceptor precursors that do not express Nrl/Nr2e3 progress towards the cone lineage. Upon downregulation of TRβ2 and RXRγ, cone precursors become S cone precursors and synthesize S-opsin. For M cone precursors to develop, S-opsin expression must then be repressed by the heterodimer TRβ2/RXRγ, and M-opsin synthesis initiated by another TRβ2-containing complex. Arrows indicate active promotion and truncated lines inhibition of a developmental stage. Dotted lines indicate tentative roles. Adapted from: I.O. Nasonkin et al. Photoreceptor development: Early steps/fate, in Encyclopedia of the Eye. Volume 3, pp. 332-339, 2010.

prior to exiting the cell cycle, RPCs fated to become photoreceptors upregulate the expression of paired-class homeodomain transcription factor orthodenticle protein homolog 2 (OTX2) (Nishida et al, 2003). OTX2 plays an important role as an early factor that specifies photoreceptor cell fate, and probably as a late factor that may promote terminal differentiation by participating in upregulation of photoreceptor-specific genes

(Koike et al, 2007). At the molecular level, OTX2 activates the promoter of cone–rod homeobox (*Crx*) transcription factor gene, encoding a closely related homeodomain transcription factor (Omori et al, 2011). OTX2 and CRX cooperate to complete photoreceptor differentiation programs (reviewed in Swaroop et al, 2010).

Postmitotic precursor cells become committed toward rod or cone fates once photoreceptor fate is specified (Figure 3). The Maf family basic motif-leucine zipper transcription factor NRL and its target, the photoreceptor-specific orphan nuclear receptor NR2E3, are the primary determinants of rod versus cone cell-fate (Cheng et al, 2006; Cheng et al, 2004; Mears et al, 2001). S cone cell fate is specified as a default pathway and inhibition of this pathway by NRL/NR2E3 is permissive to rod specification (Jia et al, 2009; Ng et al, 2011; Oh et al, 2008; Swaroop et al, 2010). Following this, NRL and NR2E3 – together with CRX – lead to the expression pattern typical of mature rod photoreceptors (Figure 3).

Cone precursors must go through an additional specification process that determines distinct cone sub-types (Figure 3). In mouse and human cone precursors, S-opsin expression is detected first, followed by M-opsin expression. In mice, onset of cone opsin expression is regulated by numerous factors; these include CRX, members of the nuclear receptor family, thyroid hormone nuclear receptor beta 2 isoform (TRβ2) and retinoid X nuclear receptor gamma (RXRγ), and of the retinoic acid (RA) receptor-related orphan receptor – RORα and RORβ2 (Ng et al, 2011).

Several extrinsic factors contribute to rod development (Figure 3). As mentioned, cell–cell interaction mediated by Notch1 is known to sustain the undifferentiated and proliferating state of RPCs, repressing neuronal fate in general (Hatakeyama et al, 2004; Henrique et al, 1997). Recently, Notch1 signaling has been shown to specifically inhibit photoreceptor fate. This function of Notch1 may allow differentiation of other neuronal cell types (Jadhav et al, 2006; Yaron et al, 2006). Other extrinsic factors inhibiting rod fate are leukemia inhibitory factor (LIF), ciliary neurotrophic factor (CNTF), and EGF (Ahmad et al, 1998; Ezzeddine et al, 1997; Graham et al, 2005). Furthermore, taurine,

secreted by RGCs, is suggested to stimulate rod photoreceptor production through glycine (Gly) and gamma aminobutyric acid (GABA(A)) receptors (Young & Cepko, 2004). Proper maturation and/or migration and integration of young rods into the ONL may require gradients of Indian Hedgehog (IHH) secreted by the RPE, and SHH secreted by RGCs. IHH may also have a role in the specification of photoreceptor fate, possibly inducing *Nrl* gene expression in photoreceptor precursors (Dakubo et al, 2008; Levine et al, 1997). Similarly, FGF family members – acidic FGF (FGF1) and basic FGF (FGF2) – are implicated in rod maturation and may induce *Nrl* expression (Bugra et al, 1994). The role of RA in promoting rod photoreceptor differentiation is still unclear, though it can induce *Nrl* expression through RA-responsive sites present in *Nrl* promoter (Khanna et al, 2006).

Maturation of committed precursors to differentiated functional photoreceptors is a lengthy process and involves expression of cell-type-specific phototransduction genes, biogenesis of OS, and formation of synapses with specific interneurons. Expression of most photoreceptor-enriched genes depends on the synergistic or antagonistic actions of NRL, NR2E3, and CRX and their interaction with other regulatory proteins. In most instances, these proteins co-occupy the promoter/enhancer regions of their target genes (Swaroop et al, 2010).

Retinal dystrophies, photoreceptor degeneration and therapeutic approaches

In 2004, the World Health Organization (WHO) estimated that 4.7% of the world population (> 500 million individuals) was visually impaired, of which, 0.7% (> 45 million) were blind (Resnikoff et al, 2008). In developing countries, the most common causes of blindness are cataract and uncorrected refractive error. However, in developed countries, progressive dysfunction and loss of retinal photoreceptors is the predominant cause of visual impairment and blindness, with age-related macular degeneration (AMD) accounting for > 50% of blindness cases.

Retinal dystrophy is a generic term that refers to pathological conditions associated with retinal photoreceptor dysfunction and loss, and includes retinitis pigmentosa (RP), AMD, Usher syndrome, Leber congenital amaurosis (LCA) and diabetic retinopathy (DR), that are for the most part incurable diseases (Wright et al, 2010). Despite the unifying feature of photoreceptor degeneration, the clinical characteristics, etiology, genetics, molecular, and cellular mechanism underlying retinal dystrophies are very diverse. Primary rod deficiencies leading to loss in early-mid life, followed by loss of cones (rod-cone dystrophies) are most common in RP (Sahel et al, 2010). However, cones also can be the primary (cone-rod dystrophy) or sole (cone dystrophy) dysfunctional cell type. Macular degeneration is distinguished from RP because degeneration is localized to the macula and it involves rod, cones, and the RPE (Swaroop et al, 2009). In particular, in AMD, progressive accumulation of deposits between the RPE and Bruch's membrane (Figure 2), render the former progressively dysfunctional with consequent effects on photoreceptor function and, ultimately, survival. Finally, in DR, photoreceptor loss has been considered for a long time secondary to defects of the retinal microcirculation caused by uncontrolled elevated glucose levels in the blood. However, more recently, the existence of primary photoreceptor deficiencies has become evident (Antonetti et al, 2006; Barber et al, 1998).

Photoreceptor death is comparable to that of any other neuron. Thus, approaches for photoreceptor regeneration share similarities to those applied to other areas of the nervous system. Like the rest of the nervous system, the mammalian retina lacks the capacity to regenerate following damage and there are at present no regenerative therapies available for degenerative retinal diseases (Comer et al, 2005; Hogg et al, 2007; Rattner & Nathans, 2006).

Current and tested treatments, aimed at slowing the degeneration process and improving photoreceptor function in RP, include laser photocoagulation (LPC), photodynamic therapy (PDT) with verteporfin (Visudyne®), transpupillary thermotherapy (TTT), and specialized surgery (Sahni et al, 2011). In DR, the standard of care is focal laser photocoagulation (FLP). Novel approaches include therapies aimed at

limiting disease progression with inhibitors of advanced glycosylation end-products (AGEs) and antioxidants (Comer & Ciulla, 2005), anti-vascular endothelial growth factor (VEGF) antibody therapies (Brown et al, 2011; Campochiaro et al, 2011a), and corticosteroid medications (Campochiaro et al, 2011b; Pearson et al, 2011) for diabetic macular edema (DME) and proliferative DR, alone or in combination (Witkin & Brown, 2011).

In AMD, the recent introduction of anti-VEGF antibody therapies has been successful in improving vision in 40% of patients treated and in stabilizing the condition of the remaining 60% (Martin et al, 2011 and E. Chu, personal communication). This therapy is classified as anti-angiogenic and targets choroidal outgrowth (abnormal angiogenesis of the choroidal circulation supplying the RPE on the basal side), which is a hallmark of late stage AMD. However, anti-VEGF treatments modify the permeability properties of the choroidal vasculature and possibly slow growth, but do not drive retraction of the newly formed vessels. In some trials, anti-platelet-derived growth factor (PDGF) antibodies have been injected together with anti-VEGF antibodies in the hope to facilitate regression of neovascularization (Mabry et al, 2010).

One successful approach is the recent gene therapy applied for LCA, a very early onset subtype of RP associated with mutations in the RPE-specific gene *RPE65*. *RPE65* mutations ultimately cause retinal degeneration by interfering with the availability of 11-cis-retinal for the phototransduction pathway (Redmond et al, 1998). Young patients treated with an AAV-based vector expressing the wild type form of RPE65 protein, permanently recovered a substantial part of their visual function (Bainbridge et al, 2008; Jacobson et al, 2011; Maguire et al, 2008; Simonelli et al, 2010). An alternative approach to gene therapy is replacement of 11-cis-retinal with a synthetic retinoid. A clinical trial (ClinicalTrials.Gov, Safety/Proof of Concept Study of Oral QLT091001 in Subjects With LCA or RP Due to RPE65 or LRAT Mutations

http://clinicaltrials.gov/ct2/show/NCT01014052?term=koenekoop+mcgill&rank=1; http://www.qltinc.com/development/products/QLT091001.htm) is currently recruiting patients in Canada (in US, Holland, Germany and the UK in the future) to evaluate the

efficacy and safety of oral administration of the drug QLT091001 in LCA and RP due to mutations in RPE65 and lecithin-retinyl acyltransferase (LRAT).

Despite current and potentially future successes, pharmacological and gene therapy approaches require a substrate of surviving photoreceptors to act upon. At mid and late stages of disease, the numbers of functional neurons might not be sufficient for rescuing visual function, making cell replacement a more promising therapeutic option.

Regeneration and cell replacement in the adult retina of lower vertebrates

In the last twenty years, our understanding of the nervous system and its adult regenerative capacity as well as insight into cell plasticity have set the ground for studies into neurogenesis in the retina and the possibility of cell replacement therapies. Adult neurogenesis is a known phenomenon in a restricted group of vertebrates. Unlike mammals, whose adult regenerative capacity is limited, some lower vertebrates including urodele amphibians (e.g., salamanders and newts) and teleost fish (e.g., zebrafish, goldfish and rainbow trout) show remarkable ability throughout their lifespan to generate and repair damaged tissues and organs, including the retina.

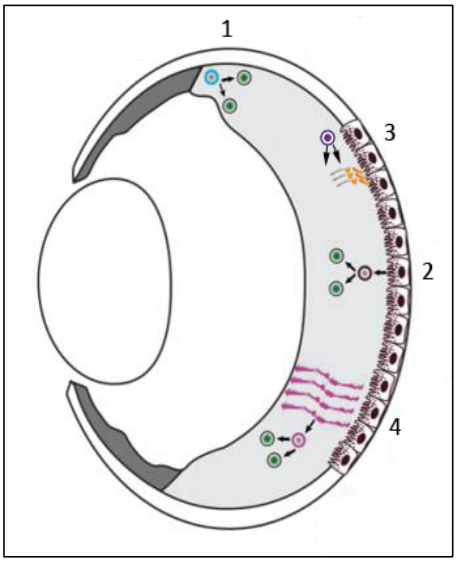


Figure 4. Stem cell niches in adult lower vertebrates. In salamanders and fish, new retinal cells are constantly added from a pool of specialized progenitor cells localized in the circumferential germinal zone/ciliary marginal zone (CGZ/CMZ) to sustain growth of the eye (1). Upon injury, salamander retinal pigment epithelial (RPE) cells de-differentiate, re-enter the cell cycle and replace lost cells by differentiating again into all retinal cell types (2). In fish, a sparse population of rod precursors (probably derived from Müller glia) proliferates at a very slow rate to add new rod photoreceptors in the healthy and damaged retina (3). Furthermore, upon injury, a subpopulation of Müller glia cells start proliferating and can differentiate to generate all types of lost retinal cells (4). Neurogenesis has also been observed from cells in the CGZ/CMZ in the post-hatched chick and from Müller glia in chicks and rodents. Adapted from: M.O. Karl & T.A. Reh, Trends in Molecular Medicine, 2010.

There are four mechanisms described for neurogenesis in the adult lower vertebrate neural retina (Figure 4): (1) differentiation of cells from the circumferential germinal zone, also known as ciliary marginal zone (CZG/CMZ), (2) transdifferentiation of the RPE, (3) migration and differentiation of rod precursors, and (4) proliferation followed by differentiation of Müller glia.

Differentiation of cells from the Circumferential Germinal Zone/Ciliary Marginal Zone

In association with continuous body growth, fish and amphibian eyes continue to enlarge throughout their entire lifetime under control of the growth hormone (GH)-insulin-like growth factor-I (IGF-I) axis (Boucher & Hitchcock, 1998; Otteson et al, 2002; Zygar et al, 2005). New retinal cells, including photoreceptors, are constantly added to the intact adult retina from at least two sources of cells (niches) and with different mechanisms (reviewed in Fleisch et al, 2011; Stenkamp, 2007): 1) cells from the CMZ/CGZ (Figure 4-1) serve as neurogenic pools from which all retinal cell types are generated (Wetts et al, 1989; Fausett & Goldman, 2006); 2) subsets of Müller glia (see below) give rise to rod photoreceptors and can respond to cell damage (Figure 4-4). CMZ/CGZ-derived newly differentiated retinal cells are constantly added to the most peripheral edge of the retina at a rate that parallels whole body growth. Neurogenic cells residing in the CMZ/CGZ have the appearance of neuroepithelial cells: they are polarized with elongated shapes, spanning the basal-apical axis, and are arranged in a single cell layer (Stenkamp, 2007). They were originally considered remnants of the embryonic retinal neuroepithelium (Johns, 1977). However, CMZ/CGZ adult neurogenesis appears to be regulated by distinct genetic pathways from those regulating developmental neurogenesis (Wehman et al, 2005), thus arguing for a distinct ontogenesis of this cell pool. CMZ/CGZ cells incorporate the S-phase marker bromodeoxyuridine (BrdU), express cell cycle markers, including proliferating cell nuclear antigen (PCNA), and key transcription factors that regulate retinal neurogenesis, such as retinal homeobox 1 (RX1), visual system homeobox 2 (VSX2/CHX10) and paired box gene 6a (*PAX6a*) (Raymond et al, 2006).

A zone of proliferating cells at the peripheral margin of the post-hatched chicken retina has also been identified, displaying features similar to those of the CMZ/CGZ of lower vertebrates and persisting up to three weeks post hatching (Fischer & Reh, 2000). Based on marker expression, these cells appear to share characteristics of embryonic multipotent progenitors. The size of a hypothetical marginal zone appears to be progressively restricted from lower to higher vertebrates, with opossums displaying only a few cells and no marginal zone visible in the mouse (Kubota et al, 2002; Moshiri & Reh, 2004). However, the human peripheral retina has been suggested to resemble the CMZ/CGZ, based on the absence of lamination and the presence of cells expressing stem cell markers, which have been shown to be Müller glia (Bhatia et al, 2009).

Transdifferentiation of the Retinal Pigment Epithelium

In adult amphibians, upon damage or removal, retinal cells and a new retina are generated predominantly from transdifferentiation of the RPE (Figure 4-2) (Keefe, 1973; Stone, 1949; Stone, 1950; Stone & Steinitz, 1957). RPE cells first de-differentiate, i.e., lose their pigmentation and detach from the basement membrane, then, proliferate and differentiate to produce a new pigmented and a non-pigmented layer (Klein et al, 1990; Mitashov, 1996; Reh, 1987; Stroeva & Mitashov, 1983; and reviewed in Del Rio-Tsonis & Tsonis, 2003; Moshiri et al, 2004). The non-pigmented layer initiates expression of retinal progenitor markers and follows a differentiation path that recapitulates developmental retinogenesis (Bugra et al, 1992; Cheon et al, 1998; Cheon et al, 2001; Cheon & Saito, 1999; Mitashov et al, 1995; Negishi et al, 1992; Sakakibara et al, 2002) and appears to be regulated by fibroblast growth factors (FGFs), bone morphogenic proteins (BMPs), and hedgehogs signaling, via MapK and Mitf transcription factors (Sakaguchi et al, 1997). Similar mechanisms underlie repair in the embryonic retina of amphibians (Mitashov, 1997) and chickens (Park & Hollenberg, 1989; Park & Hollenberg, 1991; Pittack et al, 1997). In the latter, however, the polarity of the newly formed retina is reversed. Rodent embryonic RPE cells under restricted conditions can regenerate

neural retina *in vitro* (Neill & Barnstable, 1990; Zhao et al, 1995), though the transdifferentiation potential of rodent RPE cells is limited.

Migration and differentiation of rod precursors, and proliferation followed by differentiation of Müller glia

The intact adult zebrafish INL maintains proliferating rod progenitors that migrate to the ONL (Figure 4-3), where they assume characteristics of rod precursors, and eventually differentiate to rod photoreceptors to accompany eye size expansion (Johns, 1982; Mack & Fernald, 1997). Recent data using transgenic reporter gene expression and morpholino knockdown suggest that INL proliferating rod progenitors originate from a subpopulation of Müller glia (Bernardos et al, 2007; Braisted et al, 1994; Fausett & Goldman, 2006; Raymond et al, 2006; Thummel et al, 2008b). In the intact retina, the neurogenic role of Müller glia is minimal, as indicated by the slow proliferation rate of the INL progenitors (Bernardos et al, 2007; Julian et al, 1998; Otteson et al, 2001). Yet, proliferation rate is higher toward the retinal periphery, in proximity of the CMZ/CGZ (Johns, 1982; Julian et al, 1998).

In the damaged zebrafish retina, sparse photoreceptor loss is compensated for by proliferation and terminal differentiation of the photoreceptor precursor population (Figure 4-3). However, when acute and massive retinal degeneration occurs, a subpopulation of Müller glia (Figure 4-4) re-enter the cell cycle, proliferate, and ultimately, undergo asymmetric division to generate new retinal progenitors (Bernardos et al, 2007; Montgomery et al, 2010). This process involves downregulation of the post-mitotic cell specific genes glial fibrillary acidic protein (*GFAP*) and glutamine synthetase (*GS*) and upregulation of Notch-Delta signaling pathway genes, together with brain lipid binding protein (BLBP) (Thummel et al, 2008a). At the same time, N-cadherin (Cdh2) is upregulated and relocates to the basolateral plasma membrane. De-differentiated Müller glia proliferate to form small neurogenic clusters and differentiate into all retinal

cell types to restore the integrity of all layers (Raymond et al, 2006), after which, Müller glia cells return to quiescence.

A similar response is elicited in the retina of post-hatch chicks (Fischer & Reh, 2001). However, Müller glia cell proliferation and neurogenesis are limited in chicken compared to fish (Fischer & Reh, 2002) and although markers of differentiation can be detected, there is not evidence yet of functional integration of differentiated retinal cells in the damaged retina.

Müller glia- and Ciliary Epithelium-derived cells in mammals

Generation of all retinal cell types in mammals occurs during embryonic development and extends to early postnatal development in some species. After that, no further substantial neurogenesis or gliogenesis occur in the intact or injured retina. As mentioned, in the developing mammalian retina, all cell types originate from a common RPC that undergoes transitory competence states to generate, at stereotyped times and locations, retinal neuronal and glial phenotypes (Cepko et al, 1996; Livesey & Cepko, 2001; Turner & Cepko, 1987). RPCs are no longer present in the fully laminated, functional retina upon completion of development.

Greater understanding of adult neurogenesis in lower vertebrate eyes has encouraged investigations into the existence of potentially similar, yet dormant, cell types and mechanisms in mammals. The focus in recent years has been on Müller glia- and ciliary epithelium (CE)-derived cells.

Müller glia and retinal repair in mammals

Müller glia cells generally respond to degeneration and injury in mammals by initiating a reactive response resulting in upregulation of filamentous proteins such as GFAP and vimentin, a phenomenon known as reactive gliosis (Grosche et al, 1995; Lewis & Fisher, 2003; Sarthy & Egal, 1995). Similar responses can be elicited by treatment with growth factors such as FGF2 (Lewis et al, 1992) and interleukin 6 (IL-6) family members

such as CNTF and LIF (Wahlin et al, 2000; Xue et al, 2011). Insights into adult neurogenesis in the brain, showing that neural stem cells have characteristics similar to developmental radial glia (Ming & Song, 2011), and into regenerative processes in zebrafish (Bernardos et al, 2007) and in non-mammalian vertebrates such as the chicken (Fischer & Reh, 2001; Karl et al, 2008) suggest the hypothesis that Müller glia cells are the stem cell of origin in the adult mammalian retina (Ming & Song, 2011). The similarity of Müller glia gene expression profiles with those of retinal progenitors (Blackshaw et al, 2004) and neural stem cells (Das et al, 2006a) further support that hypothesis.

In the adult rat, N-Methyl-D-aspartic acid (NMDA) neurotoxic damage elicits proliferation of a small subpopulation of Müller glia that subsequently differentiate to express mature retinal cell markers, predominantly Rho (rod) and recoverin (photoreceptor and bipolar cell) (Ooto et al, 2004; Wan et al, 2008). The proportion of Müller glia re-entering the cell cycle and differentiating to mature retinal phenotypes can be increased by stimulation with growth factors, EGF, FGF, glial cell-derived neurotrophic factor (GDNF), and insulin, or of the SHH/Wnt/β-catenin pathway (Close et al, 2006; Insua et al, 2008; Osakada et al, 2007; Wan et al, 2007). Stimulation of Notch and Wnt signaling, in fact, may be sufficient to promote Müller glia transdifferentiation to photoreceptors even in the absence of retinal damage (Del Debbio et al, 2010). Furthermore, the retinal cell phenotypes generated and their proportions can be manipulated in rat either by RA treatment, to increase bipolar cells, or by overexpression of specific transcription factors genes such as *Math3*, *NeuroD1*, *Pax6* and *Crx* (Ooto et al, 2004) to generate virtually all cell types in the retina. In mouse, injection of either EGF, FGF1, or FGF1 and insulin biases differentiation toward amacrine cells (Karl et al, 2008). Notably, light damage induces upregulation of EGF receptor (EGFR) in rat Müller glia cells, restoring the mitogenic response to EGF stimulation observed during development (Close et al, 2006). De-differentiation to retinal progenitor and differentiation to retinal cell phenotypes can also be induced in mouse Müller glia by administration of sub-toxic doses of glutamate or its analogue alpha-aminoadipate (α-AA), suggesting not only that injury-induced Müller glia

proliferation/differentiation might be mediated by glutamate but also offering a potential pharmacological approach to retinal repair (Takeda et al, 2008). Finally, Müller glia cells proliferate and migrate towards the site of injury following laser photocoagulation damage in mouse, although they do not seem to undergo transdifferentiation (Tackenberg et al, 2009).

Cells with Müller glia characteristics that proliferate in response to EFG treatment and co-express markers of differentiated glia such as GFAP, cellular retinaldehyde-binding protein (CRALBP) and vimentin, and of neural progenitors such as Nestin, CHX10, SOX2, and Notch1, were recently identified at the non-laminated margin of the intact human retina, re-proposing the existence in mammals of an area comparable to the CMZ/CGZ in fish and amphibians (Bhatia et al, 2009). Nonetheless, the degree of cell proliferation and differentiation remains limited in mammals compared to lower vertebrates. It has been suggested that adult Müller glia quiescence is maintained by at least two molecular mechanisms: transforming growth factor (TGF)β2 release from retinal neurons and downregulation of EGFR in mature Müller glia (Close et al, 2005).

Spontaneously immortalized human Müller glia cells were first cultured *in vitro* (Limb et al, 2002). Subsequently, several cultures of human Müller glia cells (MIO cell lines) have been derived from the neural retina of postmortem healthy donors spanning a wide range of ages from infancy through aging (Lawrence et al, 2007). Besides displaying features of mature Müller glia such as CRALBP, glutamine synthetase, and vimentin expression, and depolarization in response to glutamate without change in membrane resistance, MIO cells express EGFR and retinal (e.g., CHX10) and neural (e.g., SOX2) progenitor markers to different degrees, depending on culture conditions (Lawrence et al, 2007). Upon exposure to differentiating conditions *in vitro*, Müller glia cell lines can be induced to express markers of differentiated retinal neurons, including recoverin, S-opsin, peripherin, calretinin, and Brn3. Similarly, when grafted in the subretinal space of retinal degeneration rat models, MIO cells migrate and acquire markers of mature retinal cells (Lawrence et al, 2007).

In summary, Müller glia spontaneously respond to retinal damage and can be manipulated *in situ* to display retinal phenotypes. Cultures, transplantation and differentiation of human Müller glia cell lines suggest that Müller glia could be a viable source of cells for retinal replacement.

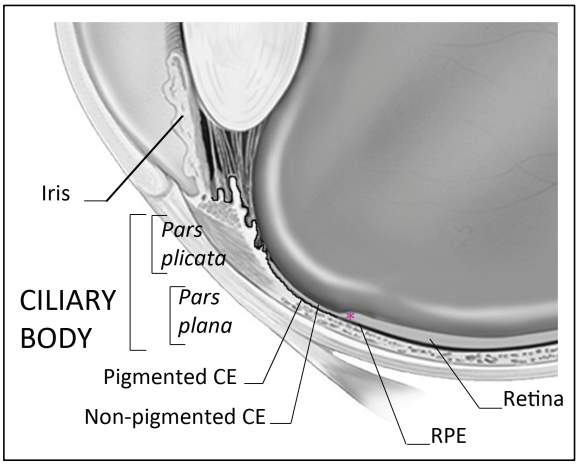


Figure 5. Ciliary body anatomy. The ciliary body is located between the peripheral margin of the retina and the iris. The neural retina extension of the ciliary body comprises two layers of epithelium that share with the retina their neuroectodermal origin, the pigmented and non pigmented ciliary epithelia (CE). Their architecture is flattened on the retinal side (*pars plana*) and folded on the iris side (*pars plicata*). The asterisk labels the peripheral retina, a non-layered portion of the retina in rodents that has been suggested to correspond to the CMZ in lower vertebrates. Designed by: Lydia Kibiuk, NIH Division of Medical Arts.

Retinal Stem Cells from Ciliary Epithelium of mammals

Retinal stem cells (RSCs) from the CE (Figure 5) were first isolated from mouse (Tropepe et al, 2000) and rat (Ahmad et al, 2000). Subsequently, reports were published on the isolation from human (Coles et al, 2004), rabbit (Inoue et al, 2005), and pig (MacNeil et al, 2007). RSCs express retinal progenitor transcription factors such as CHX10, PAX6, SIX6, SIX3, and RX (Ahmad et al, 2004; Lord-Grignon et al, 2006; Xu et al, 2007b; Yanagi et al, 2006) and share approximately 80% of their expressed genes with developmental RPCs (Das et al, 2005), including FGF, Notch, and SHH signaling pathway genes (Ahmad et al, 2004; Moshiri & Reh, 2004). Despite the definition as "stem cells", all reports concur that RSC have a limited capacity for *in vitro* self-renewal (Engelhardt et al, 2004; Inoue et al, 2005; MacNeil et al, 2007; Xu et al, 2007a). Neurosphere cultures of RSCs can be maintained *in vitro* for a relatively small number of passages (8-

10) and undergo senescence within two months from isolation (Inoue et al, 2005). Gene expression profiling of rat RSCs indicates that initial expression of the self-renewal genes *Notch1*, *Delta1*, *Hes*1 and *Hes*5 is downregulated upon passaging and that only a limited number of RPC markers continue to be expressed (James et al, 2004).

In vitro cell population expansion and number of passages can be increased by treatment with growth factors, e.g., EGF and FGF (Ahmad et al, 2000; Coles et al, 2004; Inoue et al, 2005; Mayer et al, 2005; Tropepe et al, 2000), pigment epithelium derived factor (PEDF) (De Marzo et al, 2010), as well as by activation of mitogenic pathways, such as the canonical Wnt pathway (Das et al, 2006b; Inoue et al, 2006). Since, RSCs do not self-renew indefinitely, they fail to meet the requirement to be considered *bona fide* stem cells. Notably, the origin, phenotype and "stemness" of RSCs have recently been challenged (Cicero et al, 2009; Gualdoni et al, 2010). The terms of the controversy will be illustrated in the discussion. For convenience, CE-derived neurosphere cultured cells will still be referred to as RSCs hereafter, mostly to distinguish them from RPCs present in the developing retina.

RSCs cultured *in vitro* can be induced to express genes characteristic of differentiated retinal neurons and glia (Ahmad et al, 2000; Coles et al, 2004; Inoue et al, 2005; Mayer et al, 2005; Tropepe et al, 2000). Temporally controlled activation of the canonical Wnt pathway affects the neurogenic potential of RSCs *in vitro* such that pre-induction activation promotes neurogenesis but activation of the Wnt pathway during induction represses neurogenesis (Das et al, 2006b). Similarly, inclusion of EGF and FGF during the RSC expansion period induces changes in growth factor receptor expression that result in biases in their differentiation potential (Giordano et al, 2007). Furthermore, EGF in the differentiation medium promotes neurogenesis and the appearance of bipolar cell phenotypes, whereas FGF biases differentiation towards cells expressing photoreceptor markers (Giordano et al, 2007). Notably, both mouse and human RSCs infected with a viral vector exogenously expressing the cone-rod transcription factor CRX, upregulate the photoreceptor-specific genes β-6 phosphodiesterase (*β-6PDE*), Rho, and blue opsin (*CNG3*), and hydrolyze cGMP upon

light stimulation, strongly suggestive of their acquired sensitivity to light stimulation (Jomary & Jones, 2008; Jomary et al, 2010).

However, in the absence of RPE *in vitro*, photoreceptor maturation cannot be completed and no OS are observed which would be the hallmark of fully mature functional photoreceptors. To overcome this limitation and also to test their potential for cell replacement in the retina, RSCs have been injected *in vivo*, either in the subretinal space or the vitreous. In general, RSCs survive in allogeneic and xenogeneic hosts after transplantation, showing variable degrees of integration into the intact and degenerating retina, and differentiate into cells expressing markers characteristic of retinal cells that display rudimentary morphological features of neurons (Coles et al, 2004; Kinouchi et al, 2003; Warfvinge et al, 2005). Although the number of integrated cells remains limited, recent data show more efficient generation of functional photoreceptors from human RSCs *in vitro* and *in vivo* after gene transfer and modulation of transcription factors *OTX2*, *CRX*, and *CHX10* (Inoue et al, 2010; Jomary et al, 2010). Furthermore, visual function improved upon transplantation of the transfected cells into the vitreous cavity of transducin mutant mice, a model in which photoreceptors do not degenerate but are not functional.

The evidences above support the hypothesis that cells in neurosphere cultures derived from the CE have partial stem/progenitor cell characteristics. Whether these characteristics are intrinsic or acquired in culture remains to be established. In wild type mice, rare nestin-positive cells can be detected in the non-pigmented layer of the CE up to P18 (Nishiguchi et al, 2008). Furthermore, cells in the P7-21 mouse CE proliferate in response to bFGF and insulin administration *in vivo* and express the retinal progenitor markers PAX6 and CHX10 (Abdouh & Bernier, 2006; Zhao et al, 2005).

Data obtained from *in vivo* studies of retinas undergoing pathological or injury-induced degeneration are more convincing. Proliferating cells labeled with BrdU are found up to P30 in the most peripheral retina of the *rd1* genetic mouse model of retinal degeneration (Nishiguchi et al, 2007). Furthermore, single intravitreal injection of VEGF at P9 dramatically increases the number of BrdU-positive cells in the peripheral retina

and CE. Cells expressing the photoreceptor and bipolar cell marker recoverin can be detected in the *pars plana* of the adult *rd1* mouse up to four months of age, at a time in which the ONL is absent and retinal function is completely lost in untreated animals (Nishiguchi et al, 2009). The majority of these cells appear to be of the cone lineage as shown by peanut agglutinin (PNA) double-staining, with only a small proportion belonging to the rod lineage (Rho double-positive). Some of them appear to have matured to develop cone pedicles (Nishiguchi et al, 2008; Nishiguchi et al, 2009). Nonetheless, VEGF administration does not prevent the normal course of retinal degeneration in *rd1* mice, and photoreceptors are lost by one month of age (Nishiguchi et al, 2007). Similar results can be obtained by induction of photoreceptor degeneration with N-methyl N-nitrosourea (NMU) (Nishiguchi et al, 2009), or following RGC degeneration induced by optic nerve axotomy (Nickerson et al, 2007). In another model of retinal degeneration, the Royal College of Surgeon's (RCS) rat, higher numbers of BrdU-labeled cells compared to controls were detected during the degenerating window (P15-P60) in the peripheral retina and CE (Jian et al, 2009). Cell proliferation is associated with upregulation of *Shh* and *Smo* expression and an increasing number of cells labeled with the retinal progenitor cell marker CHX10 are found in the same timeframe. However, by P90, when degeneration is terminal, both BrdU- and CHX10-labeled cells decrease to levels comparable to controls. In addition, these cells do not seem to have neurogenic potential as none of the BrdU-positive cells could be double-stained with retinal cell markers.

A recent histological/immunohistological study of three adult human pathological post-mortem eyes (from patients who underwent multiple surgeries for retinal detachment and vitreoretinopathy) reports proliferation in the CE, overexpression of EGFR, apparent migration of neurosphere structures into the adjacent vitreous, and expression of early and late photoreceptor markers, potentially indicating reactive neurogenesis in the adult human CE (DuCournau Y 2011). All together these data suggest that a subpopulation of cells in the adult mammalian CE maintains the capacity to respond to cues generated by injury or death of retinal neurons.

Final Remarks

This thesis focuses on CE-derived cells and their applications for transplantation. Cultures derived from mammalian Müller glia and CE constitute a potential source for cell therapies in retinal degenerative diseases. However, both Müller glia and CE-derived cultures require further investigations to validate their potential: a) transplantable cells need be a homogeneous, well characterized population; b) cell numbers should be expandable in the order of millions; c) differentiation should be controlled to generate the desired cell type(s); and d) efficiency of transplantation should be improved. Both cell populations have the advantage over other pluripotent cell sources, such as embryonic stem cells (ESC) and induced pluripotent stem cells (iPSC), to possess phenotypic characteristics and to be developmentally closer to the differentiated retinal cells they are to replace. Although Müller glia cells are more easily expandable, they would be derived from heterologous sources. On the other hand, CE-derived cells could allow autologous transplantations after being obtained from the patient upon a relatively simple vitrectomy procedure. Considerations have also been given to harnessing the regenerative potential of these cells *in vivo* for replacing lost photoreceptors. This approach might be feasible at the very early stages of degeneration, when the numbers of photoreceptors to replace are small and comparable to the number of Müller glia and CE cells in the eye and provided that further degeneration is also prevented. At later stages of degeneration, it is unlikely that larger numbers of progenitor cells be generated by proliferation of Müller glia or CE without increasing the risk of tumor formation, making this approach non-viable at the present status of the research.

Hypothesis

We hypothesize that cells derived from the CE of the porcine eye could be propagated in culture and differentiated to photoreceptors *in vitro* and upon transplantation in the subretinal space of allorecipient pigs.

Aims

- To study the chronological development of the pig retina as a model for retinal differentiation in human.
- To isolate and characterize cell cultures derived from the porcine CE.
- To graft porcine CE-derived cells in the normal porcine retina and evaluate their integration and differentiation potential.

Animal Model

The pig is an attractive non-primate animal model to study retinal biology for several reasons:

- The porcine eye is comparable to the human eye in size and shape;

- Fundus imaging reveals a radial (holangiotic) vasculature and an oval-shaped optic nerve head (Middleton, 2010);

- The thickness and appearance of porcine retinal layers are comparable to human (Johansson et al, 2010);

- The photoreceptor mosaic in pig and human shares a high degree of similarity (Chandler et al, 1999; Curcio et al, 1990). Although the average retinal rod:cone ratio in human is 20:1, compared to 8:1 in pig, cone density in pig is increased in a broad region dorsal to the optic disk, extending both nasally and temporally (*area centralis*), where

the rod:cone ratio decreases to 6:1 and is comparable to the average human macular rod:cone ratio of 10 (Chandler et al, 1999; Hendrickson & Hicks, 2002; Sanchez et al, 2011);

- Both human and pig retina are well developed at birth (Chandler et al, 1999; De Schaepdrijver et al, 1990; Hendrickson et al, 2008), although the gestation period for pig (112–115 days) is significantly shorter compared to human;

- Pig models of retinitis pigmentosa, glaucoma, and retinal detachment have been developed (Iandiev et al, 2006; Petters et al, 1997). Transgenic pigs with systemic expression of green (Park et al, 2001) and red fluorescent proteins (Matsunari et al, 2008) have also been produced;

- The pig eye has been useful for modeling human ocular surgery due to its size, anatomy, and vasculature (Del Priore et al, 1996; Ghosh et al, 2004).

- Pigs have been used for isolation of RPCs, and subretinal allotransplantation of these cells demonstrates their ability to migrate, morphologically differentiate, and express retinal cell markers (Klassen et al, 2007; Klassen et al, 2008).

Using the pig as an animal model was advantageous to us in that the protocols we were planning to develop for isolating CE-derived cells from the porcine eye could easily be applied to human donor tissue. Furthermore, a larger size of CE yields a higher number of cells to work with *in vitro*. Finally, we could more accurately target transplanted cells to selected sites in the subretinal space and test immune response in large animals, besides performing surgical procedures to test conditions for cell transplantation in humans.

CHAPTER 2

IMMUNOHISTOCHEMICAL STUDY OF PIG RETINAL DEVELOPMENT

Reprinted from Molecular Vision **15**, 1915-1928 (2009)

Molecular Vision 2009; 15:1915-1928 <http://www.molvis.org/molvis/v15/a204>
Received 9 April 2009 | Accepted 14 September 2009 | Published 21 September 2009

© 2009 Molecular Vision

Immunohistochemical study of pig retinal development

Jasenka Guduric-Fuchs, Laura J. Ringland, Ping Gu, Margaret Dellett, Desmond B. Archer, Tiziana Cogliati

Centre for Vision and Vascular Sciences, Queen's University Belfast, United Kingdom

Purpose: The pig eye is similar to the human eye in terms of anatomy, vasculature, and photoreceptor distribution, and therefore provides an attractive animal model for research into retinal disease. The purpose of this study was to characterize retinal histology in the developing and mature pig retina using antibodies to well established retinal cell markers commonly used in rodents.

Methods: Eyes were enucleated from fetuses in the 9th week of gestation, 1 week old piglets and 6 months old adult animals. Eyeglobes were fixed and cryosectioned. A panel of antibodies to well established retinal markers was employed for immunohistochemistry. Fluorescently labeled secondary antibodies were used for signal detection, and images were acquired by confocal microscopy. Mouse retina at postnatal day (P) 5 was used as a reference for this study to compare progression of histogenesis. Most of the primary antibodies have previously been used on mouse tissue.

Results: Most of the studied markers were detected in midgestation pig retina, and the majority had a similar distribution in pig as in P5 mouse retina. However, rhodopsin immunolabeling was detected in pig retina at midgestation but not in P5 mouse retina. Contrary to findings in all rodents, horizontal cells were Islet1-positive and cones were calbindin-immunoreactive in pig retina, as has also been shown for the primate retina. Recoverin and rhodopsin immunolabeling revealed an increase in the length of photoreceptor segments in 6 months, compared to 1 week old animals.

Conclusions: Comparison with the published data on human retina revealed similar marker distribution and histogenesis progression in the pig and human retina, supporting the pig as a valuable animal model for studies on retinal disease and repair. Furthermore, this study provides information about the dynamics of retinal histogenesis in the pig and validates a panel of antibodies that reliably detects developing and mature retinal cell phenotypes in the pig retina.

Retinal cellular inventory and development are generally conserved across many studied vertebrate species. However, a range of histological and functional differences exist between individual species. Among nonprimate mammals, the pig eye most closely resembles the human eye, with similar size and comparable histological and physiologic features. Although the gestation period for pig (112–115 days) is significantly shorter compared to human, both human and pig retina are well developed at birth [1,2]. The architecture of the pig retina comprises an area centralis enriched in cones that resembles the human macula, making it an attractive model for preclinical testing [1,3]

Pig models for retinitis pigmentosa, glaucoma, and retinal detachment have been developed [4-6]. Transgenic pigs with systemic expression of green [7] and red fluorescent proteins [8] have also been produced. Furthermore, due to its size, anatomy, and vasculature, the pig eye has been useful for modeling human ocular surgery [9-11]. Finally, pigs have been used for isolation of retinal progenitor cells, and subretinal allotransplantation of these cells demonstrates their ability to migrate, morphologically differentiate, and express retinal cell markers [12,13]. Similarly, adult retinal stem cells have been isolated and characterized from pig ciliary and iris epithelia [14,15].

Several reported in vitro studies on pig retinal neuronal survival and physiology have used immunohistochemical tools to identify cell phenotypes in the primary retinal cell culture [16-19]. At present, there are limited data on the distribution of immunohistochemical markers in the adult pig retina [20-22] and only few studies on pig retinal development [23,24]. Better understanding of pig retinal development is important to fully exploit this model's potential for the study of eye diseases. Similarly, appropriate tools to investigate retinal histology in the pig are required to follow stem cell differentiation during development, in vitro, and after transplantation.

The aim of the present study was twofold: 1) to characterize antibodies to retina-specific markers commonly used in rodents as tools for further investigations in the pig; and 2) to conduct an immunohistochemical study of retinal histogenesis in the pig.

METHODS

Animal models: All animal procedures were performed in compliance with the UK Animals (Scientific procedures) Act 1986. Mixed sex white Landrance pigs were obtained from Agri-Food and Biosciences Institute, Northern Ireland (Large Park, Hillsborough, Co. Down, Northern Ireland, UK) where animals were commercially bred on slats and fed with granulated pig food. The pigs were anaesthetised with intra-

Correspondence to: Jasenka Guduric-Fuchs, QUB-Centre for Vision and Vascular Science, RVH-Institute of Clinical Science, Belfast BT12 6BA, Northern Ireland, UK; Phone: +44-28-9063-2729; FAX: +44-28-9063-2699; email: j.guduricfuchs@qub.ac.uk

Dr. Cogliati is now at Neurobiology-Neurodegeneration & Repair Laboratory, National Eye Institute, NIH, Bethesda, MD 20892.

Molecular Vision 2009; 15:1915-1928 <http://www.molvis.org/molvis/v15/a204> © 2009 Molecular Vision

muscular azoperone (15 mg/kg) and ketamine (20 mg/kg) and euthanized with intravenous or intra-cardiac euthanasia-grade pentobarbitone (100 mg/kg).

Eyes were collected from embryos in the ninth gestational week (GW9), 1 week old piglets (1W), and 6 months (6M) old animals. Three pigs from each age group were analyzed.

Postnatal day (P) 5 in the mouse was used as control for antibody functionality and comparison of developmental stage. Wild type C57BL6 mice were bred in 12 h dark/light regime with free access to food and water. P5 mice were euthanized by intraperitoneal injection with pentobarbitone. The eyes from three P5 mice from different litters were analyzed. Comparison with adult mouse retina was performed using the data from published literature which is accordingly cited in the results section.

Preparation of retina for histology and immunohistochemistry: Eyes were enucleated from euthanized pigs, and the cornea and the lens were removed. The eyecups were fixed in 4% paraformaldehyde in PBS (137 mM NaCl, 2.7 mM KCl, 10 mM Na_2HPO_4, 2mM KH_2PO_4 pH 7.4) for 1–4 h at room temperature. After fixation the specimens were cryoprotected in 10% sucrose for 6 h followed by 30% sucrose overnight. The eyecups were embedded in optimal cutting temperature compound (OCT; Sakura, Kobe, Japan) and snap frozen in an isopentane bath on dry ice. Transverse 16 µm cryosections were cut, mounted onto Superfrost Plus glass slides (Fisher Scientific, Loughborough, UK) and stored at −80 °C until use.

Slides were thawed at room temperature and post-fixed in 4% formaldehyde (Sigma-Aldrich, Poole, UK) in PBS for 20 min at room temperature. After rinsing in PBS, sections were blocked for 1 h in 10% normal goat serum, 0.3% Triton X-100, 0.01% NaN_3 in PBS, at room temperature. Slides were rinsed in PBS and incubated for 24 h at 4 °C with primary antibody diluted in 10% normal goat serum, 0.3% Triton X-100, 0.01% NaN_3 in PBS. The source information and the dilutions for all primary antibodies used are listed in the Table 1. Following removal of the primary antibody, slides were washed 6 times for 5 min in PBS and incubated for 1 h at room temperature in 1:500 fluorescent-conjugated secondary antibody (Alexa Fluor^{488} or Alexa Fluor^{568} goat anti-mouse or goat anti-rabbit) in PBS. Slides were then washed 3 times for 5 min in PBS at room temperature and cell nuclei were counterstained with 10 µg/ml propidium iodide (Sigma-Aldrich, Poole, UK) in PBS containing 10 µg/ml RNase A (Sigma-Aldrich) for 30 min at room temperature, or with 5 µM DAPI (Invitrogen, Paisley, UK) for 10 min. Slides were mounted in fluorescent mounting medium (Dako, Ely, UK). Negative immunohistochemistry (IHC) controls were performed in parallel by omission of primary antibody. Immunoreactive cells were visualized and images recorded with an inverted confocal microscope (Nikon, Model Eclipse TE 2000-U, Tokyo, Japan) using the Nikon Confocal Microscope EZ-C1 software. Representative images were taken from the midperipheral region of the retina.

RESULTS

Progenitor cells in the developing pig retina: Antibodies to intermediate filament protein nestin and the homeodomain transcription factor Pax6 were used to identify retinal progenitor cells in the developing pig retina (Figure 1). Nestin immunoreactivity was detected throughout GW9 pig retina, reflecting the undifferentiated state of the majority of cells at this stage (Figure 1A). The staining pattern was similar to that found in the P5 mouse retina (Figure 2A), where the strongest immunoreactivity localized to fibers in the ganglion cell layer (GCL). In the postnatal pig retina, nestin immunolabeling was seen in the cell fibers in the GCL and inner plexiform layer (IPL; Figure 1B) probably representing the extensions of Müller glia cells as has been confirmed in the 8W rat retina [25].

In GW9 pig retina, Pax6 strongly labeled most cells in the GCL, cells in the inner portion of the neuroblast layer (NBL) and some cells in the prospective outer plexiform layer (OPL) (Figure 1C). The rounded cells in the inner portion of the NBL represented putative differentiating amacrine cells. Labeled cells with elongated shape and weaker staining found throughout the outer NBL appeared to be migrating progenitors. This observation was corroborated by immunolabeling for Ki67, a marker for proliferating cells, which revealed many mitotic cells throughout the NBL, excluding the innermost portion where amacrine cells differentiate (Figure 1D). Rounded Pax6-labeled cells in the developing OPL (Figure 1C) are suggestive of differentiating horizontal cells [23]. GW9 pig retina contained more migrating progenitor cells compared to P5 mouse retina in which Pax6 labeling mainly colocalized with the prospective position of ganglion, amacrine, and horizontal cells (Figure 2B). Pax6 immunoreactivity was found in ganglion, amacrine, and some horizontal cells in the 1W pig retina (Figure 1E).

Neurons of the ganglion cell layer: The antibodies to POU domain transcription factor Brn3a and intermediate neurofilament (NF)-160 were chosen to characterize ganglion cells in the developing, postnatal and mature pig retina (Figure 3). The activating protein α (AP2α) transcription factor, an exclusive marker for amacrine cells, was used to visualize the population of displaced amacrine cells within the GCL. Essentially, the same labeling of the GCL was observed in 1W and 6M pig retinas, therefore only images of 1W pig retinas are shown.

Brn3a immunoreactivity was found exclusively in the GCL in GW9 pig retina (Figure 3A). The observed staining pattern, with densely labeled cells, closely resembled that found in P5 mouse retina (Figure 2C). Brn3a-immunopositive cells were evenly spaced in the GCL of 1W pig retina (Figure 3B).

Table 1. Primary antibodies used for immunohistochemical analysis of the pig retina.

Antibody	Cell specificity	Host	Dilution	Source	Reference
Nestin	neural stem/progenitor cells, Müller glia	mouse	1:400	BD Biosciences	[25,41,44]
Pax6	retinal progenitors, ganglion, amacrine, and horizontal cells	rabbit	1:1,000	Chemicon	[28,45]
Ki67	proliferating cells	mouse	1:300	BD Biosciences	[46]
Brn3a	ganglion cells	mouse	1:40	Chemicon	[47]
Neurofilament (NF)-160	ganglion, horizontal, and bipolar cells	mouse	1:350	Sigma	[22,38,48,49]
AP2α	amacrine cells	mouse	1:50	Developmental Studies Hybridoma Bank	[26]
Calretinin	ganglion, amacrine, horizontal, cone photoreceptor, and bipolar cells	mouse	1:500	Chemicon	[33,50]
Calbindin	horizontal, ganglion, amacrine, bipolar, and cone photoreceptor cells	rabbit	1:1,500	Chemicon	[27,51,52]
GAD65	GABAergic amacrine, rare horizontal ganglion cells	mouse	1:1,000	Developmental Studies Hybridoma Bank	[27,28]
Islet1	amacrine, bipolar, ganglion, and horizontal cells	mouse	1:500	Developmental Studies Hybridoma Bank	[29,37]
PKCα	rod bipolar, amacrine, and ganglion cells, cones	mouse	1:400	Sigma	[27,30,53]
Recoverin	photoreceptors, cone bipolar cells, rare ganglion cells	rabbit	1:1,000	K. Koch	[42,51,54]
Rhodopsin (Rho4D2)	rods	mouse	1:100	R. Molday	[2,36,43]
GNAT2	cones	rabbit	1:500	Santa Cruz Biotechnology	[55-57]
P75 neurotrophin receptor	Müller glia and ganglion cells	rabbit	1:350	Promega	[31,32,58]
Glutamine synthetase	Müller glia	mouse	1:500	BD Biosciences	[35,59]
GFAP	astrocytes	rabbit	1:500	DAKO	[60-62]

The cell specificity is described according to the published literature (listed in the reference column) on the antibodies to the same proteins. Details for the primary antibodies (host, dilution used and the source) used in our study are presented.

© 2009 Molecular Vision

Molecular Vision 2009; 15:1915-1928 <http://www.molvis.org/molvis/v15/a204> © 2009 Molecular Vision

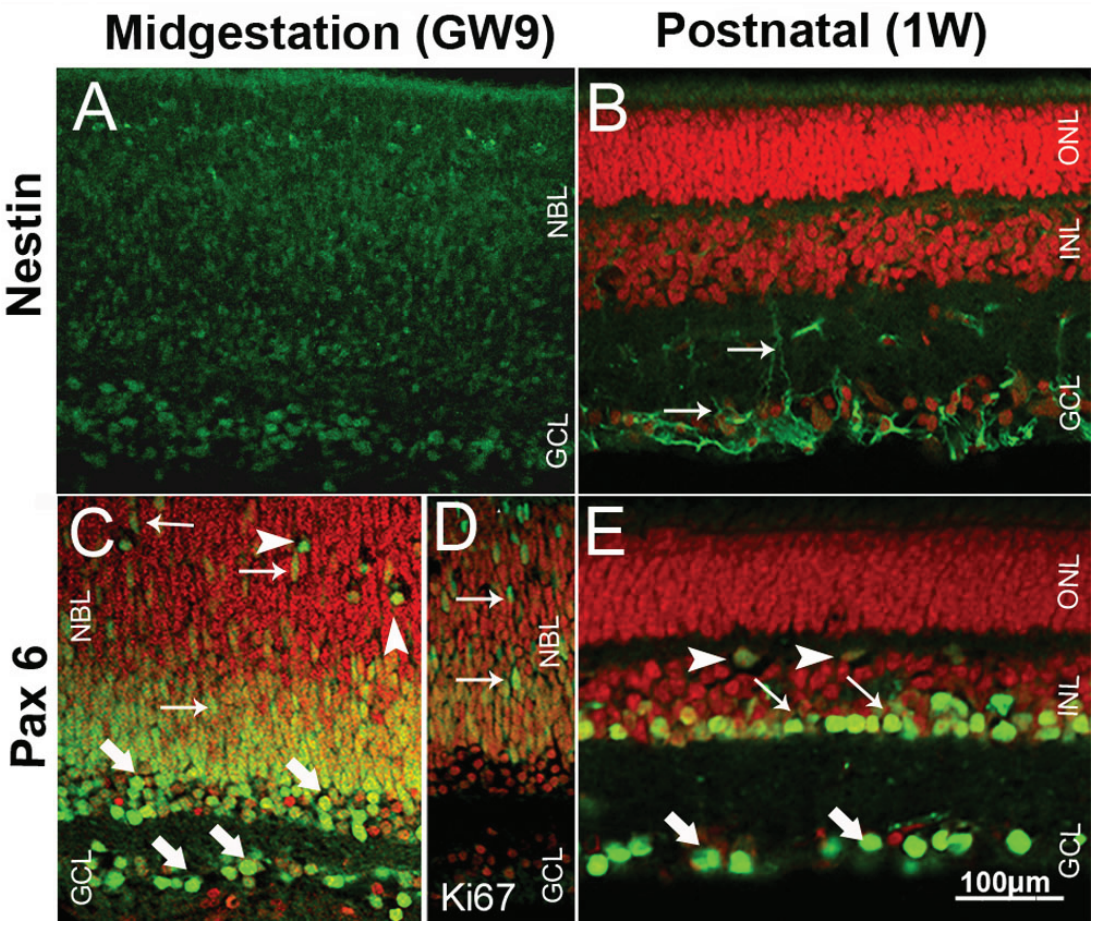


Figure 1. Pig retinal cryosections labeled immunohistochemicaly for nestin, Pax6 and Ki67. **A**: Nestin immunoreactivity is evident throughout GW9 retina. **B**: Nestin positive fibers are in the GCL and IPL (arrows) in 1W retina. **C**: Cells in the GCL, differentiating amacrine (thick arrows), horizontal (arrowheads) and putative retinal progenitors (thin arrows) are Pax6-positive in GW9 retina. **D**: Immunoreactivity for the mitotic marker Ki67 in GW9 retina reveals distribution of progenitor cells similar to that labeled for Pax6 (thin arrows). **E**: Cells in the GCL (thick arrows), amacrine (thin arrows) and some horizontal cells (arrowheads) are Pax6-positive in 1W retina. Nuclei are labeled with PI (red).

In GW9 pig retina, NF-160 staining was observed in the GCL, IPL, and in some differentiating amacrine and horizontal cells (Figure 3C). A similar pattern was found in the P5 mouse (Figure 2D), with the exception of strong staining in the OPL, suggestive of more advanced histogenesis. In the 1W pig retina, robust immunoreactivity was seen in the GCL and neurofiber layer, with fine labeling of processes in the IPL and OPL (Figure 3D).

A weak AP2α-positive signal was found in sparse cells in the GCL of GW9 pig retina (Figure 3E). In P5 mouse retina AP2α immunoreactivity was significantly stronger, labeling a large proportion of cells in the GCL and prospective inner nuclear layer (INL) (Figure 2E). Similarly to the staining pattern in adult mouse [26], AP2α in the 1W (Figure 3F) and 6M (not shown) pig retina labeled cells densely distributed in the GCL and the inner portion of the INL, suggestive of displaced amacrine and amacrine cells respectively.

Neurons of the inner nuclear layer: To characterize developing neurons in the INL, namely amacrine and horizontal cells, we used antibodies against calretinin, calbindin, and the 65 kDa isoform of glutamic acid decarboxylase (GAD65; Figure 4). Since these markers label cell processes, they also gave a good indication of the development of plexiform layers. The LIM homeodomain

Molecular Vision 2009; 15:1915-1928 <http://www.molvis.org/molvis/v15/a204> © 2009 Molecular Vision

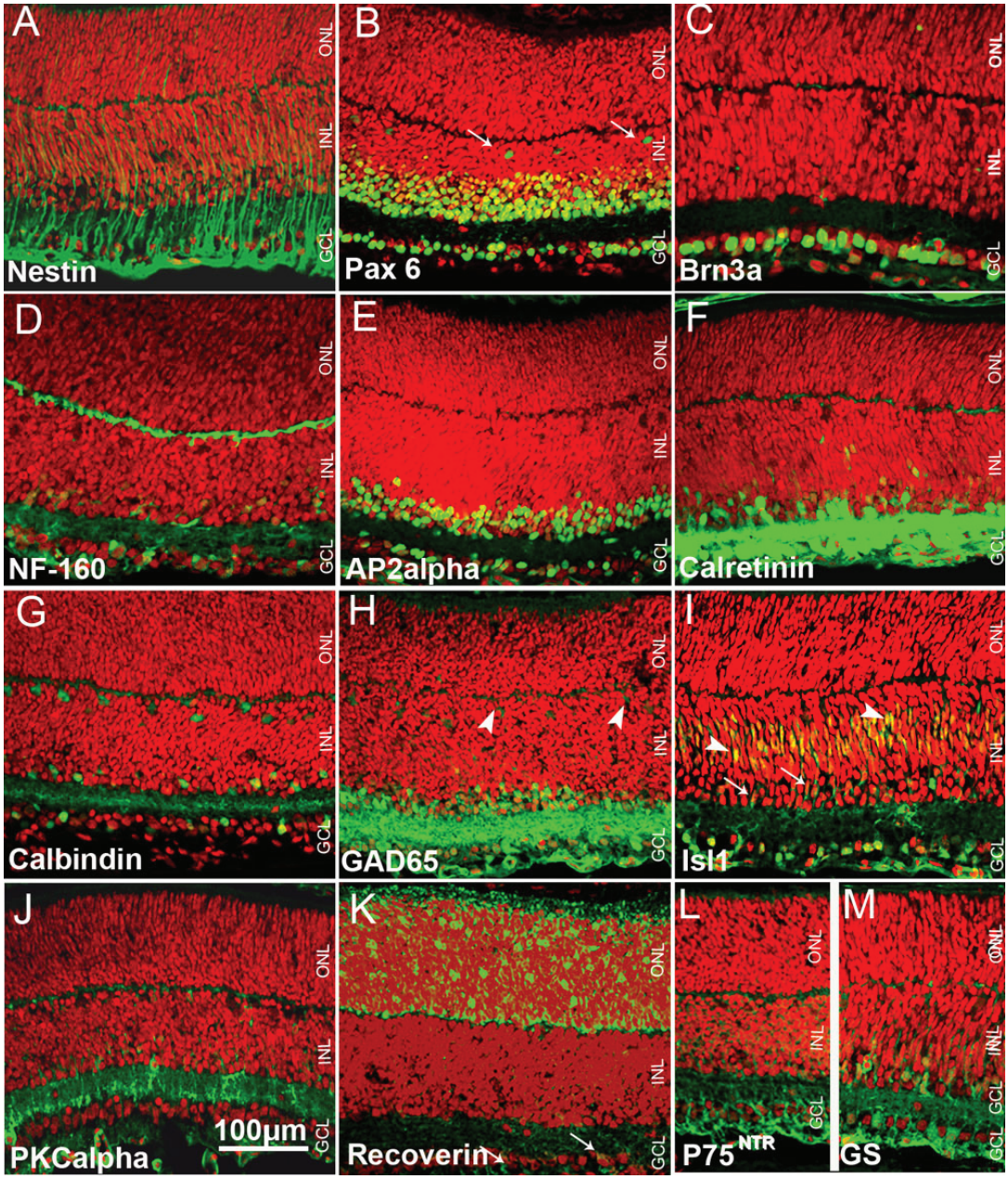


Figure 2. P5 mouse retinal sections labeled immunohistochemicaly. **A**: Radial processes are positive for nestin. **B**: Ganglion, amacrine and horizontal cells (arrows) are Pax6- positive. **C**: Ganglion cells are labeled for Brn3a. **D**: GCL, amacrine cells, IPL, and OPL are NF-160-positive. **E**: Displaced amacrine and amacrine cells are AP2α-positive. **F**: GCL, IPL, amacrine cells and OPL are labeled for calretinin. **G**: Ganglion, amacrine and horizontal cells are calbindin-positive. **H**: IPL, ganglion, amacrine and horizontal cells (arrowheads) are labeled for GAD65. **I**: Ganglion, amacrine (arrows) and bipolar cells (arrowheads) are Islet1-positive. **J**: GCL, IPL, INL and OPL are PKCα-positive. **K**: ONL and some cells in the GCL (arrows) are positive for recoverin. Neurofiber layer, INL and OPL are labeled for $P75^{NTR}$ (**L**) and GS (**M**). Nuclei are labeled with PI (red).

Molecular Vision 2009; 15:1915-1928 <http://www.molvis.org/molvis/v15/a204> © 2009 Molecular Vision

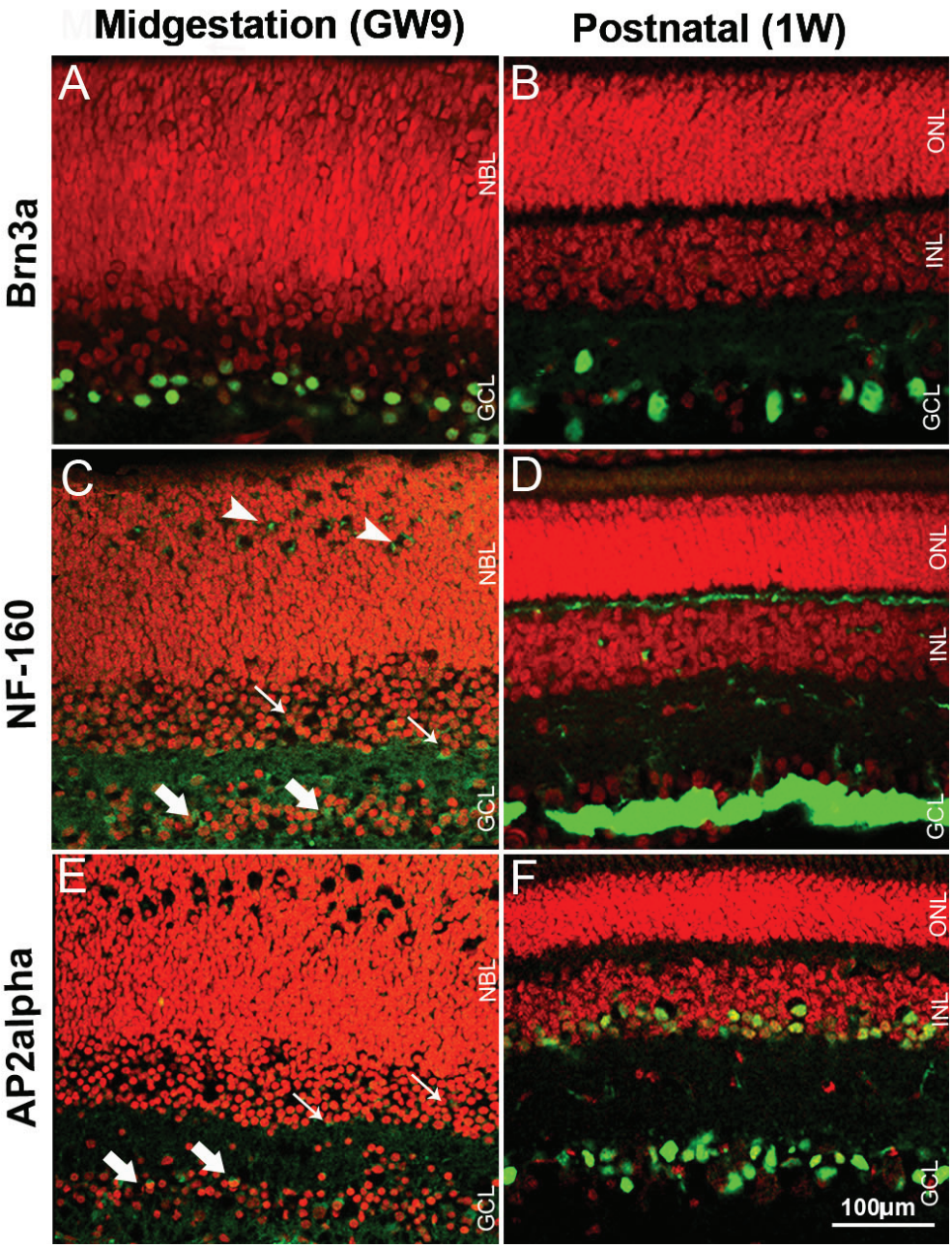


Figure 3. Pig retinal cryosections labeled immunohistochemicaly for the GCL protein markers. **A**: Only ganglion cells are labeled for Brn3a in GW9 retina. **B**: Ganglion cells are Brn3a-positive in 1W retina. **C**: Cells in the GCL (thick arrows), IPL, some developing amacrine (thin arrows) and horizontal cells (arrowheads) are positive for NF-160 in GW9 retina. **D**: GCL, neurofiber layer, and processes in IPL and OPL are NF-160-positive in 1W retina. **E**: Weak labeling for AP2α in the GCL (thick arrows) and prospective INL (thin arrows) is present in GW9 retina **F**: Cells in the GCL and amacrine cells in the INL are APα2-positive in 1W retina. Nuclei are labeled with PI (red).

Molecular Vision 2009; 15:1915-1928 <http://www.molvis.org/molvis/v15/a204> © 2009 Molecular Vision

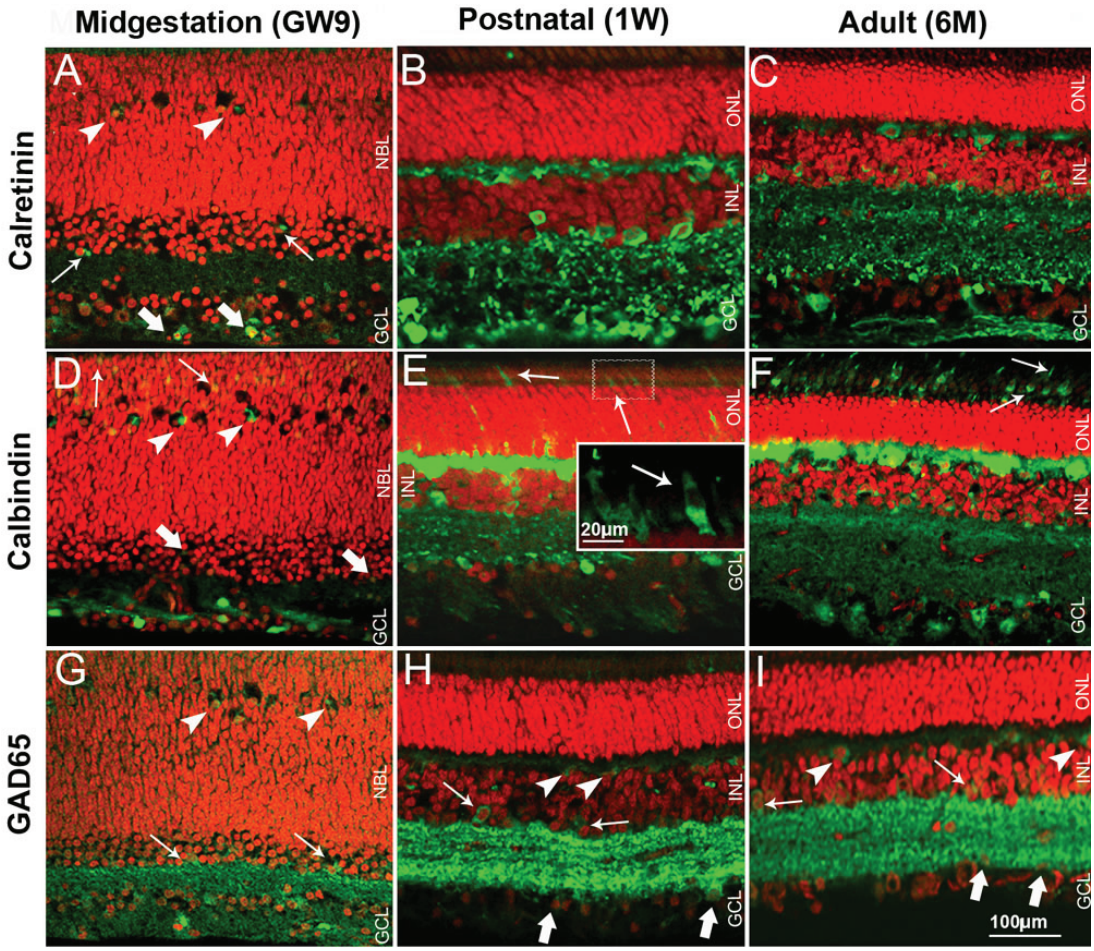


Figure 4. Pig retinal cryosections labeled immunohistochemicaly for calretinin, calbindin, and GAD65. **A**: Ganglion (thick arrows), amacrine (thin arrows) and horizontal cells (arrowheads) are calretinin-labeled in GW9 retina. GCL, IPL, amacrine and horizontal cells are calretinin-positive in 1W retina (**B**) and 6M (**C**) retina. Cells in the GCL, amacrine (thick arrows), differentiating horizontal (arrowheads), and putative cones (thin arrows) are calbindin-positive in GW9 retina. GCL, IPL, amacrine, horizontal cells, and cones (thin arrows) are calbindin-positive in 1W (**E**) and 6M (**F**) retina. **G**: GCL, IPL, amacrine (arrows) and horizontal cells (arrowheads) are GAD65-positive in GW9 retina. IPL, cells in the GCL (thick arrows), amacrine cells (thin arrows) and OPL (arrowheads) are GAD65-positive in 1W (**H**) and 6M (**I**) retina. Nuclei are labeled with PI (red).

transcription factor Islet1 and protein kinase C α isoform (PKCα) were primarily used to visualize bipolar cells (Figure 5).

In the developing pig retina at GW9, calretinin immunoreactivity was found in a subpopulation of cells in the GCL and rare cells in the inner NBL, suggestive of amacrine phenotypes (Figure 4A). Sparse cells in the developing OPL were also weakly labeled. Calretinin immunoreactivity in correspondence to ganglion and amacrine cells was significantly stronger in P5 mouse retina (Figure 2F) than in GW9 pig retina. Weaker labeling was found in mouse OPL. 1W and 6M retina (Figure 4B,C) displayed a calretinin immunostaining pattern similar to that of adult mouse (8–10W), with labeled ganglion, amacrine, and horizontal cells and the distinction of the three strata in the IPL [27].

A subpopulation of cells in the GCL and some cells in the developing OPL were strongly calbindin-immunopositive in GW9 pig retina (Figure 4D). Weak staining was found in sparse developing amacrine cells. Labeling was also seen at the outer edge of the NBL, suggesting immunoreactivity of

Molecular Vision 2009; 15:1915-1928 <http://www.molvis.org/molvis/v15/a204> © 2009 Molecular Vision

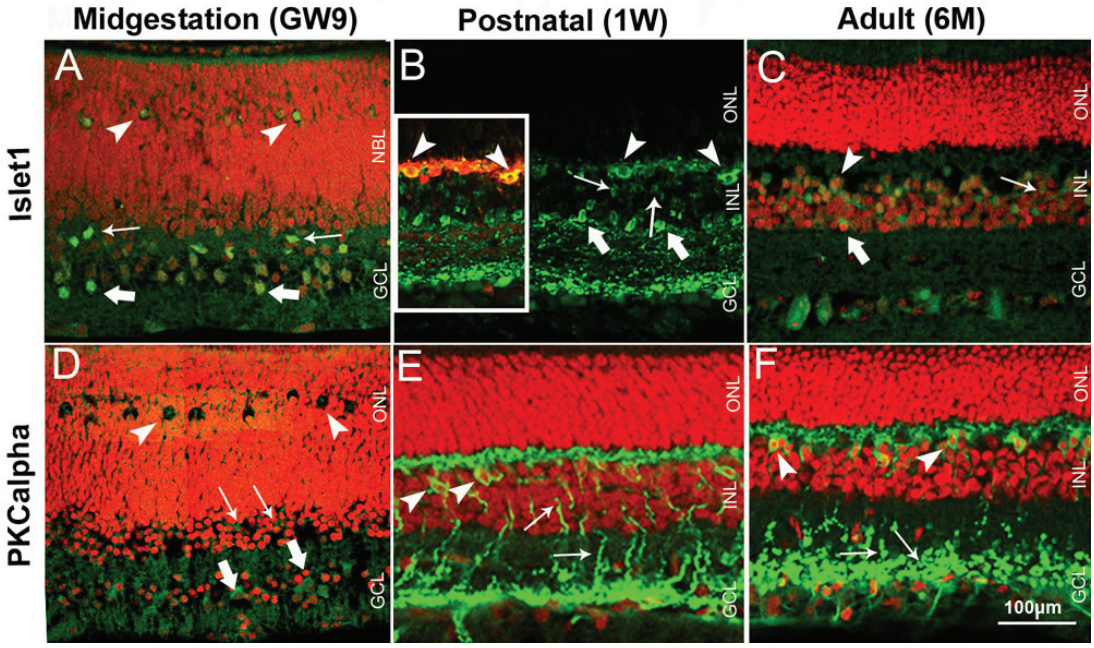


Figure 5. Pig retinal cryosections labeled immunohistochemicaly for Islet1 and PKCα. **A**: Ganglion (thick arrows), amacrine (thin arrows) and horizontal cells (arrowheads) are Islet1-positive in GW9 retina. **B**: Ganglion, amacrine (thick arrows), bipolar (thin arrows) and horizontal cells (arrowheads, also labeled with calbindin in inset **B**) are Islet1-positive in 1W (**B**) and 6M (**C**) retina. **D**: GCL (thick arrows), IPL, prospective INL (thin arrows), and developing OPL (arrowheads) are PKCα-positive in GW9 retina. **E**: Bipolar cell bodies (arrowheads) and their processes (arrows) are PKCα-positive in 1W retina. **F**: Bipolar cell bodies (arrowheads) and axonal endings (arrows) are PKCα-labeled in 6M retina. Nuclei are labeled with PI (red).

some developing photoreceptors. Labeling of amacrine cells and of the IPL was more prominent in P5 mouse retina (Figure 2G) compared to GW9 pig, where the INL and IPL only occasionally displayed weak positive signal. The labeling pattern of horizontal, amacrine, and ganglion cells and their processes in the OPL and IPL in both 1W and 6M pig retinas (Figure 4E,F) closely resembled that described for the adult mouse retina. In the pig (1W and 6M) retina, calbindin also labeled sparse photoreceptors, which had a typical wide and tapered cone-like shape (Figure 4E, inset), and did not stain for rhodopsin in double labeling experiments (not shown). Cones appeared immature and mostly inner segments were visualized in 1W pig retina (Figure 4E, inset). At 6M, cones were intensely labeled for calbindin, with inner and outer segments clearly visible (Figure 4F).

In the GW9 pig retina, GAD65 immunostaining was found in amacrine and ganglion cell bodies, with stronger signal localized to the IPL (Figure 4G). Some GAD65-positive cells with immature labeled processes, suggestive of developing horizontal cells, were also highlighted. This staining pattern was similar to P5 mouse retina (Figure 2H), albeit less intense. In mouse, weak signal was also seen in the developing horizontal cells and OPL. In postnatal and adult pig retinas, strong labeling was found in processes layering the IPL, with a characteristic striated appearance (Figure 4H,I) as seen in adult mouse retina [27,28]. Some labeled horizontal cell bodies were visible in 6M pig retina (Figure 4I).

In the GW9 pig retina, moderate to intense Islet1 immunoreactivity was observed in the GCL and in some amacrine cells at the inner border of the NBL (Figure 5A). Strongly immunopositive cells were also localized to the distal part of the NBL in the prospective OPL. The position and round shape of these cells suggests their differentiation toward horizontal cells. Contrary to findings in pig at GW9, no horizontal cells were labeled in P5 mouse retina (Figure 2I). However, developing bipolar cells in the central portion of the INL were strongly Islet1-immunopositive. From the first postnatal week onwards (Figure 5B,C) Islet1-positive staining was found in the GCL, IPL, and INL of the pig retina. At 1W and 6M, Islet1-immunoreactive amacrine cells, as well as densely distributed cell bodies, were visible in the inner and outer portion of the INL, respectively (Figure 5B,C). Some cells in the outer portion of the INL had a spindle shape characteristic of bipolar cells, whereas others appeared

Molecular Vision 2009; 15:1915-1928 <http://www.molvis.org/molvis/v15/a204> © 2009 Molecular Vision

rounded, suggestive of horizontal cell phenotypes. Double-labeling experiments with calbindin (Figure 5B, inset) confirmed the presence of Islet1-immunoreactive horizontal cells in 1W pig retina, a feature also described for human retina (12–85 years-old) [29].

Weak PKCα immunolabeling was detected in the GCL, IPL, inner NBL, and in the prospective OPL of GW9 pig retina (Figure 5D). P5 mouse retina displayed a similar labeling pattern (Figure 2J). However, the staining was more prominent compared to GW9 pig. In both 1W and 6M pig retina (Figure 5E,F) oval-shaped immunoreactive cells were found in the INL, with their cell bodies located close to the OPL and their processes extended toward both OPL and IPL, as is characteristic of rod bipolar cells. Axon processes in the IPL were clearly visualized in the 1W pig retina (Figure 5E), whereas staining in the 6M was mainly localized to the axon endings of rod bipolar cells, presented in the form of characteristic swellings or granulate labeling (Figure 5F). Some cell bodies adjacent to the vitreous and their processes were PKCα-immunoreactive in the 1W and 6M pig retinas. No PKCα-positive amacrine or cone photoreceptor cells were detected in the 1W or 6M pig retina, as reported for the mouse (8–10W) [27,30].

Photoreceptors: An antibody to calcium binding protein recoverin, which labels both rods and cones, was used as an early marker of photoreceptor differentiation (Figure 6). Rod photoreceptors were further characterized with an anti-rhodopsin antibody. Antibodies for mouse S-opsin and M-opsin used for this study did not cross-react with pig proteins (data not shown); therefore we used an antibody against Gα subunit of the cone transducin (GNAT2) to label cones in the pig retina.

In the GW9 pig retina, strong recoverin immunoreactivity was detected in putative differentiating photoreceptors, localized to the apical surface of the NBL, and in sparse cells found deeper in the inner NBL (Figure 6A). Recoverin staining was seen throughout the developing ONL in P5 mouse retina (Figure 2K). However, labeling at the apical surface of the NBL was weaker than in GW9 pig. Some recoverin-positive ganglion cells were observed in mouse P5, but not in pi GW9g developing retina. In the 1W pig retina, recoverin immunoreactivity was seen throughout the ONL, including in the inner and outer segments (Figure 6B,C). Photoreceptor segments appeared longer at 6M than at 1W. Some recoverin-positive cells localized to the prospective INL in the GW9 pig retina could be regarded as developing bipolar cells (Figure 6A). However, no conspicuous bipolar cell labeling was observed in 1W or 6M pig retina (Figure 6B,C).

In GW9 pig retina, sparse elongated rhodopsin-immunoreactive cells were observed localized to the prospective ONL, suggestive of early differentiating rod photoreceptors (Figure 6D). Some rudimentary inner segments were also weakly labeled. No rhodopsin-positive cells were detected in the P5 mouse retina with the same antibody (data not shown). Rod outer segments were strongly labeled in both 1W and 6M pig retina, whereas inner segments and some cells bodies displayed weaker staining (Figure 6E,F). Rod outer segments appeared longer and more defined in 6M compared to 1W old animals, suggesting that outer segments continue to extend in length well into the postnatal period.

No labeling with GNAT2 antibody was observed in the GW9 pig retina. Similarly, mouse cones at P5 were not positive for this marker (not shown). Cone outer segments in both 1W and 6M pig retina were strongly immunoreactive for GNAT2 (Figure 6G,H). The size of the cone outer segments slightly increased from the 1W to the 6M pig retina.

Retinal glial cells: The antibodies to low affinity neurotrophin receptor P75 ($P75^{NTR}$) and glutamine synthetase (GS) were used to characterize Müller glia, whereas an anti-GFAP antibody was used to label astrocytes. In the GW9 pig retina, strong $P75^{NTR}$ staining was present in the neurofiber layer (Figure 7A), similar to P5 mouse retina (Figure 2L). Labeled processes extended through the GCL and IPL and entered the inner portion of the NBL. Additional immunoreactivity was seen in the developing OPL, with the majority of stained cell bodies localized in the distal half of the prospective INL and some cell processes extending to the ONL. From the postnatal period onward the labeling pattern for $P75^{NTR}$ in the pig retina remained unchanged, although it appeared that IPL displayed stronger staining in the 1W compared to the 6M retina (Figure 7B,C).

In the GW9 pig retina GS positive labeling was seen mainly in the GCL, where it likely represents processes of the developing Müller glial cells. Weaker staining was also observed in the IPL and the inner portion of the NBL (Figure 7D). Interestingly $P75^{NTR}$ and GS staining pattern were almost identical in the P5 mouse retina (Figure 2L,M), whereas in the GW9 pig, $P75^{NTR}$ staining was significantly stronger, suggesting temporal advantage in the expression of this marker. GS immunolabeling pattern in the 1W and 6M pig retina was very similar to that seen for $P75^{NTR}$, revealing strong staining in the GCL, IPL and INL, suggestive of Müller glia cells, as it has also been shown for adult (8–10W) rat retina (Figure 7E,F) [31,32]. As seen also for $P75^{NTR}$, somewhat stronger staining for GS was found in the IPL of 1W compared to the 6M pig retina.

In GW9 pig retina, GFAP immunoreactivity was observed adjacent to the vitreous in cells with thin and short processes, suggestive of immature developing astrocytes (Figure 7G). In the 1W retina, the majority of the staining was localized in the neurofiber layer and GCL, with rare processes protruding into the IPL (Figure 7H). Astrocytic processes in the adult retina became denser and longer, extending from the neurofiber layer through the GCL, IPL and INL, occasionally

Molecular Vision 2009; 15:1915-1928 <http://www.molvis.org/molvis/v15/a204> © 2009 Molecular Vision

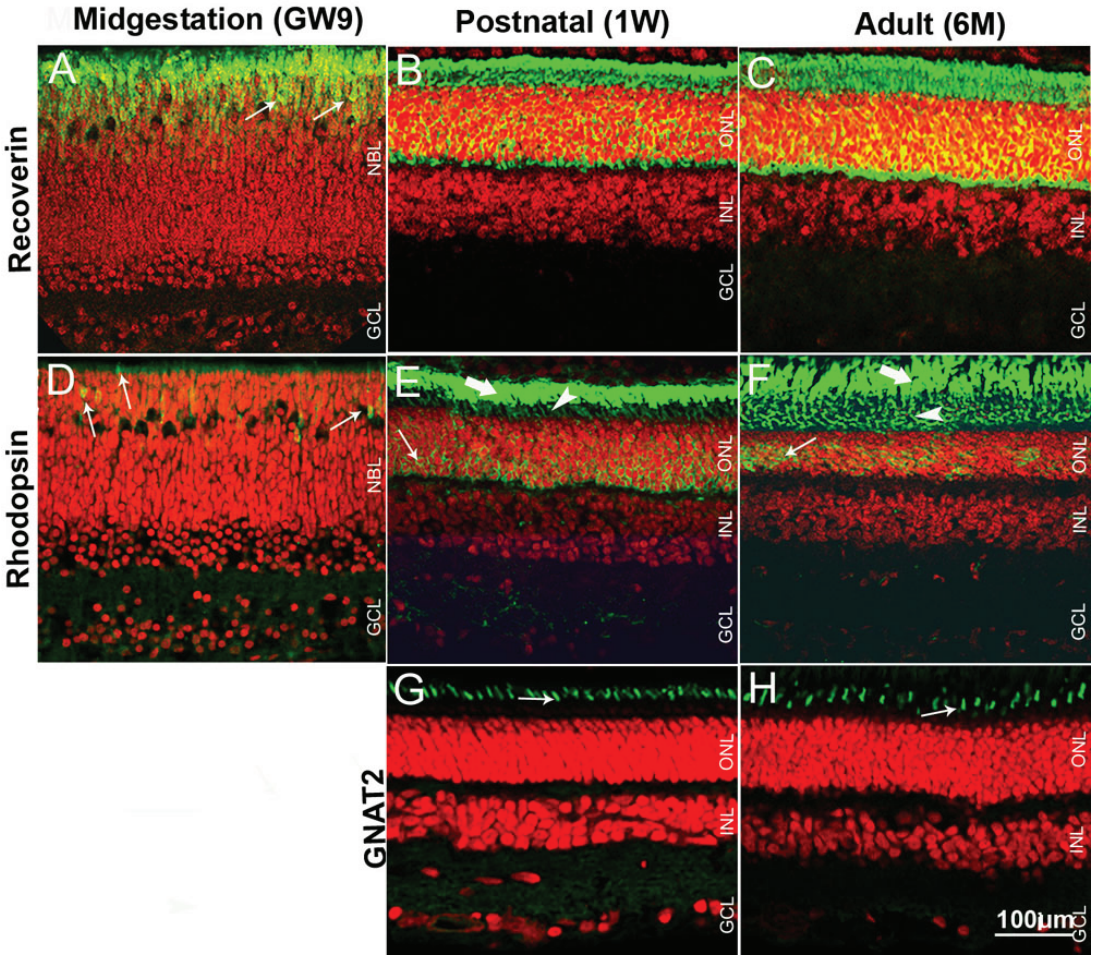


Figure 6. Pig retinal cryosections labeled immunohistochemicaly for photoreceptor protein markers. **A**: Cells in the prospective ONL are positive for recoverin (arrows) in GW9 retina. ONL and photoreceptor segments are recoverin-labeled in 1W (**B**) and 6M (**C**) retina. **D**: Some differentiating rod photoreceptors are positive for rhodopsin in GW9 retina (arrows). **E**: Strong rhodopsin-labeling is present in the outer segments (thick arrows) in 1W retina. Inner segments (arrowheads) and cell bodies (thin arrows) are less intensely stained. **F**: Rhodopsin-positive inner (arrowheads) and outer (thick arrows) segments are more elongated in 6M compared to 1W retina. Some rod cells bodies are also labeled (thin arrows) in 6M retina. Cone outer segments are labeled for GNAT2 in 1W (G) and 6M (**H**) retina (thin arrows). Nuclei are labeled with PI (red).

reaching the ONL (Figure 7I). PKCα colocalized with glial fibrillary acidic protein (GFAP) immunostaining in double labeling experiments, identifying PKCα-positive astrocytes (Figure 7J-N). Astrocytes in 1W pig retina were weakly labeled for PKCα, but in 6M pig retina these cells were strongly PKCα immunoreactive (Figure 7J-N).

DISCUSSION

We have conducted an immunohistochemical study of the pig midgestation, postnatal, and adult retina to establish the timing and progression of retinal development and define markers that reliably identify specific cell types in the pig. The majority of the studied markers were expressed at midgestation, and labeled cells were arranged in a laminar pattern according to their distribution in the mature retina. Nestin and Pax6 immunolabeling revealed a relatively large population of retinal progenitor cells at midgestation. Based on histology and retinal architecture, development appeared less advanced in GW9 pig compared to P5 mouse retina, as

Molecular Vision 2009; 15:1915-1928 <http://www.molvis.org/molvis/v15/a204> © 2009 Molecular Vision

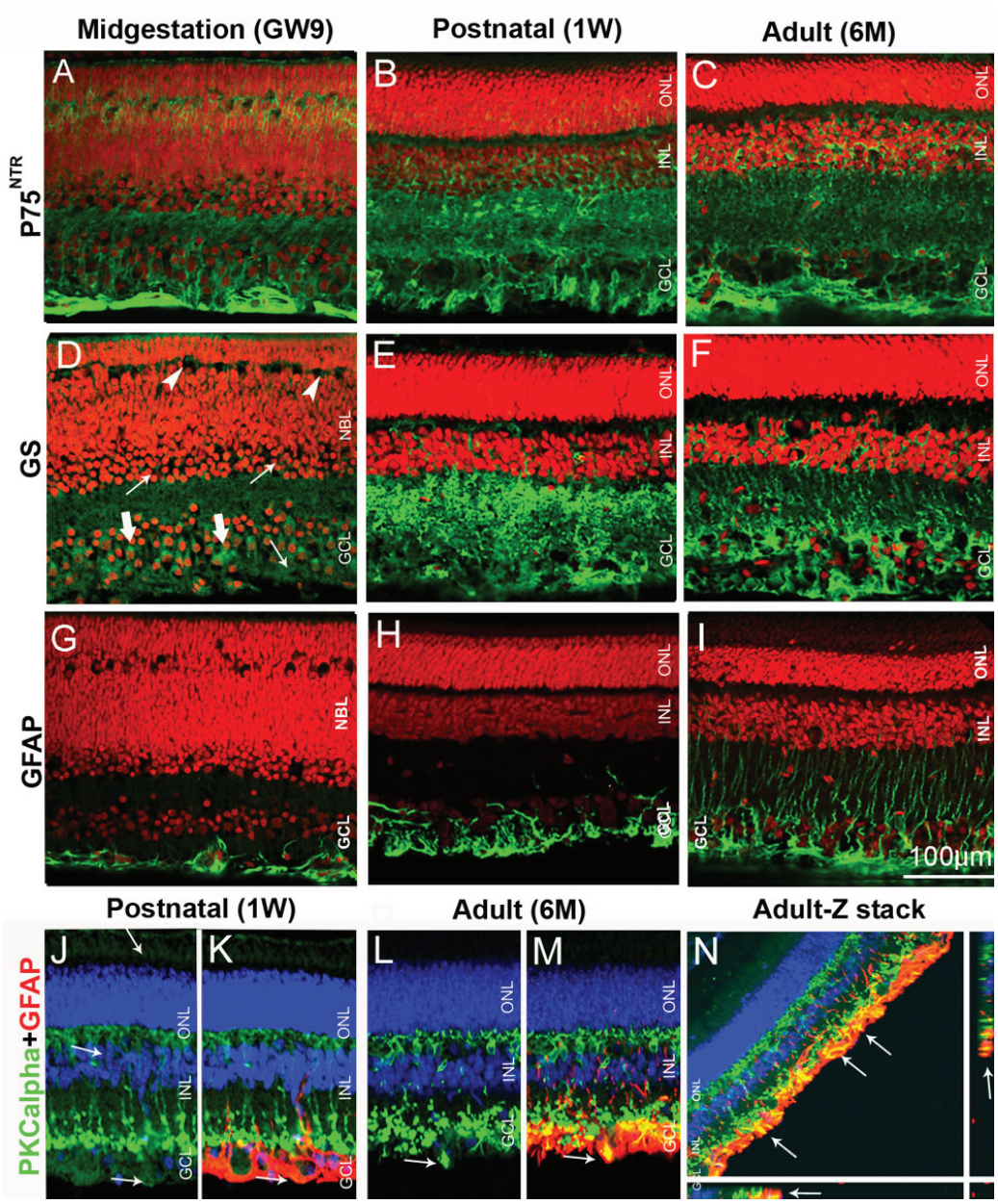


Figure 7. Pig retinal cryosections labeled for glial protein markers. **A**: Processes in the neurofiber layer, GCL, OPL, inner NBL, and developing OPL are $P75^{NTR}$-positive in GW9 retina. Processes in the GCL, IPL, and INL are $P75^{NTR}$-positive in 1W (**B**) and 6M (**C**) retina. **D**: Processes in the GCL (thick arrows), NBL (thin arrows), and developing OPL (arrowheads) are labeled for GS in GW9 retina. GS immunolabeling is present in the GCL, IPL, and INL in 1W (**E**) and 6M (**F**) retina. **G**: Immature astrocytes are GFAP-positive in GW9 retina. **H**: Processes in neurofiber and GCL are GFAP- positive in 1W retina. **I**: Elongated GFAP-positive processes in 6M retina. **J-M**: GFAP-immunopositive astrocytes are PKCα-positive, weakly in 1W (**J, K**, arrows) but strongly in 6M retina (**L, M**, arrows). **N**: A Z-stack image shows extensive double GFAP-PKCα labeling at 6M (arrows). X- and Y- planes are shown to bottom and to the right of the image.

Molecular Vision 2009; 15:1915-1928 <http://www.molvis.org/molvis/v15/a204> © 2009 Molecular Vision

suggested by the well demarcated developing OPL present in mouse but not visible in the pig retina. Histogenesis, as detected by immunohistochemistry, appeared to follow a different sequential order in pig compared to mouse. Immunoreactivity of ganglion cells in GW9 pig was similar to that in P5 mouse. Horizontal cells were strongly calbindin- and NF-160-immunoreactive in both GW9 pig and P5 mouse retina. However, AP2α, calretinin, calbindin, Islet1, and PKCα immunolabeling indicated that development of amacrine and bipolar cells was significantly less advanced in GW9 pig compared to P5 mouse. On the contrary, sparse developing rod photoreceptors were identified in GW9 pig retina, while P5 mouse retina did not show any rhodopsin immunoreactivity. These observations suggest that rod differentiation occurs earlier in pig than in mouse, relative to the development of the inner retina.

Bearing in mind the potential of the pig as a preclinical animal model for retinal disease, it is important to highlight the similarities and differences between human and pig retina. Similar to the human, the pig retina is relatively mature at birth with all layers and retinal cell types present in one-week-old animals. GW9 pig retinas appeared to be at an earlier developmental stage than GW20–21 human retina, based on published literature [33]. At GW9 in pig only early signs of OPL development were evident, whereas in human GW9 retina separation between ONL and INL is fully accomplished [33]. Pax6 labeling in GW9 pig retina revealed cells of elongated shape distributed throughout the NBL, likely migrating retinal progenitors, whereas Pax6 immunostaining has been described in the human retina at GW21 only in differentiated ganglion cells and differentiating amacrine and horizontal cells [34]. Similarly, expression of the calcium binding proteins, calretinin and calbindin, appeared to be lagging behind in GW9 pig compared to the GW20–21 human retina. In the GW21 human retina, both calretinin and calbindin robustly label ganglion and amacrine cells, with weaker staining of horizontal cells and additional labeling of cones [33]. However, only sparse cells in the GCL and NBL were calretinin- or calbindin-immunoreactive at GW9 in pig. Additionally, Müller glial cells are strongly GS positive in the GW20 human retina [35], but only weak labeling of the processes in the GCL was seen in the GW9 pig. Early immunolabeling of rhodopsin at GW9 in the pig retina is comparable to that in human, where rhodopsin immunoreactivity has been shown at GW15 in rod inner segments [36]. Although recoverin has been detected in bipolar cells in both mouse and human [27,29], only photoreceptors were labeled with anti-recoverin antibody in the pig retina.

Several antibodies labeled the same cell types in pig and human retina, but displayed different cell specificity in mouse. As in adult human retina (12–85 years old) [29], but contrary to adult mouse (10W) [37], horizontal cells in the pig retina were immunoreactive for Islet1 [29]. Moreover, as in postnatal (4 months-old) and adult (35 years-old) human retina [33], calbindin immunoreactive cones were found in 1W and 6M pig, but not in adult 8–10 week-old mouse retina [26]. However, the antibody against NF-160 subunit labeled horizontal cells in pig (GW9, 1W, 6M) as well as in mouse retina [38], but it has only been reported in retinal ganglion cells in the human retina [22,39,40].

The majority of investigated markers showed the same pattern of immunolabeling in both 1W and 6M pig retina. However, differences were found suggesting that some degree of retinal maturation occurs during the postnatal period. The same is true for the human retina, which reaches maturity by 5 years of age [2]. For example, photoreceptor outer segments continue to grow in length well into the postnatal period in pig as in human retina. Furthermore, GFAP immunolabeling revealed a significant increase in the length of astrocytic processes from 1W to the 6M pig retina. PKCα immunostaining was distributed along the axons of bipolar cells in the 1W pig retina and concentrated at the synaptic site adjacent to the GCL in the 6M retina. Finally, expression of PKCα in astrocytes was stronger in adult compared to 1W pig retina.

The data presented herein should prove useful in future investigations that use pigs as a preclinical model system for retinal disease and repair. Similarity with human retina makes such studies a viable alternative to expensive and ethically problematic experimentation on nonhuman primates.

ACKNOWLEDGMENTS

We wish to thank Alan Stitt for fruitful discussion and critical review of the manuscript, Mildred Wylie for assistance with collection of embryonic and adult tissue, Karl-Wilhelm Koch and Robert Molday for kindly donating some of the antibodies, David Beattie, Lorraine Hanna and Stephen Lloyd for technical support. This work was supported in part by funding generously provided by Fighting Blindness, ROI and TheFraser Homes Foundation for Ophthalmic Research, UK.

REFERENCES

1. Chandler MJ, Smith PJ, Samuelson DA, MacKay EO. Photoreceptor density of the domestic pig retina. Vet Ophthalmol 1999; 2:179-84. [PMID: 11397262]
2. Hendrickson A, Bumsted-O'Brien K, Natoli R, Ramamurthy V, Possin D, Provis J. Rod photoreceptor differentiation in fetal and infant human retina. Exp Eye Res 2008; 87:415-26. [PMID: 18778702]
3. Hendrickson A, Hicks D. Distribution and density of medium- and short-wavelength selective cones in the domestic pig retina. Exp Eye Res 2002; 74:435-44. [PMID: 12076087]
4. Petters RM, Alexander CA, Wells KD, Collins EB, Sommer JR, Blanton MR, Rojas G, Hao Y, Flowers WL, Banin E, Cideciyan AV, Jacobson SG, Wong F. Genetically engineered large animal model for studying cone photoreceptor survival and degeneration in retinitis

Molecular Vision 2009; 15:1915-1928 <http://www.molvis.org/molvis/v15/a204> © 2009 Molecular Vision

pigmentosa. Nat Biotechnol 1997; 15:965-70. [PMID: 9335046]

5. Ruiz-Ederra J, García M, Hernández M, Urcola H, Hernández-Barbáchano E, Araiz J, Vecino E. The pig eye as a novel model of glaucoma. Exp Eye Res 2005; 81:561-9. [PMID: 15949799]
6. Iandiev I, Uckermann O, Pannicke T, Wurm A, Tenckhoff S, Pietsch UC, Reichenbach A, Wiedemann P, Bringmann A, Uhlmann S. Glial cell reactivity in a porcine model of retinal detachment. Invest Ophthalmol Vis Sci 2006; 47:2161-71. [PMID: 16639028]
7. Park KW, Kühholzer B, Lai L, Macháty Z, Sun QY, Day BN, Prather RS. Development and expression of the green fluorescent protein in porcine embryos derived from nuclear transfer of transgenic granulosa-derived cells. Anim Reprod Sci 2001; 68:111-20. [PMID: 11600279]
8. Matsunari H, Onodera M, Tada N, Mochizuki H, Karasawa S, Haruyama E, Nakayama N, Saito H, Ueno S, Kurome M, Miyawaki A, Nagashima H. Transgenic-cloned pigs systemically expressing red fluorescent protein, kusabira-orange. Cloning Stem Cells 2008; 10:313-23. [PMID: 18729767]
9. Del Priore LV, Kaplan HJ, Hornbeck R, Jones Z, Swinn M. Retinal pigment epithelial debridement as a model for the pathogenesis and treatment of macular degeneration. Am J Ophthalmol 1996; 122:629-43. [PMID: 8909202]
10. Nicolini J, Kiilgaard JF, Wiencke AK, Heegaard S, Scherfig E, Prause JU, la Cour M. The anterior lens capsule used as support material in RPE cell-transplantation. Acta Ophthalmol Scand 2000; 78:527-31. [PMID: 11037908]
11. Ghosh F, Wong F, Johansson K, Bruun A, Petters RM. Transplantation of full-thickness retina in the rhodopsin transgenic pig. Retina 2004; 24:98-109. [PMID: 15076950]
12. Klassen H, Kiilgaard JF, Zahir T, Ziaeian B, Kirov I, Scherfig E, Warfvinge K, Young MJ. Progenitor cells from the porcine neural retina express photoreceptor markers after transplantation to the subretinal space of allorecipients. Stem Cells 2007; 25:1222-30. [PMID: 17218397]
13. Klassen H, Warfvinge K, Schwartz PH, Kiilgaard JF, Shamie N, Jiang C, Samuel M, Scherfig E, Prather RS, Young MJ. Isolation of progenitor cells from GFP-transgenic pigs and transplantation to the retina of allorecipients. Cloning Stem Cells 2008; 10:391-402. [PMID: 18729769]
14. Gu P, Harwood LJ, Zhang X, Wylie M, Curry WJ, Cogliati T. Isolation of retinal progenitor and stem cells from the porcine eye. Mol Vis 2007; 13:1045-57. [PMID: 17653049]
15. MacNeil A, Pearson RA, MacLaren RE, Smith AJ, Sowden JC, Ali RR. Comparative analysis of progenitor cells isolated from the iris, pars plana, and ciliary body of the adult porcine eye. Stem Cells 2007; 25:2430-8. [PMID: 17600111]
16. Gaudin C, Forster V, Sahel J, Dreyfus H, Hicks D. Survival and regeneration of adult human and other mammalian photoreceptors in culture. Invest Ophthalmol Vis Sci 1996; 37:2258-68. [PMID: 8843922]
17. Picaud S, Pattnaik B, Hicks D, Forster V, Fontaine V, Sahel J, Dreyfus H. GABAA and GABAC receptors in adult porcine cones: evidence from a photoreceptor-glia co-culture model. J Physiol 1998; 513:33-42. [PMID: 9782157]
18. Luo X, Heidinger V, Picaud S, Lambrou G, Dreyfus H, Sahel J, Hicks D. Selective excitotoxic degeneration of adult pig retinal ganglion cells in vitro. Invest Ophthalmol Vis Sci 2001; 42:1096-106. [PMID: 11274091]
19. Traverso V, Kinkl N, Grimm L, Sahel J, Hicks D. Basic fibroblast and epidermal growth factors stimulate survival in adult porcine photoreceptor cell cultures. Invest Ophthalmol Vis Sci 2003; 44:4550-8. [PMID: 14507904]
20. Jeon MH, Jeon CJ. Immunocytochemical localization of calretinin containing neurons in retina from rabbit, cat, and dog. Neurosci Res 1998; 32:75-84. [PMID: 9831254]
21. Jeon YK, Kim SY, Jeon CJ. Morphology of calretinin and tyrosine hydroxylase-immunoreactive neurons in the pig retina. Mol Cells 2001; 11:250-6. [PMID: 11355708]
22. Ruiz-Ederra J, Garcia M, Hicks D, Vecino E. Comparative study of the three neurofilament subunits within pig and human retinal ganglion cells. Mol Vis 2004; 10:83-92. [PMID: 14961007]
23. De Schaepdrijver L, Lauwers H, Simoens P, de Geest JP. Development of the retina in the porcine fetus. A light microscopic study. Anat Histol Embryol 1990; 19:222-35. [PMID: 2260772]
24. Engelsberg K, Johansson K, Ghosh F. Development of the embryonic porcine neuroretina in vitro. Ophthalmic Res 2005; 37:104-11. [PMID: 15746566]
25. Walcott JC, Provis JM. Muller cells express the neuronal progenitor cell marker nestin in both differentiated and undifferentiated human foetal retina. Clin Experiment Ophthalmol 2003; 31:246-9. [PMID: 12786777]
26. Bassett EA, Pontoriero GF, Feng W, Marquardt T, Fini ME, Williams T, West-Mays JA. Conditional deletion of activating protein 2alpha (AP-2alpha) in the developing retina demonstrates non-cell-autonomous roles for AP-2alpha in optic cup development. Mol Cell Biol 2007; 27:7497-510. [PMID: 17724084]
27. Haverkamp S, Wassle H. Immunocytochemical analysis of the mouse retina. J Comp Neurol 2000; 424:1-23. [PMID: 10888735]
28. de Melo J, Qiu X, Du G, Cristante L, Eisenstat DD. Dlx1, Dlx2, Pax6, Brn3b, and Chx10 homeobox gene expression defines the retinal ganglion and inner nuclear layers of the developing and adult mouse retina. J Comp Neurol 2003; 461:187-204. [PMID: 12724837]
29. Haverkamp S, Haeseleer F, Hendrickson A. A comparison of immunocytochemical markers to identify bipolar cell types in human and monkey retina. Vis Neurosci 2003; 20:589-600. [PMID: 15088712]
30. Haverkamp S, Ghosh KK, Hirano AA, Wassle H. Immunocytochemical description of five bipolar cell types of the mouse retina. J Comp Neurol 2003; 455:463-76. [PMID: 12508320]
31. Hu B, Yip HK, So KF. Localization of p75 neurotrophin receptor in the retina of the adult SD rat: An immunocytochemical study at light and electron microscopic levels. Glia 1998; 24:187-97. [PMID: 9728765]
32. Wei Y, Wang N, Lu Q, Zhang N, Zheng D, Li J. Enhanced protein expressions of sortilin and p75NTR in retina of rat following elevated intraocular pressure-induced retinal ischemia. Neurosci Lett 2007; 429:169-74. [PMID: 17997040]
33. Nag TC, Wadhwa S. Developmental expression of calretinin immunoreactivity in the human retina and a comparison with

Molecular Vision 2009; 15:1915-1928 <http://www.molvis.org/molvis/v15/a204> © 2009 Molecular Vision

two other EF-hand calcium binding proteins. Neuroscience 1999; 91:41-50. [PMID: 10336058]

34. Nishina S, Kohsaka S, Yamaguchi Y, Handa H, Kawakami A, Fujisawa H, Azuma N. PAX6 expression in the developing human eye. Br J Ophthalmol 1999; 83:723-7. [PMID: 10340984]
35. Georges P, Cornish EE, Provis JM, Madigan MC. Muller cell expression of glutamate cycle related proteins and anti-apoptotic proteins in early human retinal development. Br J Ophthalmol 2006; 90:223-8. [PMID: 16424538]
36. Bumsted O'Brien KM. Cheng H, Jiang Y, Schulte D, Swaroop A, Hendrickson AE. Expression of photoreceptor-specific nuclear receptor NR2E3 in rod photoreceptors of fetal human retina. Invest Ophthalmol Vis Sci 2004; 45:2807-12. [PMID: 15277507]
37. Elshatory Y, Deng M, Xie X, Gan L. Expression of the LIM-homeodomain protein Isl1 in the developing and mature mouse retina. J Comp Neurol 2007; 503:182-97. [PMID: 17480014]
38. Drager UC, Edwards DL, Barnstable CJ. Antibodies against filamentous components in discrete cell types of the mouse retina. J Neurosci 1984; 4:2025-42. [PMID: 6381660]
39. Straznicky C, Vickers JC, Gabriel R, Costa M. A neurofilament protein antibody selectively labels a large ganglion cell type in the human retina. Brain Res 1992; 582:123-8. [PMID: 1498675]
40. Chevez P, Font RL. Practical applications of some antibodies labelling the human retina. Histol Histopathol 1993; 8:437-42. [PMID: 7689369]
41. Xue LP, Lu J, Cao Q, Hu S, Ding P, Ling EA. Muller glial cells express nestin coupled with glial fibrillary acidic protein in experimentally induced glaucoma in the rat retina. Neuroscience 2006; 139:723-32. [PMID: 16458441]
42. Lambrecht HG, Koch KW. Recoverin, a novel calcium-binding protein from vertebrate photoreceptors. Biochim Biophys Acta 1992; 1160:63-6. [PMID: 1358206]
43. Hicks D, Barnstable CJ. Lectin and antibody labelling of developing rat photoreceptor cells: An electron microscope immunocytochemical study. J Neurocytol 1986; 15:219-30. [PMID: 3755163]
44. Ahmad I, Dooley CM, Thoreson WB, Rogers JA, Afiat S. In vitro analysis of a mammalian retinal progenitor that gives rise to neurons and glia. Brain Res 1999; 831:1-10. [PMID: 10411978]
45. Marquardt T, Ashery-Padan R, Andrejewski N, Scardigli R, Guillemot F, Gruss P. Pax6 is required for the multipotent state of retinal progenitor cells. Cell 2001; 105:43-55. [PMID: 11301001]
46. Sawhney N, Hall PA. Ki67–structure, function, and new antibodies. J Pathol 1992; 168:161-2. [PMID: 1460534]
47. Xiang M, Zhou L, Macke JP, Yoshioka T, Hendry SH, Eddy RL, Shows TB, Nathans J. The brn-3 family of POU-domain factors: Primary structure, binding specificity, and expression in subsets of retinal ganglion cells and somatosensory neurons. J Neurosci 1995; 15:4762-85. [PMID: 7623109]
48. Shaw G, Weber K. The intermediate filament complement of the retina: A comparison between different mammalian species. Eur J Cell Biol 1984; 33:95-104. [PMID: 6538136]
49. Volgyi B, Bloomfield SA. Axonal neurofilament-H immunolabeling in the rabbit retina. J Comp Neurol 2002; 453:269-79. [PMID: 12378587]
50. Bastianelli E, Takamatsu K, Okazaki K, Hidaka H, Pochet R. Hippocalcin in rat retina. comparison with calbindin-D28k, calretinin and neurocalcin. Exp Eye Res 1995; 60:257-66. [PMID: 7789406]
51. Sharma RK, O'Leary TE, Fields CM, Johnson DA. Development of the outer retina in the mouse. Brain Res Dev Brain Res 2003; 145:93-105. [PMID: 14519497]
52. Hendrickson A, Yan YH, Erickson A, Possin D, Pow D. Expression patterns of calretinin, calbindin and parvalbumin and their colocalization in neurons during development of macaca monkey retina. Exp Eye Res 2007; 85:587-601. [PMID: 17845803]
53. Kosaka J, Suzuki A, Morii E, Nomura S. Differential localization and expression of alpha and beta isoenzymes of protein kinase C in the rat retina. J Neurosci Res 1998; 54:655-63. [PMID: 9843156]
54. Yan XX, Wiechmann AF. Early expression of recoverin in a unique population of neurons in the human retina. Anat Embryol (Berl) 1997; 195:51-63. [PMID: 9006715]
55. Ying S, Jansen HT, Lehman MN, Fong SL, Kao WW. Retinal degeneration in cone photoreceptor cell-ablated transgenic mice. Mol Vis 2000; 6:101-8. [PMID: 10869099]
56. Elias RV, Sezate SS, Cao W, McGinnis JF. Temporal kinetics of the light/dark translocation and compartmentation of arrestin and alpha-transducin in mouse photoreceptor cells. Mol Vis 2004; 10:672-81. [PMID: 15467522]
57. Rosenzweig DH, Nair KS, Wei J, Wang Q, Garwin G, Saari JC, Chen CK, Smrcka AV, Swaroop A, Lem J, Hurley JB, Slepak VZ. Subunit dissociation and diffusion determine the subcellular localization of rod and cone transducins. J Neurosci 2007; 27:5484-94. [PMID: 17507570]
58. Butowt R, von Bartheld CS. Anterograde axonal transport of BDNF and NT-3 by retinal ganglion cells: Roles of neurotrophin receptors. Mol Cell Neurosci 2005; 29:11-25. [PMID: 15866043]
59. Rich KA, Figueroa SL, Zhan Y, Blanks JC. Effects of muller cell disruption on mouse photoreceptor cell development. Exp Eye Res 1995; 61:235-48. [PMID: 7556487]
60. Sarthy PV, Fu M, Huang J. Developmental expression of the glial fibrillary acidic protein (GFAP) gene in the mouse retina. Cell Mol Neurobiol 1991; 11:623-37. [PMID: 1723659]
61. Verderber L, Johnson W, Mucke L, Sarthy V. Differential regulation of a glial fibrillary acidic protein-LacZ transgene in retinal astrocytes and muller cells. Invest Ophthalmol Vis Sci 1995; 36:1137-43. [PMID: 7730023]
62. Chu Y, Hughes S, Chan-Ling T. Differentiation and migration of astrocyte precursor cells and astrocytes in human fetal retina: Relevance to optic nerve coloboma. FASEB J 2001; 15:2013-5. [PMID: 11511521]

The print version of this article was created on 16 September 2009. This reflects all typographical corrections and errata to the article through that date. Details of any changes may be found in the online version of the article.
1928

CHAPTER 3

ISOLATION OF RETINAL PROGENITOR AND STEM CELLS FROM THE PORCINE EYE

Reprinted from Molecular Vision **13**, 1045-1057 (2007)

Molecular Vision 2007; 13:1045-57 <http://www.molvis.org/molvis/v13/a114/>
Received 6 December 2006 | Accepted 30 May 2007 | Published 29 June 2007

©2007 Molecular Vision

Isolation of retinal progenitor and stem cells from the porcine eye

Ping Gu,[1] Laura Jayne Harwood,[1] Xiaohong Zhang,[1] Mildred Wylie,[2] William James Curry,[1] Tiziana Cogliati[1]

[1]Centre for Vision Sciences, Queens University Belfast, United Kingdom; [2]Veterinary Sciences Division, Department of Agriculture and Rural Development Northern Ireland, Belfast, United Kingdom

Purpose: Retinal progenitor cells (RPCs) and retinal stem cells (RSCs) from rodents and humans have been isolated and characterized in vitro. Transplantation experiments have confirmed their potential as tools for cell replacement in retinal degenerative diseases. The pig represents an ideal pre-clinical animal model to study the impact of transplantation because of the similarity of its eye to the human eye. However, little is known about porcine RPCs and RSCs. We aimed to identify and characterize in vitro RPCs and RSCs from porcine ocular tissues.

Methods: Cells from different subregions of embryonic, postnatal and adult porcine eyes were grown in suspension sphere culture in serum-free medium containing basic fibroblast growth factor (bFGF) and epidermal growth factor (EGF). Growth curves and BrdU incorporation assays were performed to establish the proliferative capacity of isolated porcine retina-derived RPCs and ciliary epithelium (CE)-derived RSCs. Self-renewal potential was investigated by subsphere formation assays. Changes in gene expression were assayed by reverse transcription polymerase chain reaction (RT-PCR) at different passages in culture. Finally, differentiation was induced by addition of serum to the cultures and expression of markers for retinal cell types was detected by immunohistochemical staining with specific antibodies.

Results: Dissociated cells from embryonic retina and CE at different postnatal ages generated primary nestin- and Pax6-immunoreactive neurosphere colonies in vitro in numbers that decreased with age. Embryonic and postnatal retina-derived RPCs and young CE-derived RSCs displayed self-renewal capacity, generating secondary neurosphere colonies. However, their self-renewal and proliferation capacity gradually decreased and they became more committed to differentiated states with subsequent passages. The expansion capacity of RPCs and RSCs was higher when they were maintained in monolayer culture. Porcine RPCs and RSCs could be induced to differentiate in vitro to express markers of retinal neurons and glia.

Conclusions: Porcine retina and CE contain RPCs and RSCs which are undifferentiated, self-renewing and multipotent and which show characteristics similar to their human counterparts. Therefore, the pig could be a useful source of cells to further investigate the cell biology of RPCs and RSCs and it could be used as a non-primate large animal model for pre-clinical studies on stem cell-based approaches to regenerative medicine in the retina.

Blinding degenerative diseases of the retina, such as retinitis pigmentosa (RP) and age-related macular degeneration (AMD) manifest with different pathologies and have heterogeneous genetic causes. However, they all involve the unifying feature of photoreceptor loss. Similar to the rest of the nervous system, the mammalian retina lacks the capability to self-regenerate in response to damage and there are at present no regenerative therapies available for such retinal diseases [1-4].

Recently, retinal progenitor cells (RPCs) have been identified in embryonic and newborn retina and retinal stem cells (RSCs) in adult ciliary epithelium (CE) of rodents and human [5-12]. These stem cells have the capacity for in vitro self-renewal and differentiation into retinal neurons and glia. Transplanted RPCs and RSCs can survive showing different degrees of integration into the intact and degenerating retina and can differentiate into cells expressing markers characteristic of retinal neurons [11,13-16]. Furthermore, recent studies have indicated that RSCs from adult mammalian CE can be reactivated in vivo upon growth factor administration [17]. A recent report also indicates that retinal neurons derived from transplanted RPCs are functional [18].

Work in rodents has provided an important and necessary step in understanding the cell biology of RPCs and RSCs and in exploring their regenerative potential upon transplantation. However, the rodent eye with its small size, small vitreal space and a low cone/rod ratio is less than ideal to test the efficacy and safety of transplanted stem cells before moving towards human clinical trials. On the other hand, the porcine eye is of similar size and anatomy to the human eye and its retina contains an area centralis rich in cones which resembles the human fovea [19,20]. Moreover, transplantation procedures performed on porcine eyes are comparable to those performed in the clinic [16,21]. Finally, porcine models of retinal degenerative diseases are available [22] and represent an excellent non-primate model system for pre-clinical tests of cell replacement treatments.

Neural precursor and stem cells (NPCs and NSCs) from embryonic and postnatal porcine brain have been isolated, expanded in vitro and tested for xenografts in rat models of Parkinson's disease where they survived and differentiated to

Correspondence to: Tiziana Cogliati, QUB-Centre for Vision Sciences, RVH-Institute of Clinical Science, Belfast BT12 6BA, N. Ireland, UK; Phone: +44-28-9063-2507; FAX: +44-28-9063-2699; email: T.Cogliati@qub.ac.uk

Dr. P. Gu is now at the Department of Ophthalmology, University of California, Irvine, CA.

Molecular Vision 2007; 13:1045-57 <http://www.molvis.org/molvis/v13/a114/> ©2007 Molecular Vision

form efferent and afferent synapses [23,24]. Conversely, murine RPCs have been xenografted into the porcine retina and shown integration and morphological differentiation [16]. Notably, porcine brain-derived NPCs express specific markers similar to their human counterparts [25]. Whether cells with characteristics of RPCs and RSCs exist in the porcine eye, whether they could be expanded in vitro and whether they could differentiate into specific retinal cell types remains unknown. In this study, we show that the porcine retina and adult CE harbour, respectively RPC and RSC displaying properties of self-renewal and multipotentiality.

METHODS

Animals: Mixed sex White Landrance pigs were obtained from the Department of Agriculture and Rural Development Northern Ireland, Hillsborough, UK. Embryos (n=30) were obtained from 40-week old gilts (n=3) at 50, 64, and 61 days of gestation. Neonatal pigs (1-3-week old) ranged in weight from approximately 3 kg to 7 kg. Fifteen-week old pigs were 50-55 kg in weight. All animal procedures were performed in compliance with the UK Animals (Scientific Procedures) Act 1986.

Preparation of retina for histology and immunohistochemistry: Eyes were enucleated from lethally anesthetized pigs at the indicated ages. The cornea and optic nerve were perforated to aid immersion-fixation in 4% (w/v) buffered paraformaldehyde (Sigma-Aldrich, Poole, UK) for 4-18 h at 4 °C. After cryoprotection in 5% (w/v) followed by 30% (w/v) sucrose in phosphate-buffered saline (PBS), ocular tissue specimens were embedded in optimal cutting temperature (OCT) compound (Sakura-Finetek, Zoeterwoude, NL) and snap frozen on dry ice/isopentane. Cryosections (15 μm) were thaw mounted onto Superfrost Plus glass slides (Fisher Scientific, Loughborough, UK) and stored at -80 °C until use. For histology, after haematoxylin and eosin (H &E) staining tissue sections were coversliped with DPX mounting medium and images recorded using a Nikon DXM1200 light microscope (Nikon, Kingston upon Thames, UK).

Isolation of retinal progenitor cells, retinal stem cells, and neural stem cells from porcine tissues: Eyes were enucleated from pigs at embryonic day (E)60 (n=30), postnatal day (PN)5 (n=13), (PN)21=3 weeks of age (n=9), (PN)150=21 weeks (n=20), 15-weeks (n=14), and 40-weeks (n=3) and placed in artificial cerebral spinal fluid [aCSF: 124 mM NaCl, 5 mM KCl, 1.3 mM $MgCl_2$, 26 mM $NaHCO_3$, and 10 mM D-glucose, (Sigma-Aldrich, Poole, UK)]. For E60 cultures embryos were obtained from 3 gilts (40 week old). Retinas from 5-7 embryos in a litter were combined to generate a single culture. All other cultures were generated combining tissue from two eyes of an individual animal. The neural retina was first dissected free of the optic nerve. A strip of ocular tissue containing the CE was then dissected after removal of cornea and lens. The CE was transferred into Earle's Balanced Salt Solution (EBSS) containing 2 mg/ml dispase (Sigma-Aldrich, Poole, UK) and incubated for 20 min at 37 °C. After digestion in trypsin mix [aCSF modified to contain 3.2 mM $MgCl_2$, 0.1 mM $CaCl_2$, 1.33 mg/ml trypsin, 0.67 mg/ml hyaluronidase, and 78 units/ml collagenase (Sigma-Aldrich, Poole, UK)] for 20 min at 37 °C, the CE cells were gently scraped off the basement membrane and the non-epithelial tissue was removed. Cells from the neural retina were isolated after incubation with the same enzymes for 10 min for each digestion. The suspensions containing CE and retina cells were mechanically triturated, and centrifuged at 1000 rpm for 10 min. The supernatants were removed, replaced with serum-free medium (SFM: DMEM/F12 (1:1) with 0.6% glucose, 2 mM glutamine, 5 mM HEPES buffer, 2% B27, 100 units/ml penicillin and 100 units/ml streptomycin) containing 1 mg/ml trypsin inhibitor (all from Invitrogen, Paisley, UK) and the tissue was further mechanically dissociated into single cells using a fire-polished pipette. Cell suspensions were cleared of debris with a 40 μm cell strainer (BD Biosciences, Oxford, UK), centrifuged at 1000 rpm for 10 min and resuspended in SFM. Cells were counted and plated at a density of $2x10^4$ cells/ml in T75 flasks in SFM containing either no exogenous growth factors or epidermal growth factor (EGF), basic fibroblast growth factor (bFGF), and EGF plus bFGF (Invitrogen, Paisley, UK). Cells were allowed to proliferate in suspension to form floating sphere colonies that were counted after 7 days in culture.

Brain NSCs were isolated from E60 pig embryos (n=6). Following removal of the brain, the striatum and periventricular areas were dissected and placed in ice-chilled sterile aCSF. Tissue was digested in PBS containing 1.33 mg/ml trypsin, 78 units/ml collagenase and 0.6% glucose for 10 min at 37 °C. The digest was decanted, replaced with SFM containing 1 mg/ml trypsin inhibitor, and the tissue mechanically dissociated into single cells with a fire-polished pipette. All subsequent preparation steps were the same as described above for RPCs and RSCs. Brain tissue from two pigs were combined to generate a single culture.

Sphere-forming capacity, expansion, and differentiation: Sphere-forming capacity was employed to assess the rate at which dissociated single cells proliferate to form sphere colonies. Single cells from the CE were plated at a density of no more than one cell per well in 96-well plates (confirmed under microscope after plating) in SFM containing 20 ng/ml EGF and 20 ng/ml bFGF. After 7 days in culture the wells were inspected and scored for the presence or absence of spheres.

Expansion capacity of RPCs and RSCs was assessed by using either suspension sphere or adherent culture conditions.

Table 1. List of primary antibodies used and dilutions

Primary antibody	Host	Dilution	Source
Nestin	Mouse	1:400	BD Biosciences
Pax6	Rabbit	1:1,000	Chemicon
β-tubulin III	Mouse	1:100	Chemicon
rhodopsin (4D2)	Mouse	1:100	Kind gift of R. Molday [32]
HuC/HuD	Mouse	1:200	Molecular Probes
recoverin	Rabbit	1:1,000	Kind gift of K. Koch [33]
Islet-1	Mouse	1:500	Developmental Studies Hybridoma Bank*
calbindin	Rabbit	1:1,000	SWANT
neurofilament-M	Rabbit	1:200	Chemicon
GFAP	Rabbit	1:500	Dako

*The monoclonal antibody developed by T.M. Jessell was obtained from the Developmental Studies Hybridoma Bank developed under the auspices of the NICHD and maintained by The University of Iowa, Department of Biological Sciences, Iowa City, IA-52242.

Molecular Vision 2007; 13:1045-57 <http://www.molvis.org/molvis/v13/a114/> ©2007 Molecular Vision

For suspension sphere culture cells were maintained in sphere-forming medium (SFM containing 20 ng/ml EGF and 20 ng/ml bFGF). Every 7 days RPC and RSC spheres were counted, collected, and digested in 0.05% trypsin-EDTA (Invitrogen, Paisley, UK) for 10 min at 37 °C. The cell suspension was then centrifuged at 1000 rpm for 10 min and the enzyme solution replaced with SFM containing trypsin inhibitor. Spheres were mechanically triturated into single cells with a fire-polished pipette and centrifuged at 1000 rpm for 10 min. Single cells were resuspended in sphere-forming medium and plated at a density of $2x10^4$ cells/ml in the same medium.

For adherent culture, dissociated RPC and RSC spheres were cultured in adherent culture medium [SFM containing 20 ng/ml EGF, 20 ng/ml bFGF, 2 μg/ml heparin (Invitrogen, Paisley, UK) and 5% fetal bovine serum (FBS; Invitrogen, Paisley, UK)]. Half volume of culture medium was changed every 2-3 days. After reaching 80-90% confluence, cells were treated with 0.05% trypsin-EDTA for 5 min at 37 °C and neutralized by trypsin inhibitor. Cells were then plated at a density of $5x10^4$ cells/ml in adherent culture medium.

To assay the differentiation capacity of RPCs and RSCs, whole or dissociated spheres ($2x10^4$ cells/ml) were plated on poly-D-lysine-coated (Sigma-Aldrich, Poole, UK) glass coverslips in 12-well dishes and incubated in differentiation medium (SFM with 10 ng/ml EGF, 10 ng/ml bFGF, 2 μg/ml heparin and 10% FBS) for 2-3 weeks, with medium changes every 3-4 days.

Immunostaining: Immunohistochemistry (IHC) was performed on retina cryosections and on cells grown or differentiated on coated glass coverslips. The former were thawed at room temperature and post-fixed in 4% formaldehyde (Sigma-Aldrich, Poole, UK) in PBS for 1 h at room temperature. The latter were fixed in 4% paraformaldehyde (Sigma-Aldrich, Poole, UK) for 20 min at room temperature. After washing, tissue or cells were incubated in antibody blocking buffer [PBS containing 10% (v/v) normal goat serum (NGS), 0.3% Triton X-100, 0.1% NaN_3 (Sigma-Aldrich, Poole, UK)] for 1 h at room temperature. Slides or coverlips were then incubated in primary antibodies (Table 1) for 48 h at 4 °C. After washing, incubation in fluorescent-conjugated secondary antibody (Alexa Fluor^{488}-goat anti-mouse or -goat anti-rabbit, 1:800 in PBS) was performed for 1 h at room temperature followed by washings. Cell nuclei were counterstained with 10 μg/ml propidium iodide (Sigma-Aldrich, Poole, UK) in dH_2O containing 10 μg/ml RNase A (Invitrogen, Paisley, UK) for 10-20 min at room temperature. After washing, slides were prepared for imaging with antifade mounting medium (Dako, Ely, UK). Negative IHC controls were performed in parallel by omission of the primary antibody. No fluorescent labeling was observed in the negative controls. Immunoreactive cells were visualized and images recorded using an Olympus BX60 fluorescent confocal microscope (Olympus, Europe, Hamburg, Germany).

5-Bromo-2-deoxyuridine (BrdU) incorporation and flow cytometry: Cells were cultured for 48 h in the presence of 10 μM BrdU (Sigma-Aldrich, Poole, UK), fixed in 4% paraformaldehyde for 20 min at room temperature and incubated with blocking buffer (PBS containing 10% NGS, 0.3% Triton X-100, and 100 μg/ml RNaseA) for 30 min at 37 °C. Cells were then washed in PBS, incubated with 2N HCl for 20 min at room temperature, and washed with Hanks' Balanced Salt Solutions (HBSS) followed by PBS at room temperature. After overnight incubation at 4 °C with anti-BrdU antibody (1:500, Sigma-Aldrich, Poole, UK) in blocking buffer, cells were washed in PBS, and incubated with fluorescent-conjugated secondary antibody (Alexa Fluor^{488}-goat anti-mouse, 1:500) for 1 h at room temperature. Cell nuclei were counterstained with 10 μg/ml propidium iodide for 10 min at room temperature. Immunoreactive cells were visualized and images recorded using an Olympus BX60 fluorescent confocal microscope (Olympus, Europe, Hamburg, Germany).

For quantification of BrdU-positive cells, after incubation with BrdU (see above) cells were trypsinized, washed, blocked and incubated with primary and secondary antibodies as described above and analyzed with a BD FACScalibur flow cytometer (BD Biosciences, Oxford, UK). Samples stained only with secondary antibody were used as negative control.

Reverse transcription-polymerase chain reaction: Total RNA was extracted from cultured cells at different passages as indicated using the RNeasy Mini kit according to manufacturer instruction (Qiagen, Crawley, UK) followed by in column treatment with DNase I (Qiagen, Crawley, UK). Reverse transcription was performed with Superscript™ II reverse transcriptase and random primers (Invitrogen, Paisley, UK). Amplification of β-actin served as the internal control. The primers and cycling conditions for RT-PCR are shown in Table 2.

RESULTS

Localization of nestin-immunoreactive cells in the porcine retina and ciliary epithelium: Three ages were selected for collection of porcine retinal tissue: embryonic day (E)60, when the retina is still developing [20,26]; postnatal day (PN)14, when retinal development is mostly complete [26]; and PN150 for mature adult retina. Retinal cryosections were H &E stained or immunolabeled with anti-nestin antibody to visualize the resident pool of immature neuroepithelial cells in the retina and CE (Figure 1). At PN14 (Figure 1B) retinal histology was characteristic of the mature (PN150) retina (Figure 1C) with

Table 2. List of primers and cycling conditions for RT-PCR

Gene	Primer sequence (5'-3')	Product size (bp)
Nestin[1]	F: GGCTTCTCTCAGCATCTTGG	
	R: AAGGCTGGCATAGGTGTGTC	150
β-tubulin III[2]	F: CAGAGCAAGAACAGCAGCTACTT	
	R: GTGAACTCCATCTCGTCCATGCCCTC	250
GFAP[1]	F: TTGACCTGCGACGTGGAGTC	
	R: AGGTGGCGATCTCGATGTCC	225
β-actin[2]	F: CTTCCCCTCCATCGTGGG	
	R: GTGGTACGGCCAGAGGCG	355

[1]Amplification conditions were 1 min/94 °C, 1.5 min/57 °C, 1.5 min/72 °C for 32 cycles. [2]Amplification conditions were 1 min/94 °C, 1.5 min/56°C, 1.5 min/72 °C for 30 cycles.

Molecular Vision 2007; 13:1045-57 <http://www.molvis.org/molvis/v13/a114/> ©2007 Molecular Vision

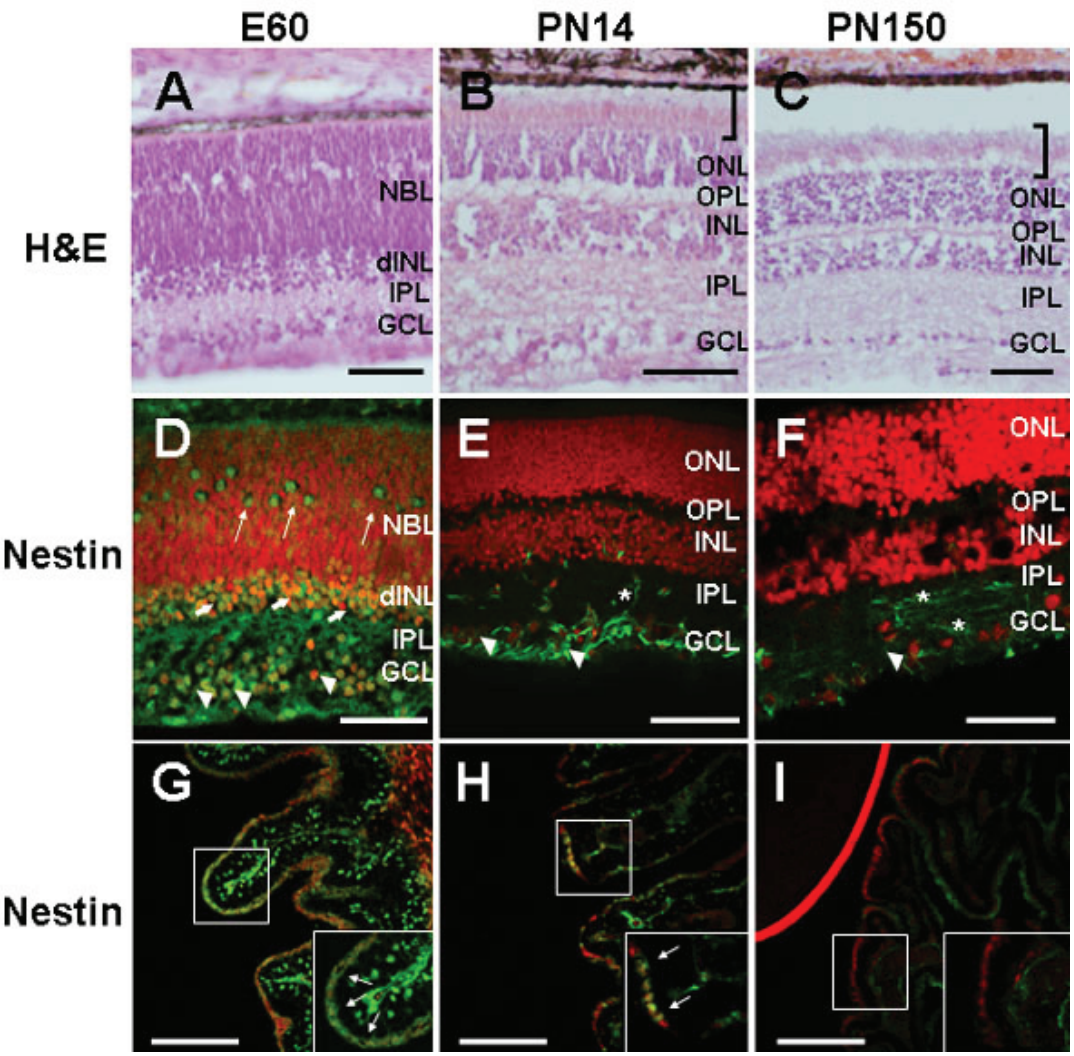


Figure 1. Identification of retinal progenitor cells and retinal stem cells in the developing and mature retina and ciliary epithelium. **A**-**C**: light microphotographs of H&E stained 15 μm retina cryosections. At PN14 (**B**) retinal histology was characteristic of the mature (PN150) retina (**C**) with each of the nuclear and plexiform layers readily identifiable. Mature outer segments of the photoreceptors (brackets) were already evident in the PN14 retina. The apparent detachment of the retina in **C** is a histological artifact. **D**-**F**: confocal fluorescent microphotographs of retina and **G**-**I**: of ciliary body (CB) cryosections (15 μm) immunostained with anti-nestin antibody (green). At E60 nestin immunoreactivity was observed in the ganglion cell layer (GCL; arrowheads), (developing) inner nuclear layer (dINL; thick arrows), neuroblast layer (NBL; thin arrows), and in the inner plexiform layer (IPL). At PN14 (**E**) nestin immunostaining was observed in the GCL (arrowheads) and IPL (asterisk). By PN150 (**F**) nestin immunoreactivity was observed in fibers in the GCL and IPL (asterisks), and in sparse cells in the GCL (arrowhead). At both E60 (**G**) and PN14 (**H**) nestin immunoreactivity was observed in cells distributed within the CB epithelium (thin arrows in insets at bottom). A higher percentage of cells with intense nestin immunostaining were observed in the E60 CB (**G**). Nestin immunoreactivity was not detected in the PN150 CB (**I**). Insets in **G**-**I** represent higher magnification images of the marked areas. Labeled stromal cells in **G** most likely represent migrating precursors of neural crest origin. The red line in I corresponds to propidium iodide (PI) staining in the adjacent lens. Nuclei were counterstained with PI (red). Scale bars: **A**, **G**-**I**, 50 μm; **D**-**F**, 100, **B**-**C**, 200 μm. ONL represents outer nuclear layer, OPL represents outer plexiform layer.

Molecular Vision 2007; 13:1045-57 <http://www.molvis.org/molvis/v13/a114/> ©2007 Molecular Vision

each of the nuclear and plexiform layers readily identifiable. Mature outer segments of the photoreceptors were already evident in the PN14 retina as compared to adult retina (bracket). At E60 (Figure 1D) nestin immunoreactivity was observed in the majority of cells in the ganglion cell layer (GCL, arrowheads) and developing inner nuclear layer (dINL, thick arrows), in a small population of cells located in the neuroblast layer (NBL, thin arrows), and in fibers in the inner plexiform layer (IPL). At PN14 immunostaining of cells in the GCL (arrowheads) and fibers in the IPL (asterisk) was observed (Figure 1E). By PN150 (Figure 1F) weak nestin immunoreactivity was detected in rare cells in the GCL (arrowhead) and in fibers in the GCL and IPL (asterisks). These observations are in agreement with the presence of nestin immunoreactive cells in the adult human retina previously described [27]. At both E60 (Figure 1G) and PN14 (Figure 1H) nestin immunoreactivity was observed in cell bodies distributed within the ciliary body (CB, thin arrows), the anatomical structure comprising the CE. A higher percentage of cells with intense immunostaining were detected at E60 than in PN14 CB (compare panels G and H). Specific nestin immunoreactivity was not observed in the PN150 CB (Figure 1I). Thus, undifferentiated nestin-immunoreactive cells were present in the developing retina and CB and their proportion decreased as retinal development progressed.

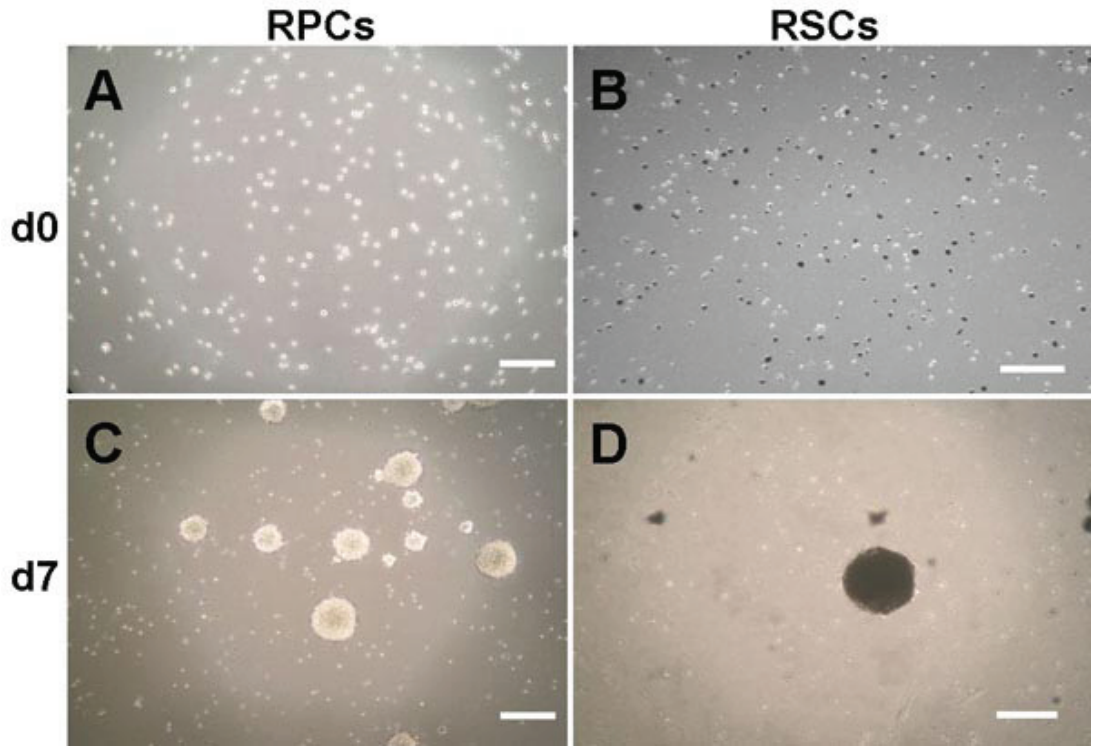
Isolation and expansion of retina-derived retinal progenitor cells and ciliary epithelium-derived retinal stem cells: Ocular tissues from embryonic, newborn, and adult pig eyes were dissected to isolate and culture in vitro RPCs from E60, PN5, PN21, and PN150=21 week old retina and RSCs from 3, 15, and 45 week old CE (Figure 2A,B). Three days after plating, small primary sphere colonies could be observed that continued to expand and, after 7 days, generated relatively large colonies, up to 300 μm in diameter (Figure 2C,D). Spheres derived from dissociation of CE contained both pigmented and non-pigmented progeny (Figure 2D). The number of primary spheres did not increase when the cultures were maintained in culture for another two weeks.

Cells proliferated to form clonal primary spheres in the absence of exogenous growth factors. To establish the effect of mitogens on cell growth, $2x10^4$ 3 week old CE-derived cells were plated in 12 multi-well plates in sphere-forming medium with or without 20 ng/ml EGF and 20 ng/ml bFGF, alone or in combination and cultured for seven days. bFGF increased by 4 times the proportion of cells forming clonal primary spheres in vitro (from 9.7±1.53 spheres/well in SFM, n=3 to 41.3±6.03 spheres/well in SFM+bFGF, n=3). When both EGF and bFGF were added to the culture medium, the number of primary sphere colonies did not increase compared to bFGF alone (42.3±7.37 spheres/well, n=3). The total number of spheres generated from dissociated retinae and maintained in the presence of EGF and bFGF was highest at E60 and decreased with increasing age to less than three spheres generated from 10^6 dissociated retinal cells at PN150 (Figure 2E). Similarly, the total number of primary spheres generated by cells dissociated from 3 week old CE was greater than those from 15 and 45 week old porcine CE (Figure 2F). The latter two generated a similar number of primary spheres suggesting that the number of cells with potential to proliferate in vitro remains constant throughout adult age. The sphere-forming capacity of 3 week old CE-derived cells was further assayed by plating in sphere-forming medium at a density of one cell per well in individual 96-well dishes. After 7 days in culture, a single sphere was observed in 3 out of 948 wells. This indicated that approximately 0.3% of porcine 3 week old (PN21) CE-derived cells were capable of self-renewal and of forming primary sphere colonies. All subsequent experiments were performed with E60 retina-derived (RPCs) and 3 week old CE-derived cells maintained in cultures enriched with EGF and bFGF.

Immunostaining of RPCs at passage (P)2 and of RSCs at P3 showed that the majority of cells within the RPC and RSC spheres were nestin- and Pax6-positive, revealing their undifferentiated phenotype (Figure 3A,B). To investigate the expandability and self-renewal potential of RPCs and RSCs their sub-sphere-forming capacity was assessed at each passage in culture. Spheres were counted, dissociated into single cells and cultured in sphere-forming medium for seven days before new sphere counts were taken. RSCs from one eye generated on average 1,773±619 primary sphere colonies which could be expanded to 65,267±8,684 sphere colonies within four passages in vitro (Figure 3D). RSC spheres could be maintained in vitro up to P10 (the longest sphere culture attempted). The total number of spheres increased up to P4, and decreased during subsequent passages. The average number of secondary spheres derived from one sphere at P1 was 4.6±1.65, it then dropped gradually to the ratio of one sphere giving rise to less than one sphere at P5 (0.99±0.076) and P6 (0.81±0.128). Furthermore, both the average sphere size and the number of pigmented cells within the spheres appeared reduced with passages (data not shown). Similarly, RPC spheres derived from dissociated E60 retinas could be subcultured in vitro (Figure 3C) up to P4 (the longest sphere culture attempted). However, the total number of spheres gradually decreased with passages and the average number of new spheres formed from dissociation of each single sphere at each passage ranged from 0.6±0.04 at P1 to 0.2±0.19 at P4. Attempts to subculture spheres derived from PN5, PN21, and PN150 retinae were unsuccessful. NSCs isolated from porcine E60 brains were cultured for comparison. As expected, primary spheres derived from brain NSCs generated subspheres continuously at a ratio of one sphere producing approximately eight new spheres at each passage (data not shown).

RT-PCR analysis of mRNA from RPC and RSC spheres at different passages in vitro was performed to investigate changes in expression of undifferentiated and differentiated cell markers. While expression of nestin decreased, expression of β-tubulin III (marker of differentiated neuronal cells) and of glial fibrillary acidic protein (GFAP, marker of differentiated glial cells) increased with increasing passages (Figure 3E,F). Together with the sphere subculture experiment, changes in gene expression suggested that increasing numbers of cells within the spheres had differentiated. This high-

Molecular Vision 2007; 13:1045-57 <http://www.molvis.org/molvis/v13/a114/> ©2007 Molecular Vision



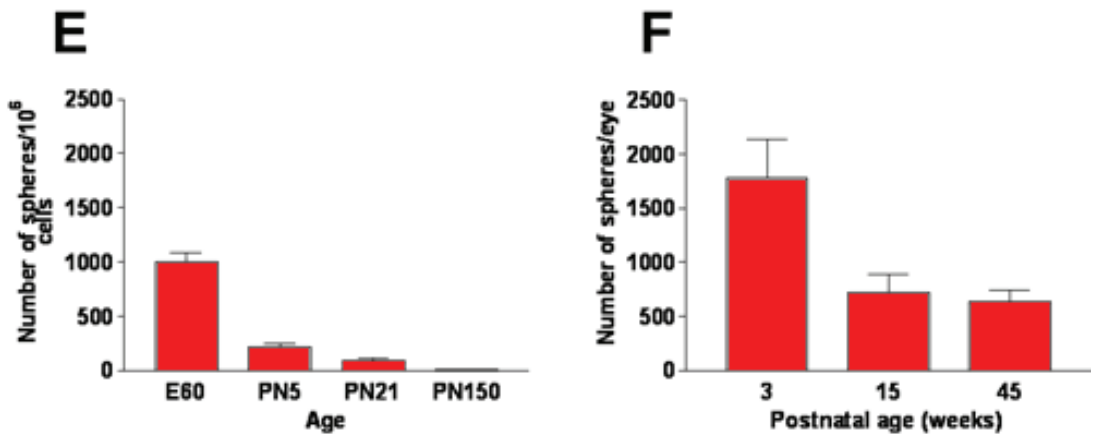


Figure 2. Primary sphere formation in serum-free medium in vitro. **A**: single cells from primary cultures of dissociated E60 retina-derived cells and **B**: of 3 week old ciliary epithelium (CE)-derived cells at day 0. Dissociated CE cultures comprise pigmented and non-pigmented cells (**B**). **C**, **D**: primary sphere colonies at day 7 after plating, showing pigmented spheres in CE-derived RSC cultures (**D**). Scale bars represent 200 µm. **E**, **F**: number of primary spheres formed from retina (**E**) and CE-derived (**F**) primary cultures at different ages. Three week old CE cultures generated more primary spheres than those from 15 and 45 week old pigs (**F**). Data are expressed as mean±SD from three independent experiments.

Molecular Vision 2007; 13:1045-57 <http://www.molvis.org/molvis/v13/a114/> ©2007 Molecular Vision

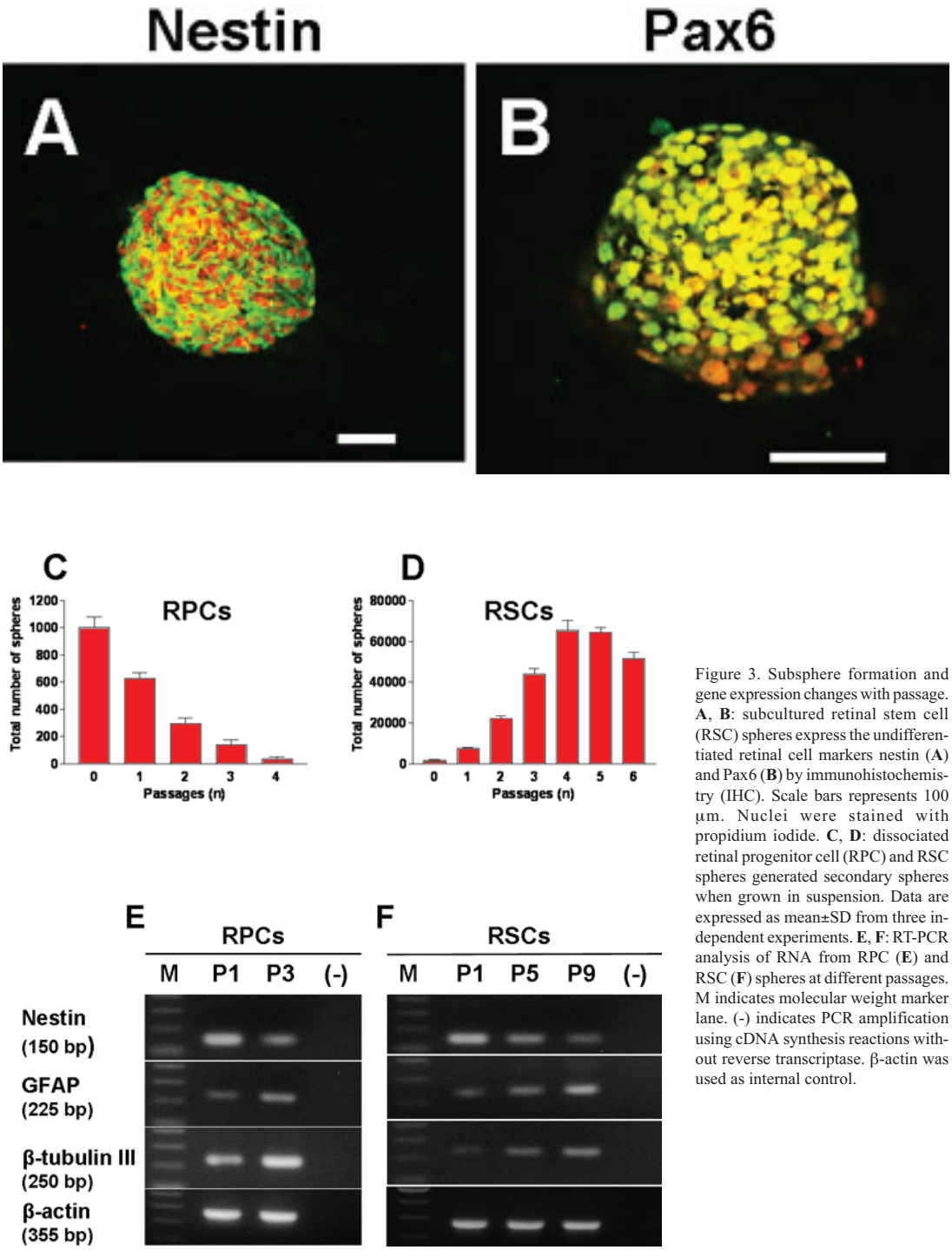


Figure 3. Subsphere formation and gene expression changes with passage. **A**, **B**: subcultured retinal stem cell (RSC) spheres express the undifferentiated retinal cell markers nestin (**A**) and Pax6 (**B**) by immunohistochemistry (IHC). Scale bars represents 100 μm. Nuclei were stained with propidium iodide. **C**, **D**: dissociated retinal progenitor cell (RPC) and RSC spheres generated secondary spheres when grown in suspension. Data are expressed as mean±SD from three independent experiments. **E**, **F**: RT-PCR analysis of RNA from RPC (**E**) and RSC (**F**) spheres at different passages. M indicates molecular weight marker lane. (-) indicates PCR amplification using cDNA synthesis reactions without reverse transcriptase. β-actin was used as internal control.

Molecular Vision 2007; 13:1045-57 <http://www.molvis.org/molvis/v13/a114/> ©2007 Molecular Vision

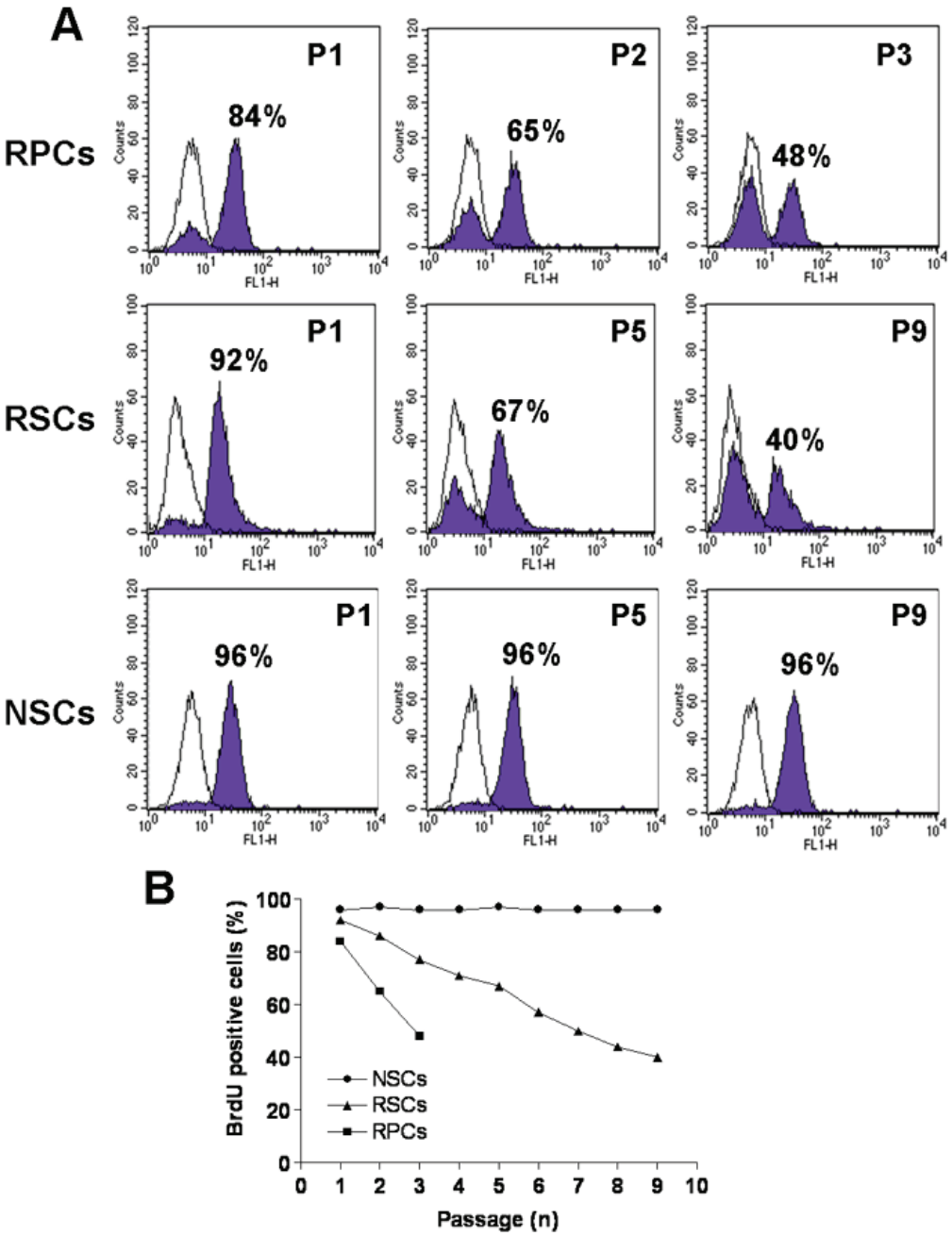


Figure 4. BrdU incorporation of retinal progenitor cell, retinal stem cell, and neural stem cell spheres at different passages. **A**: 84% and 92% of cells within retinal progenitor cell (RPC) and retinal stem cell (RSC) spheres, respectively were positive for BrdU at P1. The proportion of BrdU-positive cells decreased with increasing passages to less than 50% at P3 for RPCs and P9 for RSCs. The proportion of BrdU-positive cells within brain NSC-spheres remained constant at around 96% from P1 to P9. For each plot the shaded profile shows counts of cells after BrdU labeling detected by FACS, the white profile represents counts of control cells reacted with secondary antibody only. Individual values at each passage are plotted in **B**.

Molecular Vision 2007; 13:1045-57 <http://www.molvis.org/molvis/v13/a114/> ©2007 Molecular Vision

lighted the limited self-renewal potential of CE-derived RSCs and even more so of retina-derived RPCs.

To assess if the proliferative capacity of CE-derived RSCs and of retina-derived RPCs changed under suspension sphere culture conditions the percentage of proliferative cells in the spheres was quantified by combining incorporation of the thymidine analog bromodeoxyuridine (BrdU) and FACS analysis (Figure 4). Cultures of porcine embryonic brain NSCs were used as control in this experiment as NSCs from other species are known to proliferate for prolonged periods of time in vitro. Approximately 84% of the cells derived from RPC spheres and 92% of cells derived from RSC spheres at P1 incorporated BrdU (Figure 4A). The percentage of BrdU-positive cells decreased with increasing passages and less than 50% of the cells were labeled with BrdU in cultures of RPCs at P3 and of RSCs at P9 (Figure 4B). On the contrary, the proportion of BrdU-positive cells within brain NSC spheres remained constant at around 96% from P1 to P9.

Monolayer culture conditions have been shown to facilitate expansion of RPCs and RSCs numbers in vitro [11,28]. The expansion capacity of porcine RPCs and RSCs grown in monolayer was compared to that of cells grown as suspended spheres. Approximately $6x10^5$ RPCs were generated within three passages from 10^5 cells under adherent culture conditions compared to $2.4x10^4$ cells in the suspension sphere cultures. Similarly, more than $5x10^{11}$ RSCs were generated from $5x10^4$ cells after 10 passages in monolayer culture conditions.

Differentiation in vitro of retinal stem cells and retinal progenitor cells: Under differentiation conditions RPCs at P2 and RSCs at P3 showed morphological hallmarks of neural differentiation and expressed retinal neuronal and glial markers (Figure 5). Some cells had a small soma and several long, thin cell processes (Figure 5A, thin arrows), often connected to each other (thick arrows). A small number of cells were large and polygonal in shape (arrowhead). Expression of undifferentiated and retinal cell-specific markers was investigated by IHC with specific antibodies (Figure 5B-L). Approximately 65-70% of RSCs initiated differentiation as indicated by the number of nestin-negative cells counted (Figure 5B). The coincidental expression of Pax6 in retinal progenitors and differentiated amacrine cells makes it difficult to establish the degree of differentiation using this marker which resulted positive in 32±4.7% of cells (Figure 5C). Differentiated RSCs were immunoreactive for the glial cell marker GFAP (19±4.9%, Figure 5D) and for the neuronal marker neurofilament-M (12±4.0%, Figure 5E). Rare cells (less than 1%) expressed the cone and rod photoreceptor marker recoverin (Figure 5G), the rod photoreceptor-specific marker rhodopsin (Figure 5H), the marker of newborn horizontal, amacrine, and RGCs HuC/HuD (Figure 5F), the interneuron and RGC marker Islet-1 (Figure 5I), and the horizontal cell marker calbindin (Figure 5L). Cells immunoreactive for a specific antibody tended to appear in clusters. Thus, microphotographs document the quality of the immunostaining rather than the proportion of labeled cells. For comparison, E60 retina-derived RPCs at P2 were also differentiated in the presence of serum (see representative immunostaining with the antibodies against recoverin and rhodopsin in Figure 5J and K, respectively) and the proportion of cells immunopositive with retina-specific markers was counted (Figure 6). CE-derived RSCs seemed to possess the potential to differentiate along retinal neuronal and glial cell lineages in vitro in percentages that were comparable to those obtained for E60 retina-derived RPCs (compare GFAP, and neurofilament-M). However, the proportion of cells expressing the photoreceptor markers recoverin and rhodopsin was lower in CE-derived differentiated RSC cultures.

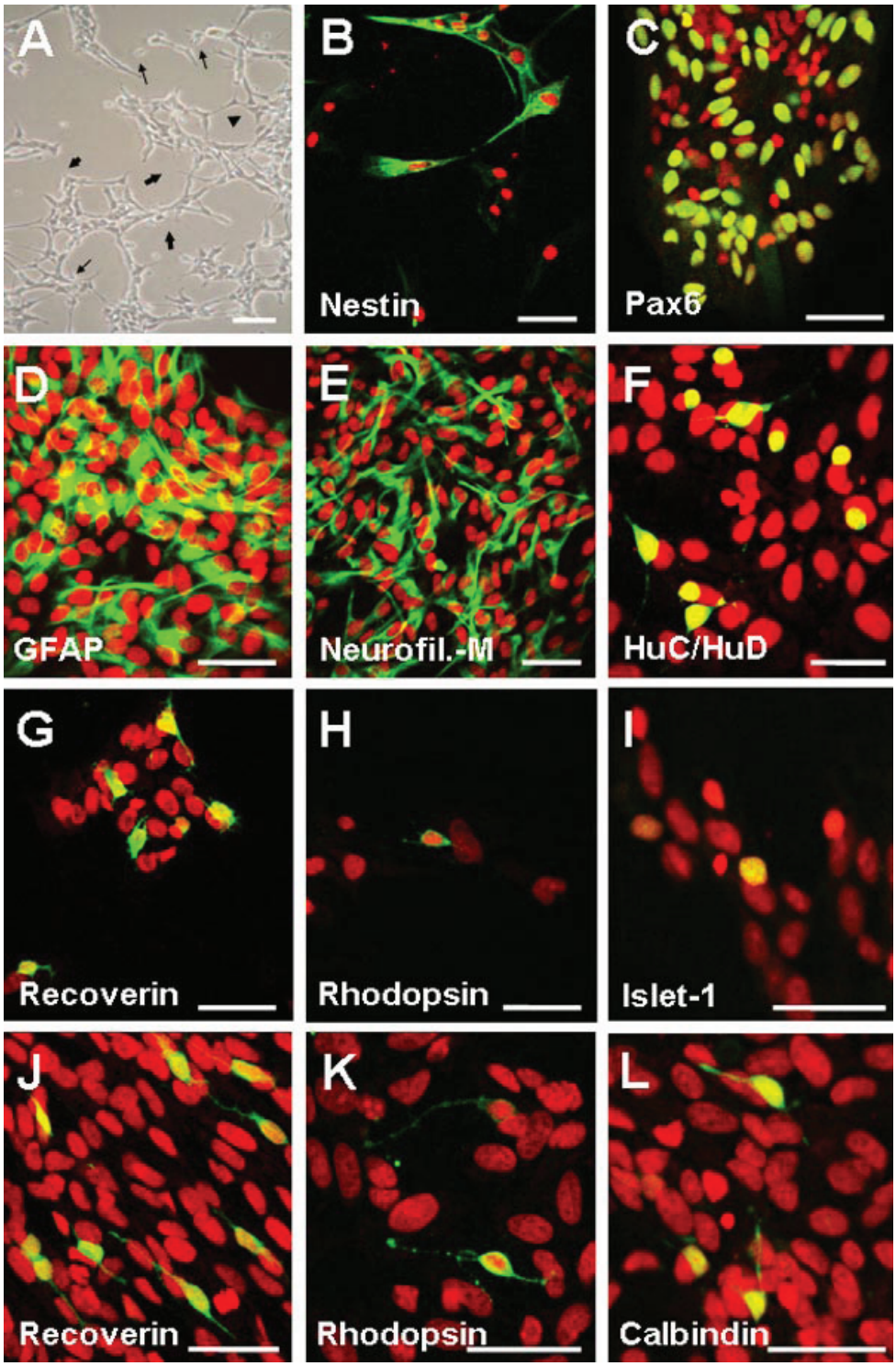
DISCUSSION

The present study describes the isolation and initial in vivo and in vitro characterization of porcine retina-derived RPCs and CE-derived RSCs. The porcine eye was chosen because of its similar size, anatomy, and histology to the human eye [19,20]. Furthermore, retinal development in the pig shows substantial similarities to human retinal development [26]. These characteristics make the pig an ideal pre-clinical animal model for transplantation experiments.

Our data indicates that the highest yields of RPCs and RSCs can be obtained from dissociated E60 retina and 3 week-old CE, respectively. Porcine RPCs and RSCs displayed properties similar to those isolated from rodent and human. RPCs were derived from adult (PN150) retina at a frequency of approximately $1:3.5x10^6$, which is comparable to the 1:2.0-$3.0x10^6$ ratio obtained for adult human RPCs [12]. Similarly, RSCs were derived from porcine 3 week-old CE at a frequency of approximately 1:350, comparable to the 1:600 ratio in human [11]. Together these data indicate that the proportion of RPCs in the retina and of RSCs in the CE are conserved between pig and human. In apparent contrast with the data on human CE-derived RSCs [11], our data showed a decrease in

Figure 5 (next page). Multipotentiality of retinal stem cells and retinal progenitor cells. Retinal progenitor cells (RPCs) and retinal stem cells (RSCs) were plated on coverslips coated with poly-D-lysine and incubated in differentiation medium for 2 weeks. **A**: phase contrast microphotograph of serum-treated RPCs showing cells with small bodies and elongated dendritic processes (thin arrows), some apparently connected (thick arrows) as well as cells with large, polygonal shapes (arrowhead) to indicate morphological changes associated with neuronal and glial differentiation. **B-I**, **L**: RSCs maintained in differentiation medium for 2 weeks were fixed and immunostained with antibodies to: nestin (**B**); Pax6 (retinal progenitors, amacrine cells; **C**); GFAP (glial cells; **D**); neurofilament-M (RGCs, interneurons; **E**); HuC/HuD (horizontal, amacrine cells; **F**); recoverin (cone and rod photoreceptors; **G**); rhodopsin (rod photoreceptors; **H**); Islet-1 (bipolar, amacrine cells **I**); and calbindin (horizontal, amacrine, RGCs; **L**). **J-K**: RPCs maintained in differentiated medium for two weeks were fixed and immunostained with antibodies to: recoverin (**J**), and rhodopsin (**K**). Cells expressing the same marker differentiated in clusters. Thus, microphotographs of recoverin and rhodopsin immunostaining in RPCs and RSCs are not for quantitative comparison and are not representative of the counts reported in Figure 6. Nuclei were stained with propidium iodide. Scale bars: **A**, **C**, and **F** represents 100 μm; **B**, **D-E**, and **G-K** represents 50 μm.

Molecular Vision 2007; 13:1045-57 <http://www.molvis.org/molvis/v13/a114/> ©2007 Molecular Vision



Molecular Vision 2007; 13:1045-57 <http://www.molvis.org/molvis/v13/a114/> ©2007 Molecular Vision

the frequency of RSCs obtained from adult (15 and 45 week old) CE compared to newborn. This difference reflected the presence of higher proportions of nestin-positive cells in the porcine CE at two weeks (PN14) compared to 21 weeks (PN150). The pool of undifferentiated cells at PN14 might be a transitional, short lived pool which persists only shortly after birth and it might be a peculiarity of the developmental process in the pig which requires further investigation.

Under sphere-forming culture conditions, the expansion capacity of CE-derived RSCs was initially comparable to that of brain-derived NSCs but decreased with increasing passages. On the other hand, retina-derived RPCs exhibited a more restricted expansion capacity when compared to CE-derived RSCs and could not be maintained for more than a few passages in suspension sphere cultures. This study employed for the first time BrdU incorporation assay in association with flow cytometry to quantify the number of proliferating RPCs, RSCs and NSCs across different passages. Besides establishing a quantitative approach to determine proliferation in culture, these experiments showed that the proportion of cells within the RPC and RSC spheres that synthesized DNA during a 48 h period decreased with time in culture while the proportion of proliferating brain-derived NSCs remained constant. This suggests that some of the cells within the RPC/RSC spheres had stopped proliferating and had undergone differentiation, or had longer doubling times at late passages in culture. Gene expression analysis suggested that the decrease in cell proliferation was in fact associated with an increase in cell differentiation. These results support the notion that RPCs and RSCs exhibit a restricted self-renewal potential compared to NSCs [8,29]. Whether the limited self-renewal is an intrinsic characteristic or it is determined by culture conditions remains to be established. Notably, the expansion capacity of porcine RPCs and RSCs maintained in monolayer cultures was increased, as it has been shown also for rodent and human cells [7,11,28]. Conclusive evidence awaits the identification of markers that unequivocally distinguish between progenitor and stem cell populations.

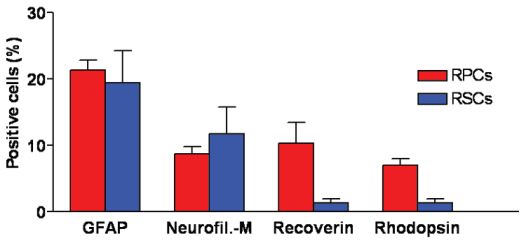


Figure 6. Quantification of E60 retina-derived retinal progenitor cells and 3 week old ciliary epithelium-derived retinal stem cells displaying distinct immunoreactivity after serum-induced differentiation in vitro. Dissociated retinal progenitor cell (RPC) and retinal stem cell (RSC) spheres were incubated in differentiation medium for two weeks, fixed, and immunostained with the indicated antibodies. Quantification was performed by recording the number of immunopositive cells over the number of nuclei counterstained with PI in random fields. Two hundred-1,000 cells for each immunostaining reaction for each culture were counted. Differentiated cells manifested retinal neural phenotypes in different proportions as indicated. A relatively large percentage of cells in both cultures displayed GFAP immunoreactivity. Data represent the mean±SD of three independent experiments.

Assessing the differentiated phenotype of porcine retina-derived RPCs and CE-derived RSCs had two scopes: to establish their multipotentiality and to investigate their potential to generate retinal cell types which would render them useful for transplantation experiments. Since porcine CE-derived RSCs have the potential to give rise to different retinal cell phenotypes, but predominantly earlier-born (neurofilament-M-immunoreactive neurons), it implies that CE-derived RSCs possess properties of early RPCs. This hypothesis is also supported by a recent report indicating that mouse CE-derived RSCs have more characteristics (e.g. proliferative capacity, potential to generate retinal cell phenotypes, and gene expression pattern) in common with early retinal progenitors than late retinal progenitors [30]. This report also suggests that CE-derived RSCs may be a residual population of stem cells from the optic neuroepithelium, representing a stage antecedent to retinal progenitors. This could be the case also for porcine CE-derived cells. However, whether the CE-derived RSC population is composed of pure early progenitor cells or of heterogeneous subsets of progenitors with distinct competencies still remains to be established since CE-derived RSCs also gave rise to cells expressing markers for late born neurons (e.g. GFAP for glial cells, rhodopsin for rod photoreceptors, and recoverin for cone and rod photoreceptors). Ultimately, the low proportion of rhodopsin-positive cells observed under the present differentiation protocol is a limitation that needs to be addressed in view of potential therapeutic approaches. Recently, the adoption of "priming" protocols has generated high yields of mouse retina-derived RSCs committed to the photoreceptor fate [31]. Similar approaches could be applied to drive photoreceptor-specific commitment from porcine CE-derived RSCs.

In summary, RPCs and RSCs from the porcine eye can be expanded in culture, differentiate in vitro to express markers specific to retinal cell types and show remarkable similarity to their human counterpart. The availability of a pre-clinical model (the pig) whose eye is comparable in size, anatomy, and histology to the human eye can benefit the advancement of the efforts leading to RPC and RSC transplantation in the diseased human eye. Our study opens the way to further characterization of porcine-derived RPCs and RSCs in vitro to investigate the molecular mechanisms regulating their proliferation and differentiation. In the future, in vivo allotransplantation of porcine RSCs using available porcine models of retinal degeneration [22] will reveal their capacity to survive, integrate and differentiate to promote cell repair. Furthermore, the use of the pig model would facilitate pre-clinical development of surgical procedures which could be directly utilized for cell transplantations in the diseased human retina.

Molecular Vision 2007; 13:1045-57 <http://www.molvis.org/molvis/v13/a114/> ©2007 Molecular Vision

ACKNOWLEDGEMENTS

We thank R. Fiocco and M. Ader for advice on RSC cultures, and R. Molday and K. Koch for kindly providing the anti-rhodopsin and anti-recoverin antibodies, respectively, T. Gardiner for help with the confocal microscope, M. Ader, B. Kennedy, M. Gadina, T. Gardiner, and D. McCance for critically reading this manuscript. This work was supported by grants from the Research and Regional Services, Northern Ireland and by funding generously provided by the Fraser Homes Foundation, Northern Ireland and by Fighting Blindness, Republic of Ireland. PG was supported by an ORS Award.

REFERENCES

1. Berson EL. Retinitis pigmentosa and allied diseases. In: Albert DM, Jakobiec FA, editors. Principles and practice of ophthalmology: clinical practice. Philadelphia: Saunders; 1994. p. 1214-37.
2. Mendes HF, van der Spuy J, Chapple JP, Cheetham ME. Mechanisms of cell death in rhodopsin retinitis pigmentosa: implications for therapy. Trends Mol Med 2005; 11:177-85.
3. Hogg RE, Chakravarthy U. Visual function and dysfunction in early and late age-related maculopathy. Prog Retin Eye Res 2006; 25:249-76.
4. Rattner A, Nathans J. Macular degeneration: recent advances and therapeutic opportunities. Nat Rev Neurosci 2006; 7:860-72.
5. Ahmad I, Dooley CM, Thoreson WB, Rogers JA, Afiat S. In vitro analysis of a mammalian retinal progenitor that gives rise to neurons and glia. Brain Res 1999; 831:1-10.
6. Yang P, Seiler MJ, Aramant RB, Whittemore SR. In vitro isolation and expansion of human retinal progenitor cells. Exp Neurol 2002; 177:326-31.
7. Klassen H, Ziaeian B, Kirov II, Young MJ, Schwartz PH. Isolation of retinal progenitor cells from post-mortem human tissue and comparison with autologous brain progenitors. J Neurosci Res 2004; 77:334-43.
8. Engelhardt M, Wachs FP, Couillard-Despres S, Aigner L. The neurogenic competence of progenitors from the postnatal rat retina in vitro. Exp Eye Res 2004; 78:1025-36.
9. Tropepe V, Hitoshi S, Sirard C, Mak TW, Rossant J, van der Kooy D. Direct neural fate specification from embryonic stem cells: a primitive mammalian neural stem cell stage acquired through a default mechanism. Neuron 2001; 30:65-78.
10. Ahmad I, Tang L, Pham H. Identification of neural progenitors in the adult mammalian eye. Biochem Biophys Res Commun 2000; 270:517-21.
11. Coles BL, Angenieux B, Inoue T, Del Rio-Tsonis K, Spence JR, McInnes RR, Arsenijevic Y, van der Kooy D. Facile isolation and the characterization of human retinal stem cells. Proc Natl Acad Sci U S A 2004; 101:15772-7.
12. Mayer EJ, Carter DA, Ren Y, Hughes EH, Rice CM, Halfpenny CA, Scolding NJ, Dick AD. Neural progenitor cells from postmortem adult human retina. Br J Ophthalmol 2005; 89:102-6.
13. Kinouchi R, Takeda M, Yang L, Wilhelmsson U, Lundkvist A, Pekny M, Chen DF. Robust neural integration from retinal transplants in mice deficient in GFAP and vimentin. Nat Neurosci 2003; 6:863-8.
14. Klassen HJ, Ng TF, Kurimoto Y, Kirov I, Shatos M, Coffey P, Young MJ. Multipotent retinal progenitors express developmental markers, differentiate into retinal neurons, and preserve light-mediated behavior. Invest Ophthalmol Vis Sci 2004; 45:4167-73.
15. Qiu G, Seiler MJ, Mui C, Arai S, Aramant RB, de Juan E Jr, Sadda S. Photoreceptor differentiation and integration of retinal progenitor cells transplanted into transgenic rats. Exp Eye Res 2005; 80:515-25.
16. Warfvinge K, Kiilgaard JF, Lavik EB, Scherfig E, Langer R, Klassen HJ, Young MJ. Retinal progenitor cell xenografts to the pig retina: morphologic integration and cytochemical differentiation. Arch Ophthalmol 2005; 123:1385-93.
17. Abdouh M, Bernier G. In vivo reactivation of a quiescent cell population located in the ocular ciliary body of adult mammals. Exp Eye Res 2006; 83:153-64.
18. MacLaren RE, Pearson RA, MacNeil A, Douglas RH, Salt TE, Akimoto M, Swaroop A, Sowden JC, Ali RR. Retinal repair by transplantation of photoreceptor precursors. Nature 2006; 444:203-7.
19. Hendrickson A, Hicks D. Distribution and density of medium- and short-wavelength selective cones in the domestic pig retina. Exp Eye Res 2002; 74:435-44.
20. Engelsberg K, Johansson K, Ghosh F. Development of the embryonic porcine neuroretina in vitro. Ophthalmic Res 2005; 37:104-11.
21. Del Priore LV, Tezel TH, Kaplan HJ. Survival of allogeneic porcine retinal pigment epithelial sheets after subretinal transplantation. Invest Ophthalmol Vis Sci 2004; 45:985-92.
22. Petters RM, Alexander CA, Wells KD, Collins EB, Sommer JR, Blanton MR, Rojas G, Hao Y, Flowers WL, Banin E, Cideciyan AV, Jacobson SG, Wong F. Genetically engineered large animal model for studying cone photoreceptor survival and degeneration in retinitis pigmentosa. Nat Biotechnol 1997; 15:965-70.
23. Armstrong RJ, Tyers P, Jain M, Richards A, Dunnett SB, Rosser AE, Barker RA. Transplantation of expanded neural precursor cells from the developing pig ventral mesencephalon in a rat model of Parkinson's disease. Exp Brain Res 2003; 151:204-17.
24. Uchida K, Okano H, Hayashi T, Mine Y, Tanioka Y, Nomura T, Kawase T. Grafted swine neuroepithelial stem cells can form myelinated axons and both efferent and afferent synapses with xenogeneic rat neurons. J Neurosci Res 2003; 72:661-9.
25. Schwartz PH, Nethercott H, Kirov II, Ziaeian B, Young MJ, Klassen H. Expression of neurodevelopmental markers by cultured porcine neural precursor cells. Stem Cells 2005; 23:1286-94.
26. De Schaepdrijver L, Lauwers H, Simoens P, de Geest JP. Development of the retina in the porcine fetus. A light microscopic study. Anat Histol Embryol 1990; 19:222-35.
27. Mayer EJ, Hughes EH, Carter DA, Dick AD. Nestin positive cells in adult human retina and in epiretinal membranes. Br J Ophthalmol 2003; 87:1154-8.
28. Yang P, Seiler MJ, Aramant RB, Whittemore SR. Differential lineage restriction of rat retinal progenitor cells in vitro and in vivo. J Neurosci Res 2002; 69:466-76.
29. Inoue T, Kagawa T, Fukushima M, Shimizu T, Yoshinaga Y, Takada S, Tanihara H, Taga T. Activation of canonical Wnt pathway promotes proliferation of retinal stem cells derived from adult mouse ciliary margin. Stem Cells 2006; 24:95-104.
30. Das AV, James J, Rahnenfuhrer J, Thoreson WB, Bhattacharya S, Zhao X, Ahmad I. Retinal properties and potential of the adult mammalian ciliary epithelium stem cells. Vision Res 2005; 45:1653-66.
31. Merhi-Soussi F, Angenieux B, Canola K, Kostic C, Tekaya M, Hornfeld D, Arsenijevic Y. High yield of cells committed to the photoreceptor fate from expanded mouse retinal stem cells. Stem Cells 2006; 24:2060-70.

Molecular Vision 2007; 13:1045-57 <http://www.molvis.org/molvis/v13/a114/> ©2007 Molecular Vision

32. Hicks D, Molday RS. Differential immunogold-dextran labeling of bovine and frog rod and cone cells using monoclonal antibodies against bovine rhodopsin. Exp Eye Res 1986; 42:55-71.
33. Lambrecht HG, Koch KW. Recoverin, a novel calcium-binding protein from vertebrate photoreceptors. Biochim Biophys Acta 1992; 1160:63-6.

The print version of this article was created on 29 Jun 2007. This reflects all typographical corrections and errata to the article through that date. Details of any changes may be found in the online version of the article.

CHAPTER 4

PREDICTION OF MICRO-RNAs AFFECTING mRNA EXPRESSION DURING RETINAL DEVELOPMENT

Reprinted from BMC Developmental Biology **10**, 1-15 (2010)

Arora et al. BMC Developmental Biology 2010, 10:1
http://www.biomedcentral.com/1471-213X/10/1

BMC Developmental Biology

RESEARCH ARTICLE Open Access

Prediction of microRNAs affecting mRNA expression during retinal development

Amit Arora†, Jasenka Guduric-Fuchs†, Laura Harwood, Margaret Dellett, Tiziana Cogliati, David A Simpson*

Abstract

Background: MicroRNAs (miRNAs) are small RNA molecules (~22 nucleotides) which have been shown to play an important role both in development and in maintenance of adult tissue. Conditional inactivation of miRNAs in the eye causes loss of visual function and progressive retinal degeneration. In addition to inhibiting translation, miRNAs can mediate degradation of targeted mRNAs. We have previously shown that candidate miRNAs affecting transcript levels in a tissue can be deduced from mRNA microarray expression profiles. The purpose of this study was to predict miRNAs which affect mRNA levels in developing and adult retinal tissue and to confirm their expression.

Results: Microarray expression data from ciliary epithelial retinal stem cells (CE-RSCs), developing and adult mouse retina were generated or downloaded from public repositories. Analysis of gene expression profiles detected the effects of multiple miRNAs in CE-RSCs and retina. The expression of 20 selected miRNAs was confirmed by RT-PCR and the cellular distribution of representative candidates analyzed by *in situ* hybridization. The expression levels of miRNAs correlated with the significance of their predicted effects upon mRNA expression. Highly expressed miRNAs included miR-124, miR-125a, miR-125b, miR-204 and miR-9. Over-expression of three miRNAs with significant predicted effects upon global mRNA levels resulted in a decrease in mRNA expression of five out of six individual predicted target genes assayed.

Conclusions: This study has detected the effect of miRNAs upon mRNA expression in immature and adult retinal tissue and cells. The validity of these observations is supported by the experimental confirmation of candidate miRNA expression and the regulation of predicted target genes following miRNA over-expression. Identified miRNAs are likely to be important in retinal development and function. Misregulation of these miRNAs might contribute to retinal degeneration and disease. Conversely, manipulation of their expression could potentially be used as a therapeutic tool in the future.

Background

miRNAs are small RNA molecules of 18-22 nucleotides in length which regulate gene expression. Precursor RNAs transcribed either as independent genes or within introns of coding genes are processed by the RNAseIII enzymes Drosha and Dicer to form the mature miRNAs [1]. The first miRNAs were discovered as a result of their role in the timing of adult cell fate determination in *Caenorhabditis elegans*. Both *let-7* and *lin-4* are temporally regulated and cause a decrease in expression of target proteins which control developmental stage-specific events [2-4]. The significance of miRNAs in developmental processes has now been shown in many plants and animals [5].

There is growing evidence that miRNAs play an important role in regulating eye development and function. In the mouse, prevention of miRNA maturation by conditional knockout in retinal tissue of the Dicer protein resulted in formation of photoreceptor rosettes and retinal degeneration and had a profound effect upon visual function, as measured by electroretinogram (ERG) [6]. Li and Carthew reported reciprocal negative regulation between Yan protein and miR-7 in *Drosophila* retinal cells: Yan directly represses the expression of miR-7 in undifferentiated progenitor cells and miR-7 directly

* Correspondence: david.simpson@qub.ac.uk
† Contributed equally
Centre for Vision and Vascular Science, Queen's University Belfast, Ophthalmic Research Centre, Institute of Clinical Science, Royal Victoria Hospital, Belfast BT12 6BA, UK

BioMed Central

© 2010 Arora et al; licensee BioMed Central Ltd. This is an Open Access article distributed under the terms of the Creative Commons Attribution License (http://creativecommons.org/licenses/by/2.0), which permits unrestricted use, distribution, and reproduction in any medium, provided the original work is properly cited.

represses the expression of Yan in differentiated photoreceptor cells [7]. The switch between these mutually exclusive expression states occurs when Yan degradation is triggered by epidermal growth factor receptor (EGFR) signaling.

Expression of various miRNAs has been demonstrated in the retina [8-10], notably a sensory organ-specific polycistronic cluster comprising miR-96, miR-182, and miR-183 [11]. The profile of miRNAs expressed in the retina has been shown to change during degeneration in several mouse models [12,13]. Many genes with retinal-specific functions are predicted to be targeted by miRNAs and functional interactions have been demonstrated [14].

miRNAs were initially thought to act through inhibition of protein translation [2]. Whilst this mechanism has been widely confirmed [15] and the global impact of miRNAs on protein levels demonstrated [16,17], it has become apparent that miRNAs also affect mRNA levels. This was first clearly demonstrated by the observation that those mRNAs with reduced expression following over-expression of a specific miRNA were enriched for predicted target sites of that miRNA [18]. Many miRNAs display tissue-specific expression [19] and inhibit expression of genes which are found at lower levels relative to other tissues [18,20]. The action of miRNAs upon mRNA levels has been widely confirmed in subsequent studies [21,22], which have also improved understanding of the properties of functional predicted target sites [16,23].

Inhibition of gene expression by miRNAs is mediated by base pairing between the miRNA and complementary sequences in the 3'UTR of target genes. However, unlike siRNAs, which direct cleavage of perfectly matched sequences, miRNAs have imperfect complementarity with their target sites. The features required for a functional target site are not fully understood, but include a stretch of perfect complementarity with a ~7 nucleotide 'seed' region at the 5' end of the miRNA [24]. A range of target prediction algorithms have been developed and each miRNA is thought to target approximately 200 transcripts [25,26]. Over 550 human miRNAs have been defined to date (miRBase v12 [27,28]) and have been suggested to regulate 30% of genes [24].

We have shown recently that the effects of miRNAs upon mRNA levels are such that the consequences of expression of a specific miRNA can be detected within a single gene expression profile [29]. Here this approach is applied to three experimental samples chosen to indicate candidate miRNAs affecting mRNA levels in ciliary epithelium-derived retinal stem cells from the adult eye (CE-RSCs), the developing retina during rod photoreceptor differentiation (postnatal murine retina) and in the mature retina (adult murine retina). This analysis may be indicative of those miRNAs with greatest effects upon target gene expression, or may reveal a subset with targets which are more susceptible to mRNA degradation. In either case, demonstration of the expression of these miRNAs confirms them as candidates for future manipulation aimed at directing differentiation or maintaining the mature retina.

Results

In silico prediction of candidate miRNAs affecting mRNA levels

Each miRNA was mapped to its predicted target genes in each mRNA expression profile and the average levels of the transcripts of their target genes were calculated. The ranked average target gene expression values in the P4 retina are shown in Figure 1A. The probability that each miRNA has a significant effect upon gene expression was calculated using the Wilcoxon ranked sum test; the results for P4 retina are illustrated in Figure 1B. The predictions from all gene expression datasets are listed in Additional file 1: Table S1 and the significant combined probabilities are shown in Table 1 ($p < 0.05$). Multiple mRNA expression profiles were analysed for murine CE-RSCs, P4 and adult retina. Significant predicted effects upon mRNA expression were detected for multiple miRNAs in the P4 and adult retina and for a smaller number in CE-RSCs. At P4 many miRNAs had highly significant effects, with miR-124, miR-125 and miR-9 being particularly significant (Figure 1, Table 1 and Additional file 1: Table S1). In the adult retina miR-124 and miR-125 were again prominent, but others, including miR-24, miR-326, miR-370, miR-96 and let-7 also had highly significant predicted effects. The greater number of genes assayed for the adult retina may have contributed to the detection of several more miRNAs with significant predicted effects and the smaller p-values than at P4. Whilst most of the candidate miRNAs predicted to affect mRNA levels ($P < 0.05$) at P4 were also in the adult, only miR-125, miR-378 and miR-24 were detected in all the different tissue types and developmental stages. Gene expression data from human CE-RSCs from adult eyes were also analysed and although many different miRNAs were predicted to be affecting mRNA levels, it was notable that the two miRNAs with the most significant effects in murine CE-RSCs, miR-378 and miR-485-3p, were also the 3rd and 4th most significant in human CE-RSCs (Additional file 1: Table S1). We hypothesized that miRNAs with detectable effects upon mRNA expression are more highly expressed than those with no effect. We tested this hypothesis in the adult mouse retina using miRNA expression data published by Loscher *et al*. [13]. A list was compiled of miRNAs whose predicted target genes exhibited significantly low expression. Expression of miRNAs within this

Table 1 miRNAs predicted to affect retinal gene expression.

CE-RSCs		P4		Adult	
miRNA	Probability	miRNA	Probability	miRNA	Probability
miR-485-3p	2.25E-03	miR-124a	5.59E-11	miR-125	8.01E-18
miR-378	1.08E-02	miR-9	2.29E-10	miR-124a	2.86E-15
miR-30-3p	1.14E-02	miR-125	3.92E-09	let-7	8.96E-09
miR-125	1.30E-02	miR-15	1.44E-07	miR-24	6.94E-08
miR-153	2.14E-02	miR-124u	8.98E-05	miR-96	6.61E-07
miR-342	2.46E-02	miR-34	3.36E-04	miR-370	9.17E-07
miR-142-5p	2.59E-02	miR-204	3.37E-04	miR-326	1.68E-06
let-7	2.69E-02	miR-378	3.55E-04	miR-29	7.82E-06
miR-24	2.99E-02	miR-20	5.95E-04	miR-331	9.74E-06
miR-183	3.00E-02	miR-96	6.40E-04	miR-124u	5.14E-05
miR-370	4.42E-02	miR-25	1.05E-03	miR-20	8.02E-05
miR-33	4.43E-02	miR-27	1.65E-03	miR-27	5.56E-04
		let-7	2.20E-03	miR-196	1.32E-03
		miR-326	2.79E-03	miR-485-5p	2.87E-03
		miR-150	8.95E-03	miR-34	3.35E-03
		miR-196	1.26E-02	miR-378	4.73E-03
		miR-184	1.33E-02	miR-127	5.00E-03
		miR-448	1.56E-02	miR-30	6.74E-03
		miR-503	2.76E-02	miR-150	1.21E-02
		miR-485-5p	3.33E-02	miR-128	1.32E-02
		miR-30	3.44E-02	miR-15	2.30E-02
		miR-24	3.98E-02	miR-9	2.62E-02
		miR-29	4.29E-02	miR-214	2.69E-02
				miR-204	2.93E-02
				miR-184	4.05E-02

The miRNAs with significant effects (combined $p < 0.05$) upon mRNA expression in mouse adult CE-RSCs, P4 and adult retina.

group was significantly higher than that of those miRNAs for which no effect on target mRNAs was predicted (Figure 2).

Experimental analysis of miRNA expression

The following miRNAs had highly significant predicted effects on target mRNA levels and were selected for analysis by RT-PCR: miR-124, miR-125, miR-9, and miR-24. A range of other candidates with p-values < 0.05 in at least one experimental condition (miR-128, miR-150, miR-204, miR-25, miR-27, miR-326 miR-34, miR-370, miR-378 and miR-485-5p) were selected to represent different predicted patterns of activity or for their lack of previous association with neural tissue. In addition, miR-122, which had $p < 0.1$ in CE-RSCs and P4 and adult retina, was of interest because it has been previously characterised as a highly expressed, liver-specific miRNA [19,22,30]; the possibility of an alternative role in the retina is intriguing. Let7d has previously been shown to be highly expressed in the retina [14] and was used as a positive control.

The pattern of relative expression in the three samples considered (porcine CE-RSCs, mouse P4 and adult retina) varied widely amongst miRNAs (Figure 3A). The expression of each individual miRNA corresponded broadly with its predicted effects upon target gene expression (e.g. miR-25 highest at P4 and miR-124 absent in CE-RSCs but present in P4 and adult mouse retina). However, whilst this analysis indicates the sample in which the relative expression of a single miRNA is highest, it gives no indication of the inter-miRNA variation in expression in that sample. It is also important to consider the relative absolute expression of different miRNAs within a single sample when considering the impact of each upon target mRNA expression. Therefore, starting template copy numbers were estimated for each miRNA based on threshold cycle (Ct) and amplification efficiency or by the linear regression efficiency method [31], which were broadly in agreement (Additional file 2: Figure S1). The miRNAs measured in each sample are shown in Figure 3B ranked by their starting template copy number in the RT-PCR assays. Those miRNAs with the most significant predicted effects upon mRNA expression are highly expressed. Notably, miR-125 has amongst the most significant predicted effects upon mRNA expression at all stages (Table 1) and miR-125a and miR-125b are the most highly expressed miRNAs in all samples (Figure 3B). Furthermore, miR-124 is highly expressed in P4 and adult retina in accordance with its predicted effects. To test the expected relationship between predicted effects and miRNA expression, the estimated miRNA copy numbers were plotted against predicted probability (Figure 4). This revealed a significant correlation (Spearman rank correlation, p = 4.0E-04), with the majority of most highly expressed miRNAs having highly significant predicted effects.

In situ hybridization (ISH) was performed to localise expression of selected miRNAs (Figure 5). Expression in the adult murine retina of the well-characterised neural miRNA miR-124 concurred with published reports [9]. In P4 retina, miR-124 positive signal was mainly colocalised with ganglion and amacrine cells. Expression of miR-34a, which has not previously been described in the retina, was detected in the porcine CE-RSC neurospheres and throughout the mouse P4 retina. In the adult mouse retina the strongest signal was observed in the inner nuclear layer (INL) and in some cells in the ganglion cell layer (GCL). miR-128 was expressed in all samples, notably in CE-RSC neurospheres and the inner plexiform layer of the retina at P4. miR-125b was also expressed at all stages with strong signal in the inner plexiform layer at P4. In

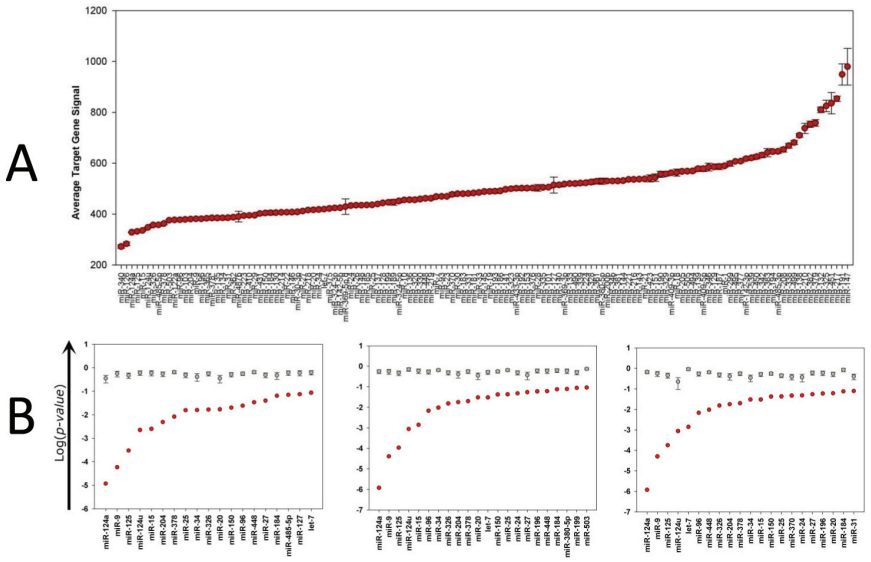


Figure 1 miRNA target gene expression. (A) miRNAs ranked by target gene expression levels (Average Target Gene Signal) in P4 retina. (B) Probabilities of each miRNA having a significant effect ($p < 0.1$) upon target gene expression according to Wilcoxon ranked sum test. The $\log_{10}$ (p-value) for each miRNA (x-axis) is plotted as a red circle and the mean probability (± standard error) derived from five random sets of predicted target genes is plotted in grey.

the adult retina miR-125b was expressed in the inner and outer nuclear layers. No expression was observed for miR-122 and miR-378 (data not shown).

Predicted targets of candidate miRNAs affecting mRNA levels

In order to identify the genes most likely regulated by miRNAs in CE-RSCs, P4 and adult retina, the target predictions for all the miRNAs shown to have a significant effect upon gene expression were combined. This revealed that some genes were predicted to be targeted by almost half of the miRNAs identified in each sample (Table 2 and Additional file 3: Table S2). These genes are the most likely to be real miRNA targets because if some predicted sites are not functional others may be active. Also, the co-operative action of multiple miRNAs may result in greater effects [23]. Six genes

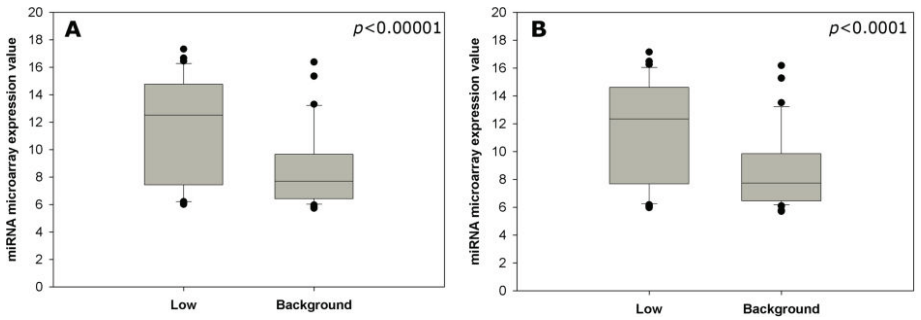


Figure 2 Association of miRNA expression with extent of predicted effect upon target mRNA expression in adult murine retina. Expression of those miRNAs with a significant effect ($p < 0.1$) upon target gene expression ('low' group) was significantly higher than that of those miRNAs with no predicted effects ('background' group). Microarray data from Loscher *et al* [13] was available for two strains of mouse, C57 (A) and 129 (B), and both showed a similar result.

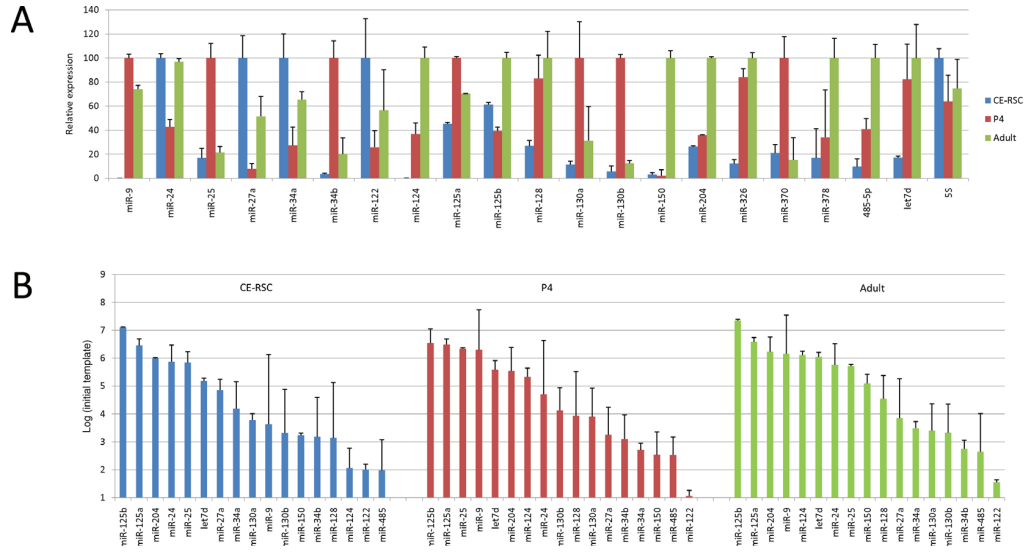


Figure 3 miRNA expression detected by RT-PCR. (A) Relative quantification of selected miRNAs in porcine CE-RSCs and murine P4 and adult retina. (B) Absolute miRNA expression levels estimated from qRT-PCR data.

targeted by three miRNAs with the highest expression and greatest predicted effects (miR-124; miR-125 and miR-9.) were selected for validation: ACCN2; ETS1; KLF13; LIN28B; NFIB and SH2B3. Following transfection of HEK293 cells with a pool of miR-124, miR-125 and miR-9 miRNA mimics the mRNA expression of 5 of these 6 genes was significantly reduced (Figure 6).

Comparison of the predicted miRNA target genes with those known to be involved in retinal function and disease [14] highlighted potential genes of interest (Table 3 and Additional file 3: Table S2). There was considerable overlap between known 'retinal genes' targeted by multiple miRNAs in P4 and adult retina. For example, a gene involved in the elongation of very long chain fatty acids (ELOVL4) is a predicted target of miRNAs with the most significant predicted effects on gene expression and the highest expression in RT-PCR assays. ELOVL4 has been implicated in Stargardts disease and macular dystrophy [32] and is expressed in photoreceptor inner segments [33], in agreement with the ISH localisation of miR-124 (Figure 5), its predicted regulator. Likewise, Neurocalcin delta (NCALD) is expressed in retinal amacrine and ganglion cells [34] in agreement with the expression of miR-204, one of its potential regulators [9].

To establish the cellular functions which are regulated by the miRNAs shown to affect mRNA expression, enrichment of functional annotation terms within the predicted target genes was assessed [35]. The genes with target sites for those miRNAs identified by our analyses were selected from the set of all genes with a conserved miRNA target site predicted by TargetScan; this list was therefore used as the background to assess enrichment (various categories, including many regulatory functions, are already enriched in this group in comparison to the whole genome; data not shown). In all the different tissue types at different developmental stages, genes with two or more predicted sites for candidate miRNAs affecting mRNA levels were enriched for annotations predominately relating to regulatory functions, notably gene transcription (Additional file 4: Table S3).

Discussion

miRNAs regulate mRNA expression in the retina

Gene expression is regulated by many factors at both transcriptional and posttranscriptional levels. The effect of miRNAs within these influences is detectable through analysis of microarray expression profiles; groups of mRNAs defined by presence of a putative target site for specific miRNAs were expressed at a significantly lower level than the group of non-target genes. These effects were observed in developing and adult retina and to a lesser extent in CE-RSCs. Not surprisingly, these effects were related to the expression level of the miRNA; those with extremely significant effects, such as miR-125, miR-124 and miR-9 were amongst the most highly expressed in the P4 and adult murine retina. The

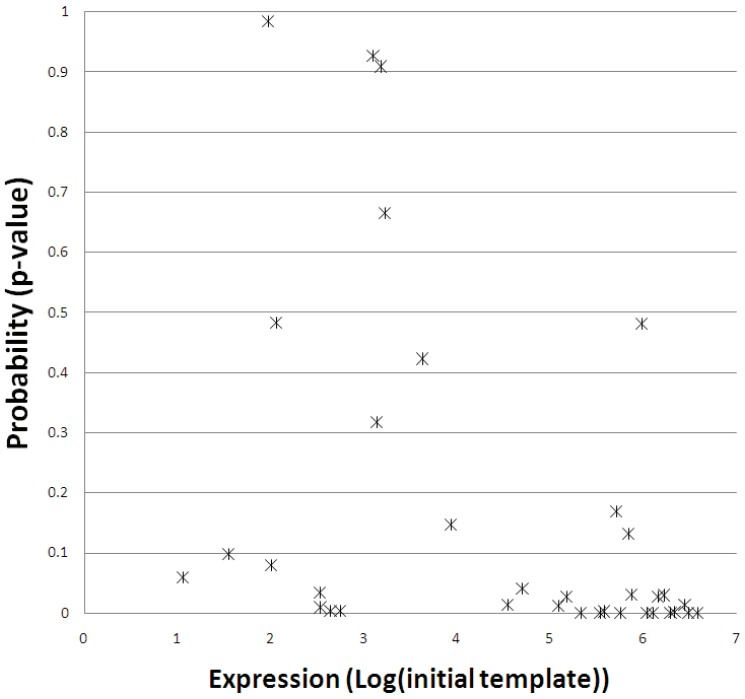


Figure 4 Comparision between the predicted effects of miRNAs and their expression as determined by RT-PCR. The estimated copy number (Log(initial template)) of each miRNA in a given sample is plotted against the probability (Wilcoxon ranked sum test) that it is having an effect upon target gene expression. The most highly expressed miRNAs have very significant effects upon predicted target gene expression and the overall correlation between miRNA expression and significance of effect upon target gene expression is significant (p = 4.0E-04; Spearman rank correlation).

miRNA expression patterns determined in this study were consistent with previous reports. For example, miR-125, miR-124 and miR-9 have all been independently reported to be highly expressed in the retina [9-11]. The association between the expression level of a miRNA and its predicted effects on mRNA expression is robust because it was demonstrated for both our qRT-PCR analysis of a relatively small number of miRNAs and for global miRNA expression profiles determined by other investigators [13].

Genes predicted to be targeted by multiple candidate miRNAs affecting mRNA levels are the best candidates for *in vivo* regulation by this mechanism. It is difficult to test this assertion in retinal cells, however the predicted effects on mRNA expression were observed for five of six genes in an *in vitro* model. This provides some support to the predictions of individual genes affected by miRNAs, at least for those targeted by multiple miRNAs with highly significant overall effects on mRNA expression,

The pattern of miRNA activity suggests a role in retinal differentiation

The predicted effects of miRNAs were less significant in mouse CE-RSCs than in the P4 and adult retina. miRNA expression was correspondingly lower, with only 4 of 20 miRNAs displaying highest expression in the CE-RSCs (although this may have been partly due to the porcine origin of the CE-RSCs used for RT-PCR analyses). The absolute levels of these miRNAs were also lower than those highly expressed in P4 and adult retina. This is consistent with reports that miRNA expression increases from very low levels at embryonic day 10, when the retina is comprised of retinal progenitor cells with similar properties and gene expression patterns to CE-RSCs [36], to higher levels in the P1 and adult retina [11]. This pattern of miRNA expression and predicted effects supports a role for miRNAs in retinal differentiation, maturation and maintenance of the adult retina. A similar observation was noted by Wienholds and co-authors, when they

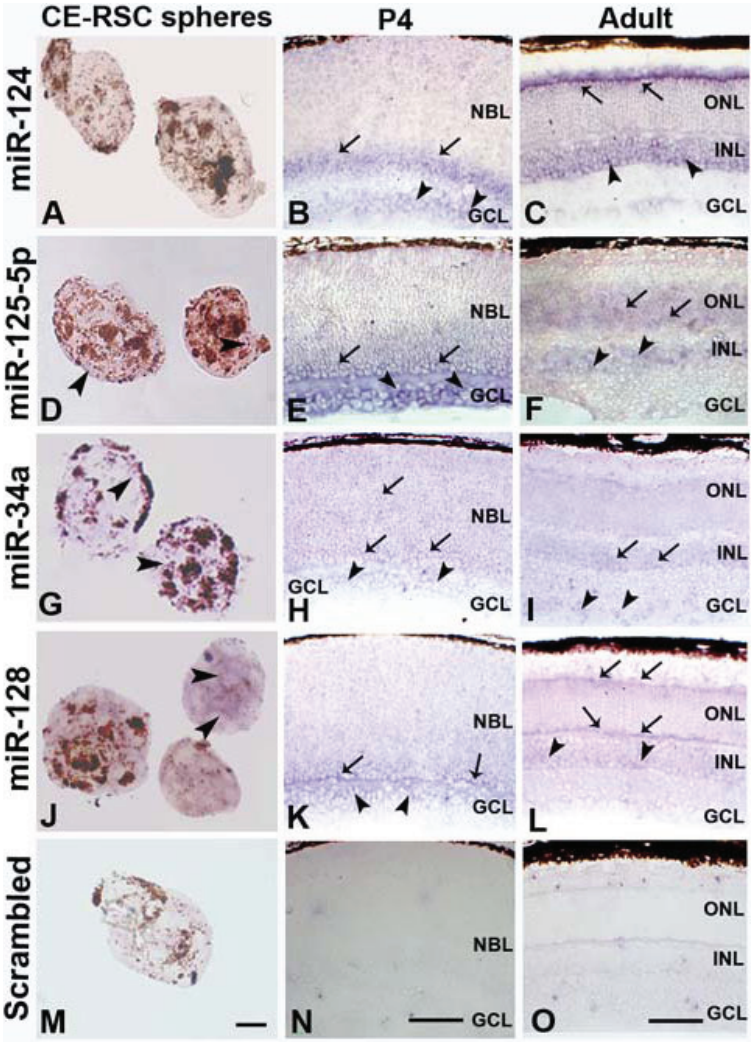


Figure 5 Cellular expression of selected miRNAs. ISH was performed on porcine CE-RSC neurospheres, and P4 and adult mouse retinas. Some neurosphere cells are naturally pigmented (dark brown). **A**: No positive signal was detected for miR-124 in CE-RSC neurospheres. **B**: Expression of miR-124 at P4 corresponded to the location of amacrine (arrows) and ganglion cells (arrowheads). **C**: In the adult retina, miR-124 was expressed in all layers with the highest intensity in the photoreceptor inner segments (arrows) and cells in the INL (arrowheads). **D**: miR-125b-5p was detected in the RSC neurospheres (purple staining depicted with arrowheads). **E**: In the P4 retina strong expression of miR-125b-5p was found in the inner portion of the NBL (arrows) and GCL (arrowheads). **F**: In the adult retina expression of miR-125b was detected in the ONL (arrows) and INL (arrowheads). G: Weak hybridisation signal for miR-34a was observed in CE-RSC neurosphere cells (arrowheads). H: P4 retina displayed week miR-34a signal throughout NBL (arrows) and ganglion (arrowheads) **I**: In the adult retina the strongest signal for miR-34a was observed in the INL (arrows) and in some cells in the GCL (arrowheads). **J**: Strong hybridisation signal was detected for miR-128 in the CE-RSC neurospheres (arrowheads). **K**: In the P4 retina a hybridisation signal for miR-128 was observed in the inner portion of the NBL (arrows) and in some cells of the GCL (arrowheads). **L**: In the adult retina strongest miR-128 hybridisation signal was detected in the INL (arrowheads), the outer portion of the outer plexiform layer and photoreceptor inner segments (arrows). ISH with scrambled negative control gave no signal in CE-RSCs (M), P4 (N), or adult mouse retina (O). NBL-neuroblast layer, GCL-ganglion cell layer, INL-inner nuclear layer, ONL-outer nuclear layer. Scale bars 50 μm.

Table 2 Genes predicted to be targets of the candidate miRNAs affecting mRNA levels.

CE-RSCs		P4		Adult	
Gene	miRNAs	Gene	miRNAs	Gene	miRNAs
CUGBP2	153; 24; 183; 378; 33; 30-3p; 342	ACVR2A	27; 96; 29; 128; 196; 150; let-7/98; 124.1; 125/351; 362; 378	ACVR2A	503; 27; 96; 448; 378; 29; 196; 125/351; 150; 124.1; let-7/98
KPNA4	142-5p; 33; 153; 378; let-7/98; 183; 24	TNRC6B	362; 184; 27; 124.1; 9; 204/211; 378; 485-5p; 150; 29; 22	TNRC6B	150; 503; 378; 448; 9; 184; 485-5p; 29; 204/211; 124.1; 27
ZNF148	183; 125/351; 370; 142-5p; 24; 378; 153	**NFIB**	125/351; 331; 22; 128; 485-5p; 124.1; 29; 27; 9; 24	RICTOR	196; 448; 124.1; 96; 503; 326; 27; let-7/98; 204/211; 29
CLCN5	30-3p; let-7/98; 378; 24; 142-5p; 153	ZNF148	34b; 196; 204/211; 378; 124.1; 24; 128; 370; 125/351; 27	CLCN5	448; 503; 378; 9; 29; 24; let-7/98; 27; 485-5p
CPEB4	142-5p; 33; 342; 125/351; 153; let-7/98	MECP2	34b; 22; 204/211; 378; let-7/98; 196; 326; 96; 124.1	HMGA2	196; 125/351; 204/211; 9; 485-5p; 503; 150; 326; let-7/98
DAGLA	153; 183; 485-3p; 125/351; 24; let-7/98	RP11-130N24.1	362; 96; 9; 29; 125/351; 196; 27; 34b; 124.1	ZNF148	204/211; 196; 124.1; 34b; 125/351; 24; 448; 27; 378
EPHA4	153; 125/351; 33; 30-3p; let-7/98; 183	SP1	125/351; 29; 24; 27; 326; 378; 22; 128; 124.1	CPEB3	196; 125/351; 503; 29; let-7/98; 9; 27; 34b
NARG1	153; 378; 33; 342; 30-3p; 370	ZBTB39	9; 128; 485-5p; 22; 124.1; let-7/98; 27; 331; 370	MECP2	326; 34b; 378; let-7/98; 96; 196; 124.1; 204/211
PTPRD	485-3p; let-7/98; 30-3p; 153; 24; 142-5p	ATXN1	125/351; 29; 9; 370; 326; 96; let-7/98; 34b	**NFIB**	124.1; 448; 485-5p; 29; 9; 24; 27; 125/351
ACVR2A	125/351; 153; 378; let-7/98; 183	CCNJ	let-7/98; 196; 27; 128; 204/211; 370; 125/351; 96	RP11-130N24.1	9; 125/351; 124.1; 27; 29; 196; 96; 34b
BTBD7	342; 30-3p; 153; 378; 142-5p	CLCN5	29; 9; 485-5p; 378; 24; 128; 27; let-7/98	AKT3	124.1; 150; 503; 29; 448; 326; 125/351
CPEB2	153; 33; let-7/98; 183; 142-5p	CPD	196; 204/211; 370; 128; 150; let-7/98; 331; 27	ATXN1	34b; 125/351; 326; 96; let-7/98; 29; 9
DDX3X	30-3p; 33; 370; 183; 342	CPEB3	128; 9; let-7/98; 125/351; 196; 29; 27; 34b	BRPF3	96; 326; 204/211; 125/351; 27; 503; 9
E2F3	125/351; 153; 370; 378; 342	HMGA2	196; 150; 485-5p; 204/211; 326; 125/351; 9; let-7/98	BSN	448; 124.1; 24; 125/351; 150; 9; 503
FBXO33	; 142-5p; 30-3p; 342; 33; 153	IGF2BP1	370; 331; let-7/98; 196; 24; 96; 326; 9	CCND2	29; 196; 503; 96; let-7/98; 448; 124.1
MLL2	; 142-5p; 342; let-7/98; 370; 33	QKI	128; 485-5p; 9; 125/351; 370; 24; 124.1; 27	CCNJ	204/211; 27; 503; 196; 96; 125/351; let-7/98
PDE4D	; 183; 33; 24; 378; 485-3p	RICTOR	27; 196; 96; 204/211; 29; 326; 124.1; let-7/98	**KLF13**	9; 96; 125/351; 29; 448; 124.1; 378
QKI	; 24; 370; 33; 125/351; 142-5p	RIMS4	9; 96; 22; 27; 362; 127; 326; 331	MGA	326; 124.1; 378; 29; 9; let-7/98; 485-5p
RNF165	; let-7/98; 153; 24; 33; 142-5p	STC1	485-5p; 124.1; 9; 125/351; 22; 378; 34b; 96	ONECUT2	27; 29; let-7/98; 485-5p; 9; 96; 503
RSBN1	; 342; 183; 153; 378; 485-3p	BRPF3	27; 9; 96; 128; 125/351; 204/211; 326	PAPPA	27; 96; 150; let-7/98; 503; 448; 326
SETD7	; 485-3p; 153; 33; 125/351; 342	CPEB4	362; 96; 125/351; 128; 9; 27; let-7/98	PTPRD	24; 124.1; 204/211; 29; 503; let-7/98; 448
SIX4	; 153; 378; 33; 30-3p; 142-5p	DCX	27; let-7/98; 128; 29; 362; 9; 96	QKI	125/351; 124.1; 9; 503; 24; 485-5p; 27
SLC4A4	; 153; 125/351; 370; 142-5p; let-7/98	DTNA	9; 124.1; 378; 22; 24; 27; 128	RNF165	124.1; 448; let-7/98; 485-5p; 150; 29; 24
SOX11	; 125/351; 153; 33; 142-5p; 485-3p	FRMD4A	29; 9; 204/211; 128; 124.1; 96; 34b	SP1	326; 124.1; 125/351; 29; 378; 27; 24
SP1	; 24; 125/351; 485-3p; 378; 33	GABBR2	128; 9; 22; 378; 326; 204/211; 370	STC1	485-5p; 378; 34b; 124.1; 9; 125/351; 96
STC1	; 125/351; 30-3p; 142-5p; 378; 183	ISL1	27; 29; 128; 96; 9; 362; 378	ZFHX4	204/211; 96; 503; 485-5p; 448; 27; 9
THRAP1	; 485-3p; 142-5p; 183; 153; 24	KLF12	34b; 370; 204/211; 124.1; 29; 9; 27	**ACCN2**	9; 29; 326; 125/351; 124.1; 27
YOD1	; let-7/98; 183; 24; 30-3p; 125/351	MGA	378; 485-5p; 326; 29; let-7/98; 9; 124.1	APPBP2	9; 448; 378; 27; let-7/98; 29

Table 2: Genes predicted to be targets of the candidate miRNAs affecting mRNA levels. *(Continued)*

ZFPM2	; 183; 142-5p; 485-3p; 153; 33	MITF	27; 331; 34b; 378; 124.1; 485-5p; 96	CPEB4	448; 9; 27; 125/351; 96; let-7/98
ARID4B	; 370; 183; 378; 142-5p	MMP16	150; 27; 370; 24; 124.1; 9; 96	CUGBP2	96; 326; 34b; 378; 196; 24

The top 30 genes in each tissue ranked by number of different miRNAs predicted to target them. Genes for which certain miRNA interactions were assessed experimentally are marked in bold. The full list of genes targeted by at least one of the candidate miRNAs affecting mRNA levels is shown in Table S2.

were able to detect only a few miRNAs during early zebrafish development [37].

Although generally lower than in retina, miRNA expression was described for the first time in this study in CE-RSCs. Human and porcine eyes are similar in terms of morphology and physiology. We have previously characterised porcine CE-RSCs [38] and therefore, although the availability of mouse expression data for CE-RSCs, P4 and adult retina made it the choice for in silico analyses, porcine CE-RSCs were used to confirm expression of predicted miRNAs. CE-RSCs from various species have been shown to have very similar properties and gene expression patterns [38-41] Of the 4 miRNAs expressed most highly in CE-RSCs according to RT-PCR, miR-24 was also predicted to have a significant effect ($p < 0.05$) upon mRNA expression and miR-122 had $p = 0.08$. It has recently been shown that miR-24a represses apoptosis and is required for proper retinal development [42]. These miRNAs could also play a role in maintaining the progenitor cell state, as has been shown in other tissues; over-expression of miR-24 causes a delay in maturation of hematopoietic progenitor cells [43] and over-expression of miR-122 delays differentiation of human embryonic stem cells [44].

Many of the specific miRNAs shown to affect mRNA expression in the P4 and adult retina have previously been implicated in neuronal differentiation. For example, miR-124 has been associated with the transition from neural progenitor to differentiated neuron in the zebrafish brain [45]. In mouse brain miR-124 expression is restricted to mature neurons [46] and it promotes neuronal differentiation by triggering brain-specific alternative pre-mRNA splicing [47]. The reported absence of miR-124 in neural and retinal stem/progenitor cells *in vivo* [9,48,49] concurs with the lack of detectable expression in the CE-RSC spheres. Expression of miR-124 in the immature retina (P4) was lower than that in the adult retina and the ISH signal at P4 mainly corresponded to early differentiating neurons, retinal ganglion and amacrine cells. Our ISH for miR-124 in the adult retina confirmed previous reports [9] and showed miR-124 expression in all retinal layers, with particularly high levels in photoreceptor inner segments.

miR-9 promotes progression of neurogenesis in the zebrafish brain [50]. Expression of miR-9 was not detected in CE-RSCs, but in contrast to miR-124 it peaked in the P4 retina. This pattern is in agreement with Xu *et al* [11], who reported a very low level of miR-9 expression at E10 which gradually increased and

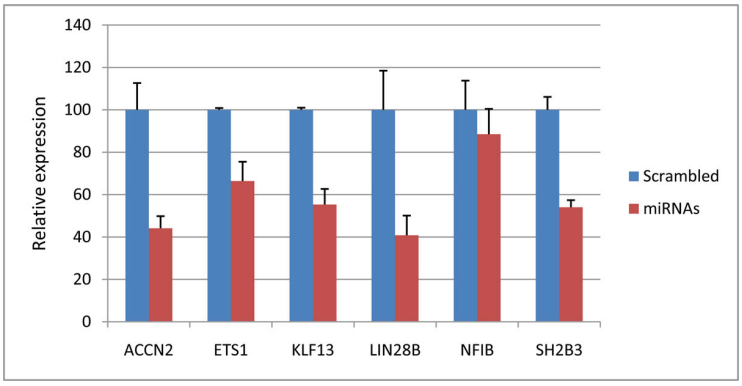


Figure 6 Overexpression of miRNAs reduces predicted target mRNA levels. Pools of miR-124, miR-125 and miR-9 miRNA mimics (miRNAs) or scrambled controls (Scrambled) were transfected into HEK293 cells. The mRNA expression of six genes predicted to be targeted by these three miRNAs was subsequently assessed by qRT-PCR. The graph shows the significant ($P < 0.01$) reduction in expression of ACCN2, ETS1, KLF13, LIN28B and SH2B3 following transfection with miRNAs relative to the scrambled control (error bars show standard deviation). There was no significant difference in expression of NFIB.

Table 3 Predicted target genes known to be involved in retinal function and disease.

CE-RSCs		P4		Adult	
4: NLK	1: NEFL	6: CAMTA1	1: COL18A1	5: NCOR2	1: DDIT4
3: DMD	1: PCDHGC3	6: NCOR2	1: COL2A1	4: CAMTA1	1: DUSP1
2: ADD1	1: PPP1R3F	5: ELOVL4	1: DUSP1	4: ELOVL4	1: FAM57B
2: CAMTA1	1: PSAP	5: NCALD	1: FAM57B	4: NCALD	1: H2AFZ
2: GNB1	1: RARB	4: NLK	1: H2AFZ	4: NLK	1: HSP90AB1
2: GPX3	1: RARG	4: RARG	1: IGFBP5	4: TP53INP2	1: IGFBP5
2: GRIA4	1: RDH10	4: TSPAN9	1: IMPDH1	4: TSPAN9	1: IMPDH1
2: HSPA8	1: RGS16	3: FZD4	1: KIAA0143	3: DMD	1: KIF1B
2: JAG1	1: RHO	3: TEAD1	1: KIF1B	3: FZD4	1: MAK
2: PAX2	1: RIMS1	3: TP53INP2	1: MAK	3: JAG1	1: MAPT
2: RB1	1: SGIP1	3: ZNF385	1: MAPT	3: RARG	1: PCDHGC3
2: SLC17A7	1: SLC12A5	2: CFL1	1: PAX2	3: TEAD1	1: PITPNA
2: TEAD1	1: SLC25A18	2: CSDA	1: PITPNA	2: CSDA	1: PPP1R3F
1: APP	1: SPP1	2: DMD	1: PPP1R3F	2: GPX3	1: PRELP
1: ATP8B1	1: STAC2	2: GPX3	1: PRELP	2: GRIA4	1: PSAP
1: BHLHB3	1: SYP	2: GRIA4	1: PSAP	2: PAX2	1: RARA
1: CAMSAP1	1: TFAP2B	2: JAG1	1: RARB	2: SLC12A5	1: RARB
1: CCNI	1: TP53INP2	2: RARA	1: RB1	2: SLC17A7	1: RB1
1: CFL1	1: TSPAN9	2: RIMS1	1: RDH10	2: TRPM3	1: RDH10
1: CLASP2	1: USH2A	2: SGIP1	1: RGS16	2: ZNF385	1: RGS16
1: COL2A1	1: ZNF385	2: SLC12A5	1: RGS9	1: ACTB	1: RGS9
1: CP		2: SLC17A7	1: RHO	1: ACTG1	1: RHO
1: DDIT4		2: TAGLN	1: RS1	1: ADD1	1: RIMS1
1: DUSP1		2: TRPM3	1: SLC1A3	1: AFF1	1: RS1
1: EEF1A1		1: ACTB	1: SLC25A18	1: ANXA2	1: SGIP1
1: EIF1		1: ACTG1	1: SMOC2	1: ATP8B1	1: SLC25A18
1: ELOVL4		1: AFF1	1: SPARC	1: ATXN7	1: SMOC2
1: FZD4		1: ANXA2	1: SPG20	1: CAMK2D	1: SPARC
1: HSP90AB1		1: ATP8B1	1: STAC2	1: CCNI	1: SPG20
1: IGFBP5		1: ATXN7	1: SYP	1: CFL1	1: STAC2
1: KIF1B		1: CAMK2D	1: TFAP2B	1: CLASP2	1: SYP
1: MSH6		1: CCNI		1: COL11A1	1: TAGLN
1: NCALD		1: CLASP2		1: COL18A1	1: TFAP2B
1: NCOR2		1: COL11A1		1: COL2A1	

Genes predicted to be targeted by one or more candidate miRNA affecting mRNA levels were compared with genes implicated in retinal function[14]. The overlapping genes are listed, with the number of different miRNAs predicted to target them followed by the gene symbol.

peaked at P10, being lower in the adult retina. Notably, the transcription factor Hes1, which maintains retinal progenitor pools during development is a predicted target for miR-9 [50]. Similarly to retinal progenitor cells, high levels of Hes1 mRNA are found in CE-RSC spheres (Yanagi et al 2006, our unpublished data). Decrease of miR-9 expression past P10 correlates with the completion of retinal cell differentiation. miR-125 is another miRNA with highly significant predicted effects upon mRNA expression and the high expression levels for miR-125a and miR-125b detected by RT-PCR are in agreement with previous miRNA array data [8,11]. Together with miR-124 and miR-9, miR-125b is also induced during neural differentiation of embryonic stem cells [51].

miRNAs differ in their effects upon mRNA turnover and translational repression

Our results suggest that, although many miRNAs are present in the retina, only a few affect mRNA levels sufficiently to have a detectable influence on target gene expression. Despite conclusive evidence of the high expression of miRNAs such as miR-181, -182 and -183 in the retina [8,9] the genes targeted by these miRNAs did not show significant down regulation at the mRNA

level in our analysis. Conversely miR-122, which has previously been shown to direct mRNA cleavage [21], was expressed at a low level, but had a significant predicted effect upon target gene expression in several samples (combined p = 0.08). Interestingly, miR-125b, one of the miRNAs with the strongest predicted effect upon mRNA levels, has been shown to accelerate deadenylation leading to rapid mRNA decay [52]. It is now accepted that miRNAs can mediate both translational repression and accelerated mRNA turnover [53]. One explanation for the detection of the effect of some highly expressed retinal miRNAs upon mRNA levels and not others could be that they are acting preferentially at the level of mRNA turnover.

Conclusions

The evidence presented in this study suggests that many miRNAs affect the expression levels of their target mRNAs during retinal development. The enrichment of the predicted target genes of these miRNAs for regulatory functions is in keeping with the proposed regulatory role of miRNAs. The lack of a mRNA 'signature' for other miRNAs which are also known to be highly expressed in the retina, suggests that certain miRNAs are less active at the mRNA level and perhaps act predominately upon translation. The identity and expression pattern of those miRNAs which were detected by analysis of target gene expression, such as miR-124, miR-125 and miR-9, provides further evidence that miRNAs play a central role in neuronal differentiation during retinal development.

Methods

Animal procedures

All animal procedures were performed in compliance with the UK Animals (Scientific Procedures) Act 1986. Adult mice were euthanised in a CO_2 chamber and P4 neonatal mice were lethally anesthetised by intra-peritoneal (IP) injection of an overdose of pentobarbitone. Eyes were enucleated and either processed for ISH or the retinas dissected and snap frozen in liquid nitrogen for RNA isolation.

Isolation and culture of CE-RSCs

Mixed sex White Landrace pigs were obtained from the Department of Agriculture and Rural Development Northern Ireland, Hillsborough, UK. CE-RSCs were isolated and grown as described previously [38]. Briefly, 1-2 week old pigs were lethally anesthetised, eyes were enucleated and placed into oxygenated artificial cerebral spinal fluid [aCSF: 124 mM NaCl,5 mM KCl,1.3 mM MgCl2, 26 mM NaHCO3, and 10 mM D-glucose, (Sigma-Aldrich, Poole, UK)]. A strip of ciliary body was dissected and enzymatically digested in Hanks' Balanced Salt Solution (HBSS) containing 2 mg/ml dispase (Sigma-Aldrich, Poole, UK) for 20 minutes at 37°C, followed by digestion in EBSS containing 1.33 mg/ml trypsin, 0.67 mg/ml hyaluronidase and 78 units/ml collagenase (Sigma-Aldrich, Poole, UK) for 20 min at 37°C. The supernatant was decanted and replaced with serum-free medium (SFM, DMEM/F12 (1:1) containing 0.6% (w/v) glucose, 2 mM glutamine, 5 mM HEPES buffer, 2% (v/v) B27, 100 units/ml penicillin and 100 units/ml streptomycin) with 1 mg/ml trypsin inhibitor (Invitrogen, Paisley UK). The cellular debris was gently triturated and dissociated into single cells with a fire-polished pipette. Cells were pelleted at 800 rpm for 10 minutes, resuspended in SFM and passed through a 40 μm cell strainer (BD Biosciences, USA). Cells were counted and plated at a density of 3×10^4 cells/ml in SFM supplemented with 20 ng/ml of epidermal growth factor (EGF) and 10 ng/ml basic fibroblast growth factor (bFGF) (Invitrogen, Paisley, UK). After 7 days newly formed sphere colonies were collected, pelleted at 800 rpm for 10 minutes and digested in Accumax cell counting solution (ICT, San Diego, USA) for 20 min at RT and mechanically dissociated into single cells by pipetting. Cells were washed once in SFM and plated at a density of 3×10^4 cells/ml. After 7 days secondary spheres were collected.

miRNA target confirmation

HEK293-T cells were transfected at 80% confluency with miRNA mimics (Qiagen, Crawley, UK) using Turbofect transfection reagent (Fermentas, York, UK). Cells were collected for RNA isolation at 48 hours post transfection.

RNA isolation

For mRNA analyses RNA was extracted using an RNeasy Micro Kit with on column DNAse digestion (Qiagen, West Sussex, UK) according to the manufacturer's protocol. For miRNA analyses total RNA was extracted using a mirVana extraction kit (Ambion, Foster City, CA) according to the manufacturer's protocol.

mRNA microarray analysis and gene expression datasets

RNA samples from retinas of three P4 mice were labeled and hybridized to GeneChip® 430A 2.0 mouse microarrays (Affymetrix, Santa Clara, Ca.) according to the manufacturer's protocols. Raw data were analysed using the Affymetrix MAS 5.0 algorithm and the results deposited in NCBI's Gene Expression Omnibus (GEO) [54,55]. Publicly available mRNA expression data were downloaded from GEO. All the data were generated from Affymetrix genechips. Samples analysed on the MOE430A platform were available for CE-RSC and are directly comparable with the Mouse 430A 2.0 platform used for the P4 retina samples (~14,000 well characterised transcripts). Data from the MOE430B platform (~22,000 transcripts) was also available for several CE-RSC samples. The Mouse430_2 platform used for adult

Table 4 Gene expression datasets.

GEO accession	Type	Organism	Tissue
GSM87191	mRNA	Human	Retinal spheres from ciliary epithelium of adult eye
GSM87193	mRNA	Human	Retinal spheres from ciliary epithelium of adult eye
GSM87194	mRNA	Human	Retinal spheres from ciliary epithelium of adult eye
GSM87195	mRNA	Mouse	Retinal spheres from ciliary epithelium of adult eye
GSM87196	mRNA	Mouse	Retinal spheres from ciliary epithelium of adult eye
GSM87197	mRNA	Mouse	Retinal spheres from ciliary epithelium of adult eye
GSM87198	mRNA	Mouse	Retinal spheres from ciliary epithelium of adult eye
GSM87199	mRNA	Human	Retinal spheres from ciliary epithelium of adult eye
GSM87200	mRNA	Human	Retinal spheres from ciliary epithelium of adult eye
GSM87201	mRNA	Mouse	Retinal spheres from ciliary epithelium of adult eye
GSM87202	mRNA	Mouse	Retinal spheres from ciliary epithelium of adult eye
GSM32153 [64]	mRNA	Mouse	Adult Retina
GSM81691 [65]	mRNA	Mouse	Adult Retina
GSM92629 [66]	mRNA	Mouse	Adult Retina
GSM107514	mRNA	Mouse	Adult Retina
GSM419995*	mRNA	Mouse	P4 Developmental Retina
GSM419996*	mRNA	Mouse	P4 Developmental Retina
GSM419997*	mRNA	Mouse	P4 Developmental Retina

The mRNA expression datasets analysed to detect the effect of miRNAs were downloaded from Gene expression omnibus (GEO) or created in-house (*). The GEO accession numbers and details are listed. Numbers indicate associated references.

retinal expression interrogated all the transcripts in the A and B platforms. The tissues and GEO sample accession numbers are listed in Table 4.

miRNA target predictions

Predictions from TargetScan [23,24] were used because we have previously demonstrated the ability of this algorithm to predict known tissue-specific miRNAs [29]. TargetScan's requirement for a perfect match to the seed region and cross-species conservation reduces the false-positive rate [24,25,56]. By minimising background, use of this algorithm maximises the ability to detect effects on expression of real miRNA target genes. Complete miRNA datasets published by Lewis *et al.* [24] were downloaded from the TargetScan website (version 3.1) [57]. For controls, 5 random datasets were generated for each of the gene expression datasets. For each of the random sets, the same numbers of target genes as predicted by TargetScan were randomly assigned to each of the miRNAs. The relationships between candidate miRNAs predicted to affect mRNA levels in the retina and their target genes were analysed using Microsoft Access and 'targets of conserved families' from Targetscan version 4.2. Functional characterisation of predicted target genes was performed using the DAVID bioinformatics database [35].

Bioinformatic analysis of target mRNA levels

The relative expression of the predicted target gene sets for each miRNA were compared as described previously using stand alone Java and R [58] programs in conjunction with MS Access and MS Excel [29]. Only single gene-specific Affymetrix probesets (suffix_at) were considered and only those expressed in each dataset analysed (designated by a 'present' call if available, or alternatively by a signal strength greater than the median value). Probeset IDs were converted to their cognate Gene Symbols, using the Biomart online suite [59]. For each mRNA expression dataset (Table 4), lists of expressed genes targeted by each miRNA family and their respective expression levels were compiled. The mean expression level was calculated for genes represented by > 1 probeset to provide the 'Average Target Gene Signal'. Only miRNAs with > 50 predicted targets were considered. The expression values of the predicted targets of a specific miRNA in each individual dataset were compared with the set of expression values in that dataset of all the genes predicted to be targeted by miRNAs. To determine whether there was a significant difference between the medians of the ranked gene expression values of the two sets, the nonparametric one-sided Wilcoxon rank sum test was employed. Fisher's combined probability test was used to calculate a composite test statistic from the individual p-values associated with the multiple expression datasets from CE-RSCs, P4 or adult retina[60]. For every miRNA with a combined $p < 0.05$ we considered that the expression of the set of genes targeted by that miRNA in that tissue was significantly less than the average expression of all the targeted genes.

RT-PCR

RT for detection of mRNAs was performed with 1 μg of RNA using random hexamers and SuperscriptIII (Invitrogen, Paisley, UK). Specific miRNAs were detected using a modified version of the method described by Shi and Chiang [61], in which mature miRNAs are polyadenylated and target sequences for a reverse primer are subsequently incorporated into cDNA by use of an oligo dT adapter. One microgram of RNA was polyadenylated using poly(A) polymerase (PAP; Ambion, Foster City, CA) at 37°C for 1 hour in a 25-μl reaction mixture. RNAs were then reverse transcribed with 200 U reverse

Table 5 Sequences of primers and ISH probes.

DNA oligonucleotides	
Name	5'-3' nucleotide sequence
Let-7d	AGAGGTAGTAGGTTGCATAGT
miR-9	TCTTTGGTTATCTAGCTGTATGA
miR-24	TGGCTCAGTTCAGCAGGAACAG
miR-25	CATTGCACTTGTCTCGGTCTGA
miR-27a	TTCACAGTGGCTAAGTTCCGC
miR-34a	TGGCAGTGTCTTAGCTGGTTGTT
miR-34b	TAGGCAGTGTAATTAGCTGATTG
miR-122	TGGAGTGTGACAATGGTGTTTG
miR-124	TAAGGCACGCGGTGAATGCC
miR-128	TCACAGTGAACCGGTCTCTTTT
miR-125a-5p	TCCCTGAGACCCTTTAACCTGTGA
miR-125b-5p	TCCCTGAGACCCTAACTTGTGA
miR-130a	CAGTGCAATGTTAAAAGGGCAT
miR-130b	CAGTGCAATGATGAAAGGGCAT
miR-150	TCTCCCAACCCTTGTACCAGTG
miR-204	TTCCCTTTGTCATCCTATGCCTG
miR-326	CCTCTGGGCCCTTCCTCCAGT
miR-370	GCCGGCTGGGGTGGAACGTGGTT
miR-378	CTCCTGACTCCAGGTCCTGTGT
miR-485-5p	AGAGGCTGGCCGTGATGAATTC
Poly (T) adapter	GCGAGCACAGAATTAATACGACTCA CTATAGGTTTTTTTTTTTTWN
Reverse RACE	GCGAGCACAGAATTAATACGAC
ETS1F	CCAGACAGACACCTTGCAGA
ETS1R	TGAGGCGATCACAACTATCG
KLF13F	GAAGCACAAGTGCCACTACG
KLF13R	GGCAGCTGAACTTCTTCTCG
NFIBF	AGCTGCTGGAAGTCGAACAT
NFIBR	TGAAGGTGGAGGTGGAGTTC
LIN28BF	AAGGCCTTGAGTCAATACGG
LIN28BR	CACTTCTTTGGCTGAGGAGG
SH2B3F	CTGGAGCTCTTCGACCCAC
SH2B3R	ATGTCTGTCCGGTCCTTCAC
ACCN2F	AGCTGTTACCATGGACTCGG
ACCN2R	CACGCAGTACTCCTGGTCCT

in situ probes	
Name	Sequence (enhanced with LNA) 5'-3'
mmu-miR-124	GGCATTCACCGCGTGCCTTA
mmu-miR-34a	AACAACCAGCTAAGACACTGCCA
mmu-miR-128	AAAAGAGACCGGTTCACTGTGA
mmu-miR-125b-5p	TCACAAGTTAGGGTCTCAGGGA
mmu-miR-378	CCTTCTGACTCCAAGTCCAGT
mmu-miR-122	CAAACACCATTGTCACACTCCA
Scrambled-miR	TTCACAATGCGTTATCGGATGT

Oligonucleotide primers and *in situ* probes from the miRCURY™LNA Detection system (Exiqon, Vedbaek, Denmark).

transcriptase (SuperScript III; Invitrogen, Paisley, UK) and 0.5 μg poly (T) adapter (3' rapid amplification of complementary DNA ends (RACE) adapter in the First-Choice RLM-RACE kit; Ambion). Primers for specific miRNAs were based on miRNA sequences obtained from miRBase [62,63] (Table 5). The reverse primer was the 3' adapter primer (3' RACE outer primer in the FirstChoice RLM-RACE kit; Ambion).

PCR was performed for 45 cycles with denaturation at 94°C for 30 seconds, annealing at 55°C for 30 seconds, and extension at 72°C for 30 seconds (LightCycler 480: Roche, Mannheim, Germany). PCR products were analyzed by polyacrylamide gel electrophoresis (20%; Invitrogen) to confirm the predicted size (approximately 60 bp, including mature miRNA and adapter sequences).

Relative RNA expression was determined by measuring the concentration of template in each sample at the threshold cycle (Ct) from a standard curve (Log concentration against Ct) generated from dilutions of a pooled cDNA sample. Relative expression determined by an alternative method employing delta Ct values and efficiency values calculated from a standard curve gave very similar results (Additional file 2: Figure S1). Starting template copy number was estimated from Ct values using the equation: $R_0 = R_{Ct} /(1 + E)^{Ct}$ where Ct is the threshold cycle, R_{Ct} is the fluorescence at this cycle, E is amplification efficiency (calculated from a standard curve) and R_0 is starting fluorescence, which is proportional to the starting template quantity. Starting template copy numbers estimated using the linear regression efficiency method described by Rutledge *et al* [31] were in broad agreement with the above method (Additional file 2: Figure S1) and mean values from the two methods were calculated.

In situ hybridization (ISH)

Mice were euthanised as described above. Eyes were enucleated, fixed in 4% PFA for 1 h at 4°C and cryoprotected trough series of 10, 20 and 30% sucrose, for 1-3 h, embedded in optimal cutting temperature compound (OCT, Sakura, Japan) and snap frozen in an isopentane bath on dry ice. CE-RSC spheres were collected and fixed in 4% PFA for 30 min at 4°C, cryoprotected in 30% sucrose over night, embedded in OCT and snap frozen on dry ice. Locked nucleic acid probes (miRCURY™ LNA Detection, Exiqon) for the candidate miRNAs and a scrambled miRNA control probe (Table 5), were prelabelled with digoxygenin (DIG) at the 5' end. 10 μm cryosections were fixed in 4% PFA for 10 minutes, rinsed in 1× PBS and 100 μl of hybridisation mix (50% formamide, 0.3 M NaCl, 20 mM Tris-HCl pH 8, 10% dextran sulphate, 1× Denhardt's solution, 1 mg/ml yeast rRNA) containing 2 μl of probe/ml was applied to sections. Slides were covered with glass cover slips and hybridisation was performed overnight at 20°C below the Tm.

Slides were washed twice in 1 × SSC, 50% formamide, 0.1% Tween 20 for 30 min, and once in 1 × SSC, 0.1% Tween 20 and 0.2 × SSC 0.1% Tween 20 for 30 minutes at 65°C. Two washes in 1× MABT (100 mM maleic acid, 150 mM NaCl, 0.1% Tween 20, pH 7.5) were performed at RT for 30 minutes. After incubation in blocking solution containing 1× MABT, 2% blocking reagent (Roche, Mannheim, Germany) and 20% heat inactivated sheep serum (Sigma-Aldrich, Poole, UK) for 2 hours at RT, anti-digoxygenin Fab fragments (Roche, Mannheim, Germany) were applied at 1:5,000 dilution overnight at RT. Detection staining was performed by incubation with the alkaline phosphatase chromogenic substrate 5-bromo-4-chloro-3-indolylphosphate/nitro-blue tetrazolium (BCIP/NBT) (Roche, Mannheim, Germany).

Additional file 1: Table S1. Significance of predicted effects of miRNAs upon mRNA expression in all gene expression datasets (CE-RSCs, P4 and adult retina) and p-values calculated using Fisher's combined probability test.
Click here for file
[http://www.biomedcentral.com/content/supplementary/1471-213X-10-1-S1.XLS]

Additional file 2: Figure S1. miRNA expression detected by RT-PCR. (A) Comparison of relative miRNA expression calculated using a standard curve (as shown in Figure 3A) with the values calculated using ΔCt and efficiency; for each gene the sample with highest expression was normalized to a value of 100. Each point represents the expression of one miRNA in a single sample as determined by both methods, which yielded very similar results (R^2 = 0.983). (B) Starting template copy numbers estimated for each miRNA based on threshold cycle (Ct) and amplification efficiency plotted against the values calculated by a linear regression efficiency method [31](R^2 = 0.661).
Click here for file
[http://www.biomedcentral.com/content/supplementary/1471-213X-10-1-S2.PDF]

Additional file 3: Table S2. All genes predicted to be targeted by candidate miRNAs affecting mRNA levels in each tissue. Genes assessed experimentally for miRNA interactions are highlighted in bold.
Click here for file
[http://www.biomedcentral.com/content/supplementary/1471-213X-10-1-S3.XLS]

Additional file 4: Table S3. The categories of functional annotations enriched within those genes predicted to be targeted by two or more candidate miRNAs affecting mRNA levels within CE-RSCs, PE or adult retina. Analyses were performed using the DAVID bioinformatics database [35]; categories with $p < 0.05$ after correction for multiple comparisons (Benjamini) are listed.
Click here for file
[http://www.biomedcentral.com/content/supplementary/1471-213X-10-1-S4.XLS]

Acknowledgements
The authors would like to acknowledge the contribution of all the researchers who have made their gene expression data publicly available and without whom this study would not have been possible.

Authors' contributions
AA performed bioinformatic analyses and some laboratory work; JG-F performed RT-PCR and ISH and contributed to manuscript preparation. LH performed miRNA transfections and mRNA RT-PCR. MD performed microarray analysis with P4 mice; TC contributed to supervision and manuscript preparation; DAS conceived and supervised the study, performed bioinformatic analyses and prepared the manuscript. All authors read and approved the final manuscript.

Received: 18 March 2009
Accepted: 6 January 2010 Published: 6 January 2010

References

1. Bartel DP: **MicroRNAs: genomics, biogenesis, mechanism, and function.** *Cell* 2004, **116(2)**:281-297.
2. Lee RC, Feinbaum RL, Ambros V: **The C. elegans heterochronic gene lin-4 encodes small RNAs with antisense complementarity to lin-14.** *Cell* 1993, **75(5)**:843-854.
3. Reinhart BJ, Slack FJ, Basson M, Pasquinelli AE, Bettinger JC, Rougvie AE, Horvitz HR, Ruvkun G: **The 21-nucleotide let-7 RNA regulates developmental timing in Caenorhabditis elegans.** *Nature* 2000, **403(6772)**:901-906.
4. Wightman B, Ha I, Ruvkun G: **Posttranscriptional regulation of the heterochronic gene lin-14 by lin-4 mediates temporal pattern formation in C. elegans.** *Cell* 1993, **75(5)**:855-862.
5. Stefani G, Slack FJ: **Small non-coding RNAs in animal development.** *Nat Rev Mol Cell Biol* 2008, **9(3)**:219-230.
6. Damiani D, Alexander JJ, O'Rourke JR, McManus M, Jadhav AP, Cepko CL, Hauswirth WW, Harfe BD, Strettoi E: **Dicer inactivation leads to progressive functional and structural degeneration of the mouse retina.** *J Neurosci* 2008, **28(19)**:4878-4887.
7. Li X, Carthew RW: **A microRNA mediates EGF receptor signaling and promotes photoreceptor differentiation in the Drosophila eye.** *Cell* 2005, **123(7)**:1267-1277.
8. Ryan DG, Oliveira-Fernandes M, Lavker RM: **MicroRNAs of the mammalian eye display distinct and overlapping tissue specificity.** *Mol Vis* 2006, **12**:1175-1184.
9. Karali M, Peluso I, Marigo V, Banfi S: **Identification and characterization of microRNAs expressed in the mouse eye.** *Invest Ophthalmol Vis Sci* 2007, **48(2)**:509-515.
10. Makarev E, Spence JR, Del Rio-Tsonis K, Tsonis PA: **Identification of microRNAs and other small RNAs from the adult newt eye.** *Mol Vis* 2006, **12**:1386-1391.
11. Xu S, Witmer PD, Lumayag S, Kovacs B, Valle D: **MicroRNA (miRNA) Transcriptome of Mouse Retina and Identification of a Sensory Organ-specific miRNA Cluster.** *J Biol Chem* 2007, **282(34)**:25053-25066.
12. Loscher CJ, Hokamp K, Wilson JH, Li T, Humphries P, Farrar GJ, Palfi A: **A common microRNA signature in mouse models of retinal degeneration.** *Exp Eye Res* 2008, **87(6)**:529-534.
13. Loscher CJ, Hokamp K, Kenna PF, Ivens AC, Humphries P, Palfi A, Farrar GJ: **Altered retinal microRNA expression profile in a mouse model of retinitis pigmentosa.** *Genome Biol* 2007, **8(11)**:R248.
14. Arora A, McKay GJ, Simpson DA: **Prediction and Verification of miRNA Expression in Human and Rat Retinas.** *Invest Ophthalmol Vis Sci* 2007, **48(9)**:3962-3967.
15. Pillai RS, Bhattacharyya SN, Filipowicz W: **Repression of protein synthesis by miRNAs: how many mechanisms?.** *Trends Cell Biol* 2007, **17(3)**:118-26.
16. Baek D, Villen J, Shin C, Camargo FD, Gygi SP, Bartel DP: **The impact of microRNAs on protein output.** *Nature* 2008, **455(7209)**:64-71.
17. Selbach M, Schwanhausser B, Thierfelder N, Fang Z, Khanin R, Rajewsky N: **Widespread changes in protein synthesis induced by microRNAs.** *Nature* 2008, **455(7209)**:58-63.
18. Lim LP, Lau NC, Garrett-Engele P, Grimson A, Schelter JM, Castle J, Bartel DP, Linsley PS, Johnson JM: **Microarray analysis shows that some microRNAs downregulate large numbers of target mRNAs.** *Nature* 2005, **433(7027)**:769-773.
19. Lagos-Quintana M, Rauhut R, Yalcin A, Meyer J, Lendeckel W, Tuschl T: **Identification of tissue-specific microRNAs from mouse.** *Curr Biol* 2002, **12(9)**:735-739.
20. Sood P, Krek A, Zavolan M, Macino G, Rajewsky N: **Cell-type-specific signatures of microRNAs on target mRNA expression.** *Proc Natl Acad Sci USA* 2006, **103(8)**:2746-2751.
21. Yu Z, Raabe T, Hecht NB: **MicroRNA Mirn122a reduces expression of the posttranscriptionally regulated germ cell transition protein 2(Tnp2) messenger RNA (mRNA) by mRNA cleavage.** *Biol Reprod* 2005, **73(3)**:427-433.

22. Krutzfeldt J, Rajewsky N, Braich R, Rajeev KG, Tuschl T, Manoharan M, Stoffel M: **Silencing of microRNAs in vivo with 'antagomirs'.** *Nature* 2005, **438(7068)**:685-689.
23. Grimson A, Farh KK, Johnston WK, Garrett-Engele P, Lim LP, Bartel DP: **MicroRNA targeting specificity in mammals: determinants beyond seed pairing.** *Mol Cell* 2007, **27(1)**:91-105.
24. Lewis BP, Burge CB, Bartel DP: **Conserved seed pairing, often flanked by adenosines, indicates that thousands of human genes are microRNA targets.** *Cell* 2005, **120(1)**:15-20.
25. Maziere P, Enright AJ: **Prediction of microRNA targets.** *Drug Discov Today* 2007, **12(11-12)**:452-458.
26. Krek A, Grun D, Poy MN, Wolf R, Rosenberg L, Epstein EJ, MacMenamin P, da Piedade I, Gunsalus KC, Stoffel M, Rajewsky N: **Combinatorial microRNA target predictions.** *Nat Genet* 2005, **37(5)**:495-500.
27. Griffiths-Jones S, Saini HK, van Dongen S, Enright AJ: **miRBase: tools for microRNA genomics.** *Nucleic Acids Res* 2008, , **36 Database:** D154-8.
28. **miRBase.** http://microrna.sanger.ac.uk/.
29. Arora A, Simpson DA: **Individual mRNA expression profiles reveal the effects of specific microRNAs.** *Genome Biol* 2008, **9(5)**:R82.
30. Elmen J, Lindow M, Silahtaroglu A, Bak M, Christensen M, Lind-Thomsen A, Hedtjarn M, Hansen JB, Hansen HF, Straarup EM, McCullagh K, Kearney P, Kauppinen S: **Antagonism of microRNA-122 in mice by systemically administered LNA-antimiR leads to up-regulation of a large set of predicted target mRNAs in the liver.** *Nucleic Acids Res* 2008, **36(4)**:1153-62.
31. Rutledge RG, Stewart D: **A kinetic-based sigmoidal model for the polymerase chain reaction and its application to high-capacity absolute quantitative real-time PCR.** *BMC Biotechnol* 2008, **8**:47.
32. Zhang K, Kniazeva M, Han M, Li W, Yu Z, Yang Z, Li Y, Metzker ML, Allikmets R, Zack DJ, Kakuk LE, Lagali PS, Wong PW, MacDonald IM, Sieving PA, Figueroa DJ, Austin CP, Gould RJ, Ayyagari R, Petrukhin K: **A 5-bp deletion in ELOVL4 is associated with two related forms of autosomal dominant macular dystrophy.** *Nat Genet* 2001, **27(1)**:89-93.
33. Lagali PS, Liu J, Ambasudhan R, Kakuk LE, Bernstein SL, Seigel GM, Wong PW, Ayyagari R: **Evolutionarily conserved ELOVL4 gene expression in the vertebrate retina.** *Invest Ophthalmol Vis Sci* 2003, **44(7)**:2841-2850.
34. Krishnan A, Venkataraman V, Fik-Rymarkiewicz E, Duda T, Sharma RK: **Structural, biochemical, and functional characterization of the calcium sensor neurocalcin delta in the inner retinal neurons and its linkage with the rod outer segment membrane guanylate cyclase transduction system.** *Biochemistry* 2004, **43(10)**:2708-2723.
35. Huang da W, Sherman BT, Lempicki RA: **Systematic and integrative analysis of large gene lists using DAVID bioinformatics resources.** *Nat Protoc* 2009, **4(1)**:44-57.
36. Das AV, James J, Rahnenfuhrer J, Thoreson WB, Bhattacharya S, Zhao X, Ahmad I: **Retinal properties and potential of the adult mammalian ciliary epithelium stem cells.** *Vision Res* 2005, **45(13)**:1653-1666.
37. Wienholds E, Plasterk RH: **MicroRNA function in animal development.** *FEBS Lett* 2005, **579(26)**:5911-5922.
38. Gu P, Harwood LJ, Zhang X, Wylie M, Curry WJ, Cogliati T: **Isolation of retinal progenitor and stem cells from the porcine eye.** *Mol Vis* 2007, **13**:1045-1057.
39. Coles BL, Angenieux B, Inoue T, Del Rio-Tsonis K, Spence JR, McInnes RR, Arsenijevic Y, Kooy van der D: **Facile isolation and the characterization of human retinal stem cells.** *Proc Natl Acad Sci USA* 2004, **101(44)**:15772-15777.
40. Inoue Y, Yanagi Y, Tamaki Y, Uchida S, Kawase Y, Araie M, Okochi H: **Clonogenic analysis of ciliary epithelial derived retinal progenitor cells in rabbits.** *Exp Eye Res* 2005, **81(4)**:437-445.
41. Xu S, Sunderland ME, Coles BL, Kam A, Holowacz T, Ashery-Padan R, Marquardt T, McInnes RR, Kooy van der D: **The proliferation and expansion of retinal stem cells require functional Pax6.** *Dev Biol* 2007, **304(2)**:713-721.
42. Walker JC, Harland RM: **microRNA-24a is required to repress apoptosis in the developing neural retina.** *Genes Dev* 2009, **23(9)**:1046-1051.
43. Wang Q, Huang Z, Xue H, Jin C, Ju XL, Han JD, Chen YG: **MicroRNA miR-24 inhibits erythropoiesis by targeting activin type I receptor ALK4.** *Blood* 2008, **111(2)**:588-595.
44. Tzur G, Levy A, Meiri E, Barad O, Spector Y, Bentwich Z, Mizrahi L, Katzenellenbogen M, Ben-Shushan E, Reubinoff BE, Galun E: **MicroRNA expression patterns and function in endodermal differentiation of human embryonic stem cells.** *PLoS ONE* 2008, **3(11)**:e3726.
45. Kapsimali M, Kloosterman WP, de Bruijn E, Rosa F, Plasterk RH, Wilson SW: **MicroRNAs show a wide diversity of expression profiles in the developing and mature central nervous system.** *Genome Biol* 2007, **8(8)**:R173.
46. Smirnova L, Grafe A, Seiler A, Schumacher S, Nitsch R, Wulczyn FG: **Regulation of miRNA expression during neural cell specification.** *Eur J Neurosci* 2005, **21(6)**:1469-1477.
47. Makeyev EV, Zhang J, Carrasco MA, Maniatis T: **The MicroRNA miR-124 promotes neuronal differentiation by triggering brain-specific alternative pre-mRNA splicing.** *Mol Cell* 2007, **27(3)**:435-448.
48. Bak M, Silahtaroglu A, Moller M, Christensen M, Rath MF, Skryabin B, Tommerup N, Kauppinen S: **MicroRNA expression in the adult mouse central nervous system.** *RNA* 2008, **14(3)**:432-44.
49. Visvanathan J, Lee S, Lee B, Lee JW, Lee SK: **The microRNA miR-124 antagonizes the anti-neural REST/SCP1 pathway during embryonic CNS development.** *Genes Dev* 2007, **21(7)**:744-749.
50. Leucht C, Stigloher C, Wizenmann A, Klafke R, Folchert A, Bally-Cuif L: **MicroRNA-9 directs late organizer activity of the midbrain-hindbrain boundary.** *Nat Neurosci* 2008, **11(6)**:641-648.
51. Krichevsky AM, Sonntag KC, Isacson O, Kosik KS: **Specific microRNAs modulate embryonic stem cell-derived neurogenesis.** *Stem Cells* 2006, **24(4)**:857-864.
52. Wu L, Fan J, Belasco JG: **MicroRNAs direct rapid deadenylation of mRNA.** *Proc Natl Acad Sci USA* 2006, **103(11)**:4034-4039.
53. Wu L, Belasco JG: **Let me count the ways: mechanisms of gene regulation by miRNAs and siRNAs.** *Mol Cell* 2008, **29(1)**:1-7.
54. Barrett T, Troup DB, Wilhite SE, Ledoux P, Rudnev D, Evangelista C, Kim IF, Soboleva A, Tomashevsky M, Edgar R: **NCBI GEO: mining tens of millions of expression profiles–database and tools update.** *Nucleic Acids Res* 2007, , **35 Database:** D760-5.
55. **Gene Expression Omnibus (GEO).** http://www.ncbi.nlm.nih.gov/projects/geo/.
56. Lewis BP, Shih IH, Jones-Rhoades MW, Bartel DP, Burge CB: **Prediction of mammalian microRNA targets.** *Cell* 2003, **115(7)**:787-798.
57. **TargetScan: Prediction of microRNA targets.** http://www.targetscan.org/.
58. **The Comprehensive R Archive Network.** http://cran.r-project.org/.
59. **BioMart Project.** http://www.biomart.org/.
60. Fisher RA: *Statistical Methods for Research Workers* Edinburgh: Oliver and Boyd 1932.
61. Shi R, Chiang VL: **Facile means for quantifying microRNA expression by real-time PCR.** *BioTechniques* 2005, **39(4)**:519-525.
62. **miRBase: the microRNA database.** http://www.mirbase.org/.
63. Griffiths-Jones S, Grocock RJ, van Dongen S, Bateman A, Enright AJ: **miRBase: microRNA sequences, targets and gene nomenclature.** *Nucleic Acids Res* 2006, , **34 Database:** D140-4.
64. Paper W, Kroeber M, Heersink S, Stephan DA, Fuchshofer R, Russell P, Tamm ER: **Elevated amounts of myocilin in the aqueous humor of transgenic mice cause significant changes in ocular gene expression.** *Exp Eye Res* 2008, **87(3)**:257-267.
65. Steele MR, Inman DM, Calkins DJ, Horner PJ, Vetter ML: **Microarray analysis of retinal gene expression in the DBA/2J model of glaucoma.** *Invest Ophthalmol Vis Sci* 2006, **47(3)**:977-985.
66. Akimoto M, Cheng H, Zhu D, Brzezinski JA, Khanna R, Filippova E, Oh EC, Jing Y, Linares JL, Brooks M, Zareparsi S, Mears AJ, Hero A, Glaser T, Swaroop A: **Targeting of GFP to newborn rods by Nrl promoter and temporal expression profiling of flow-sorted photoreceptors.** *Proc Natl Acad Sci USA* 2006, **103(10)**:3890-3895.

doi:10.1186/1471-213X-10-1
Cite this article as: Arora *et al.*: Prediction of microRNAs affecting mRNA expression during retinal development. *BMC Developmental Biology* 2010 **10**:1.

CHAPTER 5

RPE AND NEURONAL DIFFERENTIATION OF ALLOTRANSPLANTATED PORCINE CILIARY EPITHELIUM-DERIVED CELLS

Reprinted from Molecular Vision **17**, 2580-2595 (2011)

Molecular Vision 2011; 17:2580-2595 <http://www.molvis.org/molvis/v17/a279>
Received 10 August 2010 | Accepted 2 October 2011 | Published 5 October 2011

© 2011 Molecular Vision

RPE and neuronal differentiation of allotransplantated porcine ciliary epithelium-derived cells

Jasenka Guduric-Fuchs,[1] Wing Chen,[2] Henrietta Price,[3] Desmond B. Archer,[1] Tiziana Cogliati[1]

[1]Centre for Vision and Vascular Sciences, Queen's University Belfast, Royal Victoria Hospital, Institute of Clinical Science, Northern Ireland, UK; [2]Royal Victoria Hospital, Grosvenor Road, Belfast, Northern Ireland, UK; [3]The Agri-Food and Biosciences Institute (AFBI), Chemical Surveillance Branch, Veterinary Sciences Division, Stoney Road, Stormont, Belfast, Northern Ireland UK

Purpose: Cell replacement has the potential to be applied as a therapeutic strategy in retinal degenerative diseases such as retinitis pigmentosa and age-related macular degeneration (AMD) for which no adequate pharmacological and surgical treatments are currently available. Although controversial, the use of ciliary epithelium (CE)-derived cells is supported by evidence showing their differentiation into retinal phenotypes. This study examines the differentiation potential of porcine CE-derived cells in vitro and their survival, migration, morphological characteristics, and immunohistochemical phenotype in vivo, upon transplantation into the subretinal space of normal pigs.

Methods: Cells were isolated from the CE of postnatal pigs and were grown in a suspension sphere culture. Differentiation was assessed in vitro after exposure to laminin and the addition of serum. For transplantation, CE-derived spheres were dissociated, labeled with CM-DiI vital dye, and the cells were injected subretinally into one eye of eight week-old allorecipients. The eyes were examined at eight days and at two and four weeks after transplantation.

Results: Cells positive for neuronal and retinal pigment epithelium (RPE) markers were detected by immunohistochemistry in differentiation cultures. Reverse Transcriptase-Polymerase Chain Reaction (RT–PCR) revealed upregulation of neuronal markers after in vitro differentiation. CM-DiI dye-labeled CE-derived cells dissociated from primary spheres survived for up to four weeks after transplantation in vivo. Some of the surviving cells migrated distantly from the injection site. Large clusters of transplanted cells integrated into the RPE layer and multilayered RPE-like structures positive for RPE65 were often observed. Grafted cells were also identified in the neuroretina where 5%–10% were positive for recoverin, protein kinase C alpha (PKCα), and calbindin.

Conclusions: The efficient conversion to an RPE-like phenotype suggests that CE-derived cells could be a potential source of RPE for cell replacement. Our data also suggest that the ability of these cells to acquire neuronal phenotypes is influenced by the environment. Thus, pre-differentiated or (re)programmed CE-derived cells may be more amenable for retinal repair.

Cell replacement is a promising approach to restore neural function in the degenerating nervous system, including the retina. Since retinal dystrophies are ultimately characterized by the loss of photoreceptors, efforts have been made in the last decade to identify suitable sources of stem/progenitor cells and drive their differentiation along the photoreceptor lineage in vitro and in vivo. Several cell populations with retinal progenitor properties have been identified in the eye, including Müller glia, ciliary epithelium (CE)-derived, and iris-derived, and their ability to generate retinal cell types has been reported [1-4]. CE-derived cells have been shown to display stem/progenitor cell features, including clonal expansion and differentiation toward retinal phenotypes under appropriate conditions in vitro and in vivo [5-8]. The CE is located in a surgically accessible part of the eye, therefore, cells derived from this tissue offer an attractive possibility for autologous transplantation.

It is well established that continuous growth of the eye in lower vertebrates such as fish and frogs depends on the retinal stem cells located in the ciliary marginal zone [9]. A similar but less potent stem cell zone has also been identified in chickens [10]. Although an analogous structure does not exist in mammals, it has been proposed that multipotent retinal stem cells can be isolated from the CE [5,6]. However, the nature and the developmental potential of cells derived from the CE have been the object of controversy in recent literature. First, the existence of a small quiescent population of retinal stem cells (RSCs) in the CE that can be propagated in vitro has been challenged [11]. Second, the "stemness" of cells in neurospheres derived from the CE has been questioned on the basis of the persistence of pigmentation and of their expression of makers and the characteristics of pigmented CE [11]. Finally, doubts have been expressed about the developmental potential of CE-derived cultures and their

Correspondence to: Jasenka Guduric-Fuchs, QUB-Centre for Vision and Vascular Science, RVH-Institute of Clinical Science, Belfast BT12 6BA, N. Ireland, UK; Phone: +44-28-9063-2729; FAX: +44-28-9063-2699; email: j.guduricfuchs@qub.ac.uk

Dr. Tiziana Cogliati is now at Neurobiology-Neurodegeneration & Repair Laboratory, NIH - National Eye Institute, Bldg 6, Rm 302, Bethesda, MD 20892-0610.

Molecular Vision 2011; 17:2580-2595 <http://www.molvis.org/molvis/v17/a279> © 2011 Molecular Vision

capacity to differentiate along retinal lineages [11,12]. While all published literature is concordant in reporting the limited self-renewal capacity of CE-derived cells [5,7,8,13,14], work from several laboratories has shown their differentiation, both in vitro and in vivo, into neuronal and photoreceptor-like phenotypes [7,13,15,16]. Thus, although the definition as RSCs might not be the most appropriate, further investigation is needed to test the potential of CE-derived cells to generate retinal photoreceptors either by direct differentiation, transdifferentiation, or genetic manipulation.

Due to its close similarity to the human eye, a pig eye provides an appropriate system for the evaluation of potential therapeutic strategies for retinal degeneration [17,18]. Furthermore, the size of a pig eye enables accurate dissection of the ciliary epithelium without contamination from tissues such as the retina or RPE. In addition, pig eyes can be freshly harvested from euthanized animals, offering an advantage over human specimens that are usually available for research after a prolonged post-mortem period. Although porcine CE-derived cells have been isolated and studied before by the authors of this report and by others [8,19], this is the first study to include the subretinal transplantation of these cells. To date, the transplantation studies using CE derived cells have only been performed in murine animal models, although xenotransplantation of human cells into a developing mouse eye has also been performed [7,11,20]. Here, we evaluated the ability of postnatal porcine CE-derived cells to generate retinal cell types in vitro and when injected subretinally into allorecipient eyes. We adopted surgical procedures similar to those used for subretinal transplantation of fetal retinal progenitor cells in pigs [21,22].

METHODS

All animals procedures were approved by The Queen's University of Belfast Animal Ethics Committee and were performed in accordance with the UK Animals (Scientific Procedures) Act, 1986 and the ARVO statement on animal use. Mixed sex, white Landrance pigs were obtained from Agri-Food and Biosciences Institute (Hillsborough, Northern Ireland).

Cell isolation and culture: One to two week-old piglets were anaesthetized with 15 mg/kg of intra-muscular azaperone (Stresnil, Janssen Animal Health, Saunderton, UK) and 20 mg/kg ketamine (Ketaset, Fort Dodge Animal Health, Southampton, UK) and were euthanized by intravenous or intra-cardiac injection of 100 mg/kg pentobarbitone (Pentoject, Animalcare, Masham Ripon, UK). The eyes were enucleated and placed into oxygenated artificial cerebral spinal fluid (aCSF: 124 mM NaCl, 5 mM KCl, 1.3 mM $MgCl_2$, 26 mM $NaHCO_3$, and 10 mM D-glucose, pH 7.5). The eyes were bisected at the ora serrata. The vitreous was decanted from the anterior half and the lens was removed. The ciliary body was dissected from the iris and pars plana. The strips of ciliary body were enzymatically digested in Hanks' Balanced Salt Solution (HBSS) containing 2 mg/ml dispase (all from Sigma-Aldrich, Poole, UK) for 20 min at 37 °C, followed by digestion in Earle's Balanced Salt Solution (EBSS) containing 1.33 mg/ml trypsin, 0.67 mg/ml hyaluronidase, and 78 units/ml collagenase (Sigma-Aldrich) for 20 min at 37 °C. The supernatant was decanted and replaced with a serum-free medium (SFM, DMEM/F12 [1:1] containing 0.6% [w/v] glucose, 2 mM glutamine, 5 mM HEPES buffer, 2% [v/v] B27, 100 units/ml penicillin, and 100 units/ml streptomycin) with 1 mg/ml trypsin inhibitor (Invitrogen, Paisley, UK) and was incubated for 5 min at room temperature. The strips of ciliary body were subsequently placed in a 60 mm cell culture dish containing the SFM. Epithelial cells were peeled off and the non-epithelial tissue was discarded. The epithelial cellular debris was gently triturated 10–15 times using a pipette. Cells were pelleted at 1,000× g for 10 min, resuspended in the SFM, and were passed through a 40 µm cell strainer (BD Biosciences, Franklin Lakes, NJ). The cells were counted and plated at a density of 3×10^4 cells/ml in the SFM supplemented with 20 ng/ml of an epidermal growth factor (EGF, Invitrogen) and 20 ng/ml of a basic fibroblast growth factor (bFGF, Invitrogen). After seven days, newly formed sphere colonies were collected, pelleted at 1,000× g for 10 min, digested in an Accumax cell counting solution (ICT, San Diego, CA) for 20 min at 20 °C, and were mechanically dissociated into single cells by pipetting and replating at a density of 3×10^4 cells/ml.

For differentiation, CE-derived spheres were collected at the first passage, plated on poly-D-lysine and laminin-coated glass coverslips (BD Biosciences), and were allowed to differentiate for 20 days in the presence of either fetal calf serum (1%, 5%, and 10%), or of 1% serum with growth factors (10 ng/ml of EGF and bFGF). The medium was replaced every three days. After 20 days of differentiation, the cells were fixed in 4% PFA for 20 min at room temperature and were processed for immunocytochemistry.

For cell transplantation, spheres from the first passage were collected and dissociated into single cells using Accumax (ICT, San Diego, CA). The cells were labeled with CM-DiI (Invitrogen) following the manufacturer's protocol and were injected as described below.

Conventional RT–PCR: Total RNA was extracted using an RNeasy Mini Kit (Qiagen, Crawley, UK). On column DNaseI digestion was performed to digest any contaminating genomic DNA. One µg of RNA was reverse transcribed using random primers and SuperScript II (Invitrogen) according to the manufacturer's instructions. No RT controls were performed by omission of reverse transcriptase in the reaction. PCR was performed in a 30 µl reaction volume containing 1 µl of cDNA, 0.2 µM sense and anti-sense primers, 1× PCR buffer (Qiagen), 10 mM dNTP mix (Roche, Burgess Hill, UK), and 1 µl Hot Start DNA polymerase (Qiagen). Primer sequences are shown in Table 1. PCR was performed for 40

Molecular Vision 2011; 17:2580-2595 <http://www.molvis.org/molvis/v17/a279> © 2011 Molecular Vision

Table 1. Primer sequences used for RT–PCR.

Gene	Accession No (reference)	Forward primer	Reverse primer	Product size (bp)
Nanog	NM_001129971.1	TGGAGTAACCCAACCTGGAG	ATGATTTGCTGCTGGGTACC	269
0ct4	NM_001113060.1	GTTTTGAGGCTTTGCAGCTC	TCTCCAGGTTGCCTCTCACT	183
cMyc	NM_001005154.1	GGAAGGACTATCCCTCTGCC	TCCAACTCTGGGATCTGGTC	208
Klf4	NM_001031782.1	CAGCTTCAGCTATCCGATCC	TGATGTCTGCCAGGTTGAAG	128
Sox2	[21]	GGCAGCTACAGCATGATGCAGGAGC	CTGGTCATGGAGTTGTACTGCAGG	131
Six3	[21]	AGCGGACTCGGAGCCTGTTG	AGCGCATGCCGCTCGGTCCA	202
Otx2	XM_003121824.1	GCTGTGTGAATTGTGCGACT	GGTGGAGTTCAAGGTTGCAT	193
Mitf	NM_001038001.1	GGGCCGCCTAAAGCGTGGT	GGTCGCCAGGCTGGTTTGGAC	198
Chx10	NM_182894.2	AGGGAGAACAGCATTGCGGTGC	GCGCCTTGACCTAAGCCATGTCC	193
Hes1	NM_001195231.1	CAGCCAGTGTCAACACGACAC	TCGTTCATGCACTCACTGA	307
HPRT	NM_001032376.2	CCAGTCAACGGGCGATATAA	CTTGACCAAGGAAAGCAAGG	130
PKC alpha	XM_003131278.1	GACCATCCGCTCTACACTCAAC	CCCAGTCCCAGATTTCTACAG	104
Calbindin	NM_001130226.1	TCTGCTGGGGACAACTAAATTT	CAGCCTACTCCGTTACAGTGCA	93
Rhodopsin	NM_214221.1	TCCATCTACAACCCCGTCAT	CTGTCTTGGAAGTGGTGGTG	127

Primers were either designed from sequences retrieved under the accession numbers shown, or taken from published studies.

cycles using a thermocycler (ABI 2720, Applied Biosystems, Foster City, CA). PCR products were resolved on 1.5% agarose gel.

Real time RT–PCR: For differentiation, CE-derived spheres were collected at the first passage, plated on poly-D-lysine and laminin-coated six well plates (BD Biosciences), and were allowed to differentiate for 20 days in the presence of 1% serum and 10 ng/ml of EGF and bFGF. The medium was replaced every three days. After 20 days, the cells were harvested and RNA was isolated and reverse transcribed as outlined above. Real time PCR was performed with 2× Maxima SYBR Green qPCR Mastermix (Fermentas, Cambridge, UK) in 10 µl reactions containing 2 µl of 1:15 cDNA dilution and 0.5 µM of the gene specific primer. Primer efficiencies were determined from standard curves constructed using serial dilutions of pooled cDNA. Hypoxathineposphoribosyltransferase (*HPRT*) was used as the housekeeping gene for normalization. Primer sequences are shown in Table 1. Reactions were performed on a LightCycler PCR system (Roche) with the following program: initial denaturation at 95 °C for 10 min, followed by 40 cycles at 95 °C for 15 s, 58 °C for 10 s, and 72 °C for 15 s. Relative gene expression (including statistical analysis) was determined using REST software. The RNA from three independent experiments was analyzed and all reactions were performed in triplicate.

Surgical procedure: One eye from eight week-old (weight from 17.5 to 21 kg) female pigs (n=8) was transplanted. Prior to transfer to the operating theater, the animals were sedated with 2 mg/kg of azaperone (Stresnil; Janssen Animal Health, Saunderton, UK) by intramuscular injection. In the theater, the animals were sedated by intramuscular injection of 1 mg/kg xylazine (Rompun 2%; Bayer, Newbury, UK) and 4 mg/kg of ketamine hydrochloride (Ketaset 100 mg/ml; Fort Dodge, Southampton, UK), followed by administration of 0.2 mg/kg morphine (Morphine sulfate 10mg/ml; controlled drug [CD], UK). Anesthesia was induced for tracheal intubation with 1 mg/kg intravenous alfaxalone (Alfaxan 10mg/ml; Vetoquinol, Buckingham, UK), and was maintained using 1%–1.75% isoflurane in oxygen. Approximately 0.5 l of lactated Ringer's (Hartman's) isotonic solution was infused intravenously during anesthesia.

The pupil in each eye was dilated with topical medication (1 to 3 drops each of Gt cyclopentolate 1% and Gt phenylephrine 2.5%). A standard three-port pars plana vitrectomy was performed. The sclerotomies were positioned 2 mm posterior to the limbus. A retinotomy in the area centralis was performed using a 42G needle (Bausch and Lomb, Whelehan Group, Dublin). A small subretinal air bubble was created through the retinotomy, followed by the injection of $1x10^6$ cells in a maximum volume of 0.1 ml of phosphate-buffered saline (PBS) into the subretinal space. The sclerotomies were closed using 7/0 braided polyglactin sutures (Vicryl; Ethicon, Livingston, UK).

One pig was killed before recovery from anesthesia by intravenous pentobarbitone overdose at the end of the surgery. An intravenous injection of 2–4 mg/kg carprofen (Rimadyl Large Animal 50 mg/ml; Pfizer, Sandwich, UK) was administered to the other pigs after transplantation and before recovery from the anesthetic (by discontinuation of isoflurane), and xylazine sedation was reversed as necessary using approximately 0.2 mg/kg atipamezole (Antisedan 5 mg/ml; Pfizer). The animals were kept in a warm chamber for the first day after surgery. Topical eye drops containing 0.3% tobramycin and 0.1% dexamethasone (Tobradex; Alcon, Hemel Hempstead, UK) were instilled at the end of surgery, and then daily for 14 days post surgery.

At 8, 14, or 28 days after transplantation the animals were lethally anaesthetized with intravenous injection of pentobarbitone (2–4 g), and their eyes were enucleated and

Molecular Vision 2011; 17:2580-2595 <http://www.molvis.org/molvis/v17/a279> © 2011 Molecular Vision

Table 2. Primary antibodies used for immunohistochemical analysis.

Antibody	Host	Dilution	Source
Recoverin	rabbit	1:1000	Kind gift from Karl-Wilhelm Koch
Rhodopsin (Rho4D2)	mouse	1:100	Kind gift from Robert Molday
PKCα	mouse	1:400	Sigma-Aldrich
Calbindin	rabbit	1:1500	Chemicon, Millipore
RPE65	mouse	1:400	Chemicon, Millipore
Ki67	mouse	1:300	BD Biosciences
Neurofilament (NF)-M	mouse	1:350	Sigma-Aldrich
HuC/D	mouse	1:200	Molecular probes, Invitrogen

Host animal, dilution and source for each antibody are shown.

washed in PBS. After removal of the cornea and lens, the eyes were fixed in 4% PFA in PBS for 1 h at room temperature. The eyecups were cryoprotected in 10% sucrose for 6 h followed by 30% sucrose overnight, embedded in an optimal cutting temperature (OCT) compound (Sakura, Kobe, Japan), and were snap frozen in an isopentane bath on dry ice. Transverse cryosections (20 µm) were cut, mounted onto Superfrost Plus glass slides (Fisher Scientific, Loughborough, UK), and stored at −80 °C until used.

Immunohistochemistry: Immunohistochemistry on tissue sections was performed as described previously [18]. Briefly, slides were thawed at room temperature and were post-fixed in 4% formaldehyde (Sigma-Aldrich) in PBS for 20 min at room temperature. After rinsing in PBS, sections were blocked for 1 h in 10% normal goat serum (NGS), 0.3% Triton X-100, 0.01% NaN_3 in PBS, at room temperature. Slides were incubated for 24 h at 4 °C with a primary antibody diluted in 10% NGS, 0.3% Triton X-100, and 0.01% NaN_3 in PBS. The primary antibodies used are listed in Table 2. After removal of the primary antibody, slides were washed 6×5 min in PBS and were incubated for 1 h at room temperature in a secondary antibody (Alexa Fluor^{488} goat anti-mouse or goat anti-rabbit), 1:500 in PBS. After 3×5 min washing steps in PBS, cell nuclei were counterstained with 5 µM DAPI (Invitrogen) for 10 min. The slides were mounted in a fluorescent mounting medium (Dako, Ely, UK). Negative immunohistochemistry controls were performed in parallel by omission of the primary antibody. Immunoreactive cells were visualized and images were recorded using an inverted confocal microscope (Nikon, Model Eclipse TE 2000-U, Tokyo, Japan) and Nikon EZ-C1 software. Every tenth or twentieth section (200–400 µm step) was stained for the same antibody.

For isolectin B4 staining, sections were blocked in 5% BSA for 30 min, incubated with biothynilated Griffonia simplicifolia Isolectin B4 (Vector) 1:100 for 1 h, washed for 3×5 min with PBS, and were finally incubated with streptavidin-FITC 1:200 for 1 h.

For the immunocytochemistry of the differentiated cells, post-fixation glass slides were washed 3× in PBS, incubated in 10% NGS, 0.3% Triton X-100, and 0.01% NaN_3 in PBS for 1 h at room temperature, followed by overnight incubation at 4 °C. The slides were incubated for 24 h at 4 °C with the primary antibody diluted in 10% NGS, 0.3% Triton X-100, and 0.01% NaN_3 in PBS. For double labeling, the second primary antibody was added after removal of the first primary antibody and was incubated for another 24 h at 4 °C. After removal of the second primary antibody, the slides were washed for 6×5 min with PBS and were incubated in the first secondary antibody (Alexa Fluor488 goat antimouse) diluted 1:500 in PBS for 1 h. Subsequently, incubation with another secondary antibody (Alexa Fluor568 goat antirabbit), was performed for 1 h. The slides were washed for 3×5 min with PBS and were counterstained and mounted as described above. The cells were visualized and the images were captured with an epifluorescence microscope (Nikon) using Nis Elements (Nikon) software. The number of positive cells was counted in 20 random fields at 40× magnification.

RESULTS

Analysis of the gene expression of CE-derived spheres: Expression of the key pluripotency genes [23,24] and the genes active during normal retinal development was analyzed by RT–PCR using RNA extracted from P1 CE-derived spheres. Transcripts for three pluripotency genes, namely *cMyc*, *Klf4*, and *Sox2* were present in CE-derived cultures, while mRNAs for *Nanog* and *Oct4* were not detected (Figure 1A). Transcription factors associated with the eye specification and retinal histogenesis, including Six3, Mitf, Hes1, Otx2 and Chx10, were also expressed in CE-derived spheres (Figure 1B).

In vitro differentiation of CE-derived spheres: The capacity of CE-derived cells from newborn pigs to differentiate into retinal phenotypes was first evaluated in vitro, after plating CE spheres on adherent substrates (poly-D-lysine and laminin) and culturing for 20 days with a differentiation medium containing serum and growth factors. Growth factors (10 ng/ml bFGF and EGF) enhanced retinal differentiation in the presence of 1% serum (Figure 2). Photoreceptor markers

Molecular Vision 2011; 17:2580-2595 <http://www.molvis.org/molvis/v17/a279> © 2011 Molecular Vision

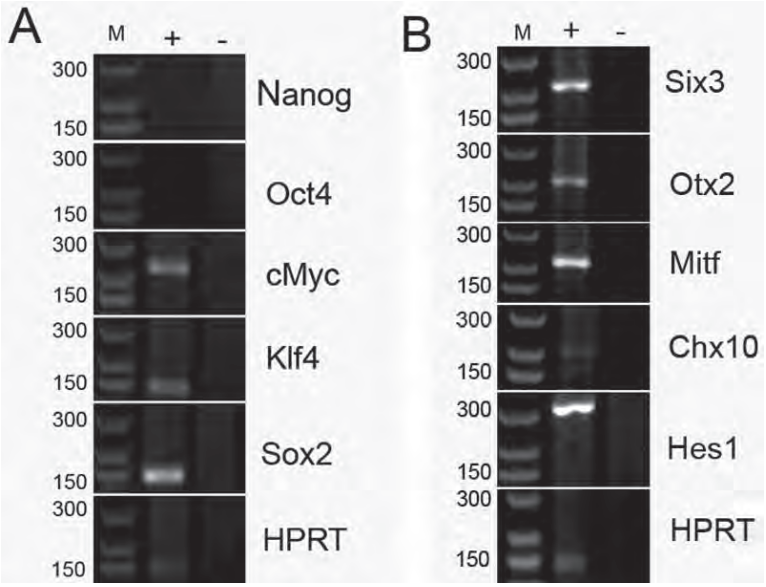


Figure 1. Gene expression of ciliary epithelium (CE)-derived cells determined by RT–PCR. RNA was isolated from passage 1 and was subjected to conventional RT–PCR. PCR products were resolved on 1.5% agarose gel. **A**: Amplification of mRNA for pluripotency markers. **B**: Amplification of mRNA for retinal progenitor genes. Sizes in base pairs for the corresponding marker bands (M) are shown on the left, adjacent to the gel images. PCR reactions performed with cDNA template are shown in lanes marked as '+' and negative control reactions performed with templates from the RT where reverse transcriptase was omitted are shown in lanes marked as '–'. Amplicons for a housekeeping gene (HPRT) under the same conditions are shown in the bottom panels.

recoverin (Figure 2A-C) and rhodopsin (Figure 2D-F), the bipolar cell marker PKCα (Figure 2G-I), the ganglion, amacrine, and horizontal cell marker calbindin (Figure 2J-L) and the RPE marker RPE65 (Figure 2P-R) were detected by immunocytochemistry in different proportions of cells. Labeling specificity was verified on mouse skin fibroblasts as negative controls and on pig retinal progenitor cells as positive controls (data not shown). Recoverin labeling was detected in about 20±3.2% of cells, rhodopsin labeling in 14.5±3.2%, PKCα labeling in 19.3±4.1%, and calbindin labeling in 21.4±2.4% of cells. Cells immunopositive for neuronal markers in vitro extended thin, long processes, which are suggestive of neuronal differentiation. Rhodopsin-labeled cells were positive for recoverin in double labeling experiments (Figure 2D,E). Double labeling also revealed that PKCα and recoverin antibodies stained a distinct population of cells and there was no overlap between these two markers. However, PKCα-labeled cells were usually found adjacent to recoverin-positive cells (Figure 2G). RPE65 immunoreactivity was detected in 12.2±3.8% cells. Cells within the spheres remained pigmented and although rare, pigment granules were sometimes observed within the cells expressing retinal markers (Figure 2M-O).

Real time PCR confirmed upregulation of PKCα ($p<0.05$), calbindin ($p<0.05$), and rhodopsin ($p=0.053$) in differentiation cultures, relative to their expression level before differentiation. Concomitantly, the retinal progenitor marker Hes1 was downregulated after differentiation (Figure 3).

Transplantation of CE-derived cells: Prior to initiating in vivo transplantation experiments, the CM-DiI dye was tested for long-term stability. CM-DiI showed long-term retention in CE-derived cells in proliferating (10 day follow-up) and differentiating (4 week follow-up) conditions in vitro (Figure 4A-B). In vivo, subretinal localization of CM-DiI-labeled cells 10 min after grafting was confirmed in cryosections from one animal. CM-DiI-labeled cells (red) were found between the RPE and outer nuclear layer (ONL). Retinal detachment at the injection area was also observed (Figure 4C,D).

Incorporation of transplanted cells into the RPE layer and formation of multilayered RPE-like structures: Eight days following transplantation, large CM-DiI positive cell aggregates were observed within the RPE layer (Figure 5). Clusters of CE-derived cells in the RPE were either RPE65-negative (Figure 5A), or showed strong RPE65 immunoreactivity (Figure 5B,C). At two and four weeks after transplantation, many CM-DiI-labeled cells were localized in the RPE layer (Figure 5D-I). Due to the phagocytic nature of the RPE, some of the CM-DiI labeling in this layer may be attributed to the uptake of the dye from dead transplanted cells. However, four weeks following transplantation, areas of the RPE were often multilayered, suggesting the de novo formation of additional RPE-like layers on top of the host RPE on the basal side (Figure 5G-I). The thickness of the RPE increased due to the formation of multilayers; in some areas it was comparable to that of the ONL (Figure 5G-I). Some CM-DiI-labeled cells were also observed at the level of the choroid, but they were negative for RPE65.

Molecular Vision 2011; 17:2580-2595 <http://www.molvis.org/molvis/v17/a279> © 2011 Molecular Vision

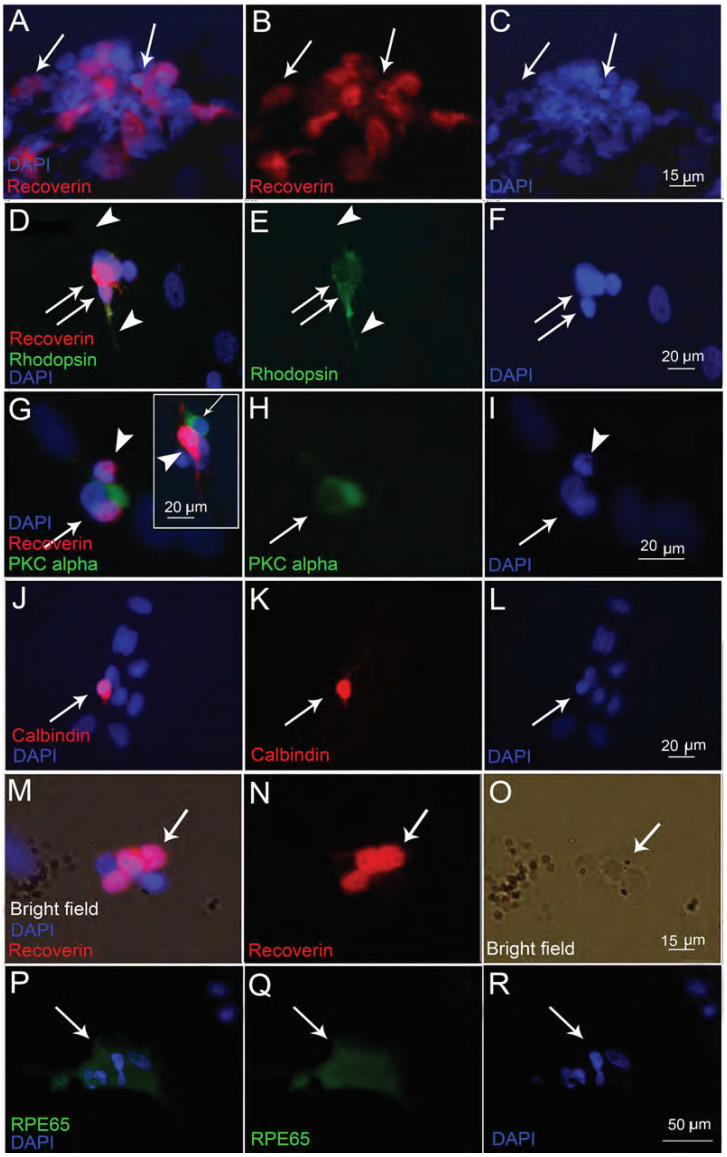


Figure 2. Microphotographs of the immunolabeling of newborn pig ciliary epithelium (CE)-derived cells after in vitro differentiation on poly-D-Lysine, laminin coated coverslips in the presence of 1% serum and 10 ng/ml basic fibroblast growth factor (bFGF) and epidermal growth factor (EGF). The images were acquired using an epifluorescent microscope. **A**, **B**: Cells labeled for recoverin are clustered together (arrows). **C**: 4',6-diamidino-2-phenylindole (DAPI) nuclear staining corresponding to **A** and **B**. **D**, **E**: Cells double-labeled for recoverin (red, **D**) and rhodopsin (green, **D** and **E**) are depicted by arrows. The focus is set to show rhodopsin-positive cell processes. Strong recoverin staining in the cytoplasm masks the nuclear DAPI staining, which is shown separately in **F**. Cells positive for protein kinase α (PKCα; green in **G** and **H**, arrows) did not co-label with recoverin (red in **G** and **H** and another example in the inset in **G**, arrowheads). The focus is set to show the processes of PKCα-labeled cells in **G** and **H**, and the recoverin-labeled processes in the inset in **G**. Corresponding DAPI nuclear stain is shown in **I**. **J**-**K**: A calbindin immunopositive cell is depicted by the arrow. The focus is set to show the processes of the labeled cell. Corresponding DAPI nuclear stain is shown in **L**. **M**, **N**: Recoverin-positive cells (arrows in **M** and **N**) that had retained pigmented granules (arrow in the bright-field image in **O**). **P**, **Q**: RPE-65 immunopositive cells (arrows) and the corresponding nuclear DAPI staining in **R**.

Molecular Vision 2011; 17:2580-2595 <http://www.molvis.org/molvis/v17/a279> © 2011 Molecular Vision

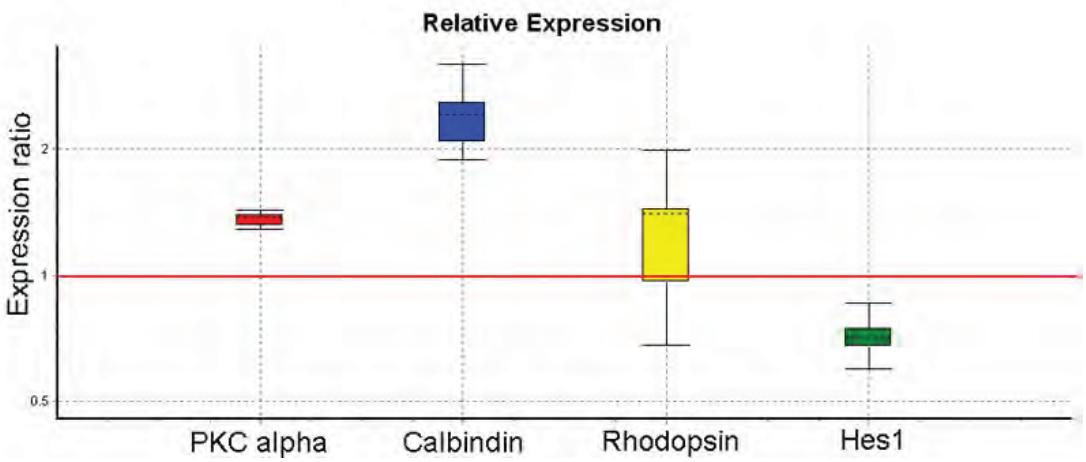


Figure 3. Quantitative real time PCR data for ciliary epithelium (CE)-derived cell cultures following in vitro differentiation. RNA was isolated from CE-derived cells after in vitro differentiation on poly-D-Lysine, laminin coated plates in the presence of 1% serum and 10 ng/ml basic fibroblast growth factor (bFGF) and epidermal growth factor (EGF) for 20 days. The data was analyzed using REST software for the relative quantification. The expression ratio represents the ratio of expression in differentiated compared to undifferentiated cultures. After differentiation, protein kinase α (PKCα; $p<0.05$), calbindin ($p<0.05$), and rhodopsin ($p=0.054$) were upregulated, while the retinal progenitor marker Hes1 was downregulated ($p<0.01$). The data are from a representative experiment performed in triplicate. Similar results were obtained from three independent differentiation experiments.

Migration of transplanted cells into the neuroretina and expression of retinal markers: Some transplanted cells migrated into the neuroretina and both CM-DiI positive pigmented and non-pigmented cells were observed interspersed with host retinal cells. The number of CM-DiI-labeled cells in the central and peripheral neurororetina was quantified by counting the cells in transverse sections containing the optic nerve head. At all time points, a proportion of surviving CM-DiI-labeled cells was found in the peripheral retina, indicating that transplanted cells had migrated tangentially from the site of injection in the central retina to more peripheral sites (Figure 6A). Cell proliferation of the transplanted cells was assessed by immunolabeling for the cell proliferation marker Ki67. A small number of imunopositive cells were found within the CM-DiI-labeled cell aggregates in the subretinal space, but no Ki67 staining was observed in the neuroretina (Figure 6B,C). Therefore, the increase in CM-DiI cell numbers in the neuroretina—from 8 to 14 and 28 days—post transplantation is likely to be due to cell migration rather than proliferation of the transplanted cells within the retina. Isolectin B4 labeling was performed to identify the distribution of immune cells (macrophage/microglia) in the injected retinas. Round, large cells positive for isolectin were identified in the subretinal space. These cells contained red particles, suggesting phagocytosis of transplanted cells by macrophages (Figure 6D,E). However, cells double-labeled with CM-DiI and isolectin were not found within the neuroretina.

To assess whether transplanted CE-derived cells that had migrated into the neuroretina displayed features suggestive of neuronal differentiation, sections of the transplanted eyes were assayed with antibodies for retinal cell markers. CM-DiI cells positive for the photoreceptor marker recoverin were detected in the ONL (Figure 7A-E). Double CM-DiI/PKCα-positive cells displayed oval shapes and were usually found outside the inner nuclear layer (INL), adjacent to bipolar cells (Figure 7F,G). PKCα labeling in pigs and cows is more intense in the ganglion cell layer (GCL), where it has been colocalized with astrocytes [18,25]. CM-DiI cells positive for the early neuronal marker HuC/D (Figure 7H,I) and calbindin-immunopositive cells were found in the GCL (Figure 7J,K), where they had a rounded or oval shape, with short thin processes (Figure 7J, inset). Since those cells were often observed close to the vitreal side, it cannot be excluded that they were retracted to the vitreous after the injection procedure, or had migrated back to the vitreous through the needle track. The percentage of CM-DiI-labeled cells localized in the neuroretina and positive for retinal neuronal markers was at an average of 8%–10% for recoverin, 5%–6% for PKCα, and 6%–9% for calbindin. The CM-DiI-labeled cells in the neuroretina always appeared slightly displaced from the pattern of the host retina and their morphology remained distinguishable from the recipients' cells.

DISCUSSION

Recent reports have highlighted the limited understanding we have of the nature and developmental potential of CE-derived

Molecular Vision 2011; 17:2580-2595 <http://www.molvis.org/molvis/v17/a279> © 2011 Molecular Vision

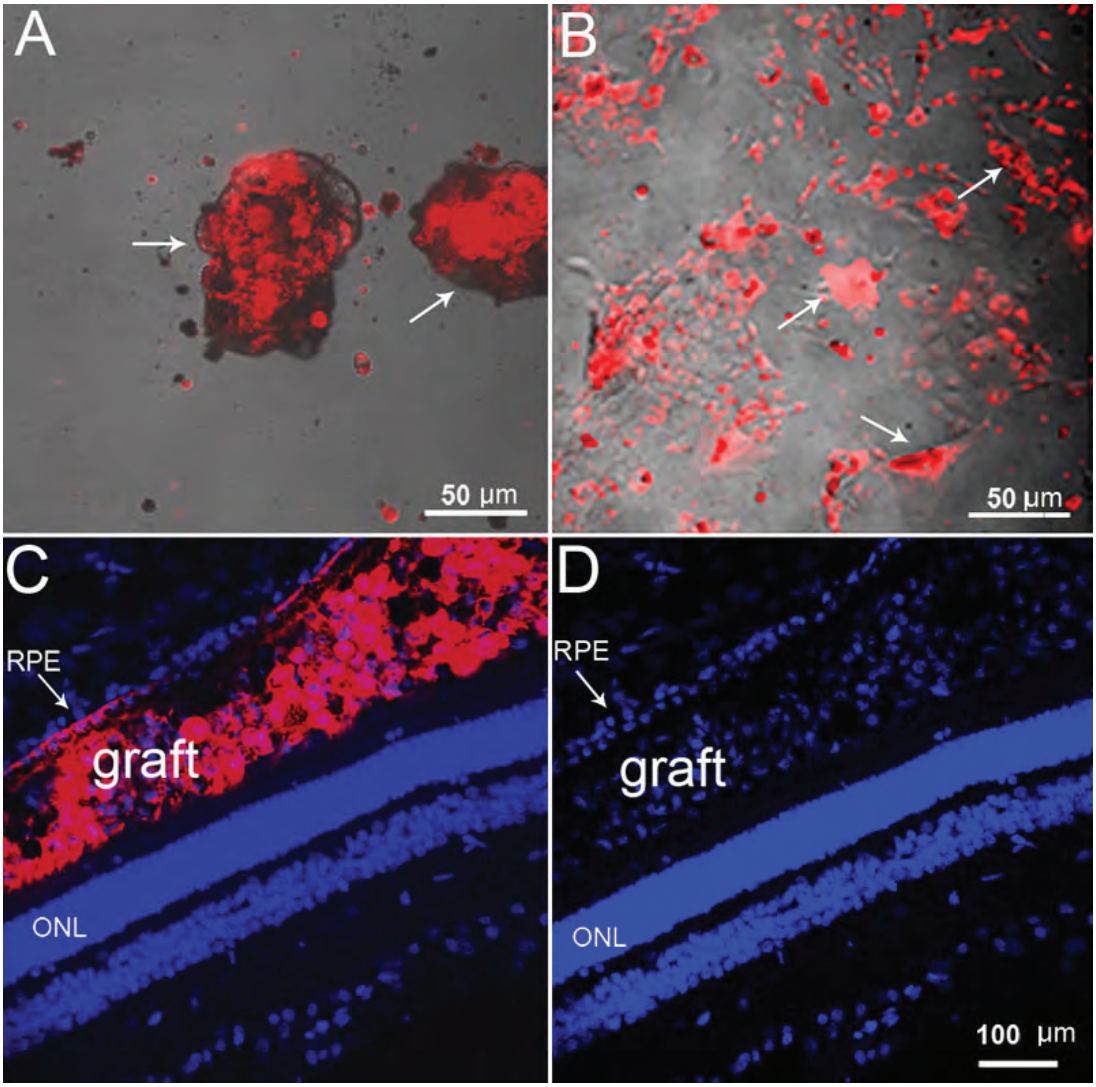


Figure 4. CM-DiI labeling of ciliary epithelium (CE)-derived cells. Dissociated cells at passage 1 were labeled and cultured in a suspension culture to form spheres (**A**), or were plated on poly-D-Lysine, laminin coated coverslips in differentiation conditions. The CM-DiI label was retained for up to 10 days in proliferating spheres (depicted by arrows in **A**), and up to four weeks in differentiating conditions (arrows in **B**) in vitro. **C**, **D**: Microphotographs of grafted CM-DiI-labeled CE-derived cells (red) in the recipient retina 10 min after subretinal injection. **C**: CM-DiI labeling merged with nuclear DAPI staining. **D**: 4',6-diamidino-2-phenylindole (DAPI) staining only. Red CM-DiI-labeled cells were found between the RPE (arrow) and the ONL. Retinal pigment epithelium (RPE); outer nuclear layer (ONL).

cells and the need for further investigations to re-evaluate their biology and potential for cell therapies in retinal degenerative diseases.

Several sources of cells have been considered for retinal cell replacement therapies and tested for their ability to generate retinal cell types. Transplanted retinal progenitors have been shown to express retinal cell markers in mice and pigs [21,26]. Functional cell replacement was demonstrated for the first time in a study by MacLaren et al. [27], where dissociated photoreceptor precursors from postnatal mice

Molecular Vision 2011; 17:2580-2595 <http://www.molvis.org/molvis/v17/a279> © 2011 Molecular Vision

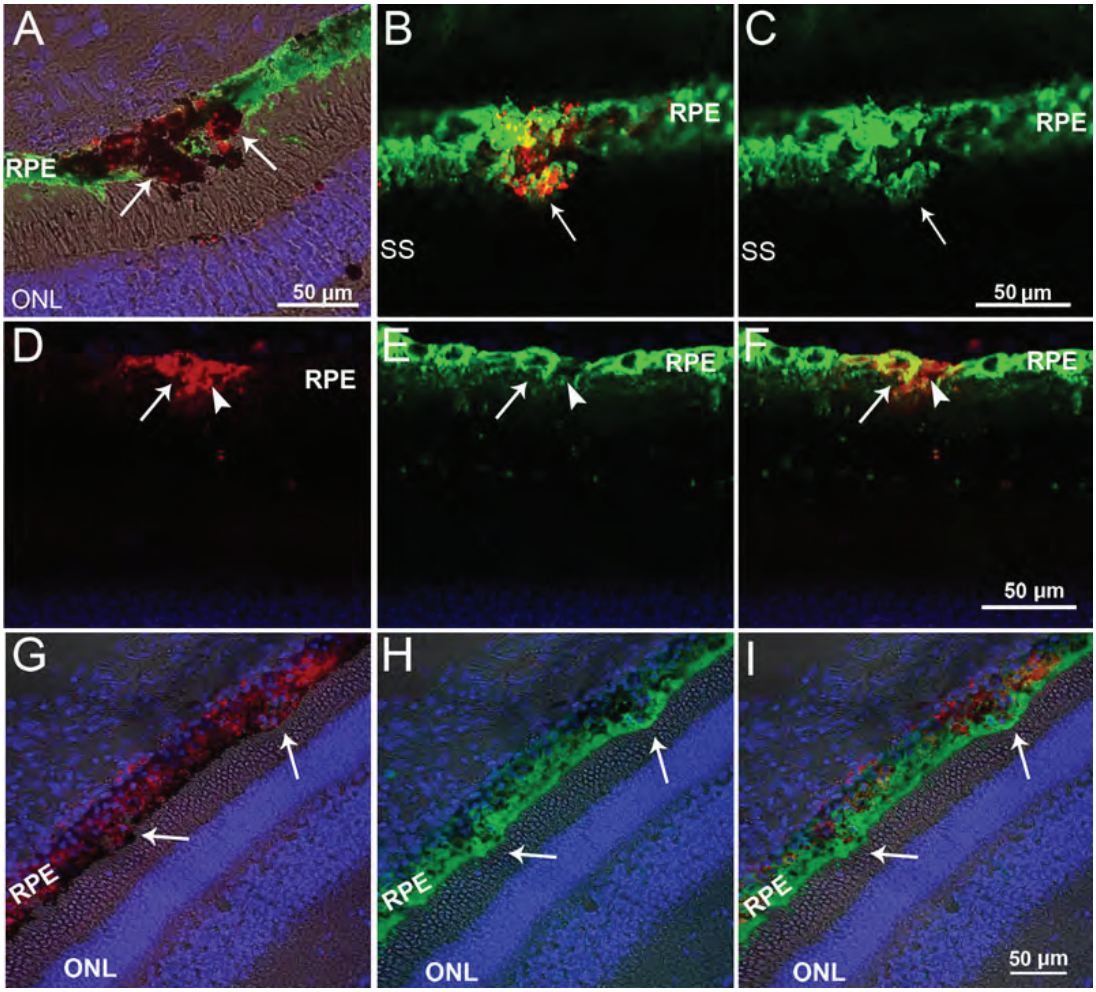


Figure 5. Microphotographs of red CM-DiI-labeled ciliary epithelium (CE)-derived cells in the retinal pigment epithelium (RPE) layer. **A**: Red-labeled pigmented CE-derived cells localized to the RPE layer, which were negative for RPE65 (arrows). **B**: At the same time point, transplanted red-labeled RPE65-positive cells were also found (red and green merged in **B** and green RPE65 labeling only in **C**, arrows). **D-F**: Two weeks following transplantation, CM-DiI-labeled cells in the RPE layer were strongly (arrow) and weakly (arrowhead) positive for RPE65. **G-I**: Four weeks after transplantation, the RPE appeared uneven and multilayered (arrows). Nuclei are labeled with 4',6-diamidino-2-phenylindole (DAPI; blue). Bright-field images are merged with the dark field in **A**, **G**, **H,** and **I.** Subretinal space (SS); and outer nuclear layer (ONL).

were used for transplantation. However, this strategy would be inadequate in humans, where the cells of the comparable ontogenic stage would have to be obtained from fetal retina, and being postmitotic, could not be expanded.

Human embryonic (hES) stem cells and induced pluripotent stem (iPS) cells are very attractive sources of cells for cell replacement. Efficient protocols for retinal differentiation of ES cells have been developed and are constantly improving [28-31]. The feasibility of using ES-derived photoreceptors has been demonstrated after their transplantation into adult $Crx^{-/-}$ mice with subsequent improvement in visual function [32]. Similarly, photoreceptors have been generated from iPS cells and their integration into both mice and pig retina has been reported [33,34]. Recently, transplantation of iPS-derived photoreceptor precursors from mice has been shown to restore

Molecular Vision 2011; 17:2580-2595 <http://www.molvis.org/molvis/v17/a279> © 2011 Molecular Vision

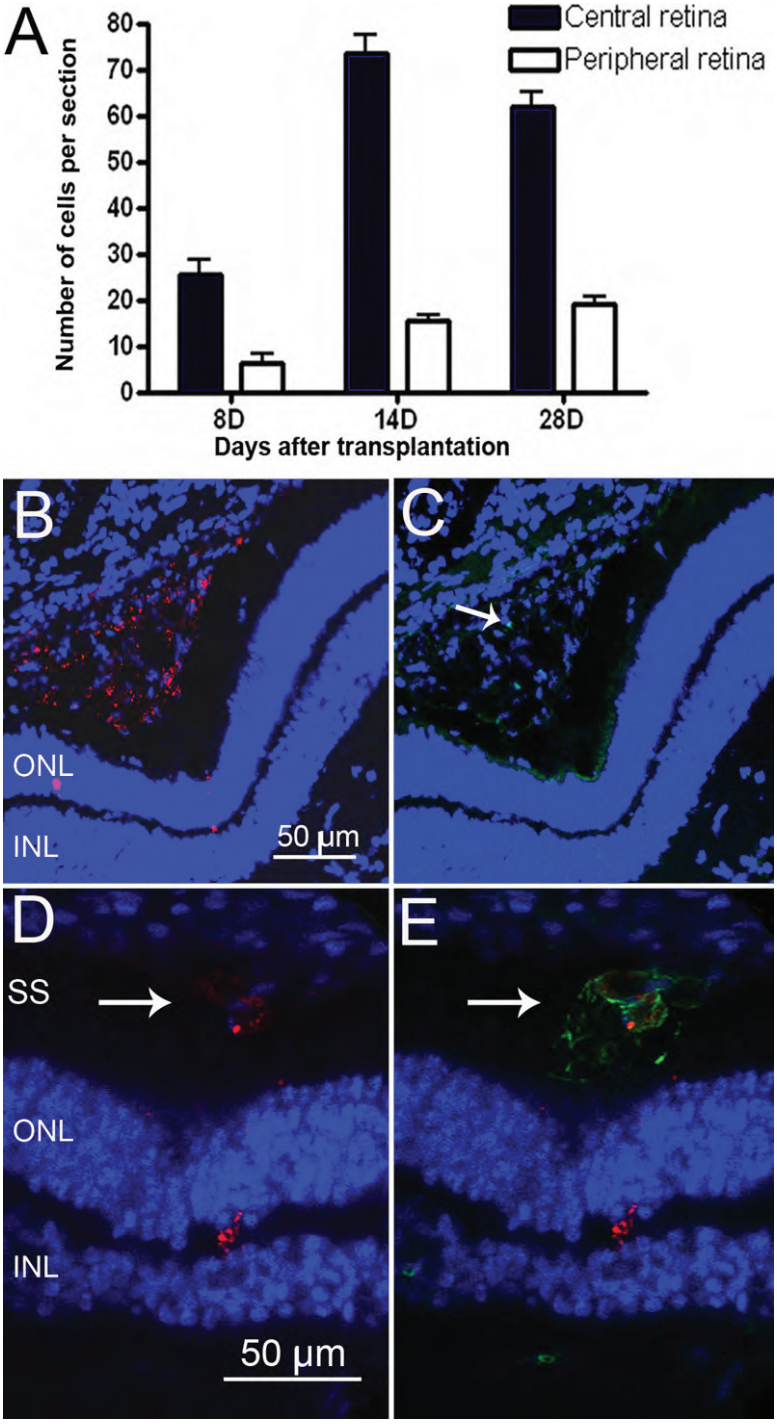


Figure 6. Analysis of migration, proliferation, and death of porcine ciliary epithelium (CE)-derived cells after subretinal transplantation. **A**: Quantification of the transplanted cells that had migrated into the neuroretina. CM-DiI-labeled cells were counted in 20 random sections from each eye. The middle third, containing the optic nerve, was considered to be the central retina and the two peripheral thirds, including the ora serrata, were considered to be the peripheral retina. The results are presented as the mean±SEM **B**, **C**: Cell proliferation assessed by Ki67 labeling in transplanted retinas. CM-DiI-positive cell aggregates in the subretinal space (red in **B**) contained rare Ki67-labeled cells (green, arrow in **C**), eight days after transplantation. **D**, **E**: Phagocytosis of transplanted cells by macrophages. CM-DiI-labeled particles (red in **D**, arrow) contained within isolectin B4-positive macrophages (green in **E**, arrow). The nuclei are labeled with 4',6-diamidino-2-phenylindole (DAPI; blue). Outer nuclear layer (ONL); inner nuclear layer (INL); and subretinal space (SS).

Molecular Vision 2011; 17:2580-2595 <http://www.molvis.org/molvis/v17/a279> © 2011 Molecular Vision

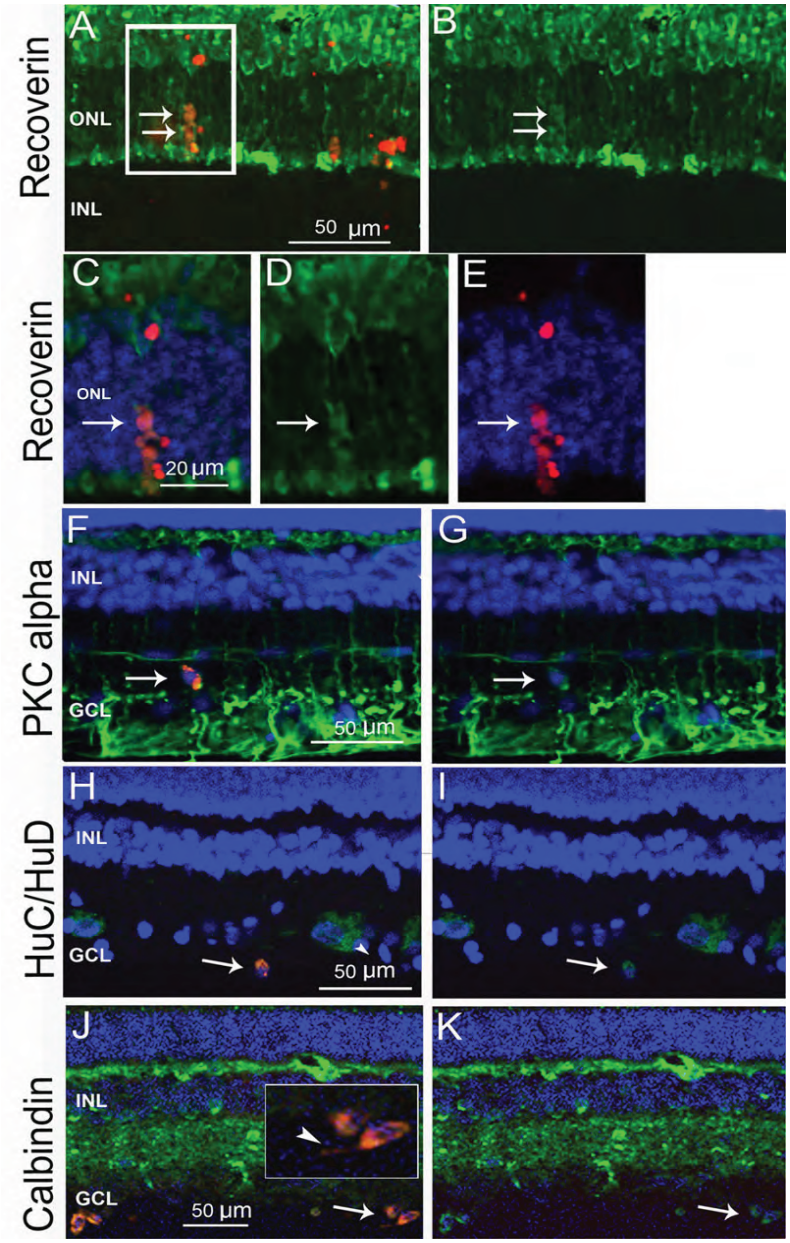


Figure 7. The immunoreactivity of transplanted ciliary epithelium (CE)-derived cells in the neuroretina. **A**: Microphotograph (1 . m confocal stack) showing red CM-DiI-labeled cells positive for recoverin (green, arrows) in the outer nuclear layer (L). **B**: Recoverin-only labeling of the same confocal stack as in **A**. The arrows point to the transplanted cells. **C**: A 0.7 m confocal slice from the boxed area in **A** showing double-labeled CM-DiI/recoverin positive cells (arrows) **D**: Green recoverin labeling in the same area (arrow). **E**: Red CM-DiI labeling and 4',6-diamidino-2-phenylindole (DAPI) nuclear staining of the same area. **F**, **G**: CM-DiI-labeled, protein kinase α (PKCα)-positive cell (green) in the inner plexiform layer (arrows). **H**, **I**: uC/D (green) and CM-DiI-positive cell in the ganglion cell layer (GCL arrow in **H** and **I**). **J**, **K**: Calbindin (green) and CM-DiI-labeled cells in the GCL (arrows). The inset is at a higher magnification with visible processes (arrowhead). The nuclei are labeled with DAPI (blue). Inner nuclear layer (I L).

Molecular Vision 2011; 17:2580-2595 <http://www.molvis.org/molvis/v17/a279> © 2011 Molecular Vision

visual function in rho$^{-/-}$ mice [35]. RPE cells have also been generated from hESC [36-40] and their transplantation rescued visual function in a rat model of retinal degeneration [41,42]. Cells with RPE features have also been differentiated from human iPSCs and they were able to delay retinal degeneration in animal transplantation studies [37,43]. Although the use of ES and iPS for cell replacement therapies shows great promise, issues such as oncogenic potential and immunogenicity have to be fully addressed before ES or iPS cells can be considered for treatment. Transplantation strategies for retinal replacement also require optimization due to the low rate of cell survival and the integration of transplanted cells. Efforts have been made to improve cell survival by transplanting cells on biodegradable scaffolds [44-47]. It has been identified that the outer limiting membrane (OLM) represents a barrier to cell integration and several approaches to controlling OLM disruption have led to enhanced integration of transplanted cells [48-52]. Until a successful method and a reliable cell-type for cell-based therapies in the retina have been identified, it is preferable to continue the investigation of cells from different sources and developmental origins with the potential to generate the differentiated progeny of interest. Although the differentiation potential of CE-derived cells is currently debatable, literature from the past decade suggests that the behavior of these cells in differentiation cultures is dependent on the experimental conditions. Such conditions could either promote a direct transition to the epithelial RPE-like phenotype or the development of retinal neuronal phenotypes, possibly through transdifferentiation or via de-differentiation and a stem-like transition state [53].

To gain insight into the differentiation potential of postnatal porcine CE-derived cells, we determined the expression of the key pluripotency genes in P1 spheres [23, 24]. We were able to detect mRNAs for *Klf4*,*Sox2*, and *cMyc*, while the transcripts for *Nanog* and *Oct4* were absent. Cells positive for *cMyc*, but negative for *nMyc* were recently identified as a retinal stem cell population in *Xenopus* and in zebrafish ciliary margins. Therefore, it has been suggested that the expression patterns of *cMyc* and *nMyc* could be used to localize stem cells in the mammalian developing retina and CE [54]. The lack of expression of the whole set of pluripotentcy genes highlights the important differences between CE-derived cells and embryonic or iPS cells. Our PCR data are in agreement with recently published analysis of NRL-eGFP mice CE-derived cultures that could not be differentiated into photoreceptors when subjected to the retinal differentiation protocol for ES cells [12]. However, porcine CE-derived cells contained mRNAs for genes expressed during retinal development, from the optic vesicle stage (*Six3* and *Mitf*) to retinal histogenesis (*Hes1*,*Chx10*, and *Otx2*). Mitf transcription factor also plays a role in promoting and maintaining the RPE [55].

Our previous study has shown that the proliferation capacity of porcine CE-derived cells decreases with the age of the donor animal [8], suggesting that the cells from younger animals may be more stem-like, with a higher ability for retinal differentiation. However, it is important to note that retinal histogenesis is complete after birth, with all retinal layers and cell types present in newborn pigs [18]. It remains to be evaluated whether the capacity of porcine CE-derived cells to generate retinal cell types actually decreases with the age of the cell donor.

Cells from the first passage in our current study generated a higher number of photoreceptor-like cells compared to our previous study, where cells were used for differentiation after passage three [8]. The fact that cells from earlier passages possess higher differentiation potential is a limiting factor for the expansion of CE-derived cells. This issue requires our attention and it will have to be resolved if these cells are to be used for cell replacement. In our current study, colabeling for rhodopsin and recoverin and the lack of cells double-labeled for recoverin and PKCα confirmed the photoreceptor-like phenotype of the differentiated cells. Interestingly, PKCα-labeled cells were always found to be closely associated with recoverin-positive cells, suggesting that they might influence each other's differentiation.

Expression of neuronal cell markers in our differentiation cultures coincided with significant, though not always complete, loss of pigmentation. Persistence of some pigmented granules in differentiated cells indicates that they originate from pigmented cells, but may require additional time to clear their pigment content.

The differentiation potential of porcine CE-derived cells in vitro was also previously studied by MacNeil et al. [19]. Although the expression of generic neuronal markers such as β-III-Tubulin and Neu-N was demonstrated, no expression of more specific retinal markers was detected in differentiation cultures in their study. The discrepancy relative to our results could be explained by the difference in the donor animal's age, the post-mortem time before cell isolation, or by the conditions for in vitro differentiation. Retention of growth factors in our differentiation cultures increased the number of differentiated cells, suggesting a role for growth factors in the differentiation and/or survival of CE-derived cells. Notably, EGF does not affect in vitro photoreceptor survival in rats [56], but it can stimulate the survival of porcine photoreceptors under the same conditions [57]. In addition to the role of both bFGF and EGF in neuronal and retinal differentiation [58-61], bFGF has been shown to play a role in transdifferentiation of RPE and iris pigment epithelium into retinal tissue [62-64]. Finally, although EGF was reported to be a negative regulator of photoreceptor differentiation during retinal development [65,66], it has been shown, in vitro, to act as a neuronal differentiation factor for retinal stem cells [67].

In vivo, transplanted CE-derived cells showed remarkable migration potential as they were found in the

Molecular Vision 2011; 17:2580-2595 <http://www.molvis.org/molvis/v17/a279> © 2011 Molecular Vision

peripheral regions of the RPE and retina. The injection of dissociated cells rather than of intact spheres, as performed in other studies, might have facilitated migration [11].

We identified the recruitment of isolectin B-positive macrophages to the subretinal space of injected eyes with the presence of red particles contained within the phagocytes. Given the relatively short timeframe, an active immune rejection of subretinal allografts is unlikely to have been induced [21,27], therefore the macrophages are probably responsible for scavenging cell debris from the dead transplanted cell.

Some transplanted CE-derived cells that had migrated into the neuroretina displayed positive and specific immunostaining for neuronal cell markers. The markers shown to be expressed in vitro in our current and previous study [8] were also detected in CE-derived cells after transplantation. All antibodies used in this study have been carefully and extensively characterized on pig tissue [18], therefore, nonspecific antibody labeling of transplanted cells is unlikely. Furthermore, the CM-DiI dye was previously successfully used for the long-term follow-up of neural stem cells after transplantation, and no diffusion of the dye was reported [68].

The majority of transplanted cells formed multilayered RPE-like structures positive for RPE65. Although, in vivo we observed preferential differentiation of CE-derived cells along the RPE lineage, immunoreactivity for the RPE marker RPE65 in vitro was relatively low, suggesting that the differentiation protocol we adopted was not optimal for the efficient generation of RPE-like phenotypes. Indeed, our protocol was designed to generate retinal neurons. However, the culture conditions for efficient in vitro differentiation of CE-derived cells into the RPE phenotype have recently been reported [69]. Cells generated with this protocol had epithelilal morphology, immunocytochemical, and ultrastructural features of RPE and a capacity for phagocytosis. Another study has shown that high expression of RPE65 can be induced in CE-derived cells in a medium supplemented with vasoactive intestinal peptide (VIP) or in a RPE cell-conditioned medium [70].

In vivo, differentiation along both the RPE and neuronal lineages could be advantageous. Cell therapies can be most effective if the contribution of different cell types is harnessed, not only to replace lost cells, but also to maintain existing function and prevent further degeneration. CE-derived RPE-like cells could contribute a protective effect by promoting photoreceptor survival [37], while newly differentiated photoreceptors could replace lost ones. Indeed, subretinal transplantation of sheets of human retinal progenitor cells together with their RPE is the only method thus far shown to be effective in humans [46]. Promising results in generating functional photoreceptors from CE-derived cells in vitro and in vivo after gene transfer and modulation of transcription factors have recently been reported [15,16].

In conclusion, our study shows that the cells from postnatal pig CEs have the ability to generate cells with the morphological and immunohistochemical features of retinal neurons and RPE, both in vitro and after subretinal transplantation in vivo. Revealing the paracrine effects and the influence of the cellular environment in determining the fate of these cells may identify specific factors that enable controlled differentiation, or in vivo activation of these cells. Understanding the pathways behind this cell plasticity may provide important clues for the development of future cell replacement therapies to combat retinal degeneration.

ACKNOWLEDGMENTS

The authors thank Alan Stitt for valuable comments, Taz McClintock, Paul Crawford, David Beattie, Lorraine Hanna and Mildred Wylie for technical support, Elaine Latimer for project coordination, Robert Molday and Karl-Wilhelm Koch for kindly donating antibodies. This work was supported in part by funding generously provided by Fighting Blindness, ROI and The Fraser Homes Foundation for Ophthalmic Research, UK.

REFERENCES

1. Lamba D, Karl M, Reh T. Neural regeneration and cell replacement: a view from the eye. Cell Stem Cell 2008; 2:538-49. [PMID: 18522847]
2. West EL, Pearson RA, MacLaren RE, Sowden JC, Ali RR. Cell transplantation strategies for retinal repair. Prog Brain Res 2009; 175:3-21. [PMID: 19660645]
3. Bhatia B, Singhal S, Jayaram H, Khaw PT, Limb GA. Adult retinal stem cells revisited. Open Ophthalmol J 2010; 4:30-8. [PMID: 20871757]
4. Wallace VA. Concise review: making a retina–from the building blocks to clinical applications. Stem Cells 2011; 29:412-7. [PMID: 21425405]
5. Tropepe V, Coles BL, Chiasson BJ, Horsford DJ, Elia AJ, McInnes RR, van der Kooy D. Retinal stem cells in the adult mammalian eye. Science 2000; 287:2032-6. [PMID: 10720333]
6. Ahmad I, Tang L, Pham H. Identification of neural progenitors in the adult mammalian eye. Biochem Biophys Res Commun 2000; 270:517-21. [PMID: 10753656]
7. Coles BL, Angenieux B, Inoue T, Del Rio-Tsonis K, Spence JR, McInnes RR, Arsenijevic Y, van der Kooy D. Facile isolation and the characterization of human retinal stem cells. Proc Natl Acad Sci USA 2004; 101:15772-7. [PMID: 15505221]
8. Gu P, Harwood LJ, Zhang X, Wylie M, Curry WJ, Cogliati T. Isolation of retinal progenitor and stem cells from the porcine eye. Mol Vis 2007; 13:1045-57. [PMID: 17653049]
9. Agathocleous M, Harris WA. From progenitors to differentiated cells in the vertebrate retina. Annu Rev Cell Dev Biol 2009; 25:45-69. [PMID: 19575661]
10. Fischer AJ, Reh TA. Identification of a proliferating marginal zone of retinal progenitors in postnatal chickens. Dev Biol 2000; 220:197-210. [PMID: 10753510]
11. Cicero SA, Johnson D, Reyntjens S, Frase S, Connell S, Chow LM, Baker SJ, Sorrentino BP, Dyer MA. Cells previously

Molecular Vision 2011; 17:2580-2595 <http://www.molvis.org/molvis/v17/a279> © 2011 Molecular Vision

identified as retinal stem cells are pigmented ciliary epithelial cells. Proc Natl Acad Sci USA 2009; 106:6685-90. [PMID: 19346468]

12. Gualdoni S, Baron M, Lakowski J, Decembrini S, Smith AJ, Pearson RA, Ali RR, Sowden JC. Adult ciliary epithelial cells, previously identified as retinal stem cells with potential for retinal repair, fail to differentiate into new rod photoreceptors. Stem Cells 2010; 28:1048-59. [PMID: 20506130]
13. Inoue T, Kagawa T, Fukushima M, Shimizu T, Yoshinaga Y, Takada S, Tanihara H, Taga T. Activation of canonical Wnt pathway promotes proliferation of retinal stem cells derived from adult mouse ciliary margin. Stem Cells 2006; 24:95-104. [PMID: 16223856]
14. De Marzo A, Aruta C, Marigo V. PEDF Promotes Retinal Neurosphere Formation and Expansion In Vitro. Adv Exp Med Biol 2010; 664:621-30. [PMID: 20238066]
15. Inoue T, Coles BL, Dorval K, Bremner R, Bessho Y, Kageyama R, Hino S, Matsuoka M, Craft CM, McInnes RR, Tremblay F, Prusky GT, van der Kooy D. Maximizing functional photoreceptor differentiation from adult human retinal stem cells. Stem Cells 2010; 28:489-500. [PMID: 20014120]
16. Jomary C, Jones SE, Lotery AJ. Generation of light-sensitive photoreceptor phenotypes by genetic modification of human adult ocular stem cells with Crx. Invest Ophthalmol Vis Sci 2010; 51:1181-9. [PMID: 19850845]
17. Hendrickson A, Hicks D. Distribution and density of medium- and short-wavelength selective cones in the domestic pig retina. Exp Eye Res 2002; 74:435-44. [PMID: 12076087]
18. Guduric-Fuchs J, Ringland LJ, Gu P, Dellett M, Archer DB, Cogliati T. Immunohistochemical study of pig retinal development. Mol Vis 2009; 15:1915-28. [PMID: 19784390]
19. MacNeil A, Pearson RA, MacLaren RE, Smith AJ, Sowden JC, Ali RR. Comparative analysis of progenitor cells isolated from the iris, pars plana, and ciliary body of the adult porcine eye. Stem Cells 2007; 25:2430-8. [PMID: 17600111]
20. Chacko DM, Das AV, Zhao X, James J, Bhattacharya S, Ahmad I. Transplantation of ocular stem cells: the role of injury in incorporation and differentiation of grafted cells in the retina. Vision Res 2003; 43:937-46. [PMID: 12668063]
21. Klassen H, Kiilgaard JF, Zahir T, Ziaeian B, Kirov I, Scherfig E, Warfvinge K, Young MJ. Progenitor cells from the porcine neural retina express photoreceptor markers after transplantation to the subretinal space of allorecipients. Stem Cells 2007; 25:1222-30. [PMID: 17218397]
22. Klassen H, Warfvinge K, Schwartz PH, Kiilgaard JF, Shamie N, Jiang C, Samuel M, Scherfig E, Prather RS, Young MJ. Isolation of progenitor cells from GFP-transgenic pigs and transplantation to the retina of allorecipients. Cloning Stem Cells 2008; 10:391-402. [PMID: 18729769]
23. Yamanaka S, Takahashi K. [Induction of pluripotent stem cells from mouse fibroblast cultures]. Tanpakushitsu Kakusan Koso 2006; 51:2346-51. [PMID: 17154061]
24. Takahashi K, Tanabe K, Ohnuki M, Narita M, Ichisaka T, Tomoda K, Yamanaka S. Induction of pluripotent stem cells from adult human fibroblasts by defined factors. Cell 2007; 131:861-72. [PMID: 18035408]
25. Shin T, Kim S, Ahn M, Kim H. An immunohistochemical study of protein kinase C in the bovine retina. J Vet Med Sci 2006; 68:71-4. [PMID: 16462121]
26. Klassen HJ, Ng TF, Kurimoto Y, Kirov I, Shatos M, Coffey P, Young MJ. Multipotent retinal progenitors express developmental markers, differentiate into retinal neurons, and preserve light-mediated behavior. Invest Ophthalmol Vis Sci 2004; 45:4167-73. [PMID: 15505071]
27. MacLaren RE, Pearson RA, MacNeil A, Douglas RH, Salt TE, Akimoto M, Swaroop A, Sowden JC. Ali RRl. Retinal repair by transplantation of photoreceptor precursors. Nature 2006; 444:203-7. [PMID: 17093405]
28. Lamba DA, Karl MO, Ware CB, Reh TA. Efficient generation of retinal progenitor cells from human embryonic stem cells. Proc Natl Acad Sci USA 2006; 103:12769-74. [PMID: 16908856]
29. Osakada F, Ikeda H, Sasai Y, Takahashi M. Stepwise differentiation of pluripotent stem cells into retinal cells. Nat Protoc 2009; 4:811-24. [PMID: 19444239]
30. Lamba DA, Reh TA. Microarray characterization of human embryonic stem cell-derived retinal cultures. Invest Ophthalmol Vis Sci 2011; 52:4897-906. [PMID: 21345990]
31. Eiraku M, Takata N, Ishibashi H, Kawada M, Sakakura E, Okuda S, Sekiguchi K, Adachi T, Sasai Y. Self-organizing optic-cup morphogenesis in three-dimensional culture. Nature 2011; 472:51-6. [PMID: 21475194]
32. Lamba DA, Gust J, Reh TA. Transplantation of human embryonic stem cell-derived photoreceptors restores some visual function in Crx-deficient mice. Cell Stem Cell 2009; 4:73-9. [PMID: 19128794]
33. Lamba DA, McUsic A, Hirata RK, Wang PR, Russell D, Reh TA. Generation, purification and transplantation of photoreceptors derived from human induced pluripotent stem cells. PLoS ONE 2010; 5:e8763. [PMID: 20098701]
34. Zhou L, Wang W, Liu Y, de Castro JF, Ezashi T, Telugu BP, Roberts RM, Kaplan HJ, Dean DC. Differentiation of induced pluripotent stem cells of Swine into rod photoreceptors and their integration into the retina. Stem Cells 2011; 29:972-80. [PMID: 21491544]
35. Tucker BA, Park IH, Qi SD, Klassen HJ, Jiang C, Yao J, Redenti S, Daley GQ, Young MJ. Transplantation of Adult Mouse iPS Cell-Derived Photoreceptor Precursors Restores Retinal Structure and Function in Degenerative Mice. PLoS ONE 2011; 6:e18992. [PMID: 21559507]
36. Klimanskaya I, Hipp J, Rezai KA, West M, Atala A, Lanza R. Derivation and comparative assessment of retinal pigment epithelium from human embryonic stem cells using transcriptomics. Cloning Stem Cells 2004; 6:217-45. [PMID: 15671670]
37. Carr AJ, Vugler AA, Hikita ST, Lawrence JM, Gias C, Chen LL, Buchholz DE, Ahmado A, Semo M, Smart MJ, Hasan S, da Cruz L, Johnson LV, Clegg DO, Coffey PJ. Protective effects of human iPS-derived retinal pigment epithelium cell transplantation in the retinal dystrophic rat. PLoS ONE 2009; 4:e8152. [PMID: 19997644]
38. Lu B, Malcuit C, Wang S, Girman S, Francis P, Lemieux L, Lanza R, Lund R. Long-term safety and function of RPE from human embryonic stem cells in preclinical models of macular degeneration. Stem Cells 2009; 27:2126-35. [PMID: 19521979]
39. Carr AJ, Vugler A, Lawrence J, Chen LL, Ahmado A, Chen FK, Semo M, Gias C, da Cruz L, Moore HD, Walsh J, Coffey PJ. Molecular characterization and functional analysis of

Molecular Vision 2011; 17:2580-2595 <http://www.molvis.org/molvis/v17/a279> © 2011 Molecular Vision

phagocytosis by human embryonic stem cell-derived RPE cells using a novel human retinal assay. Mol Vis 2009; 15:283-95. [PMID: 19204785]

40. Liao JL, Yu J, Huang K, Hu J, Diemer T, Ma Z, Dvash T, Yang XJ, Travis GH, Williams DS, Bok D, Fan G. Molecular signature of primary retinal pigment epithelium and stem-cell-derived RPE cells. Hum Mol Genet 2010; 19:4229-38. [PMID: 20709808]
41. Lund RD, Wang S, Klimanskaya I, Holmes T, Ramos-Kelsey R, Lu B, Girman S, Bischoff N, Sauve Y, Lanza R. Human embryonic stem cell-derived cells rescue visual function in dystrophic RCS rats. Cloning Stem Cells 2006; 8:189-99. [PMID: 17009895]
42. Vugler A, Carr AJ, Lawrence J, Chen LL, Burrell K, Wright A, Lundh P, Semo M, Ahmado A, Gias C, da Cruz L, Moore H, Andrews P, Walsh J, Coffey P. Elucidating the phenomenon of HESC-derived RPE: anatomy of cell genesis, expansion and retinal transplantation. Exp Neurol 2008; 214:347-61. [PMID: 18926821]
43. Buchholz DE, Hikita ST, Rowland TJ, Friedrich AM, Hinman CR, Johnson LV, Clegg DO. Derivation of functional retinal pigmented epithelium from induced pluripotent stem cells. Stem Cells 2009; 27:2427-34. [PMID: 19658190]
44. Tomita M, Lavik E, Klassen H, Zahir T, Langer R, Young MJ. Biodegradable polymer composite grafts promote the survival and differentiation of retinal progenitor cells. Stem Cells 2005; 23:1579-88. [PMID: 16293582]
45. Tao S, Young C, Redenti S, Zhang Y, Klassen H, Desai T, Young MJ. Survival, migration and differentiation of retinal progenitor cells transplanted on micro-machined poly(methyl methacrylate) scaffolds to the subretinal space. Lab Chip 2007; 7:695-701. [PMID: 17538710]
46. Radtke ND, Aramant RB, Petry HM, Green PT, Pidwell DJ, Seiler MJ. Vision improvement in retinal degeneration patients by implantation of retina together with retinal pigment epithelium. Am J Ophthalmol 2008; 146:172-82. [PMID: 18547537]
47. Redenti S, Neeley WL, Rompani S, Saigal S, Yang J, Klassen H, Langer R, Young MJ. Engineering retinal progenitor cell and scrollable poly(glycerol-sebacate) composites for expansion and subretinal transplantation. Biomaterials 2009; 30:3405-14. [PMID: 19361860]
48. West EL, Pearson RA, Tschernutter M, Sowden JC, MacLaren RE, Ali RR. Pharmacological disruption of the outer limiting membrane leads to increased retinal integration of transplanted photoreceptor precursors. Exp Eye Res 2008; 86:601-11. [PMID: 18294631]
49. Tucker B, Klassen H, Yang L, Chen DF, Young MJ. Elevated MMP Expression in the MRL Mouse Retina Creates a Permissive Environment for Retinal Regeneration. Invest Ophthalmol Vis Sci 2008; 49:1686-95. [PMID: 18385092]
50. Pearson RA, Barber AC, West EL, MacLaren RE, Duran Y, Bainbridge JW, Sowden JC, Ali RR. Targeted disruption of outer limiting membrane junctional proteins (Crb1 and ZO-1) increases integration of transplanted photoreceptor precursors into the adult wild-type and degenerating retina. Cell Transplant 2010; 19:487-503. [PMID: 20089206]
51. Jiang C, Klassen H, Zhang X, Young M. Laser injury promotes migration and integration of retinal progenitor cells into host retina. Mol Vis 2010; 16:983-90. [PMID: 20577598]
52. Yao J, Tucker BA, Zhang X, Checa-Casalengua P, Herrero-Vanrell R, Young MJ. Robust cell integration from co-transplantation of biodegradable MMP2-PLGA microspheres with retinal progenitor cells. Biomaterials 2011; 32:1041-50. [PMID: 21030072]
53. Tsonis PA, Del Rio-Tsonis K. Lens and retina regeneration: transdifferentiation, stem cells and clinical applications. Exp Eye Res 2004; 78:161-72. [PMID: 14729349]
54. Xue XY, Harris WA. Using myc genes to search for stem cells in the ciliary margin of the Xenopus retina. Dev Neurobiol 2011; ▪▪▪ [PMID: 21465669]
55. Wang SZ. Tales of retinogenesis told by human stem cells. Proc Natl Acad Sci USA 2009; 106:16543-4. [PMID: 19805334]
56. Fontaine V, Kinkl N, Sahel J, Dreyfus H, Hicks D. Survival of purified rat photoreceptors in vitro is stimulated directly by fibroblast growth factor-2. J Neurosci 1998; 18:9662-72. [PMID: 9822727]
57. Traverso V, Kinkl N, Grimm L, Sahel J, Hicks D. Basic fibroblast and epidermal growth factors stimulate survival in adult porcine photoreceptor cell cultures. Invest Ophthalmol Vis Sci 2003; 44:4550-8. [PMID: 14507904]
58. Hicks D, Courtois Y. Fibroblast growth factor stimulates photoreceptor differentiation in vitro. J Neurosci 1992; 12:2022-33. [PMID: 1535104]
59. Hunter DD, Murphy MD, Olsson CV, Brunken WJ. S-laminin expression in adult and developing retinae: a potential cue for photoreceptor morphogenesis. Neuron 1992; 8:399-413. [PMID: 1550669]
60. Israsena N, Hu M, Fu W, Kan L, Kessler JA. The presence of FGF2 signaling determines whether beta-catenin exerts effects on proliferation or neuronal differentiation of neural stem cells. Dev Biol 2004; 268:220-31. [PMID: 15031118]
61. Garcez RC, Teixeira BL, Schmitt Sdos S, Alvarez-Silva M, Trentin AG. Epidermal growth factor (EGF) promotes the in vitro differentiation of neural crest cells to neurons and melanocytes. Cell Mol Neurobiol 2009; 29:1087-91. [PMID: 19415484]
62. Opas M, Dziak E. bFGF-induced transdifferentiation of RPE to neuronal progenitors is regulated by the mechanical properties of the substratum. Dev Biol 1994; 161:440-54. [PMID: 8313994]
63. Thumann G. Development and cellular functions of the iris pigment epithelium. Surv Ophthalmol 2001; 45:345-54. [PMID: 11166346]
64. Vergara MN, Del Rio-Tsonis K. Retinal regeneration in the Xenopus laevis tadpole: a new model system. Mol Vis 2009; 15:1000-13. [PMID: 19461929]
65. Lillien L. Changes in retinal cell fate induced by overexpression of EGF receptor. Nature 1995; 377:158-62. [PMID: 7675083]
66. Ahmad I, Dooley CM, Afiat S. Involvement of Mash1 in EGF-mediated regulation of differentiation in the vertebrate retina. Dev Biol 1998; 194:86-98. [PMID: 9473334]
67. Angénieux B, Schorderet DF, Arsenijevic Y. Epidermal growth factor is a neuronal differentiation factor for retinal stem cells in vitro. Stem Cells 2006; 24:696-706. [PMID: 16179425]
68. Vossmerbaeumer U, Kuehl S, Kern S, Kluter H, Jonas JB, Bieback K. Induction of retinal pigment epithelium properties in ciliary margin progenitor cells. Clin Experiment Ophthalmol 2008; 36:358-66. [PMID: 18700924]

69. Imitola J, Raddassi K, Park KI, Mueller FJ, Nieto M, Teng YD, Frenkel D, Li J, Sidman RL, Walsh CA, Snyder EY, Khoury SJ. Directed migration of neural stem cells to sites of CNS injury by the stromal cell-derived factor 1alpha/CXC chemokine receptor 4 pathway. Proc Natl Acad Sci USA 2004; 101:18117-22. [PMID: 15608062]

70. Aruta C, Giordano F, De Marzo A, Comitato A, Raposo G, Nandrot EF, Marigo V. In vitro differentiation of retinal pigment epithelium from adult retinal stem cells. Pigment Cell Melanoma Res 2011; 24:233-40. [PMID: 21232026]

Articles are provided courtesy of Emory University and the Zhongshan Ophthalmic Center, Sun Yat-sen University, P.R. China. The print version of this article was created on 10 October 2011. This reflects all typographical corrections and errata to the article through that date. Details of any changes may be found in the online version of the article.

CHAPTER 6

GENERAL DISCUSSION

Our studies in the pig complement and expand previous works in rodents and humans. We have conducted an immunohistochemical study of porcine retinal histogenesis and characterized antibodies to retina-specific markers commonly used in rodents. We conclude that retinal development in pigs parallels retinal development in humans (Chapter 2). We show that a small proportion of cells from the newborn pig CE can proliferate and give rise to sphere cultures with limited self-renewal potential *in vitro* under controlled culture conditions (Chapter 3). Our data reveal that CE-derived cells can generate not only retinal, but also RPE phenotypes *in vivo* and *in vitro*, and suggest the hypothesis that these cells posses a broad developmental potential (Chapter 5). Similar results were recently reported in other mouse studies *in vitro* (Aruta et al, 2011) and *in vivo* (Ballios et al, 2010), further supporting our work. The dual lineage potential of CE-derived cells might be advantageous in the context of cell replacement. On the one hand, CE-derived RPE-like cells could contribute a protective effect by promoting photoreceptor survival (Carr et al, 2009b; Lin et al, 1996) while, at the same time, newly differentiated photoreceptors could replace lost ones. Finally, our studies confirmed that the pig is a viable animal model in alternative to non-human primates for pre-clinical testing of cell-based therapies in the retina. We have also shown that allotransplantation in the large porcine eye is successful and does not appear to cause any obvious immune response, providing pre-clinical data and support for translation to the human eye (Chapter 5).

Some aspects of our work require further investigation: the age of CE-derived cells; the demonstration of functional differentiation; and the use of disease models.

Optimal age of CE-derived cells - We chose to collect CE-derived cells from newborn piglets (1-2 week old) because they were more readily available and cost-effective. These cells may possess greater plasticity and enhanced capacity to generate retinal and RPE phenotypes compared to cells isolated from adult CE that would be used in human autologous transplantation procedures. Although earlier reports indicate that CE-derived cells from neonatal, young and old human donors possess at least

comparable *in vitro* proliferation and clonogenic properties (Coles et al, 2004), the true potential for auto-transplantation of porcine CE-derived cells should be confirmed with cells from adult donors.

Demonstration of functional differentiation of CE-derived cells - The use of reporter genes upregulated coincidentally with differentiation of a specific cell type (i.e. rod photoreceptors) has provided convincing evidence of the capacity of RPC and ES cells to generate the correct cell type for replacement (Decembrini et al, 2011; Lamba et al, 2009; Lamba et al, 2006; Lamba et al, 2010; MacLaren et al, 2006; Zhou et al, 2011). In our studies, we base our assessment of the transplanted cells on morphology and co-localization of cell-specific markers with a labeling dye. The use of viral constructs to express reporter genes under control of photoreceptor-specific promoters as shown in the cited papers could strengthen our results. Furthermore, the unequivocal direct proof that cells expressing photoreceptors genes possess photoreceptor function would validate their identity. The vital dye we used in this studies should be sufficient to localize the transplanted cells and record neuronal function by Ca^{++} imaging and patch clamping in retinal slice preparations (Homma K. et al., unpublished data).

Transplantation in porcine models of retinal degeneration - We have completed a full round of cell isolation and transplantation in the normal pig with relative success in terms of cell integration, expression of phenotypic markers of differentiated retinal and RPE cells, and no immune rejection. The next step would be transplantation in a pig model of retinal degeneration. Work in rodents suggests that the partially degenerated retina might be more permissive to cell integration and differentiation, depending on the degree of degeneration at the time of transplantation (Chacko et al, 2003) and supports the working hypothesis that transplanting pig models with retinal degeneration might yield visible improvements of retinal histology and function.

The debate on Retinal Stem Cells

The nature and developmental potential of cells derived from the adult CE have been the object of controversy in recent literature. Mike Dyer and his group, based on

morphological and molecular criteria, conclude that CE-derived spheres do not consist of stem cells, but rather of proliferating pigmented CE cells with epithelial morphology that fail to differentiate into retinal neurons *in vitro* and *in vivo* (Cicero et al, 2009). Furthermore, Robin Ali's and Jane Sowden's groups provide evidence that CE-derived cells expanded in monolayer culture lose their pigmentation, and despite lacking neuronal morphology, co-express markers of eye field, retinal progenitor, and differentiated CE. Upon stimulation, these cells fail to activate the Nrl-regulated rod photoreceptor differentiation program (Gualdoni et al, 2010).

Three earlier publications had also reported detailed data on the epithelial properties of CE-derived cells. However, all concur that CE-derived spheres contain a mixed population of proliferative cells with epithelial and neural properties (Kohno et al, 2006; Moe et al, 2009; Xu et al, 2007a). The epithelial phenotype is manifested in some of the cells by the presence of pigmentation, of junctional complexes (desmosomes, gap, adherent, and tight junctions), expression of epithelial markers, and flattened/polarized appearance. Neural properties are evidenced by the expression, among others, of the immature neuroepithelial marker nestin, the retinal field markers PAX6 and SOX2, and the retinal progenitor marker CHX10. The balance between epithelial and neural properties is regulated by central signaling pathways (Moe et al, 2009). The epithelial phenotype is sustained by activation of the canonical Wnt pathway while the neureoepithelial phenotype depends upon increased expression of TGF-β receptor. These data can reconcile the terms of the controversy in that slight changes in culture conditions (e.g., concentration of growth factors and culture density) might tilt the balance towards one phenotype or the other. Furthermore, they explain the limited self-renewal capacity of CE-derived cells that has been consistently reported in the published literature (Ahmad et al, 2000; Coles et al, 2004; De Marzo et al, 2010; Inoue et al, 2006; Inoue et al, 2005; Mayer et al, 2005; Tropepe et al, 2000). Thus, although the nature of RSCs remains controversial, the partial self-renewal capacity of CE-derived cells is suggestive of the undifferentiated and mitotic state.

In our studies by IHC and RT-PCR, we focused on the neuronal properties of CE-derived cells. Although we did not specifically look for epithelial properties, we reported that a fraction of the cells in the CE-derived spheres were pigmented. However, in our experimental conditions, the proportion of pigmented cells diminished with passages in culture. Furthermore, we anecdotally observed that CE-derived spheres were more difficult to dissociate than RPC or neural stem cell (NSC) spheres. This characteristic did not change over passages in culture and could provide indirect evidence of the presence of epithelial junctions in CE-derived cells. Our data are therefore compatible with the existence of mixed epithelial and neural phenotypes in CE-derived cells that can be manipulated by changing culture conditions. Notably, while some reports indicate that pigmented CE-derived cells constitute the proliferating RSC population (Tropepe et al, 2000), others suggest that non-pigmented CE cells are proliferating RSCs (Bhatia et al, 2009).

Work from several laboratories has shown differentiation *in vitro* and *in vivo* of CE-derived cells into neuronal- and photoreceptor-like phenotypes (Coles et al, 2004; De Marzo et al, 2010; Inoue et al, 2006; Inoue et al, 2005; Jomary & Jones, 2008; Jomary et al, 2010). Our differentiation cultures are different from Dyer's in that we plated dissociated cells and not intact spheres. By disrupting cell-cell interactions, we might have biased the cells towards neural differentiation. Furthermore, we differentiated our cultures in the presence of high serum or low serum and growth factors; this too might have contributed to driving the cells along the neural lineage. Most importantly, we used cells from newborn pig, which corresponds to <1 month old mouse, whereas Dyer used 6-8 week old mice. As already discussed, newborn cells might maintain neuronal progenitor properties that are lost in cells from later ages.

Similarly, our experiments are not comparable to those from Ali's and Sowden's groups since they differentiate cells maintained in monolayer cultures and we used cells cultured as neurospheres. When we used monolayer culture conditions in our initial studies, we could only detect differentiated cells positive for the glial marker GFAP and none of the other retinal neuronal markers. Since Ali's and Sowden's groups were

specifically looking for rod photoreceptor differentiation in their experiments, they might have missed glial differentiation that probably occurred in their cultures.

Concluding remarks

Based on the literature and on our data, a small proportion of porcine CE-derived cells can proliferate and give rise to characteristic spheres under controlled culture conditions *in vitro*. Cells in the spheres have limited self-renewal potential and display mixed epithelial and neural properties. Under permissive differentiating conditions *in vitro*, cells from dissociated spheres can express markers of mature retinal cells. Similarly, *in vivo*, CE-derived cells migrate from the site of injection and express markers of mature retinal cells, including photoreceptors and RPE. Further investigations are required to improve the expandability and differentiation potential of CE-derived cells if they are to be considered for translational applications. In addition, stronger functional data should be generated to provide evidence of their regenerative capacity in the diseased retina. Finally, recent concerns on the rapid accumulation of severe chromosomal aberrations during cultivation remain to be addressed (Djojosubroto et al, 2009).

The exact nature of CE-derived cells in culture remains unclear. The literature strongly suggests that cellular environment and paracrine factors play an important role in determining their phenotype and fate *in vitro* and *in vivo*. Thus, cell amplification followed by genetic (re)programming and pre-differentiation may be required to facilitate the generation of the desired cell phenotypes and to restore retinal function. Recent advances in differentiating retinal neurons from other pluripotent stem cell sources such as ESCs and iPSCs have overshadowed studies on CE-derived cells. Retinal neurons have been successfully differentiated from human ESCs *in vitro* under culture conditions that recapitulate retinal development, using known developmental cues (Hirano et al, 2003; Ikeda et al, 2005; Lamba et al, 2006; Osakada et al, 2008; Osakada et al, 2009a; Osakada et al, 2009b; Reh et al, 2010; Zhao et al, 2002), small-molecule induction protocols (Osakada et al, 2009b), and guiding morphogenesis using

biomaterial scaffolds (McUsic et al, 2012). Once transplanted in animal models of retinal degeneration, human ESC-derived retinal cells populate the ONL, express markers of rod and cone photoreceptors (Hambright et al, 2012), and partially restore function (Lamba et al, 2009). Similarly, photoreceptor progenitors have been differentiated from human iPSCs (Hirami et al, 2009), and successfully integrated in the mouse retina (Lamba et al, 2010). Finally, iPSC-derived photoreceptors allotransplanted in the swine retina have been shown to integrate and express markers of differentiation (Zhou et al, 2011). In retinal degenerative diseases such as LCA and AMD, although vision impairment is consequent to photoreceptor death, the latter fail because of a dysfunctional RPE. Thus, at early stages of disease, when the ONL is still preserved, RPE replacement could prevent photoreceptor loss. RPE derived from human and other non-human primate ESCs and iPSCs is functional and can phagocytose shed photoreceptor membranes *in vitro* and *in vivo* after transplantation in rodent models of retinal degeneration (Carr et al, 2009a; Carr et al, 2009b; Idelson et al, 2009; Okamoto & Takahashi, 2011; Wang et al, 2010). Furthermore, the first clinical trial for safety and tolerability of transplanted human ESC-derived RPE was initiated in 2011 in patients with Stargardt's macular dystrophy and dry AMD (Schwartz et al, 2012). The authors suggest that it is premature to conclusively interpret data on efficacy. However, they show that RPE integrates in the host as a mature, quiescent monolayer and they observe no signs of hyperproliferation, abnormal growth, or immune rejection four months after transplantation, suggesting that the cells are safe and well tolerated and supporting the promise of this cell-based approach.

Although other cell types are currently under more intense investigation, there are still questions worth asking and answering about CE-derived cells before discarding them as a possible source for retinal transplantation and repair. This is true especially in consideration of their amenability to autologous transplantation and the relatively limited manipulation they require before injection in the degenerative retina. Finally, all data concur in showing the remarkable plasticity of CE-derived cells in neurosphere cultures. Cell plasticity is a phenomenon that is attracting increasing research interest

and CE-derived cells may provide a useful model for studies on its regulation, ultimately providing insights and methods to manipulate stem cell sources for repair in the retina.

REFERENCES

Abdouh M, Bernier G (2006) In vivo reactivation of a quiescent cell population located in the ocular ciliary body of adult mammals. *Experimental eye research* **83:** 153-164

Ahmad I, Das AV, James J, Bhattacharya S, Zhao X (2004) Neural stem cells in the mammalian eye: types and regulation. *Seminars in cell & developmental biology* **15:** 53-62

Ahmad I, Dooley CM, Afiat S (1998) Involvement of Mash1 in EGF-mediated regulation of differentiation in the vertebrate retina. *Developmental biology* **194:** 86-98

Ahmad I, Tang L, Pham H (2000) Identification of neural progenitors in the adult mammalian eye. *Biochemical and biophysical research communications* **270:** 517-521

Antonetti DA, Barber AJ, Bronson SK, Freeman WM, Gardner TW, Jefferson LS, Kester M, Kimball SR, Krady JK, LaNoue KF, Norbury CC, Quinn PG, Sandirasegarane L, Simpson IA (2006) Diabetic retinopathy: seeing beyond glucose-induced microvascular disease. *Diabetes* **55:** 2401-2411

Aruta C, Giordano F, De Marzo A, Comitato A, Raposo G, Nandrot EF, Marigo V (2011) In vitro differentiation of retinal pigment epithelium from adult retinal stem cells. *Pigment cell & melanoma research* **24:** 233-240

Bainbridge JW, Smith AJ, Barker SS, Robbie S, Henderson R, Balaggan K, Viswanathan A, Holder GE, Stockman A, Tyler N, Petersen-Jones S, Bhattacharya SS, Thrasher AJ, Fitzke FW, Carter BJ, Rubin GS, Moore AT, Ali RR (2008) Effect of gene therapy on visual function in Leber's congenital amaurosis. *N Engl J Med* **358:** 2231-2239

Ballios BG, Cooke MJ, van der Kooy D, Shoichet MS (2010) A hydrogel-based stem cell delivery system to treat retinal degenerative diseases. *Biomaterials* **31:** 2555-2564

Barber AJ, Lieth E, Khin SA, Antonetti DA, Buchanan AG, Gardner TW (1998) Neural apoptosis in the retina during experimental and human diabetes. Early onset and effect of insulin. *The Journal of clinical investigation* **102:** 783-791

Belliveau MJ, Cepko CL (1999) Extrinsic and intrinsic factors control the genesis of amacrine and cone cells in the rat retina. *Development* **126:** 555-566

Bernardos RL, Barthel LK, Meyers JR, Raymond PA (2007) Late-stage neuronal progenitors in the retina are radial Muller glia that function as retinal stem cells. *The Journal of neuroscience : the official journal of the Society for Neuroscience* **27:** 7028-7040

Bhatia B, Singhal S, Lawrence JM, Khaw PT, Limb GA (2009) Distribution of Muller stem cells within the neural retina: evidence for the existence of a ciliary margin-like zone in the adult human eye. *Experimental eye research* **89:** 373-382

Blackshaw S, Harpavat S, Trimarchi J, Cai L, Huang H, Kuo WP, Weber G, Lee K, Fraioli RE, Cho SH, Yung R, Asch E, Ohno-Machado L, Wong WH, Cepko CL (2004) Genomic analysis of mouse retinal development. *PLoS biology* **2:** E247

Boucher SE, Hitchcock PF (1998) Insulin-related growth factors stimulate proliferation of retinal progenitors in the goldfish. *The Journal of comparative neurology* **394:** 386-394

Bradford RL, Wang C, Zack DJ, Adler R (2005) Roles of cell-intrinsic and microenvironmental factors in photoreceptor cell differentiation. *Developmental biology* **286:** 31-45

Braisted JE, Essman TF, Raymond PA (1994) Selective regeneration of photoreceptors in goldfish retina. *Development* **120:** 2409-2419

Brown DM, Campochiaro PA, Bhisitkul RB, Ho AC, Gray S, Saroj N, Adamis AP, Rubio RG, Murahashi WY (2011) Sustained benefits from ranibizumab for macular edema following branch retinal vein occlusion: 12-month outcomes of a phase III study. *Ophthalmology* **118:** 1594-1602

Bugra K, Jacquemin E, Ortiz JR, Jeanny JC, Hicks D (1992) Analysis of opsin mRNA and protein expression in adult and regenerating newt retina by immunology and hybridization. *Journal of neurocytology* **21:** 171-183

Bugra K, Olivier L, Jacquemin E, Laurent M, Courtois Y, Hicks D (1994) Acidic fibroblast growth factor is expressed abundantly by photoreceptors within the developing and mature rat retina. *The European journal of neuroscience* **6:** 1062

Campochiaro PA, Brown DM, Awh CC, Lee SY, Gray S, Saroj N, Murahashi WY, Rubio RG (2011a) Sustained benefits from ranibizumab for macular edema following central retinal vein occlusion: twelve-month outcomes of a phase III study. *Ophthalmology* **118:** 2041-2049

Campochiaro PA, Brown DM, Pearson A, Ciulla T, Boyer D, Holz FG, Tolentino M, Gupta A, Duarte L, Madreperla S, Gonder J, Kapik B, Billman K, Kane FE (2011b) Long-term benefit of sustained-delivery fluocinolone acetonide vitreous inserts for diabetic macular edema. *Ophthalmology* **118:** 626-635 e622

Carr AJ, Vugler A, Lawrence J, Chen LL, Ahmado A, Chen FK, Semo M, Gias C, da Cruz L, Moore HD, Walsh J, Coffey PJ (2009a) Molecular characterization and functional analysis

of phagocytosis by human embryonic stem cell-derived RPE cells using a novel human retinal assay. *Molecular vision* **15:** 283-295

Carr AJ, Vugler AA, Hikita ST, Lawrence JM, Gias C, Chen LL, Buchholz DE, Ahmado A, Semo M, Smart MJ, Hasan S, da Cruz L, Johnson LV, Clegg DO, Coffey PJ (2009b) Protective effects of human iPS-derived retinal pigment epithelium cell transplantation in the retinal dystrophic rat. *PloS one* **4:** e8152

Cepko CL, Austin CP, Yang X, Alexiades M, Ezzeddine D (1996) Cell fate determination in the vertebrate retina. *Proceedings of the National Academy of Sciences of the United States of America* **93:** 589-595

Chacko DM, Das AV, Zhao X, James J, Bhattacharya S, Ahmad I (2003) Transplantation of ocular stem cells: the role of injury in incorporation and differentiation of grafted cells in the retina. *Vision research* **43:** 937-946

Chandler MJ, Smith PJ, Samuelson DA, MacKay EO (1999) Photoreceptor density of the domestic pig retina. *Veterinary ophthalmology* **2:** 179-184

Cheng H, Aleman TS, Cideciyan AV, Khanna R, Jacobson SG, Swaroop A (2006) In vivo function of the orphan nuclear receptor NR2E3 in establishing photoreceptor identity during mammalian retinal development. *Human molecular genetics* **15:** 2588-2602

Cheng H, Khanna H, Oh EC, Hicks D, Mitton KP, Swaroop A (2004) Photoreceptor-specific nuclear receptor NR2E3 functions as a transcriptional activator in rod photoreceptors. *Human molecular genetics* **13:** 1563-1575

Cheon EW, Kaneko Y, Saito T (1998) Regeneration of the newt retina: order of appearance of photoreceptors and ganglion cells. *The Journal of comparative neurology* **396:** 267-274

Cheon EW, Kuwata O, Saito T (2001) Muscarinic acetylcholine receptors in the normal, developing and regenerating newt retinas. *Brain research Developmental brain research* **127:** 9-21

Cheon EW, Saito T (1999) Choline acetyltransferase and acetylcholinesterase in the normal, developing and regenerating newt retinas. *Brain research Developmental brain research* **116:** 97-109

Cicero SA, Johnson D, Reyntjens S, Frase S, Connell S, Chow LM, Baker SJ, Sorrentino BP, Dyer MA (2009) Cells previously identified as retinal stem cells are pigmented ciliary epithelial cells. *Proceedings of the National Academy of Sciences of the United States of America* **106:** 6685-6690

Close JL, Gumuscu B, Reh TA (2005) Retinal neurons regulate proliferation of postnatal progenitors and Muller glia in the rat retina via TGF beta signaling. *Development* **132:** 3015-3026

Close JL, Liu J, Gumuscu B, Reh TA (2006) Epidermal growth factor receptor expression regulates proliferation in the postnatal rat retina. *Glia* **54:** 94-104

Coles BL, Angenieux B, Inoue T, Del Rio-Tsonis K, Spence JR, McInnes RR, Arsenijevic Y, van der Kooy D (2004) Facile isolation and the characterization of human retinal stem cells. *Proceedings of the National Academy of Sciences of the United States of America* **101:** 15772-15777

Comer GM, Ciulla TA (2005) Current and future pharmacological intervention for diabetic retinopathy. *Expert opinion on emerging drugs* **10:** 441-455

Comer GM, Ciulla TA, Heier JS, Criswell MH (2005) Future pharmacological treatment options for nonexudative and exudative age-related macular degeneration. *Expert opinion on emerging drugs* **10:** 119-135

Curcio CA, Sloan KR, Kalina RE, Hendrickson AE (1990) Human photoreceptor topography. *The Journal of comparative neurology* **292:** 497-523

Dakubo GD, Mazerolle C, Furimsky M, Yu C, St-Jacques B, McMahon AP, Wallace VA (2008) Indian hedgehog signaling from endothelial cells is required for sclera and retinal pigment epithelium development in the mouse eye. *Developmental biology* **320:** 242-255

Das AV, James J, Rahnenfuhrer J, Thoreson WB, Bhattacharya S, Zhao X, Ahmad I (2005) Retinal properties and potential of the adult mammalian ciliary epithelium stem cells. *Vision research* **45:** 1653-1666

Das AV, Mallya KB, Zhao X, Ahmad F, Bhattacharya S, Thoreson WB, Hegde GV, Ahmad I (2006a) Neural stem cell properties of Muller glia in the mammalian retina: regulation by Notch and Wnt signaling. *Developmental biology* **299:** 283-302

Das AV, Zhao X, James J, Kim M, Cowan KH, Ahmad I (2006b) Neural stem cells in the adult ciliary epithelium express GFAP and are regulated by Wnt signaling. *Biochemical and biophysical research communications* **339:** 708-716

De Marzo A, Aruta C, Marigo V (2010) PEDF promotes retinal neurosphere formation and expansion in vitro. *Advances in experimental medicine and biology* **664:** 621-630

De Schaepdrijver L, Lauwers H, Simoens P, de Geest JP (1990) Development of the retina in the porcine fetus. A light microscopic study. *Anatomia, histologia, embryologia* **19:** 222-235

Decembrini S, Cananzi M, Gualdoni S, Battersby A, Allen N, Pearson RA, Ali RR, De Coppi P, Sowden JC (2011) Comparative analysis of the retinal potential of embryonic stem cells and amniotic fluid-derived stem cells. *Stem cells and development* **20:** 851-863

Del Debbio CB, Balasubramanian S, Parameswaran S, Chaudhuri A, Qiu F, Ahmad I (2010) Notch and Wnt signaling mediated rod photoreceptor regeneration by Muller cells in adult mammalian retina. *PloS one* **5:** e12425

Del Priore LV, Kaplan HJ, Hornbeck R, Jones Z, Swinn M (1996) Retinal pigment epithelial debridement as a model for the pathogenesis and treatment of macular degeneration. *American journal of ophthalmology* **122:** 629-643

Del Rio-Tsonis K, Tsonis PA (2003) Eye regeneration at the molecular age. *Developmental dynamics : an official publication of the American Association of Anatomists* **226:** 211-224

Djojosubroto M, Bollotte F, Wirapati P, Radtke F, Stamenkovic I, Arsenijevic Y (2009) Chromosomal number aberrations and transformation in adult mouse retinal stem cells in vitro. *Investigative ophthalmology & visual science* **50:** 5975-5987

Dyer MA, Cepko CL (2001) Regulating proliferation during retinal development. *Nature reviews Neuroscience* **2:** 333-342

Engelhardt M, Wachs FP, Couillard-Despres S, Aigner L (2004) The neurogenic competence of progenitors from the postnatal rat retina in vitro. *Experimental eye research* **78:** 1025-1036

Ezzeddine ZD, Yang X, DeChiara T, Yancopoulos G, Cepko CL (1997) Postmitotic cells fated to become rod photoreceptors can be respecified by CNTF treatment of the retina. *Development* **124:** 1055-1067

Fausett BV, Goldman D (2006) A role for alpha1 tubulin-expressing Muller glia in regeneration of the injured zebrafish retina. *The Journal of neuroscience : the official journal of the Society for Neuroscience* **26:** 6303-6313

Fischer AJ, Reh TA (2000) Identification of a proliferating marginal zone of retinal progenitors in postnatal chickens. *Developmental biology* **220:** 197-210

Fischer AJ, Reh TA (2001) Muller glia are a potential source of neural regeneration in the postnatal chicken retina. *Nature neuroscience* **4:** 247-252

Fischer AJ, Reh TA (2002) Exogenous growth factors stimulate the regeneration of ganglion cells in the chicken retina. *Developmental biology* **251:** 367-379

Fleisch VC, Fraser B, Allison WT (2011) Investigating regeneration and functional integration of CNS neurons: lessons from zebrafish genetics and other fish species. *Biochimica et biophysica acta* **1812:** 364-380

Ghosh F, Wong F, Johansson K, Bruun A, Petters RM (2004) Transplantation of full-thickness retina in the rhodopsin transgenic pig. *Retina* **24:** 98-109

Giordano F, De Marzo A, Vetrini F, Marigo V (2007) Fibroblast growth factor and epidermal growth factor differently affect differentiation of murine retinal stem cells in vitro. *Molecular vision* **13:** 1842-1850

Graham DR, Overbeek PA, Ash JD (2005) Leukemia inhibitory factor blocks expression of Crx and Nrl transcription factors to inhibit photoreceptor differentiation. *Investigative ophthalmology & visual science* **46:** 2601-2610

Grosche J, Hartig W, Reichenbach A (1995) Expression of glial fibrillary acidic protein (GFAP), glutamine synthetase (GS), and Bcl-2 protooncogene protein by Muller (glial) cells in retinal light damage of rats. *Neuroscience letters* **185:** 119-122

Gualdoni S, Baron M, Lakowski J, Decembrini S, Smith AJ, Pearson RA, Ali RR, Sowden JC (2010) Adult ciliary epithelial cells, previously identified as retinal stem cells with potential for retinal repair, fail to differentiate into new rod photoreceptors. *Stem cells* **28:** 1048-1059

Hambright D, Park KY, Brooks M, McKay R, Swaroop A, Nasonkin IO (2012) Long-term survival and differentiation of retinal neurons derived from human embryonic stem cell lines in un-immunosuppressed mouse retina. *Molecular vision* **18:** 920-936

Hatakeyama J, Bessho Y, Katoh K, Ookawara S, Fujioka M, Guillemot F, Kageyama R (2004) Hes genes regulate size, shape and histogenesis of the nervous system by control of the timing of neural stem cell differentiation. *Development* **131:** 5539-5550

Hendrickson A, Bumsted-O'Brien K, Natoli R, Ramamurthy V, Possin D, Provis J (2008) Rod photoreceptor differentiation in fetal and infant human retina. *Experimental eye research* **87:** 415-426

Hendrickson A, Hicks D (2002) Distribution and density of medium- and short-wavelength selective cones in the domestic pig retina. *Experimental eye research* **74:** 435-444

Henrique D, Hirsinger E, Adam J, Le Roux I, Pourquie O, Ish-Horowicz D, Lewis J (1997) Maintenance of neuroepithelial progenitor cells by Delta-Notch signalling in the embryonic chick retina. *Current biology : CB* **7:** 661-670

Hirami Y, Osakada F, Takahashi K, Okita K, Yamanaka S, Ikeda H, Yoshimura N, Takahashi M (2009) Generation of retinal cells from mouse and human induced pluripotent stem cells. *Neurosci Lett* **458:** 126-131

Hirano M, Yamamoto A, Yoshimura N, Tokunaga T, Motohashi T, Ishizaki K, Yoshida H, Okazaki K, Yamazaki H, Hayashi S, Kunisada T (2003) Generation of structures formed by lens and retinal cells differentiating from embryonic stem cells. *Developmental dynamics : an official publication of the American Association of Anatomists* **228:** 664-671

Hogg RE, Stevenson MR, Chakravarthy U, Beirne RO, Anderson RS (2007) Early features of AMD. *Ophthalmology* **114:** 1028

Iandiev I, Uckermann O, Pannicke T, Wurm A, Tenckhoff S, Pietsch UC, Reichenbach A, Wiedemann P, Bringmann A, Uhlmann S (2006) Glial cell reactivity in a porcine model of retinal detachment. *Investigative ophthalmology & visual science* **47:** 2161-2171

Idelson M, Alper R, Obolensky A, Ben-Shushan E, Hemo I, Yachimovich-Cohen N, Khaner H, Smith Y, Wiser O, Gropp M, Cohen MA, Even-Ram S, Berman-Zaken Y, Matzrafi L, Rechavi G, Banin E, Reubinoff B (2009) Directed differentiation of human embryonic stem cells into functional retinal pigment epithelium cells. *Cell stem cell* **5:** 396-408

Ikeda H, Osakada F, Watanabe K, Mizuseki K, Haraguchi T, Miyoshi H, Kamiya D, Honda Y, Sasai N, Yoshimura N, Takahashi M, Sasai Y (2005) Generation of Rx+/Pax6+ neural retinal precursors from embryonic stem cells. *Proceedings of the National Academy of Sciences of the United States of America* **102:** 11331-11336

Inoue T, Coles BL, Dorval K, Bremner R, Bessho Y, Kageyama R, Hino S, Matsuoka M, Craft CM, McInnes RR, Tremblay F, Prusky GT, van der Kooy D (2010) Maximizing functional photoreceptor differentiation from adult human retinal stem cells. *Stem cells* **28:** 489-500

Inoue T, Kagawa T, Fukushima M, Shimizu T, Yoshinaga Y, Takada S, Tanihara H, Taga T (2006) Activation of canonical Wnt pathway promotes proliferation of retinal stem cells derived from adult mouse ciliary margin. *Stem cells* **24:** 95-104

Inoue Y, Yanagi Y, Tamaki Y, Uchida S, Kawase Y, Araie M, Okochi H (2005) Clonogenic analysis of ciliary epithelial derived retinal progenitor cells in rabbits. *Experimental eye research* **81:** 437-445

Insua MF, Simon MV, Garelli A, de Los Santos B, Rotstein NP, Politi LE (2008) Trophic factors and neuronal interactions regulate the cell cycle and Pax6 expression in Muller stem cells. *Journal of neuroscience research* **86:** 1459-1471

Jacobson SG, Cideciyan AV, Ratnakaram R, Heon E, Schwartz SB, Roman AJ, Peden MC, Aleman TS, Boye SL, Sumaroka A, Conlon TJ, Calcedo R, Pang JJ, Erger KE, Olivares MB, Mullins CL, Swider M, Kaushal S, Feuer WJ, Iannaccone A, Fishman GA, Stone EM, Byrne BJ, Hauswirth WW (2011) Gene Therapy for Leber Congenital Amaurosis Caused by RPE65 Mutations: Safety and Efficacy in 15 Children and Adults Followed Up to 3 Years. *Archives of ophthalmology*

Jadhav AP, Cho SH, Cepko CL (2006) Notch activity permits retinal cells to progress through multiple progenitor states and acquire a stem cell property. *Proceedings of the National Academy of Sciences of the United States of America* **103:** 18998-19003

James J, Das AV, Rahnenfuhrer J, Ahmad I (2004) Cellular and molecular characterization of early and late retinal stem cells/progenitors: differential regulation of proliferation and context dependent role of Notch signaling. *Journal of neurobiology* **61:** 359-376

Jensen AM, Wallace VA (1997) Expression of Sonic hedgehog and its putative role as a precursor cell mitogen in the developing mouse retina. *Development* **124:** 363-371

Jia L, Oh EC, Ng L, Srinivas M, Brooks M, Swaroop A, Forrest D (2009) Retinoid-related orphan nuclear receptor RORbeta is an early-acting factor in rod photoreceptor development. *Proceedings of the National Academy of Sciences of the United States of America* **106:** 17534-17539

Jian Q, Xu H, Xie H, Tian C, Zhao T, Yin Z (2009) Activation of retinal stem cells in the proliferating marginal region of RCS rats during development of retinitis pigmentosa. *Neuroscience letters* **465:** 41-44

Johansson UE, Eftekhari S, Warfvinge K (2010) A battery of cell- and structure-specific markers for the adult porcine retina. *The journal of histochemistry and cytochemistry : official journal of the Histochemistry Society* **58:** 377-389

Johns PR (1977) Growth of the adult goldfish eye. III. Source of the new retinal cells. *The Journal of comparative neurology* **176:** 343-357

Johns PR (1982) Formation of photoreceptors in larval and adult goldfish. *The Journal of neuroscience : the official journal of the Society for Neuroscience* **2:** 178-198

Jomary C, Jones SE (2008) Induction of functional photoreceptor phenotype by exogenous Crx expression in mouse retinal stem cells. *Investigative ophthalmology & visual science* **49:** 429-437

Jomary C, Jones SE, Lotery AJ (2010) Generation of light-sensitive photoreceptor phenotypes by genetic modification of human adult ocular stem cells with Crx. *Investigative ophthalmology & visual science* **51:** 1181-1189

Julian D, Ennis K, Korenbrot JI (1998) Birth and fate of proliferative cells in the inner nuclear layer of the mature fish retina. *The Journal of comparative neurology* **394:** 271-282

Karl MO, Hayes S, Nelson BR, Tan K, Buckingham B, Reh TA (2008) Stimulation of neural regeneration in the mouse retina. *Proceedings of the National Academy of Sciences of the United States of America* **105:** 19508-19513

Keefe JR (1973) An analysis of urodelian retinal regeneration. I. Studies of the cellular source of retinal regeneration in Notophthalmus viridescens utilizing 3 H-thymidine and colchicine. *The Journal of experimental zoology* **184:** 185-206

Khanna H, Akimoto M, Siffroi-Fernandez S, Friedman JS, Hicks D, Swaroop A (2006) Retinoic acid regulates the expression of photoreceptor transcription factor NRL. *The Journal of biological chemistry* **281:** 27327-27334

Kinouchi R, Takeda M, Yang L, Wilhelmsson U, Lundkvist A, Pekny M, Chen DF (2003) Robust neural integration from retinal transplants in mice deficient in GFAP and vimentin. *Nature neuroscience* **6:** 863-868

Klassen H, Kiilgaard JF, Zahir T, Ziaeian B, Kirov I, Scherfig E, Warfvinge K, Young MJ (2007) Progenitor cells from the porcine neural retina express photoreceptor markers after transplantation to the subretinal space of allorecipients. *Stem cells* **25:** 1222-1230

Klassen H, Warfvinge K, Schwartz PH, Kiilgaard JF, Shamie N, Jiang C, Samuel M, Scherfig E, Prather RS, Young MJ (2008) Isolation of progenitor cells from GFP-transgenic pigs and transplantation to the retina of allorecipients. *Cloning and stem cells* **10:** 391-402

Klein LR, MacLeish PR, Wiesel TN (1990) Immunolabelling by a newt retinal pigment epithelium antibody during retinal development and regeneration. *The Journal of comparative neurology* **293:** 331-339

Kohno R, Ikeda Y, Yonemitsu Y, Hisatomi T, Yamaguchi M, Miyazaki M, Takeshita H, Ishibashi T, Sueishi K (2006) Sphere formation of ocular epithelial cells in the ciliary body is a reprogramming system for neural differentiation. *Brain research* **1093:** 54-70

Koike C, Nishida A, Ueno S, Saito H, Sanuki R, Sato S, Furukawa A, Aizawa S, Matsuo I, Suzuki N, Kondo M, Furukawa T (2007) Functional roles of Otx2 transcription factor in postnatal mouse retinal development. *Molecular and cellular biology* **27:** 8318-8329

Kubota R, Hokoc JN, Moshiri A, McGuire C, Reh TA (2002) A comparative study of neurogenesis in the retinal ciliary marginal zone of homeothermic vertebrates. *Brain research Developmental brain research* **134:** 31-41

Lamba DA, Gust J, Reh TA (2009) Transplantation of human embryonic stem cell-derived photoreceptors restores some visual function in Crx-deficient mice. *Cell stem cell* **4:** 73-79

Lamba DA, Karl MO, Ware CB, Reh TA (2006) Efficient generation of retinal progenitor cells from human embryonic stem cells. *Proc Natl Acad Sci U S A* **103:** 12769-12774

Lamba DA, McUsic A, Hirata RK, Wang PR, Russell D, Reh TA (2010) Generation, purification and transplantation of photoreceptors derived from human induced pluripotent stem cells. *PloS one* **5:** e8763

Lawrence JM, Singhal S, Bhatia B, Keegan DJ, Reh TA, Luthert PJ, Khaw PT, Limb GA (2007) MIO-M1 cells and similar muller glial cell lines derived from adult human retina exhibit neural stem cell characteristics. *Stem cells* **25:** 2033-2043

Levine EM, Roelink H, Turner J, Reh TA (1997) Sonic hedgehog promotes rod photoreceptor differentiation in mammalian retinal cells in vitro. *The Journal of neuroscience : the official journal of the Society for Neuroscience* **17:** 6277-6288

Lewis GP, Erickson PA, Guerin CJ, Anderson DH, Fisher SK (1992) Basic fibroblast growth factor: a potential regulator of proliferation and intermediate filament expression in the retina. *The Journal of neuroscience : the official journal of the Society for Neuroscience* **12:** 3968-3978

Lewis GP, Fisher SK (2003) Up-regulation of glial fibrillary acidic protein in response to retinal injury: its potential role in glial remodeling and a comparison to vimentin expression. *International review of cytology* **230:** 263-290

Limb GA, Salt TE, Munro PM, Moss SE, Khaw PT (2002) In vitro characterization of a spontaneously immortalized human Muller cell line (MIO-M1). *Investigative ophthalmology & visual science* **43:** 864-869

Lin N, Fan W, Sheedlo HJ, Aschenbrenner JE, Turner JE (1996) Photoreceptor repair in response to RPE transplants in RCS rats: outer segment regeneration. *Current eye research* **15:** 1069-1077

Livesey FJ, Cepko CL (2001) Vertebrate neural cell-fate determination: lessons from the retina. *Nature reviews Neuroscience* **2:** 109-118

Lord-Grignon J, Abdouh M, Bernier G (2006) Identification of genes expressed in retinal progenitor/stem cell colonies isolated from the ocular ciliary body of adult mice. *Gene expression patterns : GEP* **6:** 992-999

Mabry R, Gilbertson DG, Frank A, Vu T, Ardourel D, Ostrander C, Stevens B, Julien S, Franke S, Meengs B, Brody J, Presnell S, Hamacher NB, Lantry M, Wolf A, Bukowski T, Rosler R, Yen C, Anderson-Haley M, Brasel K, Pan Q, Franklin H, Thompson P, Dodds M, Underwood S, Peterson S, Sivakumar PV, Snavely M (2010) A dual-targeting PDGFRbeta/VEGF-A molecule assembled from stable antibody fragments demonstrates anti-angiogenic activity in vitro and in vivo. *mAbs* **2:** 20-34

Mack AF, Fernald RD (1997) Cell movement and cell cycle dynamics in the retina of the adult teleost Haplochromis burtoni. *The Journal of comparative neurology* **388:** 435-443

MacLaren RE, Pearson RA, MacNeil A, Douglas RH, Salt TE, Akimoto M, Swaroop A, Sowden JC, Ali RR (2006) Retinal repair by transplantation of photoreceptor precursors. *Nature* **444:** 203-207

MacNeil A, Pearson RA, MacLaren RE, Smith AJ, Sowden JC, Ali RR (2007) Comparative analysis of progenitor cells isolated from the iris, pars plana, and ciliary body of the adult porcine eye. *Stem cells* **25:** 2430-2438

Maguire AM, Simonelli F, Pierce EA, Pugh EN, Jr., Mingozzi F, Bennicelli J, Banfi S, Marshall KA, Testa F, Surace EM, Rossi S, Lyubarsky A, Arruda VR, Konkle B, Stone E, Sun J, Jacobs J, Dell'Osso L, Hertle R, Ma JX, Redmond TM, Zhu X, Hauck B, Zelenaia O, Shindler KS, Maguire MG, Wright JF, Volpe NJ, McDonnell JW, Auricchio A, High KA, Bennett J (2008) Safety and efficacy of gene transfer for Leber's congenital amaurosis. *N Engl J Med* **358:** 2240-2248

Marquardt T (2003) Transcriptional control of neuronal diversification in the retina. *Progress in retinal and eye research* **22:** 567-577

Martin DF, Maguire MG, Ying GS, Grunwald JE, Fine SL, Jaffe GJ (2011) Ranibizumab and bevacizumab for neovascular age-related macular degeneration. *The New England journal of medicine* **364:** 1897-1908

Matsunari H, Onodera M, Tada N, Mochizuki H, Karasawa S, Haruyama E, Nakayama N, Saito H, Ueno S, Kurome M, Miyawaki A, Nagashima H (2008) Transgenic-cloned pigs systemically expressing red fluorescent protein, Kusabira-Orange. *Cloning and stem cells* **10:** 313-323

Mayer EJ, Carter DA, Ren Y, Hughes EH, Rice CM, Halfpenny CA, Scolding NJ, Dick AD (2005) Neural progenitor cells from postmortem adult human retina. *The British journal of ophthalmology* **89:** 102-106

McUsic AC, Lamba DA, Reh TA (2012) Guiding the morphogenesis of dissociated newborn mouse retinal cells and hES cell-derived retinal cells by soft lithography-patterned microchannel PLGA scaffolds. *Biomaterials* **33:** 1396-1405

Mears AJ, Kondo M, Swain PK, Takada Y, Bush RA, Saunders TL, Sieving PA, Swaroop A (2001) Nrl is required for rod photoreceptor development. *Nature genetics* **29:** 447-452

Middleton S (2010) Porcine ophthalmology. *The Veterinary clinics of North America Food animal practice* **26:** 557-572

Ming GL, Song H (2011) Adult neurogenesis in the mammalian brain: significant answers and significant questions. *Neuron* **70:** 687-702

Mitashov VI (1996) Mechanisms of retina regeneration in urodeles. *The International journal of developmental biology* **40:** 833-844

Mitashov VI (1997) Retinal regeneration in amphibians. *The International journal of developmental biology* **41:** 893-905

Mitashov VI, Arsanto JP, Markitantova YV, Thouveny Y (1995) Remodeling processes during neural retinal regeneration in adult urodeles: an immunohistochemical survey. *The International journal of developmental biology* **39:** 993-1003

Moe MC, Kolberg RS, Sandberg C, Vik-Mo E, Olstorn H, Varghese M, Langmoen IA, Nicolaissen B (2009) A comparison of epithelial and neural properties in progenitor cells derived from the adult human ciliary body and brain. *Experimental eye research* **88:** 30-38

Montgomery JE, Parsons MJ, Hyde DR (2010) A novel model of retinal ablation demonstrates that the extent of rod cell death regulates the origin of the regenerated zebrafish rod photoreceptors. *The Journal of comparative neurology* **518:** 800-814

Moshiri A, Close J, Reh TA (2004) Retinal stem cells and regeneration. *The International journal of developmental biology* **48:** 1003-1014

Moshiri A, Reh TA (2004) Persistent progenitors at the retinal margin of ptc+/- mice. *The Journal of neuroscience : the official journal of the Society for Neuroscience* **24:** 229-237

Negishi K, Shinagawa S, Ushijima M, Kaneko Y, Saito T (1992) An immunohistochemical study of regenerating newt retinas. *Brain research Developmental brain research* **68:** 255-264

Neill JM, Barnstable CJ (1990) Expression of the cell surface antigens RET-PE2 and N-CAM by rat retinal pigment epithelial cells during development and in tissue culture. *Experimental eye research* **51:** 573-583

Ng L, Lu A, Swaroop A, Sharlin DS, Forrest D (2011) Two transcription factors can direct three photoreceptor outcomes from rod precursor cells in mouse retinal development. *The Journal of neuroscience : the official journal of the Society for Neuroscience* **31:** 11118-11125

Nickerson PE, Emsley JG, Myers T, Clarke DB (2007) Proliferation and expression of progenitor and mature retinal phenotypes in the adult mammalian ciliary body after retinal ganglion cell injury. *Investigative ophthalmology & visual science* **48:** 5266-5275

Nishida A, Furukawa A, Koike C, Tano Y, Aizawa S, Matsuo I, Furukawa T (2003) Otx2 homeobox gene controls retinal photoreceptor cell fate and pineal gland development. *Nature neuroscience* **6:** 1255-1263

Nishiguchi KM, Kaneko H, Nakamura M, Kachi S, Terasaki H (2008) Identification of photoreceptor precursors in the pars plana during ocular development and after retinal injury. *Investigative ophthalmology & visual science* **49:** 422-428

Nishiguchi KM, Kaneko H, Nakamura M, Kachi S, Terasaki H (2009) Generation of immature retinal neurons from proliferating cells in the pars plana after retinal histogenesis in mice with retinal degeneration. *Molecular vision* **15:** 187-199

Nishiguchi KM, Nakamura M, Kaneko H, Kachi S, Terasaki H (2007) The role of VEGF and VEGFR2/Flk1 in proliferation of retinal progenitor cells in murine retinal degeneration. *Investigative ophthalmology & visual science* **48:** 4315-4320

Oh EC, Cheng H, Hao H, Jia L, Khan NW, Swaroop A (2008) Rod differentiation factor NRL activates the expression of nuclear receptor NR2E3 to suppress the development of cone photoreceptors. *Brain research* **1236:** 16-29

Okamoto S, Takahashi M (2011) Induction of retinal pigment epithelial cells from monkey iPS cells. *Investigative ophthalmology & visual science* **52:** 8785-8790

Oliver TG, Grasfeder LL, Carroll AL, Kaiser C, Gillingham CL, Lin SM, Wickramasinghe R, Scott MP, Wechsler-Reya RJ (2003) Transcriptional profiling of the Sonic hedgehog response: a critical role for N-myc in proliferation of neuronal precursors. *Proceedings of the National Academy of Sciences of the United States of America* **100:** 7331-7336

Omori Y, Katoh K, Sato S, Muranishi Y, Chaya T, Onishi A, Minami T, Fujikado T, Furukawa T (2011) Analysis of transcriptional regulatory pathways of photoreceptor genes by expression profiling of the Otx2-deficient retina. *PloS one* **6:** e19685

Ooto S, Akagi T, Kageyama R, Akita J, Mandai M, Honda Y, Takahashi M (2004) Potential for neural regeneration after neurotoxic injury in the adult mammalian retina. *Proceedings of the National Academy of Sciences of the United States of America* **101:** 13654-13659

Osakada F, Ikeda H, Mandai M, Wataya T, Watanabe K, Yoshimura N, Akaike A, Sasai Y, Takahashi M (2008) Toward the generation of rod and cone photoreceptors from mouse, monkey and human embryonic stem cells. *Nature biotechnology* **26:** 215-224

Osakada F, Ikeda H, Sasai Y, Takahashi M (2009a) Stepwise differentiation of pluripotent stem cells into retinal cells. *Nat Protoc* **4:** 811-824

Osakada F, Jin ZB, Hirami Y, Ikeda H, Danjyo T, Watanabe K, Sasai Y, Takahashi M (2009b) In vitro differentiation of retinal cells from human pluripotent stem cells by small-molecule induction. *Journal of cell science* **122:** 3169-3179

Osakada F, Ooto S, Akagi T, Mandai M, Akaike A, Takahashi M (2007) Wnt signaling promotes regeneration in the retina of adult mammals. *The Journal of neuroscience : the official journal of the Society for Neuroscience* **27:** 4210-4219

Otteson DC, Cirenza PF, Hitchcock PF (2002) Persistent neurogenesis in the teleost retina: evidence for regulation by the growth-hormone/insulin-like growth factor-I axis. *Mechanisms of development* **117:** 137-149

Otteson DC, D'Costa AR, Hitchcock PF (2001) Putative stem cells and the lineage of rod photoreceptors in the mature retina of the goldfish. *Developmental biology* **232:** 62-76

Park CM, Hollenberg MJ (1989) Basic fibroblast growth factor induces retinal regeneration in vivo. *Developmental biology* **134:** 201-205

Park CM, Hollenberg MJ (1991) Induction of retinal regeneration in vivo by growth factors. *Developmental biology* **148:** 322-333

Park KW, Kuhholzer B, Lai L, Machaty Z, Sun QY, Day BN, Prather RS (2001) Development and expression of the green fluorescent protein in porcine embryos derived from nuclear transfer of transgenic granulosa-derived cells. *Animal reproduction science* **68:** 111-120

Pearson PA, Comstock TL, Ip M, Callanan D, Morse LS, Ashton P, Levy B, Mann ES, Eliott D (2011) Fluocinolone acetonide intravitreal implant for diabetic macular edema: a 3-year multicenter, randomized, controlled clinical trial. *Ophthalmology* **118:** 1580-1587

Petters RM, Alexander CA, Wells KD, Collins EB, Sommer JR, Blanton MR, Rojas G, Hao Y, Flowers WL, Banin E, Cideciyan AV, Jacobson SG, Wong F (1997) Genetically engineered large animal model for studying cone photoreceptor survival and degeneration in retinitis pigmentosa. *Nature biotechnology* **15:** 965-970

Pittack C, Grunwald GB, Reh TA (1997) Fibroblast growth factors are necessary for neural retina but not pigmented epithelium differentiation in chick embryos. *Development* **124:** 805-816

Rattner A, Nathans J (2006) Macular degeneration: recent advances and therapeutic opportunities. *Nature reviews Neuroscience* **7:** 860-872

Raymond PA, Barthel LK, Bernardos RL, Perkowski JJ (2006) Molecular characterization of retinal stem cells and their niches in adult zebrafish. *BMC developmental biology* **6:** 36

Redmond TM, Yu S, Lee E, Bok D, Hamasaki D, Chen N, Goletz P, Ma JX, Crouch RK, Pfeifer K (1998) Rpe65 is necessary for production of 11-cis-vitamin A in the retinal visual cycle. *Nature genetics* **20:** 344-351

Reh TA (1987) Cell-specific regulation of neuronal production in the larval frog retina. *The Journal of neuroscience : the official journal of the Society for Neuroscience* **7:** 3317-3324

Reh TA, Lamba D, Gust J (2010) Directing human embryonic stem cells to a retinal fate. *Methods in molecular biology* **636:** 139-153

Resnikoff S, Pascolini D, Mariotti SP, Pokharel GP (2008) Global magnitude of visual impairment caused by uncorrected refractive errors in 2004. *Bull World Health Organ* **86:** 63-70

Rodieck RW (1998) *The first steps in seeing*, Sunderland, MA: Sinauer Associates.

Sahel J, Bonnel S, Mrejen S, Paques M (2010) Retinitis pigmentosa and other dystrophies. *Developments in ophthalmology* **47:** 160-167

Sahni JN, Angi M, Irigoyen C, Semeraro F, Romano MR, Parmeggiani F (2011) Therapeutic challenges to retinitis pigmentosa: from neuroprotection to gene therapy. *Current genomics* **12:** 276-284

Sakaguchi DS, Janick LM, Reh TA (1997) Basic fibroblast growth factor (FGF-2) induced transdifferentiation of retinal pigment epithelium: generation of retinal neurons and glia. *Developmental dynamics : an official publication of the American Association of Anatomists* **209:** 387-398

Sakakibara S, Hiramatsu H, Takahashi Y, Hisatomi O, Kobayashi Y, Sakami S, Saito T, Tokunaga F (2002) Opsin expression in adult, developing, and regenerating newt retinas. *Brain research Molecular brain research* **103:** 28-35

Sanchez I, Martin R, Ussa F, Fernandez-Bueno I (2011) The parameters of the porcine eyeball. *Graefe's archive for clinical and experimental ophthalmology = Albrecht von Graefes Archiv fur klinische und experimentelle Ophthalmologie* **249:** 475-482

Sanchez-Sanchez AV, Camp E, Leal-Tassias A, Mullor JL (2010) Wnt signaling has different temporal roles during retinal development. *Developmental dynamics : an official publication of the American Association of Anatomists* **239:** 297-310

Sarthy V, Egal H (1995) Transient induction of the glial intermediate filament protein gene in Muller cells in the mouse retina. *DNA and cell biology* **14:** 313-320

Schwartz SD, Hubschman JP, Heilwell G, Franco-Cardenas V, Pan CK, Ostrick RM, Mickunas E, Gay R, Klimanskaya I, Lanza R (2012) Embryonic stem cell trials for macular degeneration: a preliminary report. *Lancet* **379:** 713-720

Simonelli F, Maguire AM, Testa F, Pierce EA, Mingozzi F, Bennicelli JL, Rossi S, Marshall K, Banfi S, Surace EM, Sun J, Redmond TM, Zhu X, Shindler KS, Ying GS, Ziviello C, Acerra C, Wright JF, McDonnell JW, High KA, Bennett J, Auricchio A (2010) Gene therapy for Leber's congenital amaurosis is safe and effective through 1.5 years after vector administration. *Molecular therapy : the journal of the American Society of Gene Therapy* **18:** 643-650

Stenkamp DL (2007) Neurogenesis in the fish retina. *International review of cytology* **259:** 173-224

Stone LS (1949) Regeneration of the neural portion of the retina from pigment cells in adult urodele eyes. *Proceedings of the Society for Experimental Biology and Medicine Society for Experimental Biology and Medicine* **72:** 382-384

Stone LS (1950) Neural retina degeneration followed by regeneration from surviving retinal pigment cells in grafted adult salamander eyes. *The Anatomical record* **106:** 89-109

Stone LS, Steinitz H (1957) Regeneration of neural retina and lens from retina pigment cell grafts in adult newts. *The Journal of experimental zoology* **135:** 301-317

Stroeva OG, Mitashov VI (1983) Retinal pigment epithelium: proliferation and differentiation during development and regeneration. *International review of cytology* **83:** 221-293

Swaroop A, Chew EY, Rickman CB, Abecasis GR (2009) Unraveling a multifactorial late-onset disease: from genetic susceptibility to disease mechanisms for age-related macular degeneration. *Annu Rev Genomics Hum Genet* **10:** 19-43

Swaroop A, Kim D, Forrest D (2010) Transcriptional regulation of photoreceptor development and homeostasis in the mammalian retina. *Nature reviews Neuroscience* **11:** 563-576

Tackenberg MA, Tucker BA, Swift JS, Jiang C, Redenti S, Greenberg KP, Flannery JG, Reichenbach A, Young MJ (2009) Muller cell activation, proliferation and migration following laser injury. *Molecular vision* **15:** 1886-1896

Takeda M, Takamiya A, Jiao JW, Cho KS, Trevino SG, Matsuda T, Chen DF (2008) alpha-Aminoadipate induces progenitor cell properties of Muller glia in adult mice. *Investigative ophthalmology & visual science* **49:** 1142-1150

Thummel R, Kassen SC, Enright JM, Nelson CM, Montgomery JE, Hyde DR (2008a) Characterization of Muller glia and neuronal progenitors during adult zebrafish retinal regeneration. *Experimental eye research* **87:** 433-444

Thummel R, Kassen SC, Montgomery JE, Enright JM, Hyde DR (2008b) Inhibition of Muller glial cell division blocks regeneration of the light-damaged zebrafish retina. *Developmental neurobiology* **68:** 392-408

Tropepe V, Coles BL, Chiasson BJ, Horsford DJ, Elia AJ, McInnes RR, van der Kooy D (2000) Retinal stem cells in the adult mammalian eye. *Science* **287:** 2032-2036

Turner DL, Cepko CL (1987) A common progenitor for neurons and glia persists in rat retina late in development. *Nature* **328:** 131-136

Wahlin KJ, Campochiaro PA, Zack DJ, Adler R (2000) Neurotrophic factors cause activation of intracellular signaling pathways in Muller cells and other cells of the inner retina, but not photoreceptors. *Investigative ophthalmology & visual science* **41:** 927-936

Wan J, Zheng H, Chen ZL, Xiao HL, Shen ZJ, Zhou GM (2008) Preferential regeneration of photoreceptor from Muller glia after retinal degeneration in adult rat. *Vision research* **48:** 223-234

Wan J, Zheng H, Xiao HL, She ZJ, Zhou GM (2007) Sonic hedgehog promotes stem-cell potential of Muller glia in the mammalian retina. *Biochemical and biophysical research communications* **363:** 347-354

Wang NK, Tosi J, Kasanuki JM, Chou CL, Kong J, Parmalee N, Wert KJ, Allikmets R, Lai CC, Chien CL, Nagasaki T, Lin CS, Tsang SH (2010) Transplantation of reprogrammed embryonic stem cells improves visual function in a mouse model for retinitis pigmentosa. *Transplantation* **89:** 911-919

Warfvinge K, Kiilgaard JF, Lavik EB, Scherfig E, Langer R, Klassen HJ, Young MJ (2005) Retinal progenitor cell xenografts to the pig retina: morphologic integration and cytochemical differentiation. *Archives of ophthalmology* **123:** 1385-1393

Wehman AM, Staub W, Meyers JR, Raymond PA, Baier H (2005) Genetic dissection of the zebrafish retinal stem-cell compartment. *Developmental biology* **281:** 53-65

Wetts R, Serbedzija GN, Fraser SE (1989) Cell lineage analysis reveals multipotent precursors in the ciliary margin of the frog retina. *Developmental biology* **136:** 254-263

Witkin AJ, Brown GC (2011) Update on nonsurgical therapy for diabetic macular edema. *Current opinion in ophthalmology* **22:** 185-189

Wright AF, Chakarova CF, Abd El-Aziz MM, Bhattacharya SS (2010) Photoreceptor degeneration: genetic and mechanistic dissection of a complex trait. *Nature reviews Genetics* **11:** 273-284

Xu H, Sta Iglesia DD, Kielczewski JL, Valenta DF, Pease ME, Zack DJ, Quigley HA (2007a) Characteristics of progenitor cells derived from adult ciliary body in mouse, rat, and human eyes. *Investigative ophthalmology & visual science* **48:** 1674-1682

Xu S, Sunderland ME, Coles BL, Kam A, Holowacz T, Ashery-Padan R, Marquardt T, McInnes RR, van der Kooy D (2007b) The proliferation and expansion of retinal stem cells require functional Pax6. *Developmental biology* **304:** 713-721

Xue W, Cojocaru RI, Dudley VJ, Brooks M, Swaroop A, Sarthy VP (2011) Ciliary neurotrophic factor induces genes associated with inflammation and gliosis in the retina: a gene profiling study of flow-sorted, Muller cells. *PloS one* **6:** e20326

Yanagi Y, Inoue Y, Kawase Y, Uchida S, Tamaki Y, Araie M, Okochi H (2006) Properties of growth and molecular profiles of rat progenitor cells from ciliary epithelium. *Experimental eye research* **82:** 471-478

Yaron O, Farhy C, Marquardt T, Applebury M, Ashery-Padan R (2006) Notch1 functions to suppress cone-photoreceptor fate specification in the developing mouse retina. *Development* **133:** 1367-1378

Young TL, Cepko CL (2004) A role for ligand-gated ion channels in rod photoreceptor development. *Neuron* **41:** 867-879

Zhao S, Thornquist SC, Barnstable CJ (1995) In vitro transdifferentiation of embryonic rat retinal pigment epithelium to neural retina. *Brain research* **677:** 300-310

Zhao X, Das AV, Soto-Leon F, Ahmad I (2005) Growth factor-responsive progenitors in the postnatal mammalian retina. *Developmental dynamics : an official publication of the American Association of Anatomists* **232:** 349-358

Zhao X, Liu J, Ahmad I (2002) Differentiation of embryonic stem cells into retinal neurons. *Biochemical and biophysical research communications* **297:** 177-184

Zhou L, Wang W, Liu Y, de Castro JF, Ezashi T, Telugu BP, Roberts RM, Kaplan HJ, Dean DC (2011) Differentiation of induced pluripotent stem cells of swine into rod photoreceptors and their integration into the retina. *Stem cells* **29:** 972-980

Zygar CA, Colbert S, Yang D, Fernald RD (2005) IGF-1 produced by cone photoreceptors regulates rod progenitor proliferation in the teleost retina. *Brain research Developmental brain research* **154:** 91-100

APPENDICES

SUMMARY

This thesis reports the isolation, characterization and allotransplantation in porcine retina of ciliary epithelium (CE)-derived cells, also known as retinal stem cells (RSCs). The self-renewal capacity and differentiation potential of these cells *in vitro* and *in vivo* makes them candidate donors in cell replacement approaches for treating retinal degenerative diseases. The use of pig as the animal model should facilitate translation of these findings to applications for human conditions.

Chapter 2 presents data on retinal histogenesis in the pig, generated upon validation of antibodies commonly used in rodents. The porcine retina displays similar marker distribution and histogenesis as the human retina, supporting the pig as a preclinical model to study retinal degeneration and repair.

Chapter 3 describes the isolation and characterization of newborn porcine CE-derived RSCs in comparison with retinal progenitor cells (RPCs) derived from the developing retina and neural stem cells (NSCs) from the developing brain. Porcine CE-derived RSCs share similar characteristics with their human counterpart: their self-renewal potential is limited and they cannot be maintained indefinitely in culture, suggesting that they are not bona fide stem cells like NSCs; however, under conditions that favor differentiation, they can express markers of mature retinal cells and rudimentary morphological features of neurons.

In Chapter 4, we undertook a novel approach to predict microRNA that could have gene regulatory functions in the retina and in RSCs based on gene expression profiling data obtained by microarray hybridization. A limited number of microRNA was predicted to affect gene expression in RSCs compared to postnatal and adult retina, consistent with their undifferentiated nature. Furthermore, among the microRNAs that ranked highest in our prediction and were validated by RT-PCR, miR24 and miR122, had previously been shown to be involved in development.

Chapter 5 completes the work presented in Chapters 2 and 3 by testing the fate of newborn pig CE-derived cells after transplantation in the young porcine retina. CE-derived cells migrated both radially and tangentially from the subretinal site of injection. The majority of transplanted cells appeared integrated in multilayered RPE-like structures and expressed RPE65, while a smaller proportion of cells integrated in the neuroretina and expressed markers of mature retinal cells. Differences in cell fate observed *in vitro*, where RPE marker expression was low and retinal phenotypes comparably higher, suggest that the environment and extrinsic cues are critical in guiding the differentiation of CE-derived cells.

In summary, this thesis shows that cultures of self-renewing cells can be obtained *in vitro* from the newborn porcine CE and that these cells can differentiate into retinal and RPE phenotypes both *in vitro* and *in vivo* in allorecipients. However, the nature and physiological role of these cells in potential endogenous repair mechanisms still remain to be explored. Notably, their remarkable plasticity *in vitro* makes them an interesting cell model to study this phenomenon of recent identification.

NEDERLANDSE SAMENVATTING

Dit proefschrift beschrijft de isolatie en karakterisering van cellen afkomstig van het ciliair epitheel (CE) van het netvlies van het varken. Deze cellen hebben eigenschappen van netvlies stamcellen (retinal stem cells, RSC's). Tevens wordt het lot van deze cellen beschreven na (allo)transplantatie in het varkensoog.

De vooronderstelling bij de beschreven experimenten was tweeledig, nl. i. dat het zelf-vernieuwingsvermogen en het differentiatie potentieel van RSC's hen tot goede kandidaten maakt voor de behandeling -door middel van celvervanging- van oogziekten, waarbij het netvlies degenereert en ii. dat het varken een goed modeldier is om de vertaalslag naar toepassing bij de mens te maken van celtherapeutisch onderzoek naar netvliesherstel (Hoofdstuk 1).

Hoofdstuk 2 beschrijft de ontwikkeling van het netvlies van het varken. Bij dit onderzoek is gebruik gemaakt van immuunhistochemie met antilichamen tegen celmerker-eiwitten, die goed gekarakteriseerd zijn bij de muis. De resultaten laten zien dat de verdeling van de celmerker-eiwitten in het varkensnetvlies grote overeenkomst vertoont met die in het menselijke netvlies. Dit gegeven ondersteunt de vooronderstelling over het gebruik van het varken als modeldier bij preklinisch onderzoek naar netvlies degeneratie en herstel.

Hoofdstuk 3 gaat in op de isolatie en karakterisering van de CE-afgeleide RSC's van pasgeboren varkens. Deze RSC's worden vergeleken met retinale voorloper (progenitor) cellen (RPC's) in het zich ontwikkelende netvlies en neurale stamcellen (NSC) van het zich ontwikkelende brein. Uit dit onderzoek bleek dat varken-CE afgeleide RSC's veel overeenkomst vertonen met hun menselijke tegenhangers in de zin dat hun zelfvernieuwend vermogen beperkt is en dat ze niet onbeperkt in kweek kunnen worden gehouden. Dit laatste geeft overigens aan dat RSC's geen bona fide stamcellen zijn, zoals NSC's. Wel is echter duidelijk geworden dat ze celmerkers tot expressie

kunnen brengen, die ook in gedifferentieerde netvliescellen worden aangetroffen en dat ze morfologische kenmerken vertonen die aan neuronen doen denken.

In Hoofdstuk 4 is een nieuwe methode ontwikkeld en toegepast die voorspelt welke microRNA's een gen-regulatoire functie zouden kunnen hebben in het netvlies en RSC's. Hierbij is gebruik gemaakt van door microarray-hybridisatie verkregen genexpressieprofielen van RSC's en netvliezen van pasgeboren en volwassen varkens. Vergeleken met de netvliezen werd er voor RSC's een klein aantal microRNA's met effect op genexpressie voorspeld. Het geringe aantal strookt met het ongedifferentieerde karakter van RSC's. Onder de microRNA's, die het hoogst op de ranglijst van effectvoorspelling stonden, bevonden zich miR24 en miR122, waarvan al eerder aangetoond dat ze betrokken zijn bij de ontwikkeling. Het voorspelde effect is vervolgens kwantitatief bevestigd met behulp van RT-PCR.

In Hoofdstuk 5 wordt het werk beschreven in de Hoofdstukken 2 en 3 aangevuld met onderzoek naar het lot van CE-afgeleide cellen van pasgeboren varkens na allotransplantatie. Hiertoe is hun distributie en fenotype bestudeerd na subretinale injectie in het oog van jonge varkens. Gebleken is dat de cellen zowel radiaal als tangentieel vanaf de plek van injectie migreren, dat de meerderheid van de getransplanteerde cellen in het retina pigment epitheel (RPE) terecht komen en de RPE-merker RPE65 tot expressie brengen. Een kleiner deel van de cellen komt terecht in de neuroretina en brengt eiwitmerkers tot expressie, die karakteristiek zijn voor volwassen netvliescellen. Deze fenotypische in vivo bevindingen zijn niet helemaal congruent met de in vitro resultaten. In vitro was het percentage cellen met de RPE-merkerexpressie laag en die van cellen met netvliesfenotypes relatief hoog, hetgeen sterk suggereert dat de directe omgeving en extrinsieke signalen een kritische rol spelen bij de differentiatie van de CE-afgeleide cellen.

Samenvattend, de resultaten beschreven in dit proefschrift laten zien dat uit het ciliair epitheel van pasgeboren varkens cellen met een zelf-vernieuwend vermogen in kweek gebracht kunnen worden en dat deze cellen zowel in vitro als in vivo (na allotransplantie) kunnen differentiëren tot cellen met fenotypes die karakteristiek zijn

voor cellen van het netvlies en het retinale pigmentepitheel. Voordat ze kunnen worden toegepast zal echter hun fysiologische rol in netvliesherstelmechanismen verder onderzocht moeten worden. Vooral de nieuw ontdekte en opmerkelijke plasticiteit in vitro maakt deze cellen tot een waardevol onderwerp van verder preklinisch onderzoek.

RIASSUNTO IN ITALIANO

Questa tesi descrive l'isolamento, la caratterizzazione e il trapianto allogenico nella retina suina di cellule derivate dall'epitelio ciliare (EC), anche chiamate cellule staminali retiniche (CSR). La capacita' di autoreplicarsi e il potenziale di generare cellule differenziate *in vitro* e *in vivo* ne suggeriscono l'uso in terapie cellulari per il trattamento delle malattie degenerative della retina. La scelta del maiale come modello animale faciliterebbe l'applicazione all'uomo dei risultati di questa ricerca.

Nel Capitolo 2 e' illustrata l'istogenesi della retina nel maiale. I dati sono stati ottenuti dopo avere validato anticorpi comunemente usati in roditori. La retina suina presenta una distribuzione di marcatori cellulari e un'istogenesi simili a quelli della retina umana. Questo incoraggia l'uso del maiale come modello preclinico per studi sulla degenerazione e rigenerazione della retina.

Il Capitolo 3 descrive l'isolamento e la caratterizzazione di CSR derivate dall'EC di maiale neonato. Le loro caratteristiche vengono confrontate con quelle di cellule progenitrici retiniche (CPR) ottenute dalla retina e cellule staminali nervose (CSN) ottenute dal cervello di embrioni di maiale. The CSR derivate dall'EC suino posseggono cartteristiche simili a quelle delle corrispondenti cellule umane: il loro potenziale di autoreplicazione e' limitato e non possono essere mantenute in coltura a lungo. Queste caratteristiche suggeriscono che queste cellule non siano *bona fide* cellule staminali come the CSN. Tuttavia, in condizioni che favoriscono il differenziamento, le CSR possono esprimere marcatori cellulari tipici delle cellule retiniche mature e caratteristiche morfologiche rudimentali che suggeriscono la loro natura di neuroni.

Nel Capitolo 4 abbiamo applicato un nuovo metodo per prevedere quali microRNA potessero avere funzione regolatoria nella retina e nelle CSR basandosi sul profilo di espressione ottenuto con l'ibridazione su micro arrays. Un numero ridotto di microRNA e' risultato essere coinvolto nell'espressione genica nelle CSR rispetto alla retina postnatale e adulta, come ci si aspetterebbe sulla base della loro natura

indifferenziata. Inoltre, tra i microRNA che sono risultati in alto alla lista e che sono stati validati con la RT-PCR, miR24 e miR22 erano gia' noti per il loro ruolo nello sviluppo.

Il Capitolo 5 illustra il destino di cellule derivate dall'EC di maiale neonato dopo trapianto nella retina di giovani maiali. Questo Capitolo conclude la ricerca presentata nei Capitoli 2 e 3. Le cellule derivate dall'EC migrano in direzione radiale e tangenziale dal punto di iniezione nello spazio subretinale. La maggioranza delle cellule trapiantate sembrano integrarsi in una struttura a piu' strati simile all'epitelio retinico pigmentato (ERP) ed esprimono il marcatore cellulare RPE65. Una piccola parte delle cellule risulta integrata nella neuroretina ed esprime marcatori cellulari caratteristici delle cellule retiniche mature. Le differenze osservate rispetto al differenziamento *in vitro*, dove a confronto l'espressione di RPE65 e' minima e le cellule che esprimono marcatori retinici numerose, suggeriscono che stimoli ambientali e segnali estrinsici sono fondamentali nel guidare il differenziamento delle cellule derivate dall'EC.

In conclusione, questa tesi dimostra che colture di cellule con capacita' di autoreplicazione possono essere ottenute *in vitro* dall'EC di maiali neonati. Queste cellule possono essere differenziate per generare fenotipi retinici e ERP *in vitro* e *in vivo* dopo allotrapianto. Tuttavia, la natura e il ruolo fisiologico di queste cellule in potenziali meccanismi autologhi di rigenerazione rimangono ignoti. La plasticita' cellulare *in vitro* aumenta l'interesse per queste cellule che potrebbero essere usate come modello per studiare questo fenomeno di recente identificazione.

ABBREVIATIONS

AGE	Advanced Glycosylation End-products
AMD	Age-related Macular Degeneration
α-AA	Alpha-aminoadipate
BLBP	Brain Lipid Binding Protein
BMP	Bone Morphogenic Protein
BrdU	Bromodeoxyuridine
CE	Ciliary Epithelium
Cdh2	N-cadherin
Chx10	Visual System Homeobox 2
CMZ	Ciliary Marginal Zone
CNTF	Ciliary Neurotrophic Factor
CRALBP	Cellular Retinaldehyde-Binding Protein
CZG	Circumferential Germinal Zone
DME	Diabetic Macular Edema
DR	Diabetic Retinopathy
EGF	Epidermal Growth Factor
EGFR	Epidermal Growth Factor Receptor
ES	Embryonic Stem (cells)
FGF	Fibroblast Growth Factor
FLP	Focal Laser Photocoagulation
GCL	Ganglion Cell Layer
GFAP	Glial Fibrillary Acidic Protein
GDNF	Glial cell-Derived Neurotrophic Factor
GH	Growth Hormone
GS	Glutamine Synthetase
IGF	Insulin-like Growth Factor

IHC	Immunohistochemistry
IL	Interleukin
INL	Inner Nuclear Layer
IPL	Inner Plexiform Layer
iPS	Induced Pluripotent Stem (cell)
LCA	Leber Congenital Amaurosis
LIF	Leukemia Inhibitory Factor
LPC	Laser Photocoagulation
NFL	Nerve Fiber Layer
NMDA	N-Methyl-D-aspartic acid
NMU	N-methyl N-nItrosourea
NSC	Neural Stem Cell
ONL	Outer Nuclear Layer
OPL	Outer Plexiform Layer
OS	Outer Segments
Pax6a	Paired Box gene 6a
PCNA	Proliferating Cell Nuclear Antigen
PDGF	Platelet-Derived Growth Factor
PDT	Photodynamic Therapy
PEDF	Pigment Epithelium Derived Factor
PNA	Peanut Agglutinin
PRL	Photoreceptor Layer
β-6PDE	β-6 Phosphodiesterase
RA	Retinoic Acid
RCS	Royal College of Surgeon's
RGC	Retinal Ganglion Cell
Rho	Rhodopsin
RP	Retinitis Pigmentosa
RPC	Retinal Progenitor Cell

RPE	Retinal Pigment Epithelium
RSC	Retinal Stem Cell
RT-PCR	Reverse Transcriptase-Polymerase Chain Reaction
Rx1	Retinal Homeobox 1
SHH	Sonic Hedgehog
Smo	Smoothened
TGF	Transforming growth factor
TTT	Transpupillary thermotherapy
VEGF	Vascular Endothelial Growth Factor
Vsx2/Chx10	Visual System Homeobox 2

LIST OF PUBLICATIONS

1. F. Dosio, T. Cogliati, S. Canevari, D. Mezzanzanica, P. Brusa, L. Delprino, M.I. Colnaghi and L. Cattel (1989) Antibody-Toxin Conjugate Preparation: Effects of the Linker on Activity and Stability. **Antibody, Immunoconjugates, and Radiopharmaceuticals** 2:101-115.

2. S. Canevari, T. Cogliati, D. Mezzanzanica, R. Orlandi e M.I. Colnaghi (1990) Anticorpi Monoclonali anti carcinomi umani quali vettori di tossine. Atti del 16º Congresso Nazionale della Societa` Italiana di Chemioterapia. **Journal of Chemotherapy** suppl. 2:370-373.

3. S.M. Muñoz, M. Caldera, S. Canevari, E. Tosi, T. Cogliati, M.I. Colnaghi and F.P. Conde (1990) Fractionation of the ribosome inactivating protein preparations with triazine dyes. **Biochem. Biophys. Res. Commun.** 173(2):554-560.

4. T. Cogliati, P. Brusa, S. Canevari, M. Caldera, D. Mezzanzanica, F. Dosio, L. Cattel and M.I. Colnaghi (1991) Preparation and Biological Characterization of Conjugates Consisting of Ricin and a Tumor-Specific Non-Internalizing MAb. **Anticancer Res**. 11(1):417-422.

5. B. Berra, L. Papi, U. Bigozzi, D. Serino, R. Morichi, P. Mennonna, S. Rapelli, T. Cogliati, and E. Montali (1991) Correlation between cytogenetic data and ganglioside pattern in human Meningiomas. **Int. J. Cancer** 47(3):329-333.

6. T. Cogliati, B.K. Dunn, M. Bar-Ner, C.M. Cultraro and S. Segal (1993) Transfected wild-type and mutant max regulate cell growth and differentiation of murine Erythroleukemia cells. **Oncogene**, 8(5):1263-1268.

7. T. Cogliati, B.K. Dunn, C.M. Cultraro, L. Hearing and S. Segal (1994) Differential effects of Max proteins (long and short) on growth and differentiation of murine Erythroleukemia cells. **Oncology Reports**, 1:179-184.

8. B.K. Dunn, T. Cogliati, C.M. Cultraro, M. Bar-Ner and S. Segal (1994) Regulation of Murine Max (Myn) Parallels the Regulation of c-Myc in Differentiating Murine Erythroleukemia Cells. **Cell Growth and Differentiation,** 5(8):847-854.

9. C.M. Cultraro, T. Cogliati, L.E. Hearing and S. Segal (1996) Basic mutant Max reverses a c-Myc block to differentiation. **Oncology Reports**, 3:141-146.

10. E. Chu, T. Cogliati, S.M. Copur, A. Borrè, D.M. Voeller, C.J. Allegra and S. Segal (1996) Identification of In Vivo Target RNA Sequences Bound by Thymidylate Synthase. **Nucleic Acid Research**, 24(16):3222-3228.

11. C. Ferrarese, G. Bianchi, M. Bugiani, T. Cogliati, M. Frigo, D. Passoni, N. Pecora, R. Piolti, C. Pozzi, R. Tortorella and L. Frattola (1996) Platelets as peripheral model of glutamate-related excitotoxicity in Parkinson's Disease. In: "**Neurodegenerative diseases '95: molecular and cellular mechanisms and therapeutic advances**", G. Fiskum Ed., Plenum Press, New York, pp 63-68.

12. C. Ferrarese, R. Tortorella, G. Bogliun, E. Beghi, T. Cogliati, C. Zoia, D. Passoni and L. Frattola (1997) Decreased Density of Lymphocytic Benzodiazepine Receptors in Drug-resistant epileptic patients. **Epilepsy Research**, 27(3):181-185.

13. C. Ferrarese, T. Cogliati, R. Tortorella, C. Zucca, G. Bogliun, E. Beghi, D. Passoni, C. Zoia, B. Begni, L. Airoldi, H. Alho and L. Frattola (1998) Diazepam binding inhibitor (DBI) in the plasma of pediatric and adult epileptic patients. **Epilepsy Research**, 29(2):129-134.

14. O.S. Birk, D.E. Casiano, C.A. Wassif, T. Cogliati, L. Zhao, Y. Zhao, A. Grinberg, S. Huang, J.A. Kreidberg, K.L. Parker, F.D. Porter and H. Westphal (2000) The LIM

homeobox gene Lhx9 is essential for mouse gonad formation. **Nature**, 403(6772):909-913.

15. T. Cogliati, D.J. Good, M. Haigney, P. Delgado-Romero, M.A. Eckhaus, W.J. Koch and I.R. Kirsch (2002) Predisposition to Arrhythmia and Autonomic Dysfunction in *Nhlh1*-Deficient Mice. **Mol. Cell. Biol**., 22(14):4977-4983.

16. R. Borgatti, P. Piccinelli, D. Passoni, A. Romeo, M. Viri, S.A. Musumeci, M. Elia, T. Cogliati, D. Valseriati, R. Grasso, M.E. Raggi, and C. Ferrarese (2003) Peripheral markers of the gamma-aminobutyric acid (GABA)ergic system in Angelman's syndrome. **J. Child. Neurol**., 18(1):21-25.

17. C. Zoia, T. Cogliati, E. Tagliabue, G. Cavaletti, G. Sala, G. Galimberti, I. Rivolta, V. Rossi, L. Frattola and C. Ferrarese (2004) Glutamate transporters in platelets: EAAT1 decrease in aging and in Alzheimer's disease. **Neurobiol. Aging**, 25(2):149-157.

18. W.T. Watford, D. Li, D. Agnello, L. Durant, K. Yamaoka, Z.J. Yao, H.J. Ahn, T.P. Cheng, S.R. Hofmann, T. Cogliati, A. Chen, B.D. Hissong, M.R. Husa, P. Schwartzberg, J.J. O'Shea, and M. Gadina (2006) Cytohesin binder and regulator (cybr) is not essential for T- and dendritic-cell activation and differentiation. **Mol Cell Biol**. 26(17):6623-6632.

19. P. Gu, L.J. Harwood, X. Zhang, M. Wylie, W. J. Curry, and T. Cogliati (2007) Isolation of retinal progenitor and stem cells from the porcine eye. **Mol Vis.** 13:1045-1057.

20. R. Picciani, K. Desai, J. Guduric-Fuchs, T. Cogliati, N.S. Peachey, C.C. Morton, and S.K. Bhattacharya (2007) Cochlin in the eye: functional implications. **Prog Retin Eye Res.** 26(5):453-469.

21. T. Cogliati, P. Delgado-Romero, E.R. Norwitz, J. Guduric-Fuchs, U.B. Kaiser, S. Wray, and I.R. Kirsch (2007) Pubertal impairment in *Nhlh2* "null" mice is associated with hypothalamic and pituitary deficiencies. **Mol Endocrinol.** 21(12):3113-3027.

22. J. Guduric-Fuchs, L.J. Ringland-Harwood, P. Gu, M. Dellett, D.B. Archer, and T. Cogliati (2009) Immunohistochemical study of pig retinal development. **Mol Vis.**, 15:1915-1928.

23. A. Arora, J. Guduric-Fuchs, L. Harwood, M. Dellett, T. Cogliati, and D.A. Simpson (2010) Prediction of microRNAs affecting mRNA expression during retinal development. **BMC Dev Biol.** 10:1-15.

24. S.K. Parapuram, R. I. Cojocaru, J. R. Chang, R. Khanna, M. Brooks, M. Othman, S. Zareparsi, N. W. Khan, N. Gotoh, T. Cogliati, and A. Swaroop (2010) Distinct signature of altered homeostasis in aging rod photoreceptors: implications for retinal diseases. **PLoS ONE,** Nov 8;5(11):e13885.

25. J. Guduric-Fuchs, W. Chen, H. Price, D.B. Archer, and T. Cogliati (2011) RPE and neuronal differentiation of allotransplanted porcine ciliary epithelium-derived cells. **Mol Vis.**, 17:2580-2595.

BOOK CHAPTERS

1. I.O. Nasonkin, T. Cogliati, A. Swaroop (2010) Photoreceptor development: Early steps/fate, in Encyclopedia of the Eye. Dartt D, Dana R, Besharse J, Battelle B, Beebe D, Bex P, Bishop P, Bok D, D'Amore P, Edelhauser H, Mcloon L, Niederkorn J, Reh T, Tamm E, Eds, Academic Press (Oxford, UK) Volume 3, pp. 332-339.

2. T. Cogliati, J. Friedman, N. Gotoh, N. Agarwal, and Anand Swaroop (2012) Inherited eye diseases in developing countries, in Genomic and Health in the Developing World, Dhavendra Kumar, Ed, Oxford University Press, New York, USA, pp. 312-332.

CURRICULUM VITAE

7 September 1963	Born in Calolziocorte, Italy
1982	Scientific Lyceum Diploma, Istituto Madri Benedettine, Milano, Italy
1988	Laurea Degree in Pharmaceutical Chemistry and Technology, Universita' degli Studi di Milano, Italy
1988-1989	Postdoctoral Fellow, Istituto Nazionale Tumori, Milano, Italy
1989-1990	Postdoctoral Fellow, Department of Physiology and Biochemistry, Universita' degli Studi di Milano, Italy
1991-1993	Postdoctoral Fellow, National Cancer Institute, National Institutes of Health, Bethesda, MD, USA
1994-1995	Research Fellow, DIBIT, Milan, Italy
1995-1996	Research Fellow, Department of Neurology, Universita' di Milano, Italy
1997-2002	Research Fellow, National Cancer Institute, National Institutes of Health, Bethesda, MD, USA
2003-2008	Lecturer, Queen's University Belfast, UK
2009-present	Scientific Administrator/Staff Scientist, Neurobiology-Neurodegeneration & Repair Laboratory, National Eye Institute, National Institutes of Health, Bethesda, MD, USA